

INTERNATIONAL SERIES OF MONOGRAPHS

**Collaborative Endeavors in the
Chemical Analysis of Art and
Cultural Heritage Materials**



EDITED BY

Patricia L. Long and Keith A. Brinkley

Collaborative Endeavors in the Chemical Analysis of Art and Cultural Heritage Materials

ACS SYMPOSIUM SERIES **1103**

Collaborative Endeavors in the Chemical Analysis of Art and Cultural Heritage Materials

Patricia L. Lang, Editor

*Ball State University
Muncie, Indiana*

Ruth Ann Armitage, Editor

*Eastern Michigan University,
Ypsilanti, Michigan*

**Sponsored by the
ACS Division of Analytical Chemistry**



American Chemical Society, Washington, DC

Distributed in print by Oxford University Press, Inc.



Library of Congress Cataloging-in-Publication Data

Collaborative endeavors in the chemical analysis of art and cultural heritage materials / Patricia L. Lang, editor, Ball State University, Muncie, Indiana, Ruth Ann Armitage, editor, Eastern Michigan University, Ypsilanti, Michigan ; sponsored by the ACS Division of Analytical Chemistry.

pages ; cm. -- (ACS symposium series ; 1103)

Includes bibliographical references and index.

ISBN 978-0-8412-2730-9 (alk. paper)

1. Spectrum analysis--Congresses. 2. Cultural property--Conservation and restoration--Congresses. I. Lang, Patricia L., editor of compilation. II. Armitage, Ruth Ann, editor of compilation. III. American Chemical Society. Division of Analytical Chemistry, sponsoring body.

QD95.C617 2012

701'.5435--dc23

2012018630

The paper used in this publication meets the minimum requirements of American National Standard for Information Sciences—Permanence of Paper for Printed Library Materials, ANSI Z39.48n1984.

Copyright © 2012 American Chemical Society

Distributed in print by Oxford University Press, Inc.

All Rights Reserved. Reprographic copying beyond that permitted by Sections 107 or 108 of the U.S. Copyright Act is allowed for internal use only, provided that a per-chapter fee of \$40.25 plus \$0.75 per page is paid to the Copyright Clearance Center, Inc., 222 Rosewood Drive, Danvers, MA 01923, USA. Republication or reproduction for sale of pages in this book is permitted only under license from ACS. Direct these and other permission requests to ACS Copyright Office, Publications Division, 1155 16th Street, N.W., Washington, DC 20036.

The citation of trade names and/or names of manufacturers in this publication is not to be construed as an endorsement or as approval by ACS of the commercial products or services referenced herein; nor should the mere reference herein to any drawing, specification, chemical process, or other data be regarded as a license or as a conveyance of any right or permission to the holder, reader, or any other person or corporation, to manufacture, reproduce, use, or sell any patented invention or copyrighted work that may in any way be related thereto. Registered names, trademarks, etc., used in this publication, even without specific indication thereof, are not to be considered unprotected by law.

PRINTED IN THE UNITED STATES OF AMERICA

Foreword

The ACS Symposium Series was first published in 1974 to provide a mechanism for publishing symposia quickly in book form. The purpose of the series is to publish timely, comprehensive books developed from the ACS sponsored symposia based on current scientific research. Occasionally, books are developed from symposia sponsored by other organizations when the topic is of keen interest to the chemistry audience.

Before agreeing to publish a book, the proposed table of contents is reviewed for appropriate and comprehensive coverage and for interest to the audience. Some papers may be excluded to better focus the book; others may be added to provide comprehensiveness. When appropriate, overview or introductory chapters are added. Drafts of chapters are peer-reviewed prior to final acceptance or rejection, and manuscripts are prepared in camera-ready format.

As a rule, only original research papers and original review papers are included in the volumes. Verbatim reproductions of previous published papers are not accepted.

ACS Books Department

Preface

The chemical analysis of art and cultural heritage materials began two centuries ago. In 1815 renowned British chemist Sir Humphry Davy described the analysis of pigments on objects excavated from the ruins of Pompeii in a paper that he read to the Royal Society (1). He wrote: “*When the preservation of a work of art was concerned, I made my researches upon mere atoms of the colour, taken from a place where the loss was imperceptible: and without having injured any of the precious remains of antiquity, I flatter myself I shall be able to give some information, not without interest to scientific men, as well as to artists, and not wholly devoid of practical applications.*” Sir Davy hoped to not only become acquainted with the nature and chemical composition of the pigments, but to discover some idea of the manners and styles of the artists (2).

The scientists authoring the chapters in *Collaborative Endeavors in the Chemical Analysis of Art and Cultural Heritage Materials* have taken the same footpath as Sir Davy in regard to the practicality of their research, but they have outpaced Davy in its appeal to a broader audience. The reader will find interesting chapters describing: the process of uncovering forgeries and counterfeits (Chapters 1, 11, 12, 16); the pedagogy of teaching the chemical analysis of art to undergraduates and the history of that “movement” (Chapters 13, 14, 15); the results of scientific investigations on art and cultural objects that have been performed primarily by students and their faculty mentor (Chapters 10, 11, 16, 17); the use of the latest technology in identifying pigments on prehistoric rock paintings, the dating of ancient objects, or the characterization of dyes or biomarkers on archeological samples (Chapters 4, 5, 6, 7, 8). The reader will also enjoy reading the viewpoint of museum conservators who have played a major role in writing and contributing to the science reported in some of the chapters (Chapters 1, 2, 3, 12 and 16). Perhaps most thought-provoking, is a chapter in *Collaborative Endeavors* that asks the question, “What can science alone tell us?” (See Chapter 9.)

But the book is not just a collection of several case studies of describing the chemical composition of objects of cultural or artistic interest; the book aims to illustrate how the chemical and physical analysis of art and cultural heritage materials is a perfect model of collaboration with museum curators, with historians, with students, with religious scholars, anthropologists, and/or with other specialists who partner to answer interesting and important questions about an archeological work or piece of art worthy of study: What are the materials? How was it made? Who influenced the work? How has it changed or deteriorated? Why was it made? Since no one scholar or scientist can answer all these questions, experts from many areas using many different kinds of analytical techniques

are drawn together in *Collaborative Endeavors* to share their knowledge and experience. As a result, an understanding of how the molecular and atomic world plays a role with physical products of human expression is presented from many different perspectives.

Sir Davy was not so lucky when it came to cooperative efforts. In 1821 he read before the Society, “Some Observations and Experiments on the Papyri Found in the Ruins of the Herculaneum” (3). He wrote: “*I should gladly have gone on with the undertaking, from the mere prospect of a possibility of discovering some better results, had not the labour, in itself difficult and unpleasant, been made more so, by the conduct of the persons at the head of the department in the Museum....and these obstacles were so multiplied, and made so vexatious towards the end of February, that we conceived it would be both a waste of the public money, and a compromise of our own characters, to proceed.*” Sir Davy’s experience emphasizes the absolute necessity for cooperative efforts between various scientific, community, and/or academic units in solving these intriguing mysteries.

However, what is different between Davy’s era and the present (except the obvious advances in technology) is the *network of information and education* in regard to the analytical process of art and cultural material analysis. *Collaborative Endeavors in the Chemical Analysis of Art and Cultural Heritage Materials* shows what can be accomplished as a result of that network. There are at least 32 museums, universities, and agencies, who helped directly to make the projects presented within possible. They include but are not limited to:

Chemistry Department, Eastern Michigan University
Archaeographics, Moscow, ID
Archaeological/Historical Consultants, Oakland, MI
Conservation Department, Detroit Institute of Arts
Department of Chemistry, Washington and Lee University
University Collections of Art and History, Washington and Lee University
Balboa Art Conservation Center
The San Diego Museum of Art
Timken Museum of Art
Collections, Mount Vernon Estate and Gardens
Smithsonian National Portrait Gallery
Smithsonian American Art Museum
J. Paul Getty Museum
Royal Picture Gallery Maurishuis, The Netherlands
Scientific Research and Analysis Laboratory, Winterthur Museum
Department of Chemistry, Rhodes College
Department of Chemistry and Biochemistry, University of Mississippi
Department of Mathematics and Computer Science, Rhodes College
McCrone Associates, Westmont, IL
Book and Paper Conservation, The Walters Art Museum, Baltimore, MD
New Testament & Early Christian Literature Department, University of Chicago
Regenstein Library, University of Chicago
Department of Chemistry and Biochemistry, University of Detroit Mercy
Department of Chemistry, Millersville University

Department of Chemistry Whitman College
Department of Chemistry, Ball State University
David Owsley Museum of Art, Ball State University
Chemistry Department, University of West Georgia
Chemistry Department, Clark Atlanta University
Anthropology Department, Hofstra University
Indianapolis Museum of Art
Conservation Department, Buffalo State College

The authors of this book have been a delight with whom to work. One of the insights gained in editing a book is to see the response of the authors after the reviews come back. All have worked hard and have been gracious in providing revisions to their work, when necessary, in order to make the science presented as clear and accurate as possible. They are the experts in their field.

Collaborative Endeavors in the Chemical Analysis of Art and Cultural Heritage Materials is the result of the Chemistry of Art Symposium held at the 2011 Central Regional Meeting of the American Chemical Society at IUPUI in Indianapolis, IN on June 9th and organized by P. Lang. The editors would like to gratefully acknowledge Dr. Corinne Deibel, Professor of Chemistry, Earlham College, for her organization of that meeting and support of the symposium.

We also thank the ACS editors, especially Nikki Lazenby for her thoughtful assistance with this book, and a big thanks goes to the many colleagues who reviewed the book and its chapters.

References

1. Some Experiments and Observations of the Colours used in Paintings by the Ancients. In *The Collected Works of Sir Humphry Davy*; Davy, J., Ed.; Smith, Elder and Co. Cornhill: London, 1840; Vol. VI, pp 134–135.
2. Probing the Authenticity of Antiquities with High-Tech Attacks on a Microscale. *Science* **1988**, 239, 1374.
3. The Ruins of Herculaneum. In *The Collected Works of Sir Humphry Davy*; Davy, J., Ed.; Smith, Elder and Co. Cornhill: London, 1840; Vol. VI, pp 173–174.

Patricia L. Lang, Professor and Chair
Department of Chemistry
Ball State University, Muncie, IN 47306
765-285-5516 (telephone), plang@bsu.edu (e-mail)

Ruth Ann Armitage, Professor
Department of Chemistry
Eastern Michigan University, Ypsilanti, MI 48197
734-487-0290 (telephone), rarmitage@emich.edu (e-mail)

Editors' Biographies

Patricia L. Lang

Patricia L. Lang, Professor and Chair of Chemistry Ball State University, earned a B.S. in Chemistry from Ball State in 1983. She completed a Ph.D. in Physical Chemistry from Miami University with Dr. Jack E. Katon in 1987 on the applications of infrared and Raman microspectroscopy. Her research focuses on the spectroscopic characterization of a wide range of different materials that include asbestos, monolayers, fibers, and bacteria. She has written and presented extensively on the analysis of historic materials including parchment, paper sizing, pigments, binders, and paint additives. In her 25 years at Ball State Dr. Lang has mentored the research of over 60 students.

Ruth Ann Armitage

Ruth Ann Armitage, Professor of Chemistry at Eastern Michigan University, earned a B.A. in Chemistry from Thiel College in 1993. She completed a Ph.D. in Analytical Chemistry at Texas A&M University with Dr. Marvin Rowe in 1998 on radiocarbon dating of charcoal-pigmented rock paintings. Since joining EMU in 2001, her research focus has remained on characterizing archaeological and cultural heritage materials including rock paintings, residues, and colorants in textiles and manuscripts in collaboration with archaeologists and museum conservation scientists, as well as both undergraduate and graduate students.

Chapter 1

What's Wrong with this Picture? The Technical Analysis of a Known Forgery

Gregory D. Smith,^{*,1} James F. Hamm,² Dan A. Kushel,²
and Corina E. Rogge²

¹Indianapolis Museum of Art, 4000 Michigan Road,
Indianapolis, IN 46208

²Art Conservation Department, 1300 Elmwood Avenue,
Buffalo State College, Buffalo NY 14222

*E-mail: gdsmith@imamuseum.org

Robert Lawrence Trotter was convicted in federal court in 1990 of producing and selling fake American primitive style folk art. A methodical ‘reverse engineering’ of one of his confiscated paintings, *Village Scene with Horse and Honn & Company Factory*, was undertaken to determine what telltale signs might exist to identify this work as a forgery. Currently 39 other Trotter fakes are yet unaccounted for and are potentially circulating on the art market or belong to private or institutional collections. A crescendo approach to the critical examination of this painting began with a simple visual assessment followed by diagnostic imaging using X-ray, near infrared, and UV radiation sources. Non-sampling chemical analysis with X-ray fluorescence and Raman microspectroscopies was conducted next to determine specifically the forger’s materials. Finally, additional information was gathered from invasive sampling approaches including cross section analysis, FTIR microspectroscopy, and pyrolysis-gas chromatography-mass spectrometry. Copious clues to the work’s inauthenticity exist at every level of investigation. Although simple visual examination would raise questions as to the artwork’s genuineness, diagnostic imaging and chemical analysis prove beyond a doubt that the work is a modern fake. Anachronistic pigments and improbable construction techniques are evidence that this is not an authentic piece of 1860s folk art.

Introduction

In 1990, Robert Lawrence Trotter was sentenced to ten months in federal prison for a decade long scheme that involved the production and sale of fake American 19th-century primitive style paintings (1–3). By his own admission, Trotter conducted fifty-two sales of his fakes and forgeries from 1981 to 1988 involving six art dealers and twenty-nine auction houses in eleven states. His ill-gotten gains were in excess of \$100,000 (1), although some of his earliest fakes sold for paltry sums, one for only \$36 (1, 2). The actual crime to which he pled guilty was wire fraud related to these transactions (2).

Trotter's familiarity with the art and antiques market in the early 1980s made him aware of the innumerable fakes that exist, especially in the primitive or folk art style. Being an amateur artist himself, he joined in the production of bogus artworks in order to augment his income. Initially these generic, anonymous folk art pieces fetched only modest sums at auction and attracted little attention. His works included typical folk art scenes and sitters, and he utilized a pastiche of the physical characteristics admired in many styles of folk art to enhance the appeal of his forgeries. In 1988 Trotter, being impatient with the trivial earnings of his fakes up to this point, left the relatively safe confines of low value, anonymous primitive art and began directly imitating the styles of well-known 19th-century folk artists such as M. W. Hopkins, Ammi Phillips, and Noah North, and finally the artist best known for his trompe l'oeil paintings, John Haberle. These more ambitious attempts came to the attention of the community of scholars and collectors specializing in these artists' works, and their authenticity began to be questioned. Because of suspicions regarding Trotter's fake 'Haberle,' the FBI established a sting operation that ultimately caught him red-handed. Dan Hingston, an auction manager caught up in the scheme, noted, "We're lucky Trotter raised the stakes. If he'd stayed at this level [anonymous, generic folk art], he could still be doing it (2)."

Of the fifty-five fakes he produced, only sixteen of these works were located by the FBI in their investigation (1). Moreover, only five of these identified works were seized by the Bureau or turned over to it as part of Trotter's compensation settlement. One of these paintings, known as *Village Scene with Horse and Honn & Company Factory*, which was signed "Sarah Honn," and dated "May 5, 1866 A.D.," was actually painted by Trotter in 1985 and ultimately was given to the Art Conservation Department at Buffalo State College by the courts in 1991 to be used for study and research (1). This landscape painting is shown in Figure 1(a).

With thirty-nine of Trotter's fake paintings still unaccounted for and likely circulating on the art market or part of private or institutional collections, the Buffalo State College faculty decided to undertake a comprehensive study of the work to determine what signs might point a conservator or curator to question its authenticity. This is particularly important since the current condition of the *Village Scene* painting is poor and has noticeably worsened in the intervening years, likely the result of the techniques used by Trotter to enhance its aged appearance. Based on this observation, it is reasonable to assume that others of Trotter's oeuvre will likely be brought to conservators for stabilization, cleaning,

and treatment if they haven't already been restored – many of his works were immediately taken by their new owners to restorers (2).

This investigation brought together the combined expertise of paintings conservators, conservation scientists, and imaging specialists. The approach to the examination began with the simplest form of exploration, namely close critical observation of the painting's composition and obvious physical construction. This level of investigation is available to all conservators, curators, and collectors. Next, macroscopic imaging techniques familiar to art conservators and forensic investigators were used to capture images of the artwork using X-ray, near-infrared, and UV radiation sources. These images provide complementary information on the artist's working methods, the condition of the artwork, and hidden aspects of its construction. Finally, scientific analysis, first using only non-destructive methods and later techniques that required sampling from the artwork, were utilized to explore the materials used by the forger and to compare them to what would be expected for a true 1860s folk art painting. This level of investigation is only possible at the most technologically sophisticated cultural heritage institutions, although motivated clients could arrange for contract analysis of their paintings.

Experimental Section

Imaging Techniques

Color photographs were acquired using a Sinar view camera with a Better Light digital scanning back CCD trilinear array with 3200 K incandescent illumination. Ultraviolet-induced visible fluorescence images of the painting were captured with a Nikon D100 digital camera (CCD array) with Wratten 2E and CC40Y filters. The camera was adjusted to white balance 7000 K and Adobe Camera Raw® tint +11. The source of UVA radiation (315 to 400 nm) was a pair of high-pressure mercury lamps filtered of their visible emission lines. A near infrared (NIR) image in transmission mode was acquired with the digital scanning back mentioned above, but modified with a Wratten 87C visible blocking filter, thus restricting the camera sensitivity to 850 to 1000 nm. The painting was exposed to NIR radiation from incandescent photo lamps directed onto the verso with the camera capturing the radiation transmitted through the painting. A radiograph of the painting was recorded on Kodak Industrex Rapid 700 radiographic paper. The Philips X-ray tube voltage was 30 kV and exposure was 525 mA•sec at a 60 in. film-focus distance. The radiograph of the experimental canvas mock-up discussed below was recorded on Kodak Industrex M100 film using the same experimental parameters. Digital versions of all images were adjusted in Adobe Photoshop for color correction, tint, exposure, mosaicking, and sharpness as necessary.

Microfocus X-ray Fluorescence (XRF)

X-ray fluorescence spectra were collected using a Bruker ARTAX energy dispersive X-ray spectrometer system. The excitation source was a molybdenum

target X-ray tube with a 0.2 mm thick beryllium window, operated at 50 kV and 600 mA current. The X-ray beam was directed at the painting through a masked aperture of 0.65 mm diameter. X-ray signals were detected using a Peltier cooled XFlash 2001 silicon drift detector. Helium purging was used to enhance sensitivity to light elements. Spectra were collected over 60 sec live time.

Raman Microspectroscopy

Raman spectra of pigments were acquired using a Bruker Senterra microscope suspended on a Z-axis gantry. The 'Z-stage' allowed the entire artwork to be placed directly under the 50X ultra-long working distance objective of the microscope. Excitation at 785 nm and 1.1 mW power at the laser focus was used to stimulate Raman scattering from an area of approximately 1-2 μm diameter. To reduce the interference due to fluorescence, an area of agglomerated pigment particles was chosen in an exposed fissure in the paint film. The resulting spectrum was measured at 3-5 cm^{-1} spectral resolution with several hundred seconds of spectral coaddition. The pigment's identity was ascertained by comparing its spectrum to those of likely reference materials.

Sampling and Cross Section Preparation

Paint samples were acquired from the painting under a stereomicroscope at low magnification using chemically etched tungsten needles and a surgical scalpel. Sampling was limited to existing areas of damage, abrasion, or cracks. Disperse samples of pigments and media were collected as surface scrapings or small paint flakes from a specific area or paint passage, and these were stored on glass well slides under cover slips until analyzed. Cross section samples were acquired by cutting vertically through the varnish, paint, and ground layers to the underlying canvas substrate using a 500 μm tip microchisel (Ted Pella). The sectioned sample was generally less than 100 μm in the long dimension. These samples were mounted in Ward's Bio-plastic™ polyester resin. Once the embedding medium fully cured, the plastic block was cut and polished on a series of Micromesh™ cloths to expose the painting's cross section.

Darkfield images of the sectioned samples were acquired on a Zeiss AxioImager A1m compound microscope with a 20X objective using an MRc5 digital photomicrography camera. The same area was then examined under UV irradiation for signs of visible luminescence. A DAPI filter cube set allowed narrowband excitation between 325 and 375 nm with observation throughout the visible spectrum ($\lambda > 412 \text{ nm}$).

Fourier Transform Infrared (FTIR) Microspectroscopy

Infrared spectra were collected using a Continuum microscope coupled to a Magna 560 FTIR spectrometer (Thermo Nicolet). Samples were prepared by flattening them in a diamond compression cell (Thermo Spectra Tech), removing the top diamond window, and analyzing the thin film of sample in transmission mode on the bottom diamond window. An approximately 100 μm square

microscope aperture was used to isolate the sample area for analysis under a 15X Schwarzschild objective. The spectra are the average of 32 scans at 4 cm⁻¹ spectral resolution. Correction and subtraction routines were applied using the instrument's Omnic software as needed to eliminate interference fringes, sloping baselines, or peaks from interfering spectral components. Sample identification was aided by searching a spectral library of common conservation and artists' materials (Infrared and Raman Users Group, <http://www.irug.org>).

Pyrolysis-Gas Chromatography-Mass Spectrometry (Py-GC-MS)

A small scraping of paint was analyzed by Py-GC-MS after derivatization of the sample using tetramethylammonium hydroxide (TMAH). The sample was analyzed using a Frontier Lab Py-2020D double-shot pyrolyzer system with a 320°C interface to an Agilent Technologies 7820A gas chromatograph and 5975 mass spectrometer detector. An Agilent HP-5ms capillary column (30 m x 0.25 mm x 0.25 μm) was used for the separation with 1 mL/min of He as the carrier gas. The split injector was set to 320°C with a split ratio of 50:1. The GC oven temperature program was 40°C for 2 min, ramped to 320°C at 20°C/min, followed by a 9 min isothermal period. The MS transfer line was at 320°C, the source at 230°C, and the MS quadrupole at 150°C. The mass spectrometer was scanned from 33-600 amu at a rate of 2.59 scans/sec with no solvent delay. The electron multiplier was set to the auto-tune value. Samples were placed into a 50 μL stainless steel Eco-cup, and 3 μL of a 25% methanolic solution of TMAH were introduced for derivatization. After 3 min the cup was placed into the pyrolysis chamber where it was purged with He for 3 min. Samples were pyrolyzed using a single-shot method at 550°C for 6 sec. Sample identification was aided by searching the NIST MS library and by comparison to pyrograms of authentic samples.

Results and Discussion

Visual Examination

On the surface, the painting has all the hallmarks of a highly desirable piece of American folk art from the 19th-century. The scene, Figure 1(a), is a typical primitive style landscape showing a small village surrounded by pastures. The artist appears to be an amateur based on the naïve sense of perspective. The careful observer is rewarded by recognizing a nearly obscured signature in the lower right hand corner of the painting. The autograph, in clear block lettering in brown paint, reads "Sarah Honn May 5, 1866 A.D."

The signature is interesting on several levels. First, folk art paintings are rarely signed, and this picture would be especially valuable because the artist is presumably a woman. History has recorded very few female folk art painters outside of the well known Susan Waters and Grandma Moses. When viewed under the stereomicroscope, it is obvious that the aging cracks run through the artist's paint as well as the signature, indicating that the two were contemporary and that the entire painting with its autograph aged together.

The village scene composition might well be a nod to the historical practice of itinerant painters of the mid-19th century who traveled the country drawing or painting a client's land holdings in return for a small payment or even a place to stay. In this instance, the presence of a small sign over the door of the red brick factory, which reads "Honn & Co.," adds an interesting twist in that the artist is presumably recording her own family's property. All attempts to identify a Sarah Honn living in late 19th-century America or a Honn & Co. business were fruitless. This anonymity reveals the forger's cleverness. Sarah Honn as a person is more believable because of the existence of her place name, and yet being purely fictitious, there are no potential inconsistencies to be discovered by a studious researcher.

The verso of the painting, Figure 1(b), provides additional 'badges of authenticity' for a gullible collector. The back of the canvas is lined onto a piece of blue-striped mattress ticking, partly obscured by a dark stain, presumably due to mold. Mattress ticking has occasionally been used as a cheap canvas material by itinerant painters and folk artists. However, in this instance the mattress ticking is not the artist's canvas, but rather a glued relining fabric, which is unique in the experience of the authors. Relining of a worn canvas is a preservation intervention performed when the original is structurally too compromised or weakened to support the paint. Careful examination of the paint surface in raking light showed a friable, undulating paint layer, but no indication of tears or holes in the canvas that would have necessitated relining. The presence of the mattress ticking as a lining fabric is perhaps the most telling outward clue that the artwork has been at least embellished to enhance its desirability.

Figure 2 shows a detail shot of the bottom tacking margin, i.e. the lower flap of canvas that is used to tack the painting onto a rectangular wooden stretcher. The upper layer of fabric, the original canvas, is frayed and reveals the blue-striped ticking underneath. The metal tacks, which were removed from their original locations (dashed circles) during the relining, present an improbable situation. The artist's white priming layer runs over top of both the original tack holes and the tack heads in their current position, suggesting the canvas was removed from the stretcher, lined, re-tacked to the stretcher, and then primed and painted. This necessitates that the painting was relined before the surface image was painted, a situation that makes no logical sense in terms of a painter's normal practice.

Imaging Techniques

UV-induced visible fluorescence imaging is a useful survey technique to gauge the condition of an artwork (4, 5). Artists' paints and varnishes tend to develop fluorophores as they age, giving old paintings a characteristic luminescence when irradiated with long wavelength UVA lamps. Recent areas of retouching over damages or paint losses will not have had the time to develop the same level of fluorescence, thus appearing as darker patches in the fluorescence image. In describing his last criminal endeavor, Trotter mentioned that on the 'Haberle' painting he, ". . . used a thin coat of copal varnish. It's browner and thinner and with a blacklight it tends to throw that even overall glow that can fool people not used to using a blacklight (2)."



Figure 1. Color images of the front (a) and verso (b) of "Village Scene with Horse and Honn & Company Factory," 40.8 cm x 51.1 cm. Courtesy of Buffalo State College.

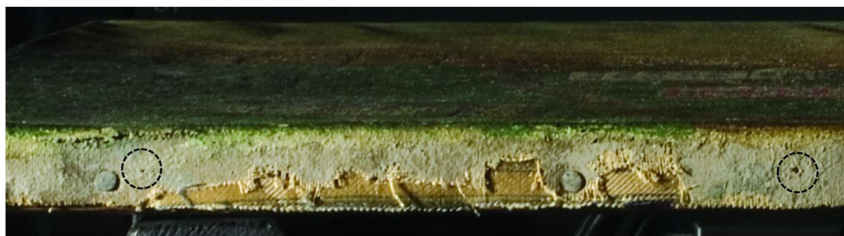


Figure 2. Detail of the lower tacking margin showing former tack holes (dashed circles). Courtesy of Buffalo State College.

Figure 3(a) shows a color image of the front of the *Village Scene* painting when exposed to UVA. It is obvious that Trotter implemented a similar coating technique, since the entire surface of the painting emits an uneven, striated cool fluorescence suggestive of a natural resin coating, although not necessarily a copal varnish, partially obscured by UV blocking dirt and grime. Conservators, however, are very used to utilizing a blacklight, and this image is startling to a highly trained eye for a painting that purports to be nearly 100 years old, has already undergone a relining, and bears extensive mold growth suggesting years of exposure to moist conditions. There are no dark patches in the fluorescence image that would indicate a history of retouching, structural repair, or restoration. Such a homogenous surface fluorescence is unusual unless a forger or dealer is trying to be duplicitous by adding an intentionally concealing surface coating.

Figure 3(b) shows the same imaging technique applied to the verso of the artwork. The heavy, seemingly brush applied mold stains are faintly fluorescent, which is not atypical for molds. However, the relining fabric, best seen in the upper right corner, is far more luminescent. Optical brighteners are applied to modern fabrics or are included in laundry detergents to give textiles a ‘whiter-than-white’ appearance. Fluorescent brighteners are a post-WWI invention (6), providing a clear indication that this lining fabric was applied in the 20th-century.

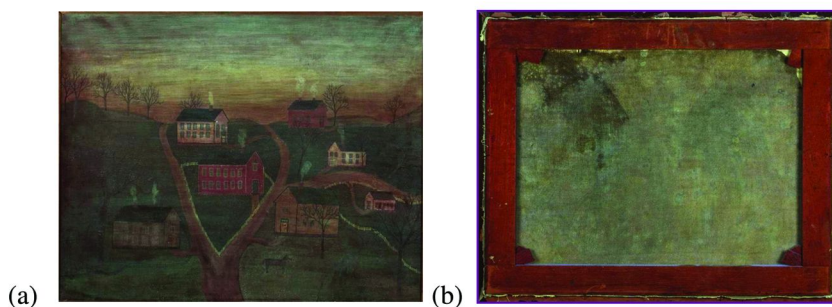


Figure 3. UV-induced visible fluorescence images of the (a) front and (b) verso of the painting. Courtesy of Buffalo State College.

Transmitted NIR photography relies on the transparency of many artists' materials to long wavelength radiation thus allowing imaging of underlying structures or compositions that include infrared opaque materials (7). Most often NIR examination is conducted to visualize underdrawings or preparatory cartoons executed in graphite or charcoal. In the transmitted NIR detail photograph of the white building on the horizon, Figure 4, there is no indication of a carbon-based underdrawing. The opaque passages are simply those surface features that utilize a carbon containing black paint. It is obvious that the artist painted in the landscape prior to placing the buildings since the horizon line is clearly running behind the central white building. These construction details evidenced by NIR imaging are not an indication of fakery for a primitive-style painting since it is easy to imagine the amateur folk artist painting what they saw in a very spontaneous way without significant planning or sketching.



Figure 4. Transmitted NIR image detail showing the horizon line running through the building and the fine craquelure pattern. Courtesy of Buffalo State College.

More importantly, the transmitted NIR image highlights in stark contrast the islands of paint separated by a scaly craquelure. This significant cracking and its evenness across the surface of the painting deviates from the typical age-induced crack patterns observed in old oil paintings. Naturally occurring cracks create a pattern perpendicular to radiating lines of stress originating in the restrained canvas corners, which are often exacerbated by low relative humidity or low temperatures (8). The cracking in *Village Scene* is similar to cracking that occurs when paint is dried by heat, causing rapid, simultaneous contraction of the entire paint surface (9). Trotter again has provided some clues to the techniques used to simulate aging. He reportedly used “. . . lots of driers [siccatives] . . .” and would age his finished paintings for a week under a sunlamp (2). No doubt the

chemical accelerators coupled with the heat from the lamp contribute to the small, even cracking observed in this forgery. In another work by Trotter, a conservator observed under the microscope that the age cracks had actually been scratched into the paint using a sharp stylus (2).

X-radiography is often utilized by conservators to image the distribution of heavy metal pigments in a painting. Until the commercialization of a synthetic route to ultrapure TiO_2 pigment in the late 1910s, the most common white artists' pigment was basic lead carbonate $[\text{2PbCO}_3 \cdot \text{Pb(OH)}_2]$ (10), being the principle white paint, but also mixed into other colors to adjust their value. As a result of this widespread use of lead white pigment, most X-ray images of historic artworks show a ghost-like image of the surface painting, but also reveal underlying artist's changes as well as abandoned compositions or reused canvases.

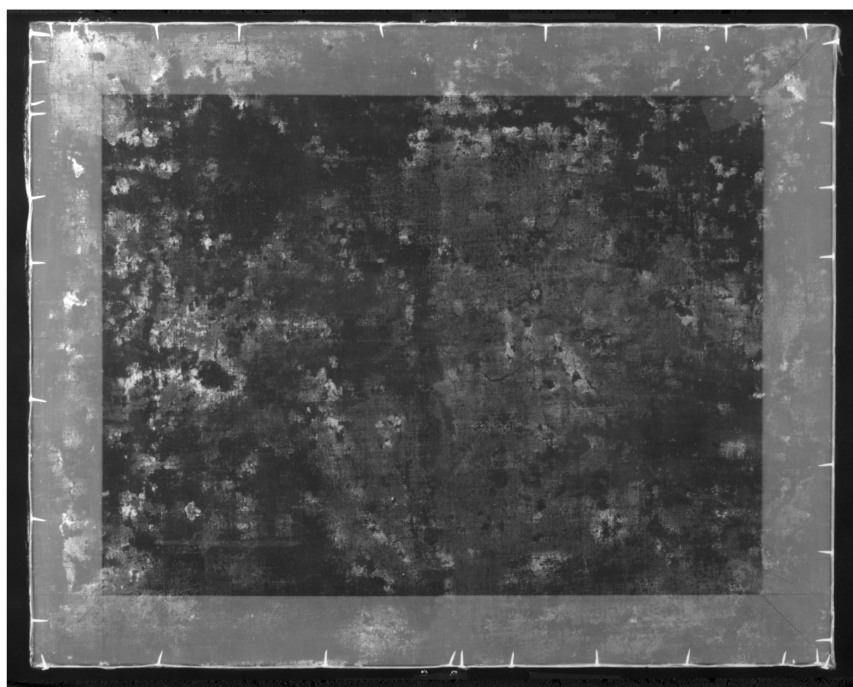


Figure 5. Radiograph of "Village Scene".

Figure 5 shows the radiograph of *Village Scene*. It is immediately obvious that no heavy metal pigments, at least none containing lead, were used to create the surface image as there is hardly any indication of the landscape. A palette devoid of lead white is inconsistent with a 1860s provenance. Moreover, one sees only amorphous, high contrast passages with blurred, indistinct borders unrelated to any figure or structure in the surface painting. In the investigation of the Trotter case, the FBI found that the forger often visited antique shops where he would buy inexpensive period paintings (1, 2). Trotter confessed that these paintings provided him with the old canvas support necessary to produce a convincing

fake. The application of commercial paint strippers removed the painted image on the authentic canvas, allowing Trotter to prepare his fakes without any telltale underlying textures. The radio-opaque indistinct passages in the X-ray image of *Village Scene* suggested that remnants of an old lead white containing ground were not removed by the paint stripper, perhaps because the ground was pushed into the canvas weave. The authors produced a mock-up using period canvas with a lead white oil ground which was removed using Zip-Strip® purchased at a local hardware store. After softening the oil paint and scraping it from the canvas with a putty knife, a radiograph of the mock-up, reproduced in (11), was captured using identical instrumental parameters to those used to collect the radiograph in Figure 5. The two images show a clear similarity, thereby confirming Trotter's reuse of canvas from an old painting for the creation of *Village Scene*.

Noninvasive Scientific Analysis

Sophisticated scientific analysis is available to many conservators and curators at larger institutions employing conservation scientists. Even at smaller institutions and in private practices, the availability of a limited number of scientific instruments, optical microscopes, and microchemical testing equipment is common. If such instrumentation is accessible, then the investigator can gain a specific knowledge of the materials used by an artist. For the sake of authentication, or more accurately 'inauthentication,' one is typically looking for anachronistic or otherwise undocumented materials or methods for a particular artist, style, or time period being employed in the creation of the suspect artwork.

X-ray fluorescence (XRF) spectroscopy is one technique that is widely available, either as a laboratory based microanalytical instrument or as the growingly popular handheld XRF units. The power of XRF lies in its non-invasive nature and the fact that the resulting elemental spectrum can be used to infer the inorganic or organometallic pigments used by the artist. *Village Scene* was subjected to an exhaustive analysis of the forger's palette using a microfocus lab-based instrument.

When creating his last forgery, i.e. the trompe l'oeil style 'Haberle' painting, Trotter is reported to have used standard tube oil colors from an art supply store and synthetic bristle brushes. He is quoted as saying, "I limited my palette to colors Haberle would have had (2)." XRF analysis of the present painting shows that Trotter was less exacting in selecting his paints for this work. Many anachronistic colorants were detected. Figure 6 shows the XRF analysis of the white paint used in the central white structure on the horizon (inset detail). Although one would expect lead white or perhaps ZnO to be used in the 1860s, the latter pigment being available at least since 1803 (10), the strongest peak in the XRF spectrum is in fact titanium. Trotter's use of TiO₂ white explains the transparency of the surface image in the radiograph in Figure 5. Based on this evidence alone, one could confidently rule out the signature date of 1866. Other colorants inferred from XRF data included Prussian blue [Fe₄[Fe(CN)₆]₃•14-16H₂O] in the blue window sills, yellow ochre in the yellow buildings and sunset [FeOOH + silicates], and red ochre in the central red building [Fe₂O₃ + silicates], all of which would have been available to 19th-century folk artists.

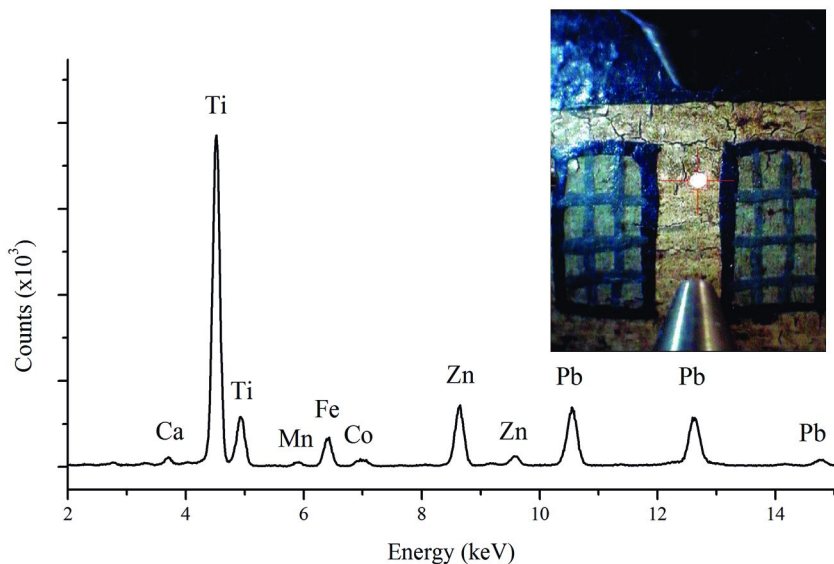


Figure 6. XRF spectrum with major element peaks identified for the white paint from the central white building. The inset shows a detail photo of the analysis spot.

In addition to these colorants, XRF revealed low levels of Co in all paints and the ground, Pb in varying amounts throughout the painting, and often concomitant peaks for Ba and Zn. The ubiquitous Co signal may represent a cobalt linoleate or naphthenate siccative added to accelerate the drying of the oil paints as confessed by Trotter. The relatively weak Pb signals in each spectrum are probably due to residual lead white ground left from stripping the reused canvas. When peaks associated with Ba and Zn occur together, this is often indicative of the use of lithopone, a co-precipitated mixture of ZnS and BaSO₄ that has been used since 1874 as an inexpensive filler in many paints (10).

Although XRF analysis provided potential pigments for most of the colors used in the painting, elemental spectra taken of the green hills showed only the omnipresent Co, Pb, Fe, Ba, and Zn. No metal could be clearly associated with a green pigment. To clarify the nature of the green colorant, the entire painting was placed under a gantry-mounted Raman microspectrometer, and vibrational spectral analysis was performed on the green pasture near the horse. The resulting Raman spectrum, shown in Figure 7(a), reveals numerous sharp spectral features indicative of an organic or organometallic pigment. The spectrum is compared to that of (b) phthalocyanine green, PG7, a chlorinated copper phthalocyanine complex first synthesized in 1938 (12), and a high degree of correlation is observed. However, under the microscope copious intermixed yellow particles were also visible, although they did not give as clear a Raman spectrum as the green component under the experimental conditions utilized.

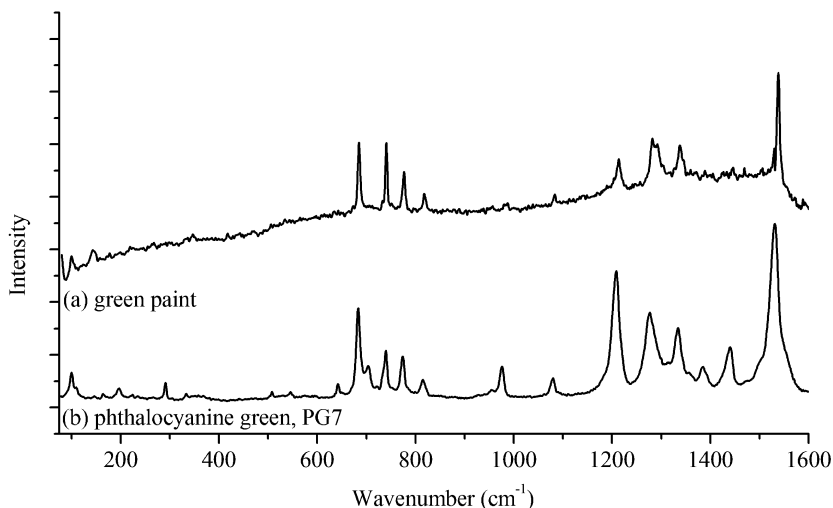


Figure 7. Raman spectra of (a) green pigment particles and (b) reference phthalocyanine green, PG7.

Invasive Scientific Analysis

Small loose fragments of the green paint analyzed above were extricated for analysis by transmission FTIR microspectroscopy. The green paint layer was separated from the other layers under the stereomicroscope prior to preparation for analysis. The resulting spectrum is shown in Figure 8(a) along with reference spectra of (b) polymerized linseed oil, and (c) hide glue. The sample spectrum shows a large oil component as revealed by methylene CH stretching bands at 2923 and 2852 cm^{-1} as well as the prominent νCO of the triglyceride esters at 1734 cm^{-1} . The broad νOH peak centered at 3420 cm^{-1} indicates that the oil binder, presumably linseed oil, is well-cured and significantly hydrolyzed. Although Trotter did reveal that he used standard tube oil colors, he never mentioned the addition of a proteinaceous component, which can be presumed present due to the weak Amide I, II, and III bands at 1651, 1533, and 1450 cm^{-1} . There are some verbal indications that Trotter did not always work in oils. At least one fake painting, an image of a ship at sea, is described by the *Maine Antique Digest* as being “tempera,” suggesting an egg binding medium, and Trotter himself in an interview with the *Digest* after sentencing cryptically described his first fake as being a “buttermilk paint,” presumably containing a casein binder (2). At this point the rationale for the protein in the green paint, whether intentional or accidental, could not be known.

With no clear indicator of the pigments used in the green paint passage based on the FTIR spectrum in Figure 8(a), a spectral subtraction was attempted to remove the overwhelming spectral features of the binding media. After scaled

subtraction of the reference spectra for linseed oil and hide glue, the resulting residual spectrum is shown in Figure 9(a). Although this spectrum appears quite noisy, a spectral library search yielded a high quality match with the spectrum of Hansa Yellow, PY3, first available in 1928 (12). The spectrum of the pure colorant is shown in Figure 9(b). Because of its high tinting strength, this strongly colored yellow pigment is often mixed with a barium sulfate (BaSO_4) filler, which is evidenced here by the sulfate stretching band triplet between 1235 and 1035 cm^{-1} and the sharp associated peak at 984 cm^{-1} . The spectrum of pure barium sulfate is shown in Figure 9(c) for comparison.

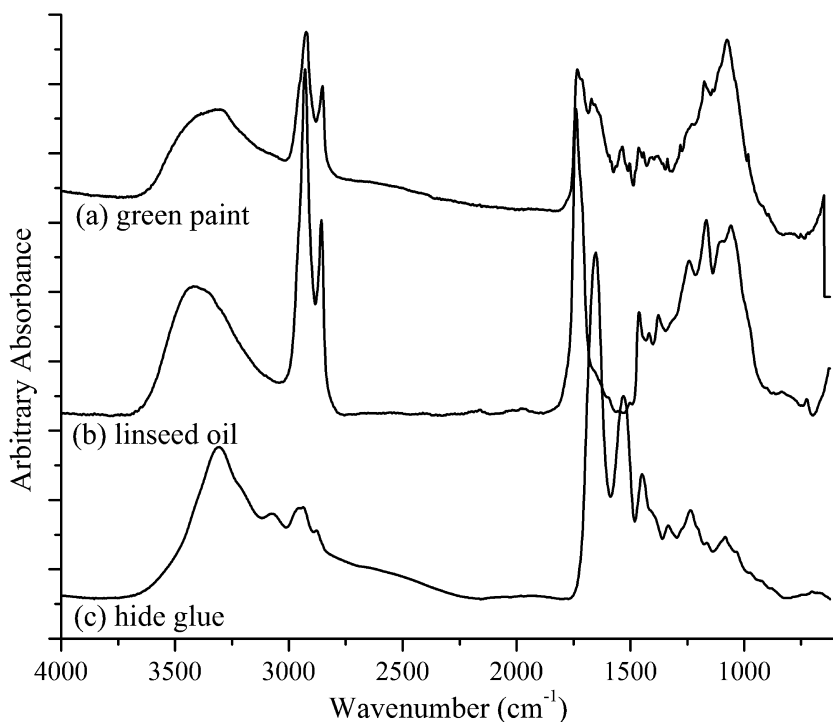


Figure 8. FTIR spectrum of (a) green paint sample compared to reference spectra of (b) polymerized linseed oil and (c) hide glue.

Through a combination of FTIR and Raman analyses, the green paint used for the landscape appears to be a mixture of phthalocyanine green and Hansa yellow, which incidentally is often given the paint color name Permanent Green Hue in the modern artist's palette (10). Permanent Green was originally a mixture of chrome oxide green with zinc yellow (ZnCrO_4), which in fact would theoretically have been available to Haberle in the 1860s (10). It is possible that Trotter may not have been aware that the modern variant no longer uses the toxic chromate containing pigment.

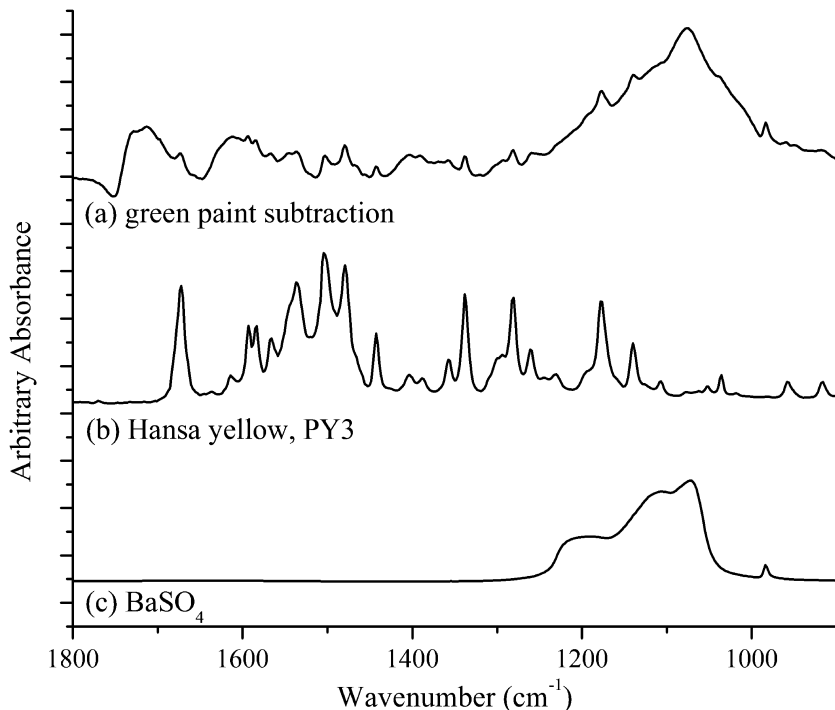


Figure 9. FTIR residual spectrum of (a) green paint after subtraction of linseed oil and hide glue reference spectra. Comparison is made to reference spectra of (b) Hansa Yellow (PY3) pigment and (c) barium sulfate.

To assess the nature of the surface coating, a thin scraping was carefully removed from the area of the horse's pasture without disturbing the underlying green paint layer. FTIR analysis (not shown) provided surprisingly an almost perfect match to well-aged shellac. Although Trotter had specifically mentioned copal as the coating of choice for his last forgery (2), the 'Haberle,' it would appear that an insect resin rather than a tree resin was used in this instance. The expected role of the shellac, which can be difficult to apply thinly and evenly by brush, in producing a convincing fake is not known. The detection of shellac required further investigation as it typically fluoresces bright orange when unbleached, unlike the cool, milky fluorescence observed in the UVA-induced visible fluorescence image in Figure 3(a).

Further analysis of the binding media and varnish was performed using Py-GC-MS of surface scrapings. The pyrogram of the TMAH-derivatized sample taken from the horse's green pasture is shown in Figure 10(a). For comparison, pyrograms for (b) linseed oil and (c) very light shellac (unbleached) are included. The major marker peaks for various artists' materials are identified in Table I (13, 14). Py-GC-MS confirms the results from FTIR analysis by revealing the simultaneous presence of oil, protein, the Hansa Yellow pigment, shellac, and trace amounts of pine resin (colophony). The shellac is most likely unbleached due to the lack of chlorinated marker compounds that have recently been reported to occur in shellac that has been decolorized by the addition of a chlorine bleach (15). Copal varnish, which was reportedly used in other Trotter fakes, is shown not to have been used in this work due to the absence of methyl sandaracopimarate, the marker compound for Manila copal, at detectable levels (16).

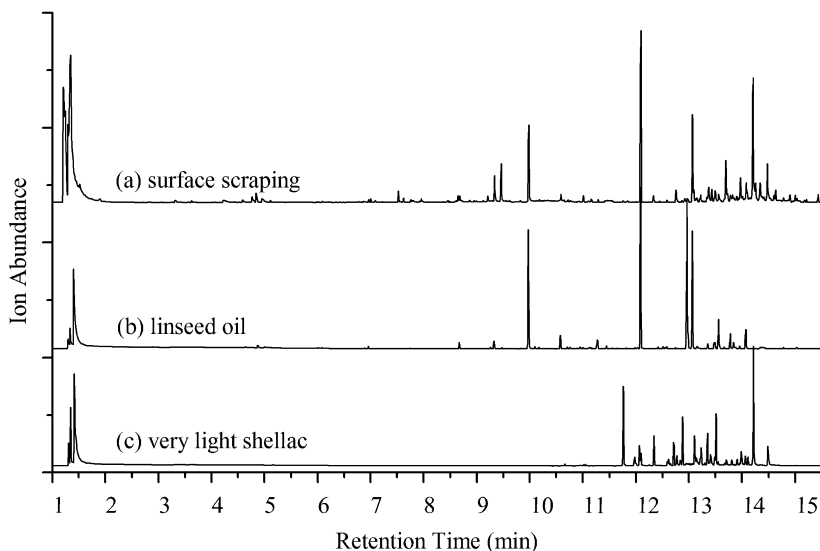


Figure 10. GC-MS pyrogram of TMAH-derivatized (a) green paint sample, (b) linseed oil, and (c) very light shellac.

The excessive craquelure of the paint in *Village Scene* provided numerous opportunities to prepare cross sections of paint passages without causing a noticeable lacuna in the painting's surface. Although an invasive approach, cross section analysis is one of the only ways to explore the working methods of an artist. To understand the layered structure of this painting, selective areas were sampled and cross sections prepared for analysis by optical microscopy.

Figure 11(a) shows a photomicrograph of one section taken from the hindquarters of the horse in the painting's foreground. Figure 11(b) shows the same section under UV irradiation. The stratigraphy of the section revealed in the two images records the process by which Trotter created the fake. At the lowest level, a chunky, fragmented white ground layer with carbon inclusions shows the incomplete removal of paint from the reused canvas. This layer is best viewed in a previously published cross section (11), but can be faintly seen in the lowest area of Figure 11(a). On top of this are two thinner, homogeneous modern white ground layers applied by the forger to prepare the reused canvas for painting. The lower of these two is only partly preserved to the far right in the cross section shown here. A translucent layer seen in Figure 11(a) separates these two grounds, and it is shown to be highly luminescent in Figure 11(b). This blue fluorescence is typical of proteinaceous materials (17). On top of the modern grounds are two green paint layers, a dark green and an upper yellow-green (the Permanent Green Hue paint layer discussed above), again interleaved with a fluorescent material consistent with a proteinaceous layer. The paint of the brown horse overlays the landscape colors, again sandwiched between fluorescent layers, the topmost of which appears to be a mostly continuous blue fluorescent layer with occasional orange fluorescent components.

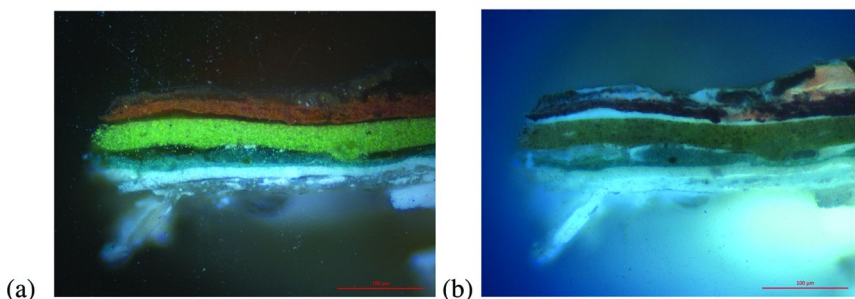


Figure 11. Visible light photomicrographs of a cross section sample from the horse's hindquarters in (a) normal illumination and (b) UV irradiation. Lower right scale = 100 μm .

It is interesting to note in the cross section the numerous thin separations that exist in all of the oil paint and ground layers. It is believed that Trotter intentionally violated the painter's "fat over lean" rule, using a fast drying medium like animal glue overtop of a slower drying medium like linseed oil (9). This type of construction inevitably leads to the oil paint being pulled apart into small islands by the rapid contraction of the surrounding protein layers, especially when heated, thus inducing nearly instantaneously the evenly random craquelure observed in *Village Scene*.

Table I. Major pyrogram peaks, their identification, and associated artists' material source of the TMAH derivatized compound

<i>Retention time (min)</i>	<i>Peak Identity</i>	<i>Origin</i>
1.2-1.3	TMAH	derivatizing agent
3.04	pyrrole	protein
3.31	methyl methoxyacetate	oil
3.63	2-methoxyacetic acid, methyl ester	oil
4.22	N-N-dimethylglycine methyl ester	protein
4.76	styrene	protein
4.84	glycerol, trimethylester	oil
4.59	1,3-dimethoxy-2-propanol	oil
5.11	hexanoic acid, methyl ester	oil
6.09	heptanoic acid, methyl ester	oil
6.20	butanedioic acid, dimethyl ester	oil
6.96	octanoic acid, methyl ester	oil
7.52	3-methoxy-2,2'-bis(methoxymethyl)-1-propanol	oil
7.62	2-chloro-N-methylbenzamine	Hansa yellow
7.75	nonanoic acid, methyl ester	oil
8.65	heptanedioic acid, dimethyl ester	oil
8.68	8-methoxyoctanoic acid, dimethyl ester	oil
9.34	octanedioic acid, dimethyl ester	oil
9.46	dimethyl phthalate	plasticizer?
9.98	nonanedioic acid, dimethyl ester	oil
10.59	decanedioic acid, dimethyl ester	oil
11.01	tetradecanoic acid, methyl ester	oil
11.16	undecanoic acid, methyl ester	oil
12.09	hexadecanoic acid, methyl ester	oil
12.33	siloxane	column
12.76	unidentified, but occurs in reference	shellac
13.06	octadecanoic acid, methyl ester	oil
13.22	derivative of aleuritic acid	shellac
13.37	butylated hydroxytoluene (BHT)	antioxidant?
13.50	tetramethyl derivative of jalaric acid	shellac

Continued on next page.

Table I. (Continued). Major pyrogram peaks, their identification, and associated artists' material source of the TMAH derivatized compound

<i>Retention time (min)</i>	<i>Peak Identity</i>	<i>Origin</i>
13.70	tetramethyl derivative of shellolic acid	shellac
13.97	derivative of aleuritic acid	shellac
14.19	dehydroabiestic acid, methyl ester	pine resin, trace
14.21	derivative of aleuritic acid	shellac
14.34	siloxane	column
14.47	derivative of aleuritic acid	shellac
14.64	7-methoxy-tetrahydroabiestic acid, methyl ester	pine resin, trace
15.18	7-oxo-dehydroabiestic acid, methyl ester	pine resin, trace
15.21	7,15-dimethoxytetrahydroabiestic acid, methyl ester	pine resin, trace

In numerous cross sections the penultimate surface layer was found to show traces of an inhomogeneous orange luminescent coating. This is consistent with the presence of unbleached shellac, which fluoresces a characteristic bright orange under UV excitation (15, 17). These cross sections confirm the FTIR and Py-GC-MS analyses that also indicated shellac along with pine resin. The presence of the coating largely in the penultimate surface layer, rather than the uppermost one, explains the cool fluorescence in the UV-induced visible fluorescence image, Figure 3(a), rather than a warm orange fluorescence typical of unbleached shellac. A topmost surface coating of glue and dirt filters the UV radiation and prevents fluorescence from the largely underlying shellac. The presence of shellac as a picture varnish is unusual (17) aside from a few notable examples (15), although it may have been added here to the uppermost layers to induce hardness to the paint surface that could not easily be achieved in a young oil paint (9) or to enhance the craquelure through shrinkage. This combination of surface layers containing glue, shellac, and pine resin is surprisingly identical to the layering found in another fake, a purported 15th century portrait group acquired in 1923 by the National Gallery in London (18).

Conclusion

A careful investigation of the artistic composition, materials, and construction techniques of one of Trotter's forgeries, namely *Village Scene with Horse and Honn & Company Factory*, has revealed numerous 'red flags' indicating that the work is not a genuine piece of 19th-century folk art. Upon casual observation, the painting appears to have all the hallmarks of a great piece of primitive-style art. This is in fact one of the indicators of its ersatz nature – it has nearly *all* of the most prized physical characteristics of the folk art genre in one painting: a

quaint composition, naïve sense of perspective, female autograph, visible mattress ticking, heavy patina and fine craquelure suggestive of aged paintings, and mold stains commensurate with years of hanging on uninsulated parlor walls. Several curious and in some instances inexplicable clues are evident with merely a close visual examination. Foremost, the use of mattress ticking as a canvas lining fabric is unique in the authors' experience, especially when no obvious canvas defects are visible to suggest relining was warranted. The applied nature of the mold and the uniform, dense surface cracking are also atypical of true primitive style paintings. Finally, the tacking margins reveal an implausible situation where the artist's ground layer and painted composition appear to have been applied after the canvas was relined.

Advanced imaging techniques also reveal several indicators of the painting's speciousness. Again, for a relined canvas, there are no signs in the UV, NIR, or X-ray images of damages, losses, or structural deficits that would explain the lining fabric, which is shown to contain anachronistic optical brighteners. Furthermore, radiography revealed that no heavy metal pigments were used in this work, which is only feasible with a purely modern palette, although amorphous radio-opaque remnants of the original ground layer from a reused "stripped" canvas are detectable. In the event that scientific analysis is possible, a Trotter fake can be definitively identified as a 20th-century product due to the presence of numerous synthetic organic and inorganic pigments that were unavailable in the previous century or by the unconventional artistic technique of interleaving animal glue and paint as seen in fluorescence microscopy of cross sections.

Since leaving prison, Robert Trotter has continued to paint 19th-century style artworks, but this time 'genuine' fakes that are sold legitimately to buyers of contemporary folk art (2, 3). When asked about the convicted forger's new career, Arthur Riordan, one of the art dealers previously fooled by Trotter and owed compensation under the court sentencing, declared, "Good, I hope he makes a million dollars because we get the first \$62,000 (2)." For the remaining thirty-nine unidentified Trotter fakes, compensation to their owners seems unlikely. Still, it is hoped that for the sake of art history and the reputations of gallery owners and collectors that the indicators revealed here might help to unmask others of Trotter's oeuvre. The consistency of the forger's methods is not at present known. However, four additional Trotter fakes confiscated by the FBI are now part of the Yale University Art Gallery's study collection. Future work will hopefully subject these forgeries to the same level of scientific scrutiny in order to establish the reliability of the 'red flags' discovered here in the condition, construction, and materials of *Village Scene*.

Acknowledgments

This work was completed at Buffalo State College and first appeared in a summary version as a presentation at the 2007 Annual Meeting of the American Institute for Conservation (11). The faculty recognizes the exhaustive research of the Trotter trial by graduate student Jennifer DiJoseph from the Class of 2010 and prosecutor Peter Jongbloed, former U.S. District Attorney in Connecticut,

for information regarding the case and ultimately the transfer of the *Village Scene* painting to Buffalo State College. GDS and CER acknowledge the financial support of the Andrew W. Mellon Foundation.

References

1. Jongbloed, P. S. *United States v. Robert Lawrence Trotter; Criminal No. N-89-59 (AHN)*; U.S. Department of Justice: District of Connecticut, 1990.
2. Pennington, S. *Maine Antique Digest*. (March 1990), pp 14-A–17-A.
3. Hewett, D. *Maine Antique Digest*. (December 1997), p 8-A.
4. Grant, M. S. In *Conserve O Gram*, Number 1/9; National Park Service: Washington, DC, 2000, pp 1–3.
5. Grant, M. S. In *Conserve O Gram*, Number 1/10; National Park Service: Washington, DC, 2000, pp 1–4.
6. Mustalish, R. A. In *Traditions and Innovation: Advances in Conservation, Contributions to the Melbourne Congress*; Roy, A., Smith, P., Eds.; IIC: London, 2000, pp 133–136.
7. Kushel, D. A. *Stud. Conserv.* **1985**, *30*, 1–10.
8. Mecklenburg, M.; Lopez, L. F. In *The Care of Painted Surfaces: Materials and Methods for Consolidation and Scientific Methods to Evaluate their Effectiveness*; Il Prato: Padova, Italy, 2006, pp 49–58.
9. Hebborn, E. *The Art Forger's Handbook*; Overlook Press: Woodstock, NY, 1997, pp 148–152.
10. *Pigment Compendium: A Dictionary of Historical Pigments*; Eastaugh, N., Walsh, V., Chaplin, T., Siddall, R., Eds.; Butterworth-Heinemann: Oxford, England, 2004.
11. Hamm, J.; Smith, G. D.; Kushel, D.; DiJoseph, J. *AIC Paintings Specialty Group Postprints* **2008**, *20*, 62–66.
12. Lomax, S. Q.; Learner, T. *J. Am. Inst. Conserv.* **2006**, *45*, 107–125.
13. Colombini, M. P.; Bonaduce, I.; Guatier, G. *Chromatographia* **2003**, *58*, 357–364.
14. van den Berg, K. J.; Pastorova, I.; Spetter, L.; Boon, J. In *ICOM Committee for Conservation, 11th Triennial Meeting, Edinburgh, Scotland*; Bridgland, J., Ed.; James and James: London, 1996; pp 930–937.
15. Sutherland, K. *J. Inst. Conserv.* **2010**, *33*, 129–145.
16. Scalalone, D.; Lazzari, M.; Chiantore, O. *J. Anal. Appl. Pyrolysis* **2003**, *68-69*, 115–136.
17. Eastaugh, N. *The Picture Restorer*; (Spring 2003), pp 11–12.
18. Wieseman, M. E. *A Closer Look: Deceptions and Discoveries*; National Gallery Co.: London, 2010; pp 36–38.

Chapter 2

Scientific Examination and Treatment of a Painting by Gijssbert Gillisz d'Hondecoeter in the Mauritshuis

Lauren Paul Bradley,^{*1} Sabrina Meloni,^{*2} Erich Stuart Uffelman,³ and Jennifer L. Mass⁴

¹J. Paul Getty Museum, 1200 Getty Center Drive, Suite 1000,
Los Angeles, CA 90049-1687

²Royal Picture Gallery Mauritshuis, Mauritshuis, Korte Vijverberg 8,
2513 AB Den Haag, Postbus 536, 2501 CM Den Haag, The Netherlands

³Department of Chemistry, Washington and Lee University,
Lexington, VA 24450

⁴Scientific Research and Analysis Laboratory, Conservation Department,
Winterthur Museum, Winterthur, DE 19735

^{*}E-mail: lpbradley@gmail.com; meloni.s@mauritshuis.nl

Gijssbert Gillisz d'Hondecoeter's (1604-1653) panel painting, *Cock and Hens in a Landscape*, recently underwent complete treatment and technical examination at The Royal Picture Gallery Mauritshuis, The Hague (inv. no. 405). The interdisciplinary application of art historical research, conservation methodology, and scientific investigation led to several discoveries about the painting, including the revelation that major compositional elements of iconographical significance had been overpainted at some point in its history. Technical examination suggested that the original paint was in sufficiently good condition for the overpaint to be removed. The painting is currently on permanent display at the Prince William V Gallery in a state closer to the painter's original artistic intent.

Introduction

One of the themes of this book is to illustrate the cooperative efforts between scientific, academic, and museum communities in gaining new knowledge about cultural heritage material and using it to educate both the general public and students at the undergraduate and graduate levels. This chapter arose from a triangle of interactions between the Winterthur/University of Delaware Program in Art Conservation (WUDPAC), The Royal Picture Gallery Mauritshuis, and Washington and Lee University (W&L)—a partnership that has now been in place for over six years. During Lauren Bradley's final year of study in the WUDPAC program, as the American Friends of the Mauritshuis Intern in Conservation, she undertook the treatment and technical study of Gijsbert Gillisz d'Hondecoeter's *Cock and Hens in a Landscape* (collection ID MH405) under the direction of Mauritshuis Paintings Conservators Petria Noble and Sabrina Meloni (1, 2). Erich Uffelman, from W&L, assisted with the pXRF analysis performed on the painting and Jennifer Mass from the Winterthur Museum and WUDPAC carried out the SEM-EDS analysis. Both Uffelman and Mass participated in the writing of this chapter. The Mauritshuis has one of the world's greatest collections of paintings from the Dutch Golden Age; WUDPAC has one of the world's leading graduate programs in art conservation; and W&L has pioneering courses in using study abroad to educate science and non-science undergraduate students about the technical examination of 17th-century Dutch paintings (3, 4). This monograph is thus intended not only as a contribution to the art conservation literature, but also to be useful in various undergraduate courses on Chemistry in Art (5), as well as in the NSF Chemistry in Art Workshops (6). [Please also see chapters by Lang; Gaquere-Parker and Parker; and Hill in this volume.]

Thus, we will briefly discuss the methodology behind the treatment and examination of Hondecoeter's *Cock and Hens in a Landscape*, how the Hondecoeter family fits into the established history of 17th-century Dutch painting, the picture's art historical context, the technical research findings, and the conservation treatment. This approach emphasizes the interdisciplinary linking of relevant cultural, socioeconomic, and historical information that undergirds the competent analysis and treatment of a painting.

Methodology

Prior to embarking on a conservation treatment project, the painting or art object is thoroughly examined and documented, adhering to the guidelines and standards of ethical practice established by the field (7). Because Hondecoeter's *Cock and Hens in a Landscape* had a complex surface that raised questions about the condition and the restoration history with implications for treatment, a variety of analytical techniques were used to study the painting on both a macroscopic and a microscopic level, including magnification under a binocular microscope, ultraviolet-induced visible fluorescence imaging (UV), infrared photography (IR), X-radiography, handheld portable X-ray fluorescence spectroscopy (pXRF), cross-sectional microscopy with UV and visible illumination, polarized light microscopy (PLM), Fourier transform infrared spectroscopy (FTIR), scanning

electron microscopy with energy dispersive X-ray spectroscopy (SEM-EDS), and SEM in the backscattered electron mode (SEM-BSE). A very well-illustrated text that cogently summarizes these conservation science techniques has recently appeared (8).

To supplement the technical data, a number of related works by Hondecoeter and his contemporaries were examined in other collections including the Rijksmuseum in Amsterdam, the Museum Boijmans van Beuningen in Rotterdam, and the Philadelphia Museum of Art in Pennsylvania, USA, in addition to several pictures at Pieter de Boer's Gallery in Amsterdam. These paintings provided insight into Hondecoeter's painting practices in addition to establishing a visual reference for how a Hondecoeter panel in good condition should appear today.

Examination generally begins by studying a painting using non-destructive imaging techniques such as magnification under visible light, UV, IR, and X-radiography. Magnification is an invaluable tool for the conservator; a trained eye can draw sophisticated conclusions about a painting's condition and the artist's working practice using magnification alone. UV irradiation provides additional information about the surface and is often used for identifying areas of restoration/overpaint as newer materials typically fluoresce differently than the aged, original material. For example, aged natural resin varnishes will fluoresce green under UV irradiation, while synthetic polymer-based materials such as acrylic paint (often used in conservation) will appear dark. Fluorescence colors can also aid in assigning preliminary pigment identifications. IR can be a useful technique for studying aspects of the picture hidden from view beneath layers of paint such as an artist's preparatory sketch or *pentimenti* (changes to the composition). If there is enough contrast between, for example, the lines in the artist's sketch and the surrounding ground, and if the proper wavelengths are selected, the intervening paint layers can become IR transparent. The IR radiation penetrates through to the ground layer and is reflected back through the paint layers to the detector, making it possible to image the hidden lines. If the ground layer is dark in color, less IR radiation is reflected, which decreases the ability to distinguish underdrawings from the surrounding ground (9, 10). The success of X-radiography in imaging a painting is based on differences in radio opacity of different artists' materials. The technique is useful for visualizing structural components such as panel or canvas joins, and the painting technique, especially when pigments containing heavy metals such as lead white ($2\text{PbCO}_3\cdot\text{Pb}(\text{OH})_2$) or vermilion (HgS) are present (11).

Scientific instrumentation can be used to address questions that are not possible to answer using imaging techniques alone. For example, pXRF provides information about the elemental composition of a painting's surface, which can be used to infer which pigments may be present. X-ray radiation has sufficient energy to penetrate the entire painting structure, meaning the spectra will typically contain information about numerous paint layers including the ground layer. When coupled with the use of a vacuum pump, pXRF can identify elements with atomic numbers of 13 (Al) or greater. It is an excellent technique for analyzing works of art because it is non-invasive and non-destructive and the data collection is relatively fast; it is often possible to get discriminatory data in two minutes or less. Limitations include the inability to target a specific

layer in the painting structure and insensitivity to elements with a lower atomic number for air path analysis. Overlapping X-ray lines and the presence of elements that could be associated with multiple compounds may also complicate qualitative interpretation of the spectra. pXRF can be a powerful tool for pigment characterization, especially when used in combination with other elemental analysis techniques or with imaging and molecular analysis methods such as cross-sectional microscopy, polarized light microscopy, SEM analysis, and FTIR. Excellent introductory discussions of the strengths and limitations of pXRF spectroscopy have recently appeared (12, 13), and a book on the applications of handheld pXRF in art and archaeology is in press (14).

Techniques which require sampling may be used when further questions arise about a pigment or a specific layer in the painting structure. Samples are typically taken under magnification from an area of the painting with pre-existing damage or at the painting's edge, where the surface is hidden from view by the frame rabbet (15). Depending on the sample size required for analysis, a tungsten needle (16) or a scalpel can be used to take the sample, which may range from a few microns in diameter to the size of a period at the end of a 12-pt font sentence.

Cross-sectional microscopy involves polishing a sample embedded in resin to reveal the sample's edge, providing a cross-sectional view of the layer structure. The polished sample can be examined under magnification using light microscopy and/or scanning electron microscopy. Cross-section samples provide information about the stratigraphy of paint and varnish layers; illumination under the microscope using a UV irradiation source coupled with different wavelength filter cubes can help clarify the boundaries between layers or the presence of varnish and glaze layers. SEM-EDS can be used to identify the elemental composition of a single pigment particle within a cross-section sample, to identify the presence of pigment alteration/degradation products, or to create elemental X-ray maps of the entire sample, providing detailed information about the distribution of elements throughout the layering structure. This technique complements pXRF data in that it allows for the detection of elements as light as boron ($Z = 5$) because it is performed under high vacuum. SEM-BSE produces grayscale images based on the local average of the atomic numbers present and is invaluable for studying the particle morphology of paint pigments and fillers (17).

FTIR is a powerful technique for characterizing general classes of organic materials such as oils, polysaccharides, proteins, resins, and waxes, as well as for identifying synthetic resins, inorganic pigments (particularly polyoxoanions), and natural minerals. In the transmission mode, the technique involves taking a microgram-sized sample, flattening the sample on a diamond half cell using a steel micro-roller, and measuring the IR absorption across the spectral range of 4000 to 650 cm^{-1} (18, 19).

Hondecoeter Family

Gijsbert Gillisz d'Hondecoeter (1604-1653) came from a family of artists; his grandfather (Nicolaes Jansz), his father (Gillis Claesz), his brother (Nicolaes II), and his son (Melchior) (20) were all painters (21, 22). The tradition of passing

craft-based knowledge down from generation to generation was widespread in the 17th century, when painters learned through the apprentice system regulated by the St. Luke's Guild. Many young painters trained under a family member or a familial connection made through marriage; others held apprenticeships with a master for a fee.

Relatively little has been written about Gijsbert Hondecoeter or the Hondecoeter family. Gijsbert trained under his father, Gillis Claesz, who predominantly painted landscapes populated by animals. Gijsbert was primarily active in Utrecht, registering with the city's St. Luke's Guild in 1626 (23). His pictures, which primarily depict live game birds and poultry, are fairly static with little drama or interaction between the birds.

Gijsbert trained his son, Melchior, until his death in 1653. According to Arnold Houbraken, an 18th-century biographer of 17th-century Dutch artists, Melchior continued painting under his uncle, Jan Baptist Weenix, who was married to his father's sister, Justina. It is likely that Melchior worked alongside his cousin, Jan Weenix, in his uncle's studio (22). Melchior remains the best-known member of the Hondecoeter family and is perhaps the greatest exponent of the poultry-yard genre. His paintings are characterized by lively compositions, accuracy of anatomical description, and expressive use of color.

In comparison to the rest of 17th-century Europe, the Dutch art market was unique. Following the Protestant Reformation in the 16th century, there was a sharp decline in ecclesiastical art patronage throughout the Northern Netherlands. Because Calvinist theology prohibited the use of images for worship, few Dutch painters depicted Biblical or devotional scenes (24, 25). Furthermore, there was little court patronage as the Dutch aristocracy was relatively small and the government was dominated by a regent class.

Dutch business and trade were highly prosperous, leading to the formation of what might be considered the first modern economy and to the formation of a substantial middle and upper class in addition to a wealthy elite (26–30). A new and thriving art market emerged to satisfy the demand for pictures created by the affluent members of the Reformed Protestant Dutch Republic. Dutch artists produced millions of paintings during the 17th century. Although some of these pictures were commissioned works, a substantial majority was prepared for the open market, which was typically regulated at the local level by the St. Luke's Guild of each city or town.

Rembrandt van Rijn, arguably the best known painter from the Dutch Golden Age (31), was unusual in that his pictures could not be grouped within a single category—he painted religious and historical paintings in addition to portraits, landscapes, still-lives, and genre scenes. An overwhelming majority of Dutch painters specialized in a particular category or sub-category of painting in order to produce paintings more efficiently and to minimize their competition. Thus, an artist might not only specialize in still-life painting, but further specialize in breakfast still-lives, “ontbijtes,” or luxury still-lives, “Pronkstilleven” (32, 33). Patrons of pictures depicting domesticated and wild birds were likely rich burghers who kept exotic and native fowl on their country estates. Occasionally, poultry breeders would commission artists to paint prize birds and common farmyard specimens rather than purchasing already completed works (34).

The Painting

Hondecoeter's *Cock and Hens in a Landscape* (Figure 1) has a complex surface that was not fully understood until after treatment began. The picture depicts a large yellow cock and two hens in an outdoor setting. The cock sits on an overturned woven basket at the center of the composition while a brown hen balances on the rim of another basket at left and a black hen rests at right. An atmospheric landscape recedes into the distance at right, behind a potted plant and a terracotta vessel. Prior to treatment, the lower right corner also contained a leafy green plant, which was determined to be a much later addition, as the plant covered small losses and cracks in the original paint layer (revealed by examination with the binocular microscope). The decision was made to remove the non-original plant during cleaning, which revealed a previously unknown animal skull, a bone, and a black and white rabbit (Figures 2 and 3). Black and white rabbits are a fairly common motif within Hondecoeter's *oeuvre*, however, the depiction of a skull and bone seems to be unique to the Mauritshuis painting. The plant was most likely added to hide the fact that the rabbit's body was truncated when the panel was cut down, and perhaps also because skulls, as *memento mori*, or reminders of death, had lost their appeal to later audiences. Vanitas symbols featured frequently in 17th-century Dutch painting, reflecting the conservative Calvinist religious views of the time (21, 24). The plant was added before the painting entered the Mauritshuis collection in 1876, as the rabbit and skull are not visible in early photographs, nor are they referenced in early descriptions. The painting has a gray-blue sky, which was repainted at some point to be brighter in color.

Hondecoeter repeated motifs and compositional arrangements throughout his career. This practice lent itself to greater productivity, as less time was spent innovating during the planning stages. The large woven basket, the yellow cock with a spotted breast, the downward facing hen, the black and white rabbit, and ribbon-like strands of grass all appear in other works by Hondecoeter, suggesting the Mauritshuis painting may have been created for the open market rather than for a specific commission. The brushwork used to render these forms is similar to representations found in pictures examined at Pieter de Boer's gallery, suggesting Hondecoeter was well practiced at their depiction.

The Mauritshuis composition, with a landscape receding in the distance and several large birds in the foreground, is almost identical to works attributed to Hondecoeter's Dordrecht-based contemporary, Aelbert Cuyp (1620–1691). A 1935 Mauritshuis catalogue links the two artists, referencing a painting by Cuyp sold at auction, which had a similar composition and a boat in the background (35, 36). Unfortunately, no further information is provided, leaving many unanswered questions about the picture's provenance, its attribution, and its whereabouts today. A reproduction of a painting that matches this description was found in the photographic archives at the Netherlands Institute for Art History in The Hague (RKD); further research would be needed, however, to draw any conclusions.



Figure 1. Gijsbert Gillisz d'Hondecoeter (1604-1653), *Cock and Hens in a Landscape*, no date. Oil on panel, 52 x 70 cm. Royal Picture Gallery Mauritshuis. Inv. no. 405. Before treatment (2010). Courtesy of The Royal Picture Gallery Mauritshuis. (see color insert)

It is possible that Cuyp was influenced by Hondecoeter's work or that both artists were working from a similar model in a workshop book. [Two useful introductions to Dutch workshops have been published (37, 38).] Archival research carried out at the RKD indicated that historically, there has been confusion over the attribution of poultry-yard scenes by Hondecoeter and by Cuyp. Another picture attributed to Hondecoeter at the Mauritshuis was previously attributed to Cuyp and has a false Cuyp signature, added sometime before the painting entered the collection in 1899.

Examining works by Hondecoeter in other collections provided insight into how he typically painted the sky and how he positioned his birds in relation to the edges of the composition. Studying these features was significant because the Mauritshuis panel has been cut down and the original sky was repainted. Hondecoeter's *Waterfowl* (A 1332), dated 1652, at the Rijksmuseum Amsterdam, served as a reference for how a Hondecoeter panel in good condition should look today. The upper half of the painting is dominated by a gray-blue sky with several small clouds; dark, horizontal striations resulting from the formation of lead soaps in an underlayer are visible throughout the sky. [Lead soaps are discussed in more detail in the Condition Section.]

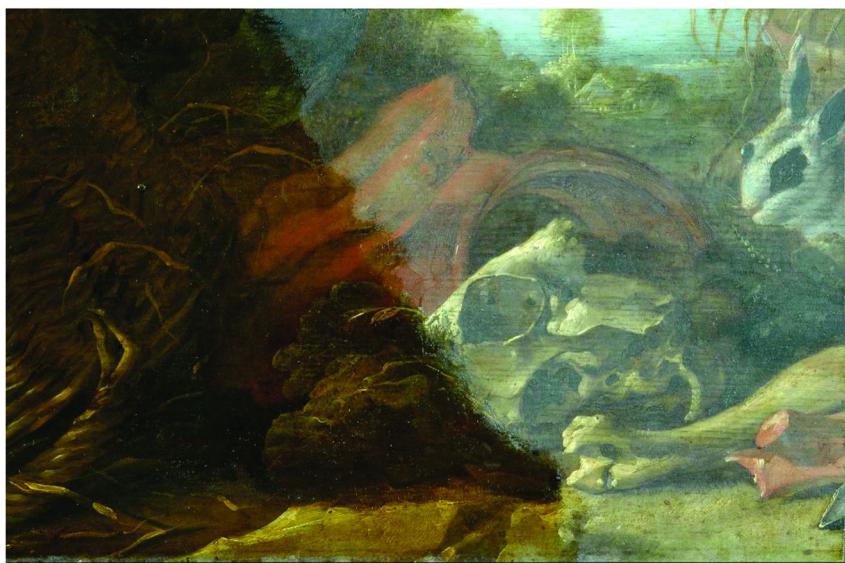


Figure 2. Detail, lower right corner during cleaning. The varnish and overpaint are intact at left and have been removed at right. (see color insert)



Figure 3. *Cock and Hens in a Landscape*. Royal Picture Gallery Mauritshuis. After treatment (2011). (see color insert)

Construction

The painting was executed on an oak wood panel comprised of two glue-joined horizontal planks with a radial grain direction (Figure 4). The panel verso has no evidence of original beveling, which would have facilitated fitting the painting into a frame (39). Shallow grooves, approximately 1 cm in length run perpendicular to the panel edge at the top and bottom of the right side as seen from the reverse (Figure 5). These grooves appear to be part of the original construction and may have served an analogous function to beveling. Similar marks have been found on Rembrandt van Rijn's *Supper at Emmaus* from the Musée du Louvre (INV#1739). On Rembrandt's painting, which has been thinned and cradled, the verso has been described as having traces of "shallow gouged grooves as was sometimes done instead of beveling" (40).



Figure 4. Panel verso showing the outline of the secondary support that was once attached; the joint runs horizontally through the center of the panel.

In preparation for painting, a thin layer of chalk (likely glue-bound CaCO_3) was applied to the surface, filling the open pores and interstices of the wood grain. This practice not only provided the artist with a smoother surface on which to paint, but also reduced costs, as chalk was a less expensive material than pigment bound in drying oil.



Figure 5. Detail, shallow grooves in upper right corner of the panel verso.
Raking light from above.

The chalk layer was followed by a gray *imprimatura* underlayer. The *imprimatura* creates a uniformly colored surface for painting in addition to setting the overall tonality of the picture; i.e., despite often being concealed under several layers of paint, the *imprimatura* affects the overall appearance of the painting (41). Dark *imprimatura* layers often remain visible on the surface, functioning as the midtone or the shadow (42). This was recently observed, for instance in a Teniers/Brueghel study (43).

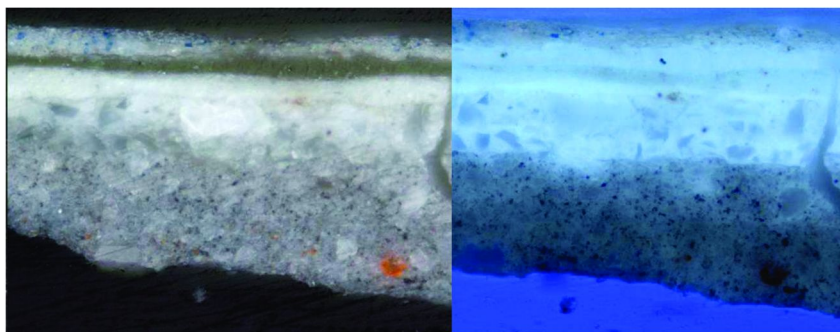


Figure 6. Cross-section sample (405 x01) taken from the overpainted sky, 400x magnification; reflected light at left, ultraviolet irradiation at right. (see color insert)

Cross-sectional microscopy coupled with SEM-EDS analysis indicates the *imprimatura* layer contains a mixture of lead white, an organic black pigment, and a calcium-based filler material. Red particles are visible near the bottom of the *imprimatura* layer under 400x magnification in reflected light (Figure 6). These particles were identified as Pb_3O_4 using SEM-EDS and may be a byproduct of lead soap formation rather than an intentional additive to the paint. Because the *imprimatura* has a lead white matrix, the brushstrokes used to apply the layer are visible in the X-radiograph. The strokes are broad and intersect in large crisscross patterns.

Examination with IR (Artist multispectral imaging camera, IR2 mode, with a long wave pass filter 1000 nm) revealed evidence of underdrawing lines in the cock that are not visible under normal lighting conditions. The lines have a slightly broken quality, suggesting they were created using a dry medium such as black chalk or charcoal rather than with a wet medium and a brush. Brush-applied drawings have a more fluid, unbroken line quality. A distinct underdrawing line runs along the back of the cock's head, along the upper edge of his comb, and around his wattle. The location of the preparatory marks visible suggests Hondecoeter used underdrawing to plot the location of the primary compositional forms, but did not go so far as to create shadow or any indication of texture.

The paint application technique used to create the picture was studied using a binocular microscope (10x – 50x magnification) and cross-sectional microscopy (40x – 400x magnification). Examination indicated the composition was worked up by painting the largest forms first, namely the birds and the central basket. The landscape was filled in around the birds, working from the background to the foreground. There are no major *pentimenti* or changes to the composition, further confirming the placement of the figures and forms had already been established when painting began.

The blue sky was applied at the beginning of the painting process, directly on top of the gray *imprimatura*, without leaving reserves for the birds or the landscape. Leaving an area in reserve is an artistic technique in which other parts of the composition are painted around an area, which the artist will later fill (42). This approach minimizes the amount of paint used and reduces the likelihood that an underlying form will become visible over time as the upper paint layers become increasingly transparent. As paints age and oxidize, the refractive index of the binding medium increases, becoming closer to that of the pigments, which causes the paint layer to become more translucent; lead soap formation also increases translucency. The paint used to render the sky was found to contain a mixture of lead white and smalt (a cobalt blue glass). [*vide infra*]

The large, woven basket and the birds were worked from dark to light with the highlights added last. Details such as the black markings on the brown hen, the spots on the cock's breast, the eyes, the beaks, and the claws were also added towards the end of the painting process. Dry brushstrokes were used around the edges of the birds to soften the edges of their forms and to make them sit more convincingly in space.

The painting has a relatively smooth surface with little impasto texture. The paint used to create the landscape along the horizon line and the shadowed side of

the basket in the center is thin and medium-rich. Washy brushstrokes are visible on the shadowed side of the large basket.

Hondecoeter used glazes in certain areas to achieve a richer surface appearance. Glazing involves the use of a thin, transparent paint to modulate or enrich the colors in the underlying paint layer. This technique is apparent in the black hen's comb and in the landscape. On the hen's comb, the glaze is visible under magnification as a fractured, translucent red layer on top of a more opaque red paint. The glaze has a bright pink fluorescence in UV, which is characteristic of an organic red pigment such as red lake. pXRF analysis suggested the opaque red paint contains vermilion (HgS).

In the landscape, there is a non-fluorescent, translucent brown layer pooled within the interstices of the underlying paint texture. This layer likely represents the combination of an original copper-containing glaze that has discolored over time and the remains of an old, discolored varnish. The presence of copper was confirmed using pXRF. [A more extensive discussion of pXRF and paintings analysis may be found in the following chapter (44).]

Condition and Previous Treatment History

Prior to treatment, the painting's condition made it unsuitable for display. There were multiple layers of thick, discolored varnish on the surface, which distorted the tonal relationships and made it difficult to interpret the darker passages (45, 46). The varnish had an uneven surface gloss with the darker passages becoming matte and crazed (micro-cracking).

The Mauritshuis records describe several restorations dating back to 1916, when Mauritshuis restorer Derex de Wild performed the first documented treatment. De Wild reduced a thick layer of varnish on the painting "by half" using a mechanical technique (47); this may have entailed rubbing the surface of the degraded, brittle varnish until it flaked and turned into a powder. The thinned varnish was regenerated several times and a new varnish was applied. Regeneration frequently involved the use of alcohol vapors and copaiba balsam. De Wild's report describes leaving the overpainted sky intact.

Mauritshuis restorer J. C. Traas treated the painting again in 1937 (48). Traas performed structural work on the panel in addition to removing discolored varnish and overpaint from the surface. He repaired the joint between the two planks and although it is not explicitly referenced in the report, he probably also inserted the butterfly cleat spanning the joint on the verso. Traas applied a new varnish and retouched the painting.

In early 2010, the painting was surface cleaned using a 1% solution of tri-ammonium citrate in demineralized water. A saturating layer of 10% Regalrez 1094 varnish in Terpentina D was applied on top of the old varnish using cotton wool wrapped in silk. This was done in an attempt to resaturate the matte areas and make the painting aesthetically acceptable for display. This minimal treatment was unsuccessful and did not achieve adequate saturation (49–53). Further testing with Laropal A81 varnish and different concentrations of Regalrez 1094 varnish

also proved unsuccessful. At this point, it was decided that the painting would benefit from a complete treatment involving varnish removal.

During the present examination and treatment campaign, it became clear that much of the painting's treatment history went undocumented and likely occurred before the picture entered the collection in 1876. A variety of analytical techniques were used to investigate the history and to identify passages of disfiguring repaint that should be removed.

Perhaps the most drastic interventions to the work were those made to the original format (the size of the support). The painting currently measures 52 x 70 cm, although the original dimensions are unknown. At some point, the panel was cut down on the right side, slightly trimmed along the upper edge, and sanded along the joint (39, 54). In the past, paintings were frequently altered to suit the needs of the collector; the picture may have been cut down to fit a frame or to serve as a pendant painting to a smaller piece.

The major alterations at the right and top edges occurred before 1876, when the painting's present dimensions first appear in a Mauritshuis inventory book recording new acquisitions to the collection (55). The sanding along the joint may have occurred as late as 1937 when Traas describes putting the joint between the two planks together; sanding was commonly done to achieve a better glue bond (48). The cock's feathers are slightly discontinuous across the joint, indicating some of the image material was removed when the joint was repaired.



Figure 7. Diagram speculating how much of the original panel is missing at the top and left edges.

The back of the panel has a ghost image outlining where a non-original secondary support structure was once attached (Figure 4). The outline is truncated at left, indicating it was in place and removed before the panel was cut down. Based on the approximate symmetry of the secondary support's vertical members to one another, it is possible that 21 cm are missing at the left (Figure 7). This calculation is based on the average distance between the vertical members, the average width of each individual member, and the distance between the member at the far right to the edge of the panel. The lower plank is approximately 5 cm wider than the upper plank, which may suggest as much as 5 cm are missing from the top. It was, however, not uncommon for panel planks in the 17th century to be asymmetrical in width. These approximations suggest the original dimensions were in the range of 52–57 cm in height and 91 cm in width, which is consistent with established height to width ratios of 17th-century marine-format panels (56). In the 17th century, artists could purchase supports according to standardized sizes intended for different subjects including marine scenes, landscapes, and portraits (57). It is significant to note that related poultry-yard scenes attributed to Cuyp, which are reproduced in the RKD archives, also appear to have a marine format.

Prior to treatment, the painting had several layers of discolored yellow varnish on the surface. In addition, Traas had intentionally tinted the uppermost varnish layer using small black pigment particles when he applied it in 1937. Historically, tinting a new varnish was done to imitate the appearance of an aged yellow varnish, which was a valued aesthetic component of old master paintings in the early part of the 20th century—almost all of the paintings Traas treated at the Mauritshuis have a tinted varnish (58). This practice is no longer in use as it does not do justice to the artist's original intention.

During cleaning, after the varnish layers were removed, it became apparent that the original sky had been repainted using a bright blue paint, and several clouds were added at the center of the picture, above the birds. The overpaint had a fractured appearance under magnification along the top and right edges, indicating it was applied sometime before the panel was cut down. A second overpaint campaign, carried out using a slightly darker blue, was present along the joint (Figure 3). The overpaint was analyzed using a variety of noninvasive and microsampling techniques including pXRF, PLM, cross-sectional microscopy, FTIR, and SEM-EDS, in an attempt to date its application and to better understand how it might be removed. Only the earlier, broadly applied overpaint will be discussed here.

Analysis performed using FTIR indicated that the bright blue overpaint applied across the entire sky contained a mixture of lead white ($2\text{PbCO}_3\cdot\text{Pb}(\text{OH})_2$) and Prussian blue (ferric ferrocyanide, $\text{Fe}_4[\text{Fe}(\text{CN})_6]_3$) bound in linseed oil. Prussian blue was synthesized in 1704 and first used as an artist's material shortly thereafter (59–61), meaning the overpaint must have been applied sometime between that date and 1876, when the painting's present dimensions first appear in print. FTIR can be used as a diagnostic indicator for Prussian blue because the pigment contains ferric ferrocyanide components that have a strong carbon nitrogen triple bond absorbance at 2083 cm^{-1} , a region of the IR spectrum in which very few other artists' materials are active.

The Prussian blue particles are barely perceptible in cross-section under 400x magnification, causing the layer of overpaint to appear white. This phenomenon can be attributed to the pigment's incredibly fine particle size and its high tinting strength. Only a small quantity of this high tinting strength pigment is required to tint lead white paint blue (59). Prussian blue particles are approximately 0.01 to 0.02 μm in diameter and are best visualized using PLM, which involves dissolving the binding media, separating the pigments from the paint matrix, and examining them using transmitted light (59). These properties make it difficult to detect Prussian blue on a painting using pXRF alone, since iron is also a major component of surface dirt and earth pigments.

Cross-sectional microscopy performed on several samples taken from the sky confirmed the presence of an uneven varnish residue between the overpaint and the original paint. This information had implications for the treatment, as oil-based overpaint can be difficult to remove from an oil painting due to similarities in solubility. Furthermore, lead-based oil paints have siccative properties—the lead ions act as driers, promoting oxidation within the film and the formation of cross-links, resulting in a tough paint layer. Having a varnish underneath the overpaint is beneficial during cleaning because the varnish can be used as a sacrificial layer; cleaning solvents and gel formulations can be tailored to target the varnish rather than the overpaint, allowing the overpaint to be removed without resorting to harsh cleaning solutions.

Hondecoeter's original sky obscured by the overpaint was found to contain a mixture of lead white and smalt using cross-sectional microscopy and pXRF. Smalt is a pigment created by grinding potassium glass colored with blue cobalt oxide into a workable powder (K, Al, Co silicate); coarse grinds result in a bluer pigment, while finer grinds result in a grayer one (62, 63). Loose smalt particles have a characteristic conchoidal fracture pattern visible under high magnification. When embedded in a paint matrix and viewed in cross-section, the pigment often has a triangular shape as was observed in the Hondecoeter sample (Figure 6). In the 17th century, smalt was produced and sold in quality grades ranging from gray to blue. Compared to the costly pigment ultramarine blue, which was often reserved for commissioned paintings or passages of the painting with iconographical significance, smalt was a fairly inexpensive alternative (63).

Characteristic peaks for cobalt and silicon (observed as a shoulder on the lead peak)—two principal elemental components of smalt—are present in pXRF spectra collected throughout the sky, corroborating the visual evidence of smalt observed in cross-section (Figure 8). Strong peaks for lead can be attributed to the presence of lead white in the overpaint, in the original sky, and in the *imprimatura* layer.

Many varieties of blue smalt are inherently prone to discoloration over time (likely due to the pigment's potash to silica ratio) (64–66), while some varieties are more stable and have retained their blue color over hundreds of years. Determining whether Hondecoeter's original sky was in good condition played a major role in the decision whether or not to reveal it through cleaning. If the original sky was in a badly deteriorated state, the overpaint might have been left intact because there would not have been a significant visual gain through removing it. Cleaning tests confirmed the original paint surface had minimal evidence of abrasion. The

small particles appeared blue in cross-section and on the surface in areas where the overpaint was abraded. X-ray maps created using SEM-EDS (17) did not reveal any evidence of chemical degradation (migration of potassium ions outside of the small particles), further indicating that the small particles were in good condition (Figure 9). The maps show the potassium is still closely associated with the particle's silica core. [Small degradation is discussed at greater length in the following chapter of this book (44).]

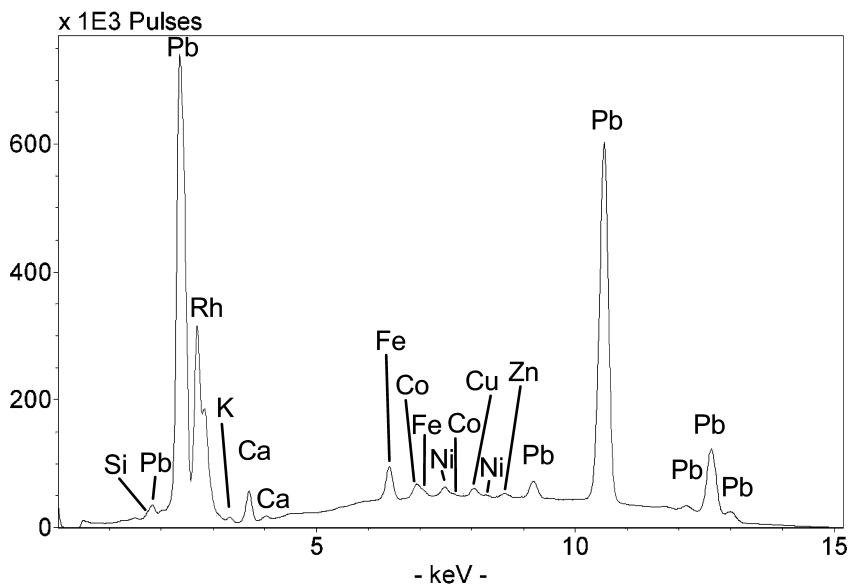


Figure 8. pXRF spectrum collected from an area of overpainted sky with characteristic peaks for smalt (Co, Si) [Bruker Tracer III-SD Rh X-ray tube at 15 kV and 55 μ amps, 20 Torr, 1080 s].

Examination under the binocular microscope confirmed the plant in the lower right corner was a later addition. The overpaint used to render the plant had a coarse, pebbly texture with large white particles visible at the surface; this contrasted with the smoother surface of the finely ground original paint. The overpaint extended across age cracks in the underlying original paint and went over the right edge of the panel, where the painting had been cut down. Cleaning tests indicated the overpaint was readily soluble in the same solvents used to remove the varnish layers (*vide infra*).

Lead soaps are forming preferentially along the wood grain in the gray *imprimatura* underlayer, resulting in the appearance of short, dark horizontal lines throughout the sky (67) (Figure 10). In other areas, lead soap aggregates have become mobile and migrated through adjacent layers, causing a deformation or rupture at the surface.

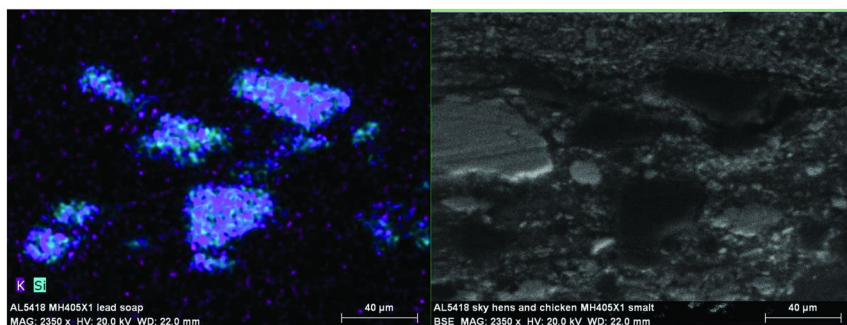


Figure 9. Left: SEM-EDS X-ray map of potassium (purple) and silicon (blue) within cross-section sample 405 x01 -- illustrating the absence of smalt degradation (no migration of K^+ away from the Si core). Right: Same sample, back scatter electron image showing the smalt particles (darker gray/black) within the cross-section (uncoated sample analyzed using variable pressure mode). (see color insert)

Lead soaps have been studied extensively in the previous decade because they occur almost ubiquitously in old master oil paintings (68–70). They likely result from the slow base-induced ester saponification of paint layers containing lead white (or other lead-containing pigments or driers). [Oil paints containing zinc and copper pigments or driers, or smalt, are also prone to metal soap formation.] Oil paint contains fatty acid triglycerides and lead white pigment is a basic lead carbonate ($2PbCO_3 \cdot Pb(OH)_2$). Over time, the basic lead white cleaves the ester linkages formed between the triglycerides to produce glycerol and lead carboxylates, commonly referred to as “lead soaps”. In some cases, these lead soaps aggregate and form globules in the paint layer that can grow large enough in size to push through the surface of the paint layers, appearing as raised white bumps on the painting’s surface (this has not happened in this painting).

That lead soaps can form preferentially along the wood grain is because the chalk ground in the interstices of the wood acts as a reservoir of free fatty acids that reacts with the lead white in the overlying lead-white containing *imprimatura*. This phenomenon has been studied in detail in several other paintings in the Mauritshuis (67). Due to saponification involving the lead white particles, the paint loses its opacity in these areas and becomes more transparent, appearing darker. This is occurring throughout the picture but is most noticeable in areas where the image paint on top of the *imprimatura* is abraded or has also become transparent—most notably in the sky and the yellow cock’s body.

The lead soaps are visible in cross-section as translucent areas. X-ray maps created using SEM-EDS show a lower concentration of elemental lead in these areas, which can be attributed to a dissolution of the lead white pigment particles during lead soap formation. This phenomenon is also apparent in images created using SEM-BSE; the lead soap aggregates appear darker than the surrounding lead white paint matrix (Figure 11). Detecting differences in average atomic number is possible because the SEM-BSE intensity (the number of beam electrons elastically

scattered back towards the electron beam) is related to the atomic number of the atoms in the interaction volume of the electron beam (17).



Figure 10. Detail, before treatment, showing disturbing dark lines visible in the sky resulting from lead soap formation in the underlying imprimatura layer that correspond to the ground-filled wood grain.

Lead soap aggregates are larger in size than lead white pigment particles; accordingly, the formation of lead soaps in the *imprimatura* layer (corresponding to the chalk ground-filled interstices of the wood grain) has led to an increase in volume. The surface paint in these areas has plastically deformed as the result of this increase, whereas in other areas the paint has fractured and cracked. The expanded paint has created prominent ridges across the surface of the entire painting (71). This texture became especially apparent after the thick layers of varnish and overpaint were removed (Figure 12).

Treatment

Treating the painting (54) was a complex endeavor due to the presence of multiple varnish and overpaint campaigns with varying solubilities. The extent of non-original material present was not fully understood until after cleaning began, as the thick discolored varnish layers made it difficult to interpret the underlying paint layers. The aged varnish had a strong fluorescence under UV illumination that masked the differences in fluorescence between the original and non-original material. More than half a dozen solvent mixtures and gel formulations were used during cleaning (72–77).

Small cleaning tests were performed at the edges of the painting to establish which solvents or gel formulations could remove the varnish and later repaint without harming the underlying original paint. Testing continued throughout the treatment as new passages of overpaint became apparent. Frequent discussion among the Mauritshuis conservators and curators guided the decisions to proceed with each step of the cleaning process.



Figure 11. 1150 \times magnification. SEM-BSE image (uncoated sample analyzed using variable pressure mode) of a lead soap aggregate in the imprimatura layer; the aggregate is the large dark oval-shaped area at the center of the image (Sample 405 x01).

Cleaning proceeded cautiously by removing one layer of non-original material at a time. The uppermost layers of discolored varnish were removed first using free solvent mixtures of isopropanol, isooctane, and acetone; these mixtures are consistent with what one would expect to use for dissolving an aged natural resin.

During cleaning, it became apparent that the painting was selectively cleaned in the past; an even older natural resin varnish was present in the dark passages on the lower half of the painting beneath the upper, pigmented varnish. Darker colors are more vulnerable during cleaning due to a higher proportion of medium to pigment in the paint and a lack of good metal ions to promote extensive oxidation and cross-linking within the paint film as it dries (78). Furthermore, dark passages are often less satisfying to clean because the resulting visual change is not as great as it is with lighter passages. It is not uncommon to find partially removed coatings on paintings that have been cleaned in the past; this phenomenon is often referred

to as “port-hole cleaning” or “dealer cleaning”. Because this underlying varnish was older and more oxidized, it required a slightly more polar solvent mixture to remove. Varnish oxidation is an autoxidation process in which the terpenoids of the resin undergo various reactions with atmospheric molecular oxygen (45, 46).



Figure 12. Detail after cleaning and varnish removal, lower right corner. Raking light from the top showing the raised horizontal ridges created by lead soap formation in the imprimatura layer.

The restorer-applied plant in the lower right corner was removed because it covered a significant portion of the original composition and cleaning tests indicated the underlying original paint was in good condition. The overpaint was soluble in the same free solvent mixtures used to remove the varnish. In order to minimize mechanical action (movement of the cotton swab) on the surface, isopropanol gelled with 5% Klucel-G by weight was used to remove the plant. Klucel-G is a hydroxypropylcellulose that is soluble in water and alcohols. It was selected as a gelling agent because it was assumed to have no independent cleaning properties and could be used to increase the viscosity of the isopropanol solvent and decrease the evaporation rate, thus minimizing the amount of solvent introduced to the surface. Based on the solubility properties of the plant, the paint was likely a drained oil mixed with a natural resin varnish; this combination of materials was a fairly common restoration technique in the past. Absorbing or “draining” the excess oil binding medium from an oil paint before it is used results in a “leaner” paint that remains more soluble than full-bodied oils over time.

The blue repaint in the sky flattened the pictorial space and the bright color was inconsistent with what one would expect to find in a 17th-century Dutch picture. Testing indicated the repaint was insoluble in most free solvent mixtures appropriate for use on an aged oil painting. Mechanical removal of the repaint using a scalpel under the microscope would prove to be time consuming and hazardous due to the lead white component of the paint; furthermore, the coarse surface texture of the original sky would make it difficult to use a scalpel without harming the original surface. Further testing with benzyl alcohol and Pemulen TR2 indicated that a 5% benzyl alcohol Pemulen gel could be used to remove the overpaint successfully without damaging the original paint. Pemulen is a polyacrylic acid copolymer used in the cosmetics industry to create oil-in-water emulsions for products such as sunscreen. During testing, the percentage of benzyl alcohol in the gel was gradually increased from 1% to 5% until the desired working efficacy was achieved. Benzyl alcohol was selected as a solvent because it had a minor effect on the overpaint as a free solvent during testing. Pemulen TR2 was selected as a gelling agent because it can be used to emulsify benzyl alcohol without the addition of a surfactant (unlike other materials such as Carbopol-Ethomeen gels, which require a large amount of surfactant), which is at risk of being left behind on the surface after cleaning. The Pemulen gel is likely effective here for a combination of reasons—the benzyl alcohol component of the gel works to swell the lead-based oil paint, while the aqueous components of the gel pass through the overpaint to swell and solubilize the uneven varnish layer below, creating an undercutting effect.

Removing the overpaint to uncover the original sky was a slow process performed under the microscope (Figure 13). Subtle details were revealed through cleaning including a flock of small birds in flight above the landscape at right and the feathered edges of the larger bird's forms, features that allow them to sit more convincingly in space. The large, amorphous clouds added above the birds at the center of the sky were also removed, restoring a sense of diagonal movement through the picture. The sky was likely overpainted to mask the disturbing effects of lead soap formation visible across the surface as short, dark horizontal lines (67–70, 79).

After cleaning, the picture was varnished and retouched. Varnishing saturates the paint, which makes it easier to match colors during retouching, in addition to providing an isolating layer between the original paint surface and the restoration material. Paraloid B72 was selected as an isolating varnish because it resulted in the most regular, even surface appearance during testing (80). It is a thermoplastic acrylic resin comprised of an ethyl methacrylate (70%) and methyl acrylate (30%) copolymer. In theory, the varnish creates a high-molecular weight “floor” on top of which other, more saturating varnishes can be applied to build up the desired appearance. B72 is fairly insoluble in many of the solvents commonly used for retouching, which keeps multiple options open for which retouch paints can be used later in the treatment.

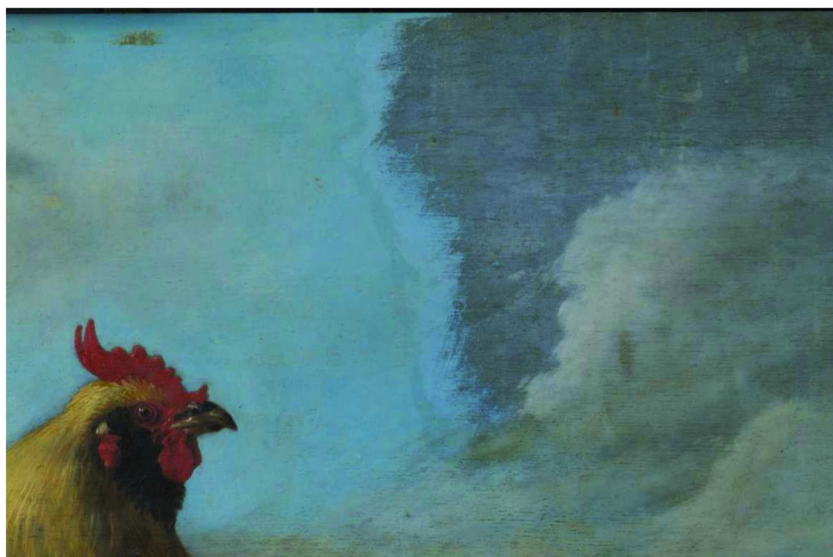


Figure 13. During overpaint removal in the sky; the bright blue overpaint is intact at left and has been removed at right to reveal the original gray-blue sky. (see color insert)

Areas of loss and abrasion were retouched using a combination of Golden PVA conservation paints, and dry pigments with Mowilith 20 in ethanol as a medium (81, 82). Because the painting was anticipated to hang at a relatively high location in the gallery, a conscious attempt was made to not retouch every damage and disturbing feature visible at close range. There are few discrete losses to the original paint; however, in many areas, the legibility of the image was disrupted by abrasion or increasing transparency of the upper paint layers. Extensive retouching was required to reintegrate the dark lines in the damaged sky; all evidence of the lines was not erased through retouching in order to maintain the picture's naturally aged patina.

Small 1 cm x 2 cm areas of discolored varnish and blue overpaint were left intact as a reference at the edge, hidden from view by the frame. The treatment restored balance within the picture, allowing the birds to feature prominently in the foreground with the landscape receding into the background. Cleaning revealed Hondecoeter's virtuoso rendering of the birds and his energetic brushwork in the feathers. Uncovering the original gray-blue sky greatly improved the overall appearance of the picture.

Conclusion

A combination of art historical research, art conservation methodology, and scientific examination has shed new light on Hondecoeter's *Cock and Hens in a Landscape*. Important, yet obscured iconographical elements were recovered,

and the tonal balance within the painting was restored to the extent possible. The picture is now on permanent display in the Prince William V Gallery, a satellite gallery of the Mauritshuis, which is hung according to 18th-century salon style, with paintings stacked from floor to ceiling. Extensive collaboration and interdisciplinary work (as revealed, in part, by the depth of the Acknowledgments section) enables powerful new insights into cultural heritage objects to be achieved.

Acknowledgments

Lauren Bradley would like to thank the American Friends of the Mauritshuis for generously funding the Mauritshuis Internship in Paintings Conservation and the Samuel H. Kress Foundation for awarding a travel grant to relocate to The Netherlands. Mauritshuis Conservators Petria Noble, Sabrina Meloni, and Carol Pottasch provided excellent mentorship and were the source of many insightful discussions throughout this project and during the internship as a whole. Conservation Scientist Annelies van Loon assisted with the interpretation of cross-section samples and fellow Mauritshuis intern Charlotte Blachon offered words of encouragement. Mauritshuis Curators Edwin Buijsen, Quentin Buvelot, Geerte Broersma, Lea van der Vinde, and Director Emilie Gordonker visited the studio on a regular basis to see the painting and provide fresh insights. Curators and conservators at other institutions graciously pulled files and brought paintings out of storage for examination including Barbara Schoonhoven at the Museum Boijmans Van Beuningen, Anna Krekeler at the Rijksmuseum Amsterdam, and Lloyd de Witt at the Philadelphia Museum of Art. Amsterdam art dealer, Pieter de Boer, kindly granted access to three Hondecoeter paintings at his gallery in addition to opening his personal photographic archives for study. A special thank you to Fred Meijer of the RKD and Joy Kearney for visiting the Mauritshuis to discuss the painting after treatment and for helping to enrich our understanding of Hondecoeter's work. WUDPAC faculty advisor Joyce Hill Stoner offered tireless guidance and support in addition to Mary McGinn, Richard Wolbers, and Stephanie Auffret. Additional gratitude is expressed to the following institutions for providing assistance to WUDPAC students: American Institute for Conservation, Foundation of the American Institute for Conservation, The Samuel H. Kress Foundation, The National Endowment for the Humanities, The Rosenberg Family, The Society of Winterthur Fellows, Tru Vue, and The WUDPAC Professional Development Fund.

The NSF is gratefully acknowledged for recently funding non-destructive analytical instrumentation (NSF 0959625) at W&L that was used in the examinations reported here; the NSF is also thanked for funding Chemistry in Art Workshops for many years. W&L Lenfest summer grants and travel grants to ESU permitted course development and the research travel that enabled the handheld pXRF to be taken to The Mauritshuis. A 2009 State Council of Higher Education for Virginia Outstanding Faculty Award assisted ESU in various aspects of these projects. ESU would like to thank Petria Noble, Carol Pottasch, and Sabrina Meloni of The Mauritshuis and Jennifer Mass and her colleagues at Winterthur

for years of collaborative help; and he would like to thank Dr. Bruce J. Kaiser for pXRF support. ESU does not have the space here to individually thank all of the W&L, U.S., and Dutch friends and colleagues who have helped support his work.

References

1. The reader should note that because this is not a review paper, the references are not intended to be comprehensive. Rather, they are provided with the intention of guiding readers new to the field of paintings conservation and technical art investigations towards relevant literature.
2. van der Vinde, L.; Bradley, L. *Mauritshuis in Focus* **2011**, *24* (1), 32.
3. Uffelman, E. S. *J. Chem. Educ.* **2007**, *84*, 1617–1624.
4. Uffelman, E. S. *J. Chem. Educ. (online paper)* **2007**, *84*, 38.
5. Uffelman, E. S. *International Council of Museums Conservation Committee Triennial 16th Conference*, Lisbon, Portugal, September 19–23, 2011; Criterio: Lisbon, Portugal, 2011; paper 312; pp 1–8.
6. Hill, P., S.; Simon, D.; Uffelman, E. S.; Bower, N.; Lagalante, A. F.; Norbutus, A. J. *American Institute for Conservation of Historic and Artistic Works 39th Annual Meeting*, Philadelphia, PA, 2011.
7. Code of Ethics and Guidelines for Practice of the American Institute for Conservation of Historic & Artistic Works. In *American Institute for Conservation of Historic and Artistic Works: Directory 2011*; AIC: Washington, DC, 2011; pp 282–288.
8. Pinna, D.; Galeotti, M.; Mazzeo, R. *Scientific Examination for the Investigation of Paintings. A Handbook for Conservator-restorers*; Centro Di della Edifimi srl: Firenze, Italy, 2009.
9. Bomford, D. *Art in the Making: Underdrawings in Renaissance Paintings*; National Gallery (London) Company: London, 2002.
10. Ricciardi, P.; Delaney, J. K.; Glinsman, L.; Thoury, M.; Facini, M.; de la Rie, R. *Proc. SPIE* **2009**, *7391*, 739106-1–739106-12.
11. Taft, W. S.; Mayer, J. W. *The Science of Paintings*; Springer-Verlag: New York, 2000.
12. Trentelman, K.; Bouchard, M.; Ganio, M.; Namowicz, C.; Patterson, C. S.; Walton, M. *X-Ray Spectrometry* **2010**, *39*, 159–166.
13. Namowicz, C.; Trentelman, K.; McGlinchey, C. *Powder Diffr.* **2009**, *24*, 124–129.
14. Shugar, A. N.; Mass, J. L. *Handheld XRF for Art and Archaeology*; Lueven: Belgium, 2012.
15. Kirsh, A.; Levenson, R. S. *Seeing Through Paintings*; Yale University Press: New Haven, 2000.
16. Appendix G: Polarized Light Microscopy in Conservation. In *Microscopy for Art Conservators: Appendices*; McCrone Research Institute: Chicago, 2005.
17. Goldstein, J. I.; Newbury, D. E.; Joy, D. C.; Lyman, C. E.; Echlin, P.; Lifshin, E.; Sawyer, L.; Michael, J. R. *Scanning Electron Microscopy and X-ray Microanalysis*; Springer: New York, 2003.

18. Hsu, C.-P. S. In *Handbook of Instrumental Techniques for Analytical Chemistry*; Settle, F., Ed.; Prentice Hall PTR: Upper Saddle River, NJ, 1997; pp 247–284.
19. Derrick, M. R.; Stulik, D.; Landry, J. M. *Infrared Spectroscopy in Conservation Science*; The Getty Conservation Trust: Los Angeles, 1999.
20. Kearney, J. *Melchior d'Hondecoeter: Catalogue Raisonne* **2012** in press.
21. Haak, B. *The Golden Age: Dutch Painters of the Seventeenth Century*; Stewart, Tabori and Chang Publishers: New York, 1996.
22. Rikken, M. *Melchior d'Hondecoeter Bird Painter*; Nieuw Amsterdam Publishers: Amsterdam, 2008.
23. Spicer, J. A.; Muhlberger, R. C. Hondecoeter, d'. . <http://www.oxfordartonline.com/subscriber/article/grove/art/T038750> (March 26, 2012).
24. Schama, S. *Embarrassment of Riches: An Interpretation of Dutch Culture in the Golden Age*; Vintage Books: New York, 1997.
25. Benedict, P. *Christ's Church Purely Reformed: A Social History of Calvinism*; Yale University Press: New Haven, 2002.
26. North, M. *Art and Commerce in the Dutch Golden Age*; Yale University Press: New Haven, 1997.
27. Hochstrasser, J. B. *Still Life and Trade in the Dutch Golden Age*; Yale University Press: New Haven, CT, 2006.
28. Bernstein, W. J. *A Splendid Exchange: How Trade Shaped the World*; Atlantic Monthly Press: New York, 2008.
29. Brook, T. *Vermeer's Hat: The Seventeenth Century and the Dawn of the Global World*; Bloomsbury Press: New York, 2008.
30. Cook, H. J. *Matters of Exchange: Commerce, Medicine, and Science in the Dutch Golden Age*; Yale University Press: New Haven, 2007.
31. Schwartz, G. *The Rembrandt Book*; Harry N. Abrams, Inc.: New York, 2006.
32. Schneider, N. *Still Life*; Taschen: Koln, Germany, 2003.
33. Biesboer, P.; Brunner-Bulst, M.; Gregory, H. D.; Klemm, C. *Pieter Claesz: Master of Haarlem Still Life*; Waanders: Zwolle, The Netherlands, 2004.
34. Rosenberg, J.; Slive, S.; Kuile, E. H. t. *Dutch Art and Architecture 1600-1800: The Pelican History of Art*; Penguin Books: New York, 1979.
35. Wheelock, A. K., Jr. *Aelbert Cuyp*; Thames & Hudson: New York, 2001.
36. Kloek, W. T. *Aelbert Cuyp: Land, Water, Light*; Waanders Printing: Zwolle, The Netherlands, 2002.
37. Bruyn, J. In *Rembrandt: the Master & his Workshop: Paintings*; Brown, C., Kelch, J., Thiel, P. v., Eds.; Yale University Press: New Haven, 1991; pp 68–89.
38. Walsh, J. *Jan Steen: The Drawing Lesson*; Getty Museum: Los Angeles, 1996.
39. Dardes, K.; Rothe, A. *The Structural Conservation of Panel Paintings*; Getty Conservation Institute: Los Angeles, 1998.
40. van de Wetering, E.; Franken, M.; Groen, K.; Klein, P.; van der Veen, J.; de Winkel, M. *A Corpus of Rembrandt Paintings V: Small Scale History Paintings*; Springer: Dordrecht, The Netherlands, 2011; Vol. IV.

41. Wetering, E. v. d. *Rembrandt: The Painter at Work*; Amsterdam University Press: Amsterdam, 1997.
42. Doherty, T.; Woollett, A. T. *Looking at Paintings: A Guide to Technical Terms Revised Edition*; The J. Paul Getty Museum: Los Angeles, 2009.
43. Woll, A. R.; Mass, J.; Bisulca, C.; Cushman, M.; Griggs, C.; Wazny, T.; Ocon, N. *Stud. Conserv.* **2008**, *53*, 93–109.
44. Uffelman, E. S.; Court, E.; Marciari, J.; Miller, A.; Cox, L. Handheld XRF Analyses of Two Veronese Paintings. In *Collaborative Endeavors in the Chemical Analysis of Art and Cultural Heritage Materials*; Lang, P. L., Armitage, R. A., Eds.; ACS Symposium Series 1103; American Chemical Society: Washington, DC, 2012; Chapter 3.
45. van der Doelen, G. A., Ph.D. Thesis, FOM-Institute of Atomic and Molecular Physics, Amsterdam, The Netherlands, 1999; 178 pages.
46. Doelen, G. A. v. d.; Berg, K. J. v. d.; Boon, J. J. *Stud. Conserv.* **1998**, *43* (4), 249–264.
47. De Wild, D. *Mauritshuis Conservation Treatment Report, Mauritshuis Conservation Department*; Den Haag, The Netherlands, 1916.
48. Traas, J. C. *Mauritshuis Conservation Treatment Report, Mauritshuis Conservation Department*; Den Haag, The Netherlands, 1937.
49. de la Rie, E. R.; Delaney, J. K.; Morales, K. M.; Maines, C. A.; Sung, L.-P. *Stud. Conserv.* **2010**, *55* (2), 134–143.
50. Delaney, J. K.; de la Rie, E. R.; Elias, M.; Sung, L.-P.; Morales, K. M. *Stud. Conserv.* **2008**, *53* (3), 170–186.
51. Berns, R. S.; De la Rie, E. R. *Stud. Conserv.* **2003**, *48* (4), 251–262.
52. Berns, R. S.; De la Rie, E. R. *Stud. Conserv.* **2003**, *48* (2), 73–82.
53. de la Rie, E. R. *Stud. Conserv.* **1987**, *32* (1), 1–13.
54. Nicolaus, K. *The Restoration of Paintings*; Konemann: Cologne, 1998.
55. *Mauritshuis Inventory Book, Mauritshuis Curatorial Department*; Den Haag, The Netherlands, 1876.
56. Wadum, J. *Vermeer Illuminated: Conservation, Restoration and Research*; V&K Publishing/Inmere: Mauritshuis, The Hague, 1995.
57. Buckley, B. *Paintings Conservation Catalog: Stretchers and Strainers*; American Institute for Conservation of Historic and Artistic Works: Washington, DC, 2008; Vol. 2.
58. Noble, P.; Meloni, S.; Pottasch, C.; Ploeg, P. v. d. *Preserving our Heritage: Conservation, Restoration and Technical Research in the Mauritshuis*; Waanders Publishers: Zwolle, The Netherlands, 2009.
59. Berrie, B. H. In *Artists' Pigments: A Handbook of Their History and Characteristics*; Fitzhugh, E. W., Ed.; Oxford University Press: New York, 1997; Vol. 3, pp 191–272.
60. Eastaugh, N.; Walsh, V.; Chaplin, T.; Siddall, R., *Pigment Compendium: A Dictionary and Optical Microscopy of Historical Pigments*. Butterworth-Heinemann: Oxford, 2008.
61. Kirby, J.; Saunders, D. In *National Gallery Technical Bulletin*; Roy, A., Ed.; National Gallery Company: London, 2004; Vol. 25, pp 77–99.

62. Muhlethaler, B.; Thissen, J. In *Artists' Pigments: A Handbook of Their History and Characteristics*; Roy, A., Ed.; Oxford University Press: New York, 1993; Vol. 2, pp 113–130.
63. Hommes, M. v. E. *Changing Pictures: Discoloration in 15th-17th Century Oil Paintings*; Archetype: London, 2004.
64. Boon, J. J.; Keune, K.; Geldof, M.; Mensch, K.; Bryan, S.; van Asperen de Boer, J. R. J. *Chimia* **2001**, *55*, 952–960.
65. Spring, M.; Higgitt, C.; Saunders, D. In *National Gallery Technical Bulletin*; Roy, A., Ed.; National Gallery/Yale University Press: London, 2005; Vol. 26, pp 56–70.
66. Robinet, L.; Spring, M.; Pages-Camagna, S.; Vantelon, D.; Trcera, N. *Analytical Chemistry* **2011**, *83*, 5145–5152.
67. Noble, P.; van Loon, A.; Boon, J. J. In *Chemical changes in old master paintings II: darkening due to increased transparency as a result of metal soap formation*; ICOM-CC 14th Triennial Meeting, The Hague, 2005; Verger, I., Ed.; James & James: The Hague, 2005; pp 496–503.
68. Boon, J. J.; Hoogland, F.; Keune, K. In *Chemical Processes in Aged Oil Paints Affecting Metal Soap Migration and Aggregation*; 34th Annual Meeting of the American Institute for Conservation of Historic and Artistic Works, June 16-19, 2006, Providence, RI, 2006; pp 1–25.
69. Keune, K. Ph.D. Thesis, FOM-Institute of Atomic and Molecular Physics, Amsterdam, The Netherlands, 2005; 301 pages.
70. Robinet, L.; Corbeil, M.-C. *Stud. Conserv.* **2003**, *48* (1), 23–40.
71. Loon, A. v. *AMOLF-FOM*; Amsterdam, 2008; p 234 (notes 24 and 25).
72. Wolbers, R. *Cleaning Painted Surfaces: Aqueous Methods*; Archetype: London, 2000.
73. Dorge, V. *Solvent Gels for the Cleaning of Works of Art: The Residue Question*; The Getty Conservation Institute: Los Angeles, 2004.
74. *Science for Conservators Series: Cleaning*, 2nd ed.; Routledge: Florence, KY, 1992; Vol. 2.
75. White, R.; Roy, A. *Stud. Conserv.* **1998**, *43*, 159–176.
76. Phenix, A.; Sutherland, K. *Rev. Conserv.* **2001**, *2*, 47–60.
77. Morrison, R.; Abigail, B.-Y.; Burnstock, A.; Van Den Berg, K. J.; Van Keulen, H. *Stud. Conserv.* **2007**, *52* (4), 255–270.
78. Mills, J. S.; White, R. *The Organic Chemistry of Museum Objects*, 2nd ed.; Butterworth-Heinemann: London, 1994.
79. Keune, K.; Boon, J. J. *Stud. Conserv.* **2007**, *52*, 161–176.
80. Ellison, R.; Smithen, P.; Turnbull, R. *Mixing and Matching: Approaches to Retouching Paintings*; Archetype Publications Ltd.: London, 2010.
81. Berger, G. A. In *Inpainting using PVA medium*; Cleaning, Retouching and Coatings, preprints of the Contributions to the IIC Brussels Congress, Brussels, 1990; pp 150–155.
82. Cove, S. In *Mixing and Matching: Approaches to Retouching Paintings*; Ellison, R., Smithen, P., Turnbull, R., Eds.; Archetype Publications Ltd.: London, 2010; pp 74–86.

Chapter 3

Handheld XRF Analyses of Two Veronese Paintings

Erich Stuart Uffelmann,^{*1} Elizabeth Court,^{*2} John Marciari,^{*3}
Alexis Miller,² and Lauren Cox²

¹Department of Chemistry, Washington and Lee University,
Lexington, VA 24450

²Balboa Art Conservation Center, P.O. Box 3755, San Diego, CA 92163-1755

³The San Diego Museum of Art, P.O. Box 122107, San Diego, CA 92112

*E-mail: uffelmane@wlu.edu; ecourt@bacc.org; jmarciari@sdmart.org

Paolo Veronese's painting of *Apollo and Daphne* at the San Diego Museum of Art was suspected of containing large areas of degraded smalt (a pigment derived from ground cobalt glass) in the sky, causing the original blue color to have turned gray. Handheld XRF analysis of the painting confirmed the presence of cobalt in all spots involving the sky. For purposes of contrast, Veronese's painting of *Madonna and Child with St. Elizabeth, the Infant St. John, and St. Catherine* at The Timken Museum of Art was analyzed by handheld XRF. The Timken's Veronese's sky is still blue, and copper (almost certainly present in the form of azurite) was found instead of cobalt.

Introduction

One of the themes of this book is to illustrate the cooperative efforts between scientific, academic, and museum communities in gaining new knowledge about cultural heritage material and using it to educate both the general public and students at the undergraduate and graduate levels. This chapter arose from collaborations between the Balboa Art Conservation Center and Washington and Lee University that date to 2004. Elizabeth Court was brought to W&L from BACC, with funds from an Associated Colleges of the South Keck Foundation Grant, to consult on Uffelmann's courses involving the technical examination of 17th-century Dutch painting (*I-3*). In the spring of 2011 an American Chemical

Society Meeting in Anaheim, CA featuring a session on art and analytical chemistry (4) made further travel to San Diego with W&L's handheld (portable) X-ray fluorescence spectrometer (pXRF) an efficient proposition. Two days of analyses of paintings at BACC, the San Diego Museum of Art, and the Timken Museum of Art ensued. Among the works investigated were two paintings by Veronese: *Apollo and Daphne* (Figure 1) at the SDMA, and the *Madonna and Child with St. Elizabeth, the Infant St. John, and St. Catherine* (Figure 2) at the Timken. This monograph is thus intended not only as a contribution to the art conservation literature, but is also intended to be useful in various undergraduate courses on Chemistry in Art (2, 3, 5), as well as the NSF Chemistry in Art Workshops (5, 6). [Please also see chapters by Lang; Gaquere-Parker and Parker; and Hill in this volume.] Thus, we briefly discuss Veronese's place in 16th century Italian Painting, the art historical context of the paintings, and the results of their technical examination. Since smalt degradation was a question surrounding the analysis of *Apollo and Daphne*, we also briefly review the degradation and detection of smalt as a colorant.

Background

Paolo Veronese

Paolo Caliari (1528–1588), better known as Paolo Veronese, was born in Verona, the son of a Lombard stonemason, and was apprenticed by the age of ten to the local painter Antonio Badile; he later trained with the painter Giovanni Caroto, also from Verona. Coming of age, Veronese quickly surpassed his local contemporaries, and by the early 1550s had moved to Venice, the most important artistic center in Northern Italy. In Verona, he had learned the principles of design associated with the artists of central Italy, and to these, upon arriving in Venice, he added the lessons in color available in the works of Titian. Titian, however, was for the most part engaged in work for foreign clients by the 1550s, and Veronese quickly began to win major commissions in Venice, rivaled only by his contemporary, Tintoretto. During a long and successful career, in which Veronese and his well-trained workshop turned out hundreds of paintings, the artist came to be known for his clarity of composition, bright colors, and lush painterliness. With his frescoes and large canvases, Veronese was the decorative painter *par excellence*. The best single introduction to Veronese in English remains the catalogue for the exhibition at the National Gallery of Art in Washington (7). See also more recent treatments (8–10).

Apollo and Daphne

Veronese's canvas of *Apollo and Daphne* in the SDMA was painted in the early 1560s. Nothing is known of the work's early history, but it was very likely to have been part of a decorative scheme with another mythological canvas, the *Diana and Actaeon* in the Philadelphia Museum of Art. Not only do the two paintings have similar subjects drawn from Ovid's *Metamorphoses*, but both have figures and trees drawn to the same scale, and the two paintings are executed

in virtually identical technique: both are on a rough canvas of approximately 10 x 10 threads per square centimeter, with a thinly applied brown ground over which the forms were built up in opaque paint, with glazes (thin transparent paint layers applied over an opaque paint layer (11)) laid over the top. These and other mythological paintings by Veronese from the late 1550s and early 1560s are generally thought to be a response to the *poesie* that Titian painted for Philip II during the 1550s. Moreover, a group of Veronese's mythological paintings follow close on the heels of his secular decorative ensembles at the Palazzo Trevisan in Murano (1557-58) and the Villa Barbaro at Maser (1560-61).



Figure 1. Paolo Veronese, Apollo and Daphne. Oil on canvas, H. 43 1/16" (109.4 cm) x W. 44 5/8" (113.4 cm). Gift of Anne R. and Amy Putnam to the San Diego Museum of Art, inv. no, 1945:27. Courtesy of the San Diego Museum of Art. (see color insert)



Figure 2. Paolo Veronese, *Madonna and Child with St. Elizabeth, the Infant St. John, and St. Catherine*. Oil on canvas, H. 40 5/8" (103.2 cm) x W. 61 3/4" (156.9 cm). Courtesy of the Putnam Foundation, Timken Museum of Art, San Diego, CA. (see color insert)

There are at least two textual versions of the Apollo and Daphne story (12), but the version that had the greatest impact on European art is from Ovid. In that version, Apollo saw Cupid, son of Venus, drawing his bow and insulted him, “What are you doing, you silly boy, with such a powerful weapon? A bow like that looks better on my shoulder, for I can hit anything---any animal I hunt, any enemy---in fact, just now I killed the poison-bloated Python with more arrows than I can count.... Be satisfied to arouse a little passion now and then with your torch, you certainly should not consider yourself in the same class as me” (13)! In response to this provocation, Cupid shot Apollo through the heart with a sharp, gold-tipped arrow and then shot Daphne, a river nymph, through the heart with a blunt, lead-tipped arrow. The consequence was that Daphne rejected the love of all men and sought to emulate the chaste goddess Diana, while Apollo lusted for Daphne. Apollo pursued the Nymph, who fled. Approaching exhaustion, she reached the waters of her father, Peneus. “Father, help me! If rivers have divine power---this beauty that has made me so attractive, rid me of it, change me” (13)! As her prayer concluded, she became encased in bark, her hair became leaves and her arms tree branches. Apollo, still love-struck, tried to kiss the tree, which even rooted to the ground, resisted his advances. Finally, Apollo declared that if she cannot be his love, she will be his tree, and he declared that he will always wear laurel leaves and that a laurel wreath will, from that day forth, be worn by Roman victors.

The story of Apollo and Daphne is among the most familiar tales of Greco-Roman mythology and a favorite subject for artists in Renaissance and Baroque Europe. The best known version is surely Bernini’s sculpture in the Villa Borghese at Rome, but other important examples include Antonio del Pollaiuolo’s famous painting (ca. 1470-1480) in the National Gallery (London); Nicolas Poussin’s painting (1625) in the Alte Pinakothek (Munich); and Giambattista Tiepolo’s painting (ca. 1744-1745) at the Louvre. All of these works focus on the dramatic point in which Daphne is in mid-transformation.

Executed in the painterly style so characteristic of Veronese’s work, the San Diego canvas presents an interesting take on the story, for it shows not the climactic moment of the chase and Daphne’s transformation, but rather, the anticlimactic moment just afterwards: Apollo has overtaken Daphne and stares upward with wonder at the metamorphosis that has occurred. Daphne would have been running from the right towards the left of the scene and staring backward at a pursuing Apollo before her transformation; she is now frozen in that pose, and Apollo has circled around to the front of her and gazes at the ongoing metamorphosis.

Madonna and Child with St. Elizabeth, the Infant St. John, and St. Catherine

Veronese’s painting at the Timken dates to around 1568-70, slightly later than *Apollo and Daphne*. The identification of the figures in the canvas has not always been clear, for the saint at right lacks Saint Catherine’s traditional attributes of a broken wheel or a ring being exchanged with the infant Christ, and she was long identified as Saint Justina. The painting seems to be based, however, on sketches that are today in the Museum Boijmans van Beuningen in Rotterdam,

and the inscription on that sheet, “Sposi di Santa [...] / con S. Zuani ...” (Marriage of St. ____, with St. John) puts an end to the question and confirms that the female figure at right in the painting is indeed Saint Catherine, for there would be no reason to show Saint Justina in a marriage scene. The Rotterdam drawing was made by Veronese on the back of a letter dated 1568, providing a *terminus post quem* for the painting.

The Timken painting is not, however, the only canvas that relates to the Rotterdam drawing, for the sketches also seem preparatory to paintings at the Musée des Beaux-Arts, Brussels; the Musée Fabre, Montpellier; and the New Orleans Museum of Art. This group of paintings shows, furthermore, Veronese’s workshop in its full burst of production. On the one hand, the Timken painting was surely of Veronese’s invention and has deftly painted passages that show it was at least partly executed by the master himself. Yet, some parts of the Timken painting—the painting of St. Catherine’s draperies, for example—are handled in a slightly abbreviated manner that is often the benchmark of workshop assistance, and the existence of the other versions likewise raise the question of how much of any one painting Veronese executed himself. It can be argued that an overwhelming majority of the paintings that emerged from the workshop from around 1570 onward were created through a similarly collaborative process. [For further commentary on Veronese and his workshop, see the (forthcoming) catalogue related to the Veronese exhibition to be held at the Ringling Museum of Art in 2012.] When assisting a master painter, however, the workshop assistants would adopt the same materials and techniques as the master, so the Timken painting, like the canvas at the San Diego Museum of Art, can be considered a typical work by Veronese from the 1560s, particularly from a technical point of view.

Degradation and Detection of Smalt Colorants

The exact date of cobalt as a colorant in glass is lost in antiquity, and the use of cobalt glass, smalt, as a pigment in painting begins prior to the 14th century (14). Its production involved melting silica with potash (potassium oxide) and a source of cobalt derived from ores that were frequently rich in arsenic, as well as containing other metals such as iron and nickel. The amount of other elements present depended on both the source of the ore and its treatment; i.e., roasting the ore lowered the arsenic content via volatilization. Smalt’s use in European painting was particularly prevalent in the 16th and 17th centuries, because it was a much cheaper alternative to azurite and ultramarine. With the advent of Prussian blue in the early 18th century, smalt’s use became increasingly infrequent. Although smalt yields a pleasing blue color when fresh, because the refractive index of glass is not dramatically different from polymerized oil binding medium, it had to be ground fairly coarsely for reasonable opacity. In addition, the ground glass-oil medium combination did not yield ideal handling properties (e.g., the oil could run down a vertical canvas). Furthermore, as early as the 17th century, smalt was known to discolor, although the early writers attributed the discoloration to the oil binding medium, rather than the pigment itself.

In the last decade, numerous studies have elucidated the nature of smalt degradation (15–20). A combination of microspectroscopy, scanning electron microscopy energy dispersive spectroscopy (SEM-EDS), and secondary ion mass spectrometry (SIMS) demonstrated that loss of potassium ions from the glass was linked to a change in smalt from blue to gray (15). Cobalt ions in blue glass are found in a tetrahedral +II oxidation state, and the cobalt in this environment produces an absorption spectrum entirely consistent with a $d^7 T_d$ Co(II) center in a weak ligand field. The basicity of the glass is essential to stabilizing the T_d coordination of Co(II) within the glass framework, and the potassium acts as a counterion to balance the charge; use of sodium to balance the charge (soda glass) produces a spectrum that has a bathochromic shift that gives the material a less-pleasing purplish appearance. As potassium leaches out of the glass and is replaced by protons, the coordination number of the Co(II) increases to O_h six-coordinate, and consistent with this change in the coordination environment is the shift in the absorption spectrum and the dramatic change in absorbance power due to the alteration from local point group symmetry without an inversion center (T_d) to a local point group symmetry with an inversion center (O_h). SEM-EDS maps and SIMS maps consistently showed that cobalt was not leaching from the glass and that potassium was, yielding potassium soaps from ester saponification of the oil binding medium (15).

The alteration of the glass caused by potassium ion leeching out into the surrounding medium can be distinguished by vibrational methods (17, 19, 21). In smalt, the asymmetric Si-O-Si stretch occurs in the region 1040–1080 cm^{-1} ; the symmetric Si-O-Si stretch occurs in the region of 780–800 cm^{-1} ; and the O-Si-O bending vibration occurs between 460–470 cm^{-1} . Crucially, additives such as Na_2O , CaO , and K_2O generate an additional vibration at approximately 920 cm^{-1} , corresponding to Si-OM (where $M = \text{Na}^+$, Ca^{2+} , or K^+ ; for potassium, this additional band is generally underneath the asymmetric Si-O-Si stretch). When the potassium leaches out of smalt, the Si-OK band is observed to diminish, and Si-OH bands are observed to grow (17, 21).

The most definitive characterization of the chemical changes at cobalt in smalt degradation has recently been published (20). By using the SOLEIL synchrotron, investigators were able to examine degraded and undegraded smalt samples at very high resolution using micro-X-ray absorption spectroscopy (μ -XAS) at the cobalt K-edge. By employing X-ray absorption near-edge spectroscopy (XANES) and extended X-ray absorption fine structure (EXAFS), as well as synchrotron-based μ -FTIR and μ -Raman, they were able to probe the different alterations. By using anhydrous blue Co(II)-silica gel and hydrated pink Co(II)-silica gel as model compounds in XANES and EXAFS measurements of degraded and undegraded smalt, they were able to conclusively show that the well-preserved smalt featured Co(II) in a T_d environment with Co-O bond distances of 1.95 Å, while the degraded smalt featured Co(II) in an O_h environment with Co-O bond distances of 2.02–2.06 Å. Although their results are generally applicable, it is noteworthy in this context that two of the five paintings studied by these synchrotron methods featured degraded and well-preserved smalt samples from works by Veronese.

Fortunately, in addition to the investigations of smalt referenced above, the National Gallery, London, published two significant papers on Veronese's technique, spanning most of his career, based on his nine paintings in their collection (22, 23), and these papers document Veronese's use of smalt in the sky of some works and the use of azurite in the sky of other works. The technical results were recently placed in a larger context of Veronese's work (24).

Veronese's reputation as a master of color was facilitated by his location in Venice, which was a trade nexus and would have given him access to all of the pigments available at that time in Europe. Venetian glass was renowned, and would have meant that smalt was readily available to Veronese. The National Gallery work demonstrated that, in several paintings featuring gray-toned skies, the color was not the result of an artistic choice by Veronese, but rather the degradation of smalt over time.

Furthermore, Veronese's green copper resins exhibit highly variable degrees of preservation/degradation, and his significant use of red lake pigments (characteristic of Venetian painting of the period) has caused many of his reds to be fugitive. A very readable reference on discoloration in paintings of this era is available (25).

Use of pXRF for the Analysis of Cultural Heritage Objects

Handheld XRF has several pros and a few cons as an analytical tool for examining cultural heritage objects (26, 27). Some of the pros are: (1) Because the instrument is portable, the instrument may be brought to the object, eliminating the chance of damage due to transport. [Of course, there is a physical risk of damage, that must be controlled, in bringing the instrument into close proximity to the object.] For paintings, as long as the artwork is not covered by glass, the instrument may be mounted on a tripod and brought directly to the painting in the gallery. (2) Significantly, the technique is non-destructive; i.e., no sample needs to be removed from the art object. (3) The amount of X-ray radiation emitted is so low that the art object will be undamaged by the analysis. Furthermore, the emitted radiation is so low that users who exercise prudent caution should never be exposed to radiation above background levels. (4) Because X-rays have penetrating power, layers below the surface of the object yield information to the analyst. (5) With the use of a portable vacuum pump (to evacuate the interior of the instrument's X-ray path) and with careful positioning of the instrument within one millimeter of the object, elements as light as aluminum can be detected (air absorbs X-rays of low energy fluoresced by the lighter elements). (6) Analyses can be performed rapidly. Two minutes of acquisition time is sufficient in many instances to get good quality signal to noise ratios for most peaks of interest. When dealing with valuable cultural heritage objects, it frequently takes longer to carefully position the spectrometer than it does to acquire the data. (7) The instrument is relatively inexpensive and is physically robust to travel in the field.

There are cons or limitations associated with the technique. (1) Unlike benchtop pXRF models which can have sampling resolutions of 70 μm , the handheld unit has a sampling area of roughly 3 mm in diameter. This can necessitate caution in selecting areas to analyze for clear results. (2) Although

it is useful to get information from different layers of the painting due to the penetrating power of the X-rays, determining which layer of the painting is causing which signals frequently requires having other forms of information; e.g., paint samples or cross sections analyzed by polarized light microscopy (PLM) or SEM-EDS. Recently, 3D resolution and mapping of pXRF spectra have been achieved by synchrotron methods (28–31), or very advanced semi-portable systems (32). (3) Quantitative information is difficult to obtain and is typically impossible to obtain for paintings. (4) The instrument's construction gives rise to element signals that sometimes cause issues with correct analysis. For instance, the instrument construction typically produces significant Rh peaks (for a rhodium anode X-ray source) as well as low level peaks for Fe, Co, and Ni (from stainless steel), and Al (instrument structure) (33). With experience, and sufficient authentic material in the sample area, real peaks from these elements in the sample can be distinguished from the intensity of the peaks present from those elements in the instrument. There are also sum peaks, escape peaks, elastic scattering of X-rays, inelastic scattering of X-rays, and other artifacts to consider (26, 33). Interested readers are referred to a significant new book in press on the use of handheld pXRF for art and archaeology applications (34), and a recent well-illustrated general survey of scientific methods for examining paintings (35).

Experimental Section

For the pXRF spectra obtained in this study, the following conditions were typically used: Bruker Tracer III-SD, Rh X-ray tube at 40 kV and 11 μ amps, 20 Torr interior pressure inside the instrument, 120 s spectrum accumulation time. The front of the instrument was carefully placed parallel to the picture plane. Because the painting surface was relatively flat in the regions surveyed, the instrument could be safely very carefully positioned (using a tripod with a manually controlled, geared instrument mount) within approximately one millimeter of the painting surface. The element assignments were made using the Bruker Artax 7.2.1.1 software, but comprehensive tables of pXRF lines are readily available in common sources (36).

Results of Technical Examination

Madonna and Child with St. Elizabeth, the Infant St. John, and St. Catherine

Prior to the 2011 pXRF investigation, *Madonna and Child with St. Elizabeth, the Infant St. John, and St. Catherine* from the Timken Museum of Art was examined as part of a project at BACC in 2000–2001 to determine the materials used by the artist. The painting was examined in normal and ultraviolet light and under a stereobinocular microscope. In addition, cross sections and pigment samples were taken. The cross sections taken from the painting were useful in determining the layered structure of the painting and how Veronese applied the paint. [For an example of a paint cross section showing layering structure, see Figure 6 of the previous chapter of this volume (37).] This technique

requires extremely small samples (generally ranging 0.5-1 mm in diameter) be taken. Samples containing as complete a representation of layering as possible are removed from areas adjacent to pre-existing structural damage (38). The samples are mounted in resin, ground and polished, and examined under a microscope. PLM is used to identify the individual pigment particles that make up paint layers (18). This technique requires that extremely small samples be taken from the surface of the painting. A small scraping of the top layer of paint is mounted on a microscope slide and viewed under a microscope with light polarizing capabilities. The pigment particles are examined under high magnification to determine standard particle characteristics, such as color, morphology, transparency, birefringence/isotropism, index of refraction, particle relief, pleochroism, polarization colors, and particle size (18). It is possible to identify the pigments in the sample by knowing the particular characteristics and then by comparing them with the characteristics of reference pigment samples. This technique should be confirmed with elemental analysis whenever possible in order to make a conclusive identification, as was done with these samples using pXRF analysis.

Madonna and Child with St. Elizabeth, the Infant St. John, and St. Catherine is oil on canvas and measures H. 40 5/8" (103.2 cm) x W. 61 3/4" (156.9 cm). The original canvas is a coarse, herring-bone-weave linen. The herring bone pattern runs horizontally and its texture is visible on the painted surface. The original canvas is lined to a finer, plain-weave, linen fabric. Canvas lining is done to paintings when the original canvas is structurally unsound and/or there is significant loss of adhesion between the paint layers and the original canvas (39).

The appearance of the paint is noticeably more colorful than the *Apollo and Daphne*, especially the sky which is bright blue. The canvas was prepared with a white ground layer that is probably gesso (gesso is calcium sulphate, gypsum, mixed with hide glue---typically rabbit-skin glue (11)). An imprimatura or toning layer was next applied over the entire gesso ground and provides a mid-tone for the composition. The paint is built up in thin layers, and the final effect depends upon interlayering of both transparent glazes and opaque scumbles (translucent light colored paint). The flesh and the red colors were underpainted in grisaille (gray) using a mixture of white and black paint, whereas the other parts of the painting were underpainted with white, blacks, and browns. The bright colors were built up with more opaque pigment and the darker colors were built up with transparent glazes. It is the combination of the layering that achieves the beautiful surface. The deep red glazes over the shadows in the dress and the brown glazes in the dark areas give the painting depth and contrast with the thicker more opaquely painted areas such as the sky, flesh, and garment details that have been highlighted with opaque touches of white and lead tin yellow. Polarized light microscopy on several samples from the painting indicated the presence of azurite blue (rather than smalt), lead tin yellow, vermilion, and possibly red lead (18). pXRF analysis (see Figure 3 for spot locations) revealed copper peaks and confirmed the presence of azurite (Figure 4), which is a copper-containing blue pigment. The occurrence of tin peaks (Figure 5) in the pXRF analysis was consistent with the presence of lead tin yellow (lead is present in all of the pXRF spectra, due to the use of lead white in the ground layer of paint). The presence of mercury and arsenic (Figure

6), was indicative of vermilion and either orpiment or realgar, respectively. Note that it was fortunate that the relative amounts of Hg and As relative to the Pb signals made the assignments possible (especially with curve fitting) even with the peak overlap issues present with these three elements (26, 36). [The Hg $L\alpha_2$ and $L\alpha_1$ lines at 9.90 and 9.99 keV respectively do not overlap with Pb or As lines or any other relevant element lines. The Pb $L\alpha_2$ and $L\alpha_1$ lines at 10.45 and 10.55 keV respectively overlap with the As $K\alpha_2$ and $K\alpha_1$ lines at 10.51 and 10.54 keV respectively; however, several other Pb lines in the spectrum do not overlap with any lines from elements that could reasonably be expected. The As $K\beta_2$ and $K\beta_1$ lines at 11.72 and 11.73 keV respectively overlap with the Hg $L\beta_2$ and $L\beta_1$ lines at 11.92 and 11.82keV respectively; however, perak deconvolution clearly resolved the As and the Hg.]

The *Madonna and Child with St. Elizabeth, the Infant St. John, and St. Catherine* was restored prior to its acquisition by the Timken. There are no large losses of ground or paint apparent. However, the painting has been cleaned in the past and has sustained solvent abrasion throughout the composition. The abrasion was carefully inpainted by a past restorer. The condition of the painting was assessed by the Balboa Art Conservation Center in 1996 and found to be satisfactory.

Apollo and Daphne

Condition Assessment

The painting of *Apollo and Daphne* was executed with oil paint on linen canvas. The original canvas measures H. 42 15/16" (109.1 cm) x W. 44 3/8" (112.7 cm); the overall size mounted onto the stretcher measures H. 43 1/16" (109.4 cm) x W. 44 1/2" (113.4 cm). The original canvas consists of two pieces of moderately heavy (10 warp/weft threads per cm), plain-, open-weave linen fabric with threads varying in thickness, butted together and sewn with thread to make a horizontal seam at H. 31 1/2". It was common practice to sew pieces of canvas together to make a larger painting surface because fabric looms only made certain widths of canvas. There are no tacking edges of the usual type remaining on the painting, but there is some evidence that this painting, like other known examples by the artist, may have been nailed to the front face of the stretcher. Apart from a slightly irregular pattern of cusping, there seem to be now-filled holes at regular intervals along the bottom and possibly right edge(s). The canvas shows cusping at the top, right, and bottom edges, but the left seems to be trimmed to a greater extent. X-radiographs taken by the BACC helped provide insight into this issue. As noted by Penny (40), Veronese at least occasionally nailed his canvases to the front face of the stretcher. Cusping (also sometimes termed scalloping) is the pattern produced in the weave of the canvas when it is prepared for painting. The canvas threads distort into a curved pattern along the edges because they are restrained by the tacks used to stretch the canvas (38, 41, 42).



Figure 3. Spot locations for the pXRF analysis of Veronese, *Madonna and Child with St. Elizabeth, the Infant St. John, and St. Catherine*.

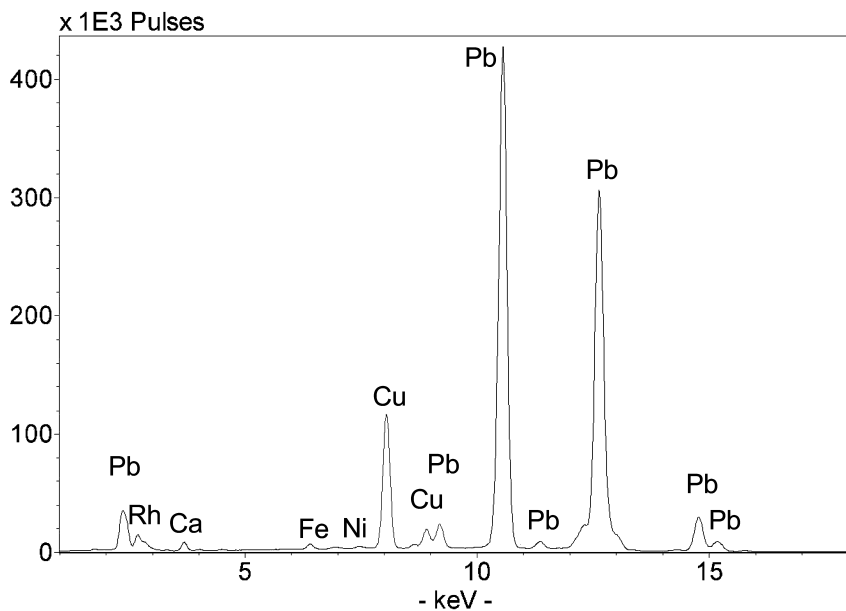


Figure 4. Veronese, *Madonna and Child with St. Elizabeth, the Infant St. John, and St. Catherine*. Blue sky featuring prominent Cu peak (confirmed as azurite by PLM) [spot 1].

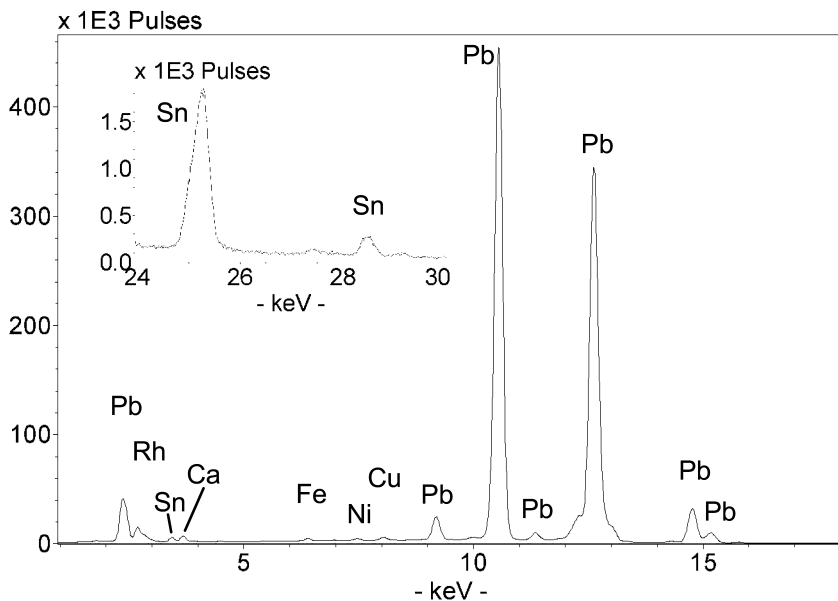


Figure 5. Veronese, *Madonna and Child with St. Elizabeth, the Infant St. John, and St. Catherine*. Bluish white and yellow dress area showing Sn (characteristic of lead tin yellow) [spot 5].

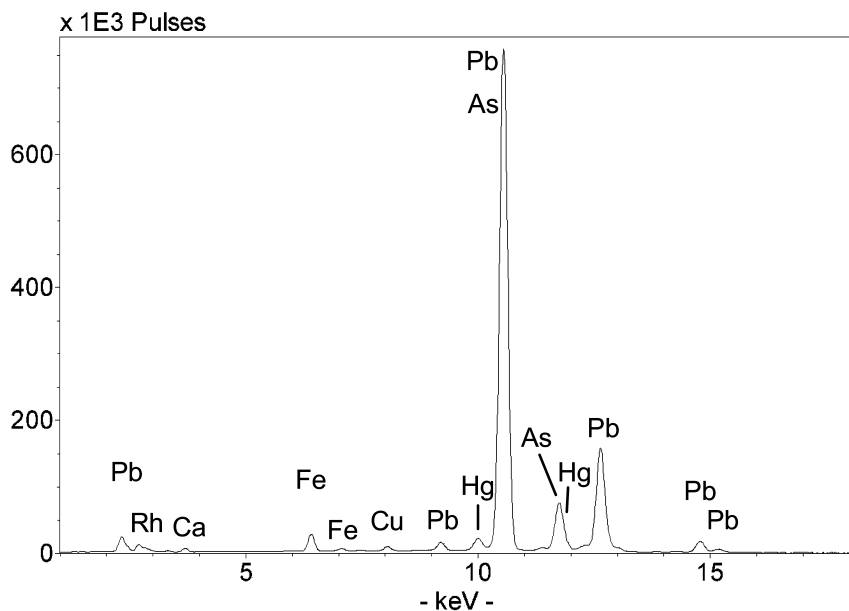


Figure 6. *Veronese, Madonna and Child with St. Elizabeth, the Infant St. John, and St. Catherine. Orange cloak featuring prominent Hg and As peaks (characteristic of vermilion and orpiment or realgar) [spot 2].*

Before painting, the canvas was prepared with a thin, aqueous (est.) ground or priming layer that does not conceal the texture of the canvas. The ground appears to be light-brown in color, although its appearance may also be darkened by penetration of glue or discolored varnish layers during its history. The paint is generally thin and ranged in application from thin transparent glazes to moderately thick soft paste with low impasto (more thickly applied paint that may retain brush texture or a three-dimensional appearance) (11). The x-radiograph revealed that the position of Daphne's outstretched arm and shoulder had been slightly changed as the artist worked out the composition. The sky appears to be an unusual beige or tan color rather than the expected blue. The color of the sky was one of the reasons the Curator and Conservators wanted further examination of the pigments to see whether this color was intentional or was a result of the aging of the materials.

The *Apollo and Daphne* painting has undergone multiple campaigns of restoration over its lifetime. This is typical for older paintings as the materials age and the paintings sustain damages. Most paintings in a museum have been restored at least once or twice. The most recent conservation/restoration treatment of this painting was conducted at the Balboa Art Conservation Center from 1981-1983. At that time the painting was examined and found to have suffered from extensive damage from past harsh cleaning (solvent abrasion) that had exposed the tops of many of the canvas threads throughout the composition, but especially in the background and the sky. In the past, powerful solvents and chemical reagents with the capacity to erode the original paint were often used

to remove layers of grime, discolored varnish, and darkened paint added by previous restorers. The solvent abrasion and other damages had been covered with restorer's paint that extended well beyond the areas of actual damage and had darkened with age. The non-original varnish was of a natural resin type that had also become yellow, and there were brownish remnants of an earlier varnish in the interstices of the weave that further detracted from the appearance of the painting. In addition to the compromised aesthetic appearance of the painting, it was structurally vulnerable. The original canvas was quite weak and had been torn in the past. It had been reinforced with two layers of linen attached to the reverse with animal skin glue perhaps 150 years earlier, but this lining had in turn become brittle and no longer gave the canvas adequate support.

The treatment at BACC in 1983 consisted of both aesthetic and structural steps. The discolored varnish and restorer's overpaint were removed to reveal the original colors. The cleaning involved using small cotton swabs to apply tailored mixtures of organic solvents that had been determined by testing under a binocular microscope to safely remove the non-original layers without further damaging the original paint. The old lining and lining adhesive were also carefully removed from the reverse, and the painting was relined to a stable synthetic fabric using a non-penetrating and reversible synthetic adhesive (BEVA 371, a proprietary poly(ethylene-co-vinyl acetate) from Adams Chemical). It was remounted onto a new self-adjusting spring stretcher. The painting was then brushed with an isolating layer of a stable synthetic varnish (Laropal K-80, a polycyclohexanone) that does not darken or turn yellow with age. [This varnish is no longer used at BACC because it may eventually cross-link. However, this is very slow under museum conditions, and it will remain safely removable in the future.] Losses were filled to the level of the original paint with gesso putty and inpainted with paint made from dry pigments mixed in the same resin to re-integrate the surface. The inpainting was confined to the actual areas of loss. Finally, a thin protective layer of the same varnish with the addition of a small amount of microcrystalline wax was sprayed on the surface to adjust the gloss. The condition of the painting is currently stable and satisfactory. [Readers new to paintings conservation might find six references particularly helpful in the context of this discussion (39, 43–47). For specific discussion of current conservation techniques and materials, visit the American Institute for Conservation of Historic and Artistic Works (AIC) (48).]

pXRF Analysis

Test spots (see Figure 7 for spot locations) in the sky of *Apollo and Daphne* (Spots 1, 2, and 12) were chosen from both lighter tan and darker brown areas shown by examination under ultraviolet light to be least likely to be contaminated by later inpainting (Because older varnish and older paint fluoresce differently under UV than newer varnish and newer paint, UV-induced visible fluorescence can be used to distinguish areas of inpainting.). All these sample locations showed a similar composition (e.g., Figure 8) with cobalt, iron, and arsenic as well as silicon (from the glass), indicative of smalt. They also each contain lead, indicative of lead white mixed with the (formerly) blue paint and calcium, presumably from

the calcium sulfate ground. In this instance, the discoloration of the smalt is extreme to the point that there is no longer any blue color visible. In the case of *Apollo and Daphne*, harsh treatment in the past has undoubtedly contributed further. Another test (Spot 8) was done in an area of the sky near the foliage on the left where a light blue color with a greenish tinge appeared to be original paint. This area contained lead, calcium, iron, silicon, cobalt, and arsenic, but also contained copper. The ratio of the peaks in Spot 8 to the peaks of Spots 1, 2, and 12 suggest that there is less cobalt and arsenic (therefore less smalt) and more of a copper containing pigment, possibly azurite.



Figure 7. Spot locations for the pXRF analysis of *Apollo and Daphne*.

Other areas of the painting that would not be expected to have cobalt were chosen for analysis to provide comparison with the cobalt-containing spectra and for general reference. Spot 3 was taken from an area in the pink dress. It contained

no cobalt, but a lot of lead from lead white. The red is likely to be a lake pigment (an organic pigment not detectable with pXRF). [Sometimes the aluminum of the substrate on which the organic dye is precipitated to produce the pigment can be detected under the conditions used in this study to obtain the pXRF spectra. However detecting aluminum can be challenging because it is a light element, and it is present as part of the instrument construction. For Spot 3, we could not be confident we were detecting aluminum above background levels.] Spot 9 from an area on Apollo's proper right thigh again contained no cobalt but lots of lead (lead white) with some iron, probably from an earth pigment. There is also a small amount of titanium (Ti), which is presumed to come from titanium white (the white pigment used for inpainting at BACC). This entire area has numerous tiny dots of inpainting that were difficult to avoid. Another test area in the sky (Spot 4, Figure 9) was chosen because it is a visual color match to the original areas found to contain smalt but is clearly an area of loss that is inpainted. This spot contained no cobalt but did contain titanium, presumed to come from titanium white, and iron, most likely from an earth pigment (ochre or umber), as well as a lot of calcium, presumably from the calcium carbonate fill. There was also some lead, although a much smaller amount than in the tests done on areas of original paint. It may be from original paint just outside the target area of inpainting or from residual original paint in the area of inpainted loss. The absence of cobalt in these samples reaffirmed its importance in the sky samples.

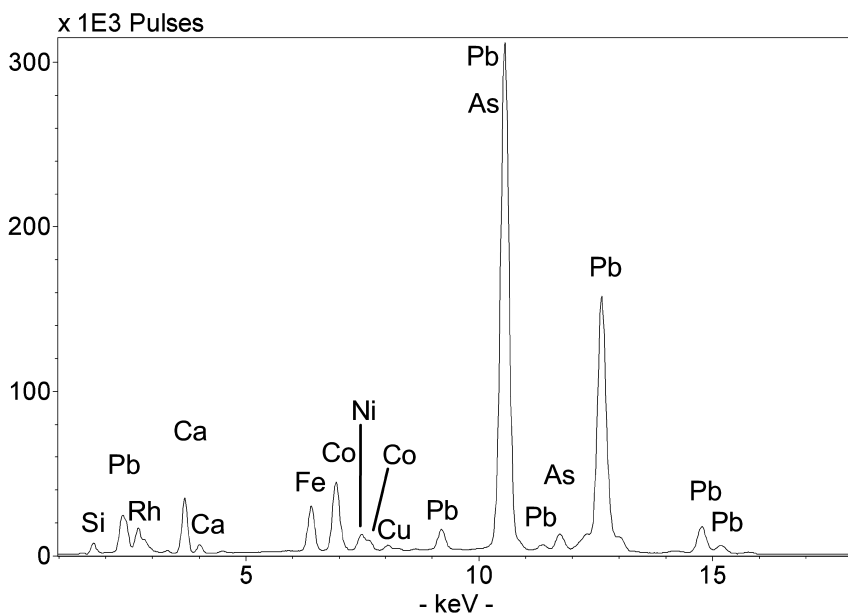


Figure 8. Veronese, Apollo and Daphne. Gray sky showing Co and As (both characteristic of smalt---cobalt glass) [spot 2].

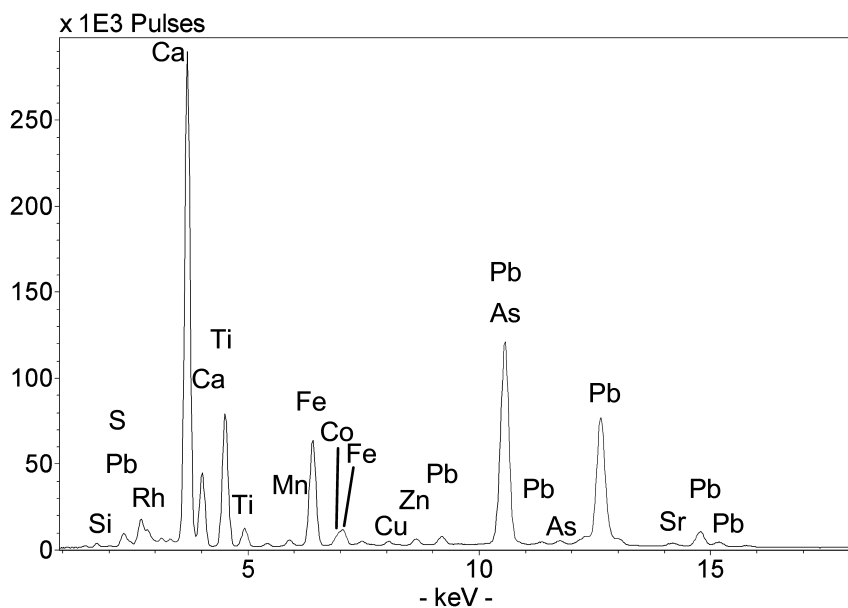


Figure 9. Veronese, *Apollo and Daphne*. Gray sky showing Ti (anachronistic titanium white---characteristic of inpainting) [spot 4].

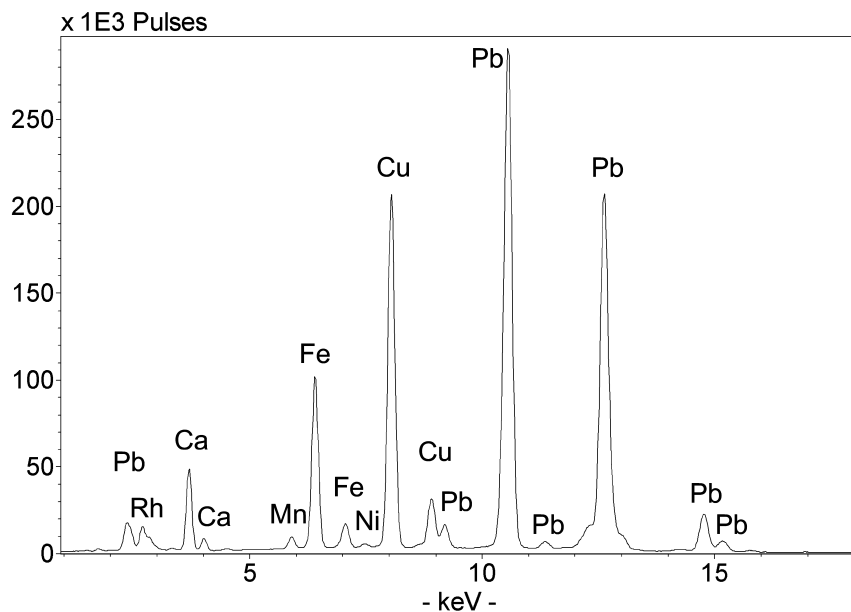


Figure 10. Veronese, *Apollo and Daphne*. Bown ivy on tree showing Cu (characteristic of discolored copper resinates) [spot 10].

The composition of the varying greens in the painting was also of interest. There are transparent brown leaves and foliage as well as more opaque green leaves and foliage. The transparent brown foliage (Spot 10, Figure 10) and the dark brown shadow of the hill (Spot 15) have similar spectra and associated peaks for Ca, Mn, Fe, Cu, Pb. The presence of copper in these samples suggests that they may be discolored copper resinate, although the organic resinate cannot be positively identified with pXRF. The opaque light green in the leaves of the central foliage (Spot 14) was found to contain Ca, Si, Fe, Co, Cu, Pb, and As. The copper in this instance could be from a green pigment like verdigris or malachite or even the blue pigment azurite mixed with a yellow pigment such as yellow ochre, possibly indicated by the fact that there appears to be more iron than is present in the original sky samples. The presence of cobalt and arsenic also points to the use of smalt, either as an admixture or a lower layer. The medium green of the hill (Spot 16) in the background has a similar composition to the light green leaf, but the medium green seems to have a higher proportion of cobalt and a lower proportion of copper. It is possible that this area also has either verdigris, copper resinate, malachite, or azurite and yellow ochre in mixtures with smalt or layered with smalt. The brown hill (Spot 5 and Spot 13) showed a similar composition to the other browns and greens - Ca, S, Fe, Cu, Co, As, Pb – with a larger amount of iron and some detectable sulfur. This indicates the use of earth pigments, a copper pigment (verdigris, copper resinate, azurite, malachite), smalt, and lead white. The calcium and sulfur peaks suggest the presence of calcium sulfate, which would be in the ground layer. In all of the brown and green samples, since lake pigments (organic dye stuffs) cannot be detected with pXRF spectrometry, it cannot be ruled out that a yellow lake is present, possibly mixed with smalt or azurite to create green. In all these cases, other techniques such as cross-sections and polarized light microscopy could give more conclusive answers about which pigments, layered or mixed, were actually used.

Lead was observed in all spots, consistent with lead white being used as an admixture in the paint layers or with lead white existing in layers beneath those analyzed. Spot 9 produced a good spectrum of lead white. Calcium was observed in all spots, consistent with calcium sulfate being used in the canvas preparation. Veronese was known to use a traditional gesso priming. The presence of manganese and iron are consistent with an earth pigment. Veronese's technique (1570's) often included a white ground layer with a thin brown imprimatura, traditionally made of black and earth pigments (23).

Conclusion

Collaboration between BACC, SDMA, The Timken, and W&L, has led to a fruitful examination of two Veronese paintings by handheld pXRF. The work reported here confirmed a curatorial and art conservation insight at BACC and SDMA that the Veronese *Apollo and Daphne* has undergone extensive smalt degradation (as well as changes in other pigments). This work extends relevant work reported from the National Gallery, London, in which some of Veronese's skies are pigmented by smalt (with varying degrees of degradation), while

others are pigmented by azurite. Combining pXRF spectroscopy with previous conservation studies by BACC of the two Veronese paintings enabled a deepened understanding of the two works. Knowing that the current appearance of the sky in *Apollo and Daphne* was not an artistic choice by Veronese (or a state of unfinished work), permits us to view the painting with renewed imagination, and to align Veronese's reputation for bright colors with the current state of the painting.

Acknowledgments

The authors wish to thank John Wilson, PhD., Executive Director of the Timken Museum of Art, for graciously permitting the project team to examine the Museum's *Madonna and Child with St. Elizabeth, the Infant St. John, and St. Catherine* 1565-70 for comparative purposes for this study. The NSF is gratefully acknowledged for recently funding non-destructive analytical instrumentation (NSF 0959625) at W&L that was used in the examinations reported here; the NSF is also thanked for funding Chemistry in Art Workshops for many years. W&L Lenfest summer grants and travel grants permitted course development and research travel. ESU's travel to BACC and the SDMA was made possible by funds from the W&L Dean of the College. A 2009 State Council of Higher Education for Virginia Outstanding Faculty Award assisted ESU in various aspects of these projects. ESU would like to thank all of the staff at BACC, SDMA, and the Timken who made his research visit possible, as well as Dr. Bruce J. Kaiser for pXRF support.

References

1. The reader should note that, because this is not a review paper, the references are not intended to be comprehensive, but should enable the reader new to paintings investigations to get into relevant literature.
2. Uffelman, E. S. *J. Chem. Educ.* **2007**, *84*, 1617–1624.
3. Uffelman, E. S. *J. Chem. Educ. online paper* **2007**, *84*, 38.
4. In *Partnerships and New Analytical Methodologies at the Interface of Chemistry and Art*, 241st American Chemical Society National Meeting, Anaheim, CA, March 27–31, 2011.
5. Uffelman, E. S. *International Council of Museums Conservation Committee Triennial 16th Conference*, Lisbon, Portugal, September 19–23, 2011; Criterio: Lisbon, Portugal, 2011; paper 312; 1-8.
6. Hill, P. S.; Simon, D.; Uffelman, E. S.; Bower, N.; Lagalante, A. F.; Norbutus, A. J. *American Institute for Conservation of Historic and Artistic Works 39th Annual Meeting*, Philadelphia, PA, 2011.
7. Rearick, W. R. *Paolo Veronese: His Life and Art*; National Gallery of Art, Washington and Cambridge University Press: Cambridge, England, 1988.
8. Cocke, R. *Paolo Veronese: Piety and Display in an Age of Religious Reform*; Ashgate Pub Ltd: Farnham, Surrey, U.K., 2002.

9. Ilchman, F. *Titian, Tintoretto, Veronese: Rivals in Renaissance Venice*; MFA Publications: Boston, 2009.
10. Salomon, X. F. *Paolo Veronese: The Petrobelli Altarpiece*; Silvana: Milan, 2009.
11. Doherty, T.; Woollett, A. T. *Looking at Paintings: A Guide to Technical Terms Revised Edition*; The J. Paul Getty Museum: Los Angeles, 2009.
12. Gantz, T. *Early Greek Myth: A Guide to Literary and Artistic Sources*; The Johns Hopkins University Press: Baltimore, MD, 1993.
13. Simpson, M. *The Metamorphoses of Ovid*; University of Massachusetts Press: Amherst, MA, 2001.
14. Muhlethaler, B.; Thissen, J. In *Artists' Pigments: A Handbook of Their History and Characteristics*; Roy, A., Ed.; Oxford University Press: New York, 1993; Vol. 2, pp 113–130.
15. Boon, J. J.; Keune, K.; Geldof, M.; Mensch, K.; Bryan, S.; van Asperen de Boer, J. R. J. *Chimia* **2001**, *55*, 952–960.
16. van der Weerd, J.; van Veen, M. K.; Heeren, R. M. A.; Boon, J. J. *Anal. Chem.* **2003**, *75*, 716–722.
17. Spring, M.; Higgitt, C.; Saunders, D. In *National Gallery Technical Bulletin*; Roy, A., Ed.; National Gallery/Yale University Press: London, 2005; Vol. 26, pp 56–70.
18. Eastaugh, N.; Walsh, V.; Chaplin, T.; Siddall, R. *Pigment Compendium: A Dictionary and Optical Microscopy of Historical Pigments*; Butterworth-Heinemann: Oxford, 2008.
19. Robinet, L.; Neff, D.; Bouquillon, A.; Pages-Camagna, S.; Verney-Carron, A.; Etcheverry, M.-P.; Tate, J. In *ICOM-CC 15th Triennial Conference New Delhi 22-26 September 2008 Preprints*; Bridgland, J., Ed.; Allied Publishers Pvt, Ltd: New Delhi, 2008; Vol. 1, pp 224–231.
20. Robinet, L.; Spring, M.; Pages-Camagna, S.; Vantelon, D.; Trcera, N. *Anal. Chem.* **2011**, *83*, 5145–5152.
21. Spring, M. Investigation of the degradation of smalt in paintings using multiple synchrotron and laboratory techniques. In *SR2A: Fourth edition of Synchrotron Radiation in Art and Archaeology*; Amsterdam, 2010.
22. Penny, N.; Spring, M. In *National Gallery Technical Bulletin*; Roy, A., Ed.; National Gallery Publications: London, 1995; Vol. 16, pp 5–29.
23. Penny, N.; Spring, M. In *National Gallery Technical Bulletin*; Roy, A., Ed.; National Gallery Publications: London, 1996; Vol. 17, pp 32–55.
24. Penny, N. *National Gallery Catalogues The Sixteenth Century Italian Paintings Volume II Venice 1540-1600*; National Gallery Company Limited: London, 2008; Vol. 2.
25. Hommes, M. v. E. *Changing Pictures: Discoloration in 15th-17th Century Oil Paintings*; Archetype: London, 2004.
26. Namowicz, C.; Trentelman, K.; McGlinchey, C. *Powder Diffraction* **2009**, *24*, 124–129.
27. Trentelman, K.; Bouchard, M.; Ganio, M.; Namowicz, C.; Patterson, C. S.; Walton, M. *X-Ray Spectrometry* **2010**, *39*, 159–166.
28. Woll, A. R.; Bilderback, D. H.; Gruner, S.; Gao, N.; Huang, R.; Bisulca, C.; Mass, J. L. In *Materials Research Society Symposium Proceedings*; Vandiver,

- P. B., Mass, J. L., Murray, A., Eds.; Materials Research Society: Warrendale, PA, 2005; Vol. 852, pp 281–290.
29. Woll, A. R.; Mass, J.; Bisulca, C.; Huang, R.; Bilderback, D. H.; Gruner, S.; Gao, N. *Appl. Phys. A* **2006**, *83*, 235–238.
 30. Mass, J.; Bisulca, C. *Antiques and Fine Art* **2010** Summer/Autumn, 222–223.
 31. Janssens, K.; Dik, J.; Cotte, M.; Susini, J. *Acc. Chem. Res.* **2010**, *43* (6), 814–825.
 32. Alfeld, M.; Janssens, K.; Dik, J.; de Nolf, W.; van der Snickt, G. *J. Anal. At. Spectrom.* **2011**, *26*, 899–909.
 33. Kaiser, B. J.; Wright, A. *Draft Bruker XRF Spectroscopy User Guide: Spectral Interpretation and Sources of Interference*; Bruker: Coventry, 2008.
 34. Shugar, A. N.; Mass, J. L. *Handheld XRF for Art and Archaeology*; Lueven: Belgium, 2012.
 35. Pinna, D.; Galeotti, M.; Mazzeo, R. *Scientific Examination for the Investigation of Paintings. A Handbook for Conservator-restorers*; Centro Di della Edifimi srl: Firenze, Italy, 2009.
 36. Bearden, J. A. In *CRC Handbook of Chemistry and Physics: A Ready-Reference Book of Chemical and Physical Data*, 60th ed.; CRC Press, Inc.: Boca Raton, Florida, 1979; pp E152–E190.
 37. Bradley, L. P.; Meloni, S.; Uffelman, E. S.; Mass, J. L. Technical Examination and Treatment of a Painting by Gijsbert Gillisz d'Hondecoeter. In *Collaborative Endeavors in the Chemical Analysis of Art and Cultural Heritage Materials*; Lang, P. L., Armitage, R. A., Eds.; ACS Symposium Series 1103; American Chemical Society: Washington, DC, 2012; Chapter 16.
 38. Kirsh, A.; Levenson, R. S. *Seeing Through Paintings*; Yale University Press: New Haven, 2000.
 39. Nicolaus, K. *The Restoration of Paintings*; Konemann: Cologne, 1998.
 40. Penny, N. In *National Gallery Catalogues The Sixteenth Century Italian Paintings Volume II Venice 1540-1600*; National Gallery Company Limited: London, 2008; Vol. 2, p 430.
 41. Wetering, E. v. d., *Rembrandt: The Painter at Work*; Amsterdam University Press: Amsterdam, 1997.
 42. Johnson, C. R. J.; Hendriks, E.; Noble, P.; Franken, M. In *Advances in Computer-Assisted Canvas Examination: Thread Counting Algorithms*; Buckley, B., Ed.; AIC Paintings Specialty Group Postprints 22: Los Angeles, 2009.
 43. Berger, G. A.; Russell, W. H. *Conservation of Paintings: Research and Innovations*; Archetype: London, 2000.
 44. Wolbers, R. *Cleaning Painted Surfaces: Aqueous Methods*; Archetype: London, 2000.
 45. Dorge, V. *Solvent Gels for the Cleaning of Works of Art: The Residue Question*; The Getty Conservation Institute: Los Angeles, 2004.
 46. Townsend, J. H.; Doherty, T.; Heydenreich, G.; Ridge, J. *Preparation for Painting: The Artist's Choice and Its Consequences*; Archetype Publications, Ltd.: London, 2008.

47. Ellison, R.; Smithen, P.; Turnbull, R. *Mixing and Matching: Approaches to Retouching Paintings*; Archetype Publications Ltd.: London, 2010.
48. *AIC Collaborative Knowledge Base*; www.conservation-wiki.com (January 10, 2012).

Chapter 4

Characterization of the Binders and Pigments in the Rock Paintings of Cueva la Conga, Nicaragua

R. Li,¹ S. Baker,² C. Selvius DeRoo,³ and R. A. Armitage^{*,1}

¹Chemistry Department, Eastern Michigan University,
501 W Mark Jefferson, Ypsilanti, MI 48197

²Archaeological/Historical Consultants,
609 Aileen St., Oakland, CA 94609

³Conservation Department, Detroit Institute of Arts,
5200 Woodward Ave., Detroit, MI 48202

*E-mail: rarmitage@emich.edu

Cueva la Conga is the first limestone cave with paintings and modified speleothems found in Nicaragua. Dating of images made with inorganic pigments generally requires the presence of an organic binder. Chemical characterization of the organic material in the paint was undertaken using thermally assisted hydrolysis/methylation-gas chromatography-mass spectrometry (THM-GC-MS). Results show that significant quantities of organic material are present in the rock itself, precluding dating of the paints based on binders. Some of the inorganic paints, however, contain traces of charcoal, possibly from calcination of the iron oxide pigments to change their color. We have successfully dated charcoal from the paintings using plasma-chemical oxidation and accelerator mass spectrometry. This study considered the composition of the substrate when sampling of the rock art to be dated, and emphasizes the importance of rigorous sampling protocols in analysis of rock art.

Introduction

The Cueva la Conga rock art site in Nicaragua has only been known outside its local area since 2006, when it was recorded by archaeologists from the United States (1). The site is located in northern Nicaragua, in a region of that country where few archaeological studies have been carried out. This is due, in part, to the isolation of the area, in the mountains near the Honduran border. In 2009, we undertook a small expedition to Cueva la Conga to collect samples from the paintings found there, in hopes of determining the age of the paintings, thereby placing them into a chronological context. The cultural implications of dating the rock art of Cueva la Conga and its importance as a ritual cave are described elsewhere (2). Here, we focus on the scientific study of the materials used to create the paintings. In particular, we were interested in determining the nature of any organic material in the paints, which would aid in the radiocarbon dating of the paintings.

Direct radiocarbon dating of rock paintings using plasma-chemical oxidation (PCO) and accelerator mass spectrometry (AMS) was pioneered by the Rowe group at Texas A&M University in the 1990s (3). Charcoal pigments are often observed, and are considered more reliable for dating, as charcoal can generally be identified microscopically. Many charcoal images from around the world have been radiocarbon dated with the PCO method developed by the Rowe group (4–7). Applying PCO-AMS to inorganic pigmented paints requires that an organic binder or vehicle was used in the paint, and that the binder/vehicle remains to the present day. Furthermore, because rock painting samples consist primarily of substrate rock, any organic material originating from the substrate must be insignificant.

The problem of substrate contamination is the most significant. To address the issue, samples of both paint and unpainted substrate rock have been collected for some studies. We have found that in at least one case in Guatemala, the substrate was heavily contaminated, casting significant doubt on the dates obtained from two other paint samples at that site (8, 9). Paint and substrate samples for that study were not collected systematically. When the Cueva la Conga project was undertaken, we carefully planned collection of matched samples of paint and substrate for a comprehensive analysis to support any attempts at dating.

Materials and Methods

Rock Painting Samples

In January 2009, two of us (SB and RAA) traveled to Cueva la Conga to collect paint samples in hopes of obtaining radiocarbon dates and identifying the pigments and materials used. Five samples of charcoal and six of inorganic pigmented paints were collected (Table I), all but two of which had unpainted substrates removed as well. Those two samples, from red handprints, were very thick paint that flaked off without significant substrate attached. Figure 1 shows the rock paintings sampled; of particular note is the variety of colors and motifs displayed amongst the paintings. Each sample was removed with a new sterile scalpel blade onto clean aluminum foil that had been baked at 500°C overnight to remove oils;

they were then wrapped in additional foil and sealed into individual labeled zip-top plastic bags. Samples were documented with photographs before and after sampling.

Microscopy Methods

Each sample of paint and substrate was visually inspected at 20x magnification under visible light. Any foreign matter, including fibers and insect parts, was removed prior to further analysis. Two of the samples, 5 and 9, contained charcoal inclusions in the red paints, and were further subjected to scanning electron microscopy. This was carried out by Dr. Glenn Walker of the EMU Biology Department, using an Amray 1820I SEM at 5 kV on gold-coated paint fragments.

X-ray Fluorescence Spectroscopy

Micro-XRF spectroscopic analyses were carried out in the Conservation Department at the Detroit Institute of Arts. The instrument used was a Bruker AXS ARTAX with a Mo source at 50 keV and 700 μ A with no filter. A 0.2 mm collimator was utilized with a helium purge. Acquisition times ranged from 120 to 300 seconds.

Thermally Assisted Hydrolysis/Methylation-Gas Chromatography-Mass Spectrometry

Gas chromatography-mass spectrometry (GC-MS) has been used to look for lipids—indicative of binder—in rock paintings (10). Pyrolysis-GC-MS has also been used to identify patinas associated with rock paintings and to look for the presence of binders (11–13). We used thermally assisted hydrolysis methylation (THM)-GC-MS, a modified pyrolysis method, to rapidly screen the mineral-pigmented paints to determine if binders were present, and to evaluate the efficacy of pretreatment on the charcoal paints. THM-GC-MS is a good method for rapid comparisons of the organic content of small samples like those from Cueva la Conga because the method is fast, requires little sample preparation and is nonselective, yielding results for lipids, amino acids, and carbohydrates at the same time.

A Varian 3800 gas chromatograph with a Saturn 2000 mass spectrometer was used for the analyses. The GC was equipped with a Varian Chromatoprobe and 1079 inlet which allowed for temperature programming of the injection port. Submilligram portions of the paint and substrate samples were weighed into Chromatoprobe vials, to which was added two microliters of internal standard-derivatizing agent mixture. This mixture was prepared from 5 μ L of a primary internal standard (5 ± 0.01 mg tri-*t*-butylbenzene in 1 mL of methanol), combined with 1 mL of 10% TMAH in methanol. The vial was placed into the Chromatoprobe and then into the GC inlet.

The inlet was cryogenically held at an initial temperature of 40°C for 0.1 minutes, then temperature programmed to 84°C at a rate of 200°C/min and held for 1.00 min at 100% split to evaporate any excess methanol. After this initial

drying step, the temperature was ramped to 300°C at a rate of 200°C/min; this is the temperature at which THM occurred. Each of the samples was run under splitless conditions. An initial eight minute solvent delay was used at the start of each GC analysis to prevent exposing the MS filament to excess TMAH.

Separation was carried out on a Varian VF-5ms column (30 m long, 0.25 mm i.d., 0.25 μm film thickness). Helium (99.999%) was used as the carrier gas, at a pressure of 40 psi. Mass spectra were collected in electron impact mode from m/z 35-650. The ion trap was maintained at 150°C for the duration of the analysis. At the start of each day, a blank consisting of a Chromatoprobe vial with 2 μL of the TMAH containing internal standard was run under the described conditions. Then the samples were run; this allowed us to correct for any contamination in the system. Each sample was run only one time, but the residue was retained for future replicate analyses.

Table I. Description of samples from Cueva La Conga

<i>Sample</i>	<i>Location and description</i>
Paint 1	Charcoal from “anthropomorph” figure on Panel 6, (two samples removed)
Substrate 1	Substrate from small pocket in rock to left of anthropomorph
Paint 2	Charcoal from upside-down anthropomorph on Panel 9,
Substrate 2	Substrate from next to Paint 2
Paint 3	Charcoal from fragmentary images in Panel 3, removed from scratches on wall
Substrate 3	Substrate from scratch without charcoal present
Paint 4	Charcoal, possibly from torch smudges, on Panel 7 (not dated)
Substrate 4	Substrate removed from lower vesicle without charcoal
Paint 5	Purple-red paint fragment isolated in vesicle, from red circle on Panel 6
Substrate 5	Substrate from nearby vesicle without paint
Paint 6	Orange paint from complex geometric figure on Panel 4
Substrate 6	Substrate from near orange geometric figure
Paint 7	Red paint from red line spanning Panels 2 and 3
Substrate 7	Substrate from below red line
Paint 8	Yellow paint from handprint underlying red line (#7) on Panels 2 and 3
Substrate 8	Substrate from next to yellow handprint
Paint 9	Red paint flake from handprint in Panel 12
Paint 10	Red paint flake from handprint in Panel 14

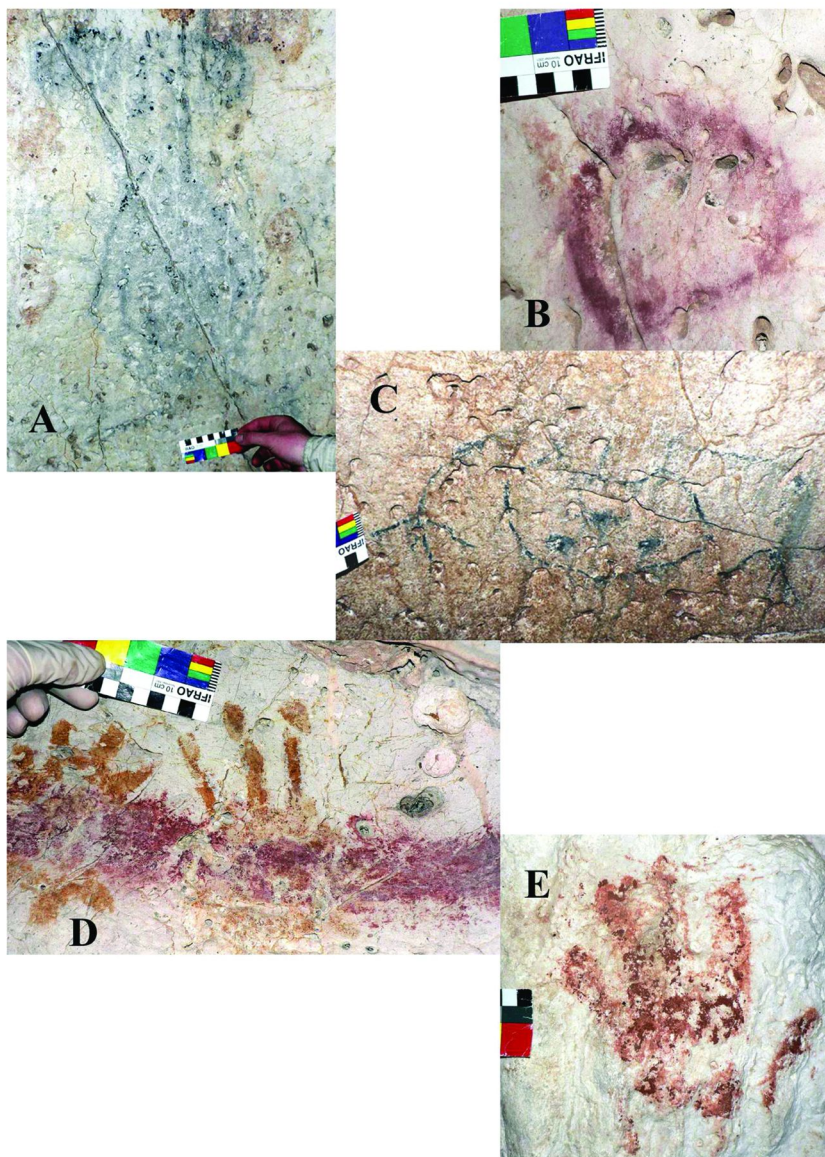


Figure 1. Photographs of some of the sampled rock paintings from Cueva la Conga: (A) Sample 1 charcoal anthropomorph; (B) Sample 5 red circle; (C) Sample 2 anthropomorph; (D) Samples 7 and 8, red line and yellow handprint; (E) Sample 9 red handprint.

Plasma-Chemical Oxidation and AMS Radiocarbon Dating

The remaining paint and substrate samples were further divided to obtain samples nearly matched in mass prior to wet chemical pretreatment and PCO-AMS. While the standard pretreatment generally consists of an acid wash to remove carbonates, a base wash to remove humic acids, and a final reacidification step to prevent adsorption of atmospheric carbon dioxide (14), we used a modified procedure developed in our laboratory that is less destructive. All samples and substrate samples were weighed into clean microcentrifuge tubes, and combined with 1 mL of phosphate buffer (1 M in phosphate ion, pH (8)). Samples were ultrasonicated at $50 \pm 5^\circ\text{C}$ for 60 min. Yellow color in the solution was considered indicative of dissolved humic acids; phosphate washes were repeated until the resulting solution was clear following the ultrasonication step.

The material resulting from the cleaning step was filtered using glassware and binder-free borosilicate glass filters that had been baked overnight at 500°C . The material was rinsed with deionized water and dried on the filter. For plasma-chemical oxidation, the filter was placed directly into the plasma-chemical oxidation chamber. The chamber was maintained at a vacuum pressure of $\sim 10^{-7}$ Torr. Vacuum integrity checks (VICs) prior to plasma-chemical treatment indicated that no significant leaks were present in the system. We assume, as a worst case scenario, that all pressure increase during the 60-min VIC arises from carbon dioxide; as long as the pressure increase corresponds to less than the contamination background in the accelerator mass spectrometer (typically 0.5-1 $\mu\text{g C}$), the increase is considered inconsequential. Oxygen gas was of ultra-high purity grade (99.999+ %). The oxygen plasma has been shown to react with organic carbon in the paint samples at a sufficiently low temperature ($\sim 150^\circ\text{C}$) that the inorganic oxalates and carbonates present are unaffected.

Table II. Pretreatment and plasma conditions

<i>Sample</i>	<i>Pretreatment</i>	<i>Oxygen plasma conditions</i>	<i>Yield, $\mu\text{g C as CO}_2$</i>
Paint 1	9x phosphate	50 W, 39 min	260
Paint 2	5x phosphate	50 W, 52 min	90
Paint 3	10x phosphate	50 W, 35 min	275
Paint 5	none	50 W, 41 min	200
Paint 5	2x phosphate	100 W, 60 min	200
Paint 9	none	50 W, 40 min	250
Paint 9	3x phosphate	100 W, 60 min	110

Ideally, 100 μg of carbon as carbon dioxide is preferred to obtain a reliable radiocarbon date. If at least 60 μg C was produced from a paint sample, it was collected by cooling a glass finger on the plasma system with liquid nitrogen. The glass tube was then sealed off and sent to the Center for Accelerator Mass Spectrometry at the Lawrence Livermore National Laboratory for radiocarbon analysis. Pretreatment and plasma conditions for the Cueva la Conga samples are listed in Table II.

Results and Discussion

Microscopy

The samples that were presumed in the field to be charcoal were inspected at 20x under visible light, and all four of the purported charcoal samples were confirmed to be charcoal. For additional information, samples of the charcoal were selected and sent to Caroline Cartwright, a microscopist and botanical specialist at the British Museum to determine the possible source of the charcoal. Dr. Cartwright is a wood anatomist and has extensive experience with Mesoamerican materials. She has determined that the charcoal pigmented images derive from three botanical sources: *Hymenaea courbari*, locally known as Jatobá; *Pinus* species; and *Pithecellobium* species. The possible cultural implications of the use of these plants are described elsewhere (2).

Microscopic examination of the inorganic pigmented samples showed primarily fibers, spider webs, insect parts, etc. Paint sample 7 contained green, algae-like material. Ms. Maria Goodrich examined wet-mounted samples under immersion microscopy at high (400x and 1000x) magnification, and concluded that the material is most likely derived from filamentous cyanobacteria. Cyanobacteria, which probably make up the thick biofilm covering the speleothems at the large entrance to Cueva la Conga, are also common when light levels are very low. Heterotrophic bacteria are ubiquitous in cave environments. This is problematic from the standpoint of radiocarbon dating rock art: significant extraneous organic material in the paint not associated with the painting event will render any date obtained meaningless at best, and misleading in cultural interpretations at worst.

Far more promising from a dating standpoint, paint samples 5, 9 and 10 were all observed to contain charcoal inclusions. Pieces of charcoal can be seen protruding from the surrounding mineral pigment, indicating that the charcoal is not superficial, and does not derive from torches or soot. Figure 2 shows an electron micrograph of a charcoal inclusion in paint sample 9. The cellular structure of the wood is clearly visible in the mineral matrix.

While there might be cultural reasons to add charcoal to mineral pigment, there are no binding or extending properties that would suggest its use in red or yellow rock paintings. There are further no reports in the literature of charcoal being found in such a manner in rock painting samples. We propose that preparation of the pigments may have led to the charcoal being incorporated into the paint. Changing colors of mineral pigments through roasting is a well-known practice in the art field. An example is the pigment umber, a mixed

iron-manganese oxide and clay mineral. Raw umber is a light brown color; heating raw umber removes water from the mineral, yielding a warmer, darker brown of burnt umber. This process of calcining iron oxide pigments to change their color has been known since antiquity (15). Because the charcoal inclusions were only observed in the darkest paints from Cueva la Conga, we believe that lighter iron oxide pigments were heated in an open fire to change their color. When the cooled mineral was removed from the hearth and ground to prepare the paint, charcoal from the heating process was incorporated incidentally.

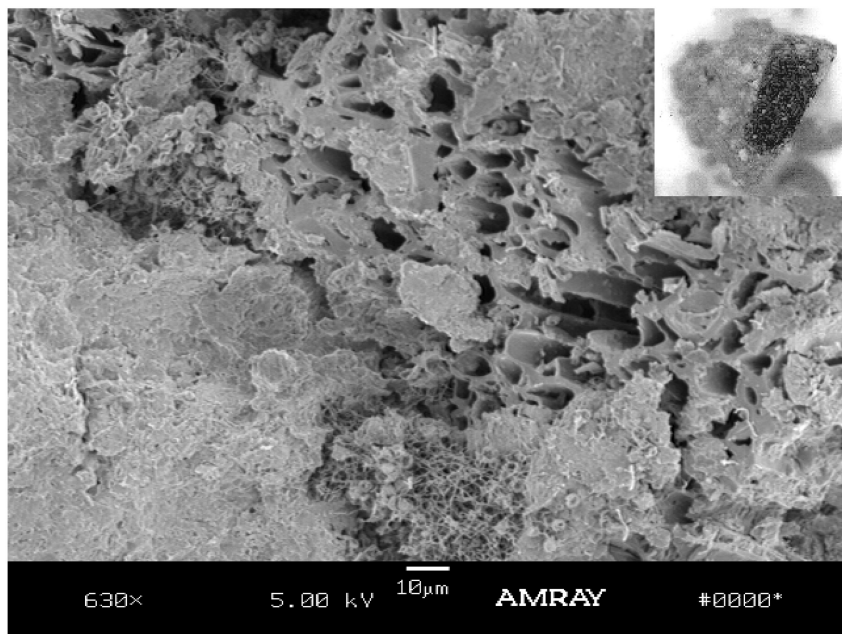


Figure 2. Electron micrograph showing charcoal inclusion in paint from red handprint in Panel 12. Inset shows the black charcoal inclusion in a portion of the paint sample.

X-ray Fluorescence Results

The results from the x-ray fluorescence analysis (Table III) support the calcination hypothesis. All of the pigments are primarily iron oxides, with significant contribution from the limestone substrate. Only one sample (5, which was nearly pure paint) did not show significant calcium from the underlying limestone. The titanium and silicon present are likely indicative of sand inclusions. Clays (aluminum phyllosilicates) do not appear to have been added to the paints as an extender, as the aluminum content of the pigments is negligible.

Table III. Elemental compositions of Cueva La Conga paint samples

<i>Paint sample</i>	<i>Acquisition time, s</i>	<i>Major components</i>	<i>Trace components</i>
5	240	Fe	Ca, Si, Br, Ti (possibly)
6	300	Fe, Ca	K, Ti, Si, Mn
7	300	Fe, Ca	K, Ti, Si, Mn, Zn, Br, As(?)
8	300	Fe, Ca	Ti, Mn, Si, K, Al (?)
9	300	Fe, Ca	Cu, Zn, Mn, Cr, P(?), Br
10	300	Fe, Ca	Ti, Si, Mn

THM-GC-MS Results

The primary goal of the THM-GC-MS analysis was to determine whether there were significant differences between the compositions of the paint and substrate samples. Ideally, the organic substances would be found only in the paint samples. Simply put, this was not the case for the samples from Cueva la Conga. The three classes of compounds indicative of binders – proteins, carbohydrates, and fatty acids – are discussed separately.

Proteins are cleaved into amino acids and derived into their corresponding N- and O-methyl esters by TMAH. The identity of these compounds was confirmed by running standards of each naturally occurring amino acid under our analysis conditions to build a user database, which was compared to literature spectra for additional confirmation (16). Only four amino acids – alanine, leucine, threonine, and glutamic acid – were observed in any of the samples. When these amino acids were present, they were not isolated in the paint, but present also in the substrate. This strongly indicates that proteinaceous binders were not likely used in Cueva la Conga, or they did not survive to the present day.

Carbohydrates are broken into monosaccharides and further converted to methyl ether and ester derivatives during the process. Unfortunately, the resulting compounds are not clearly diagnostic of specific monosaccharides. Instead, multiple compounds that can be characteristic of pentoses and hexoses are formed. Fabbri and Helleur (17) showed that several compounds and their relative ratios can be used to identify monosaccharides. To confirm that these compounds were formed during THM-GC-MS under the conditions we used, we ran seven monosaccharides standards (glucose, fructose, ribose, xylose, galactose, arabinose and mannose) and found that each monosaccharide does indeed yield several peaks, making the identification of any single sugar complex. A few compounds were selected as markers for sugars, including 2, 4-dimethoxybutanoic acid methyl ester and the permethylated saccharinic acids. The paint and substrate pairs for samples 6 and 7 were of the same composition; for sample pairs 5 and 8, two of the carbohydrate markers were found in the substrates while only one was observed in the paints. This indicates that carbohydrate-based binders either were not used or did not survive at Cueva la Conga.

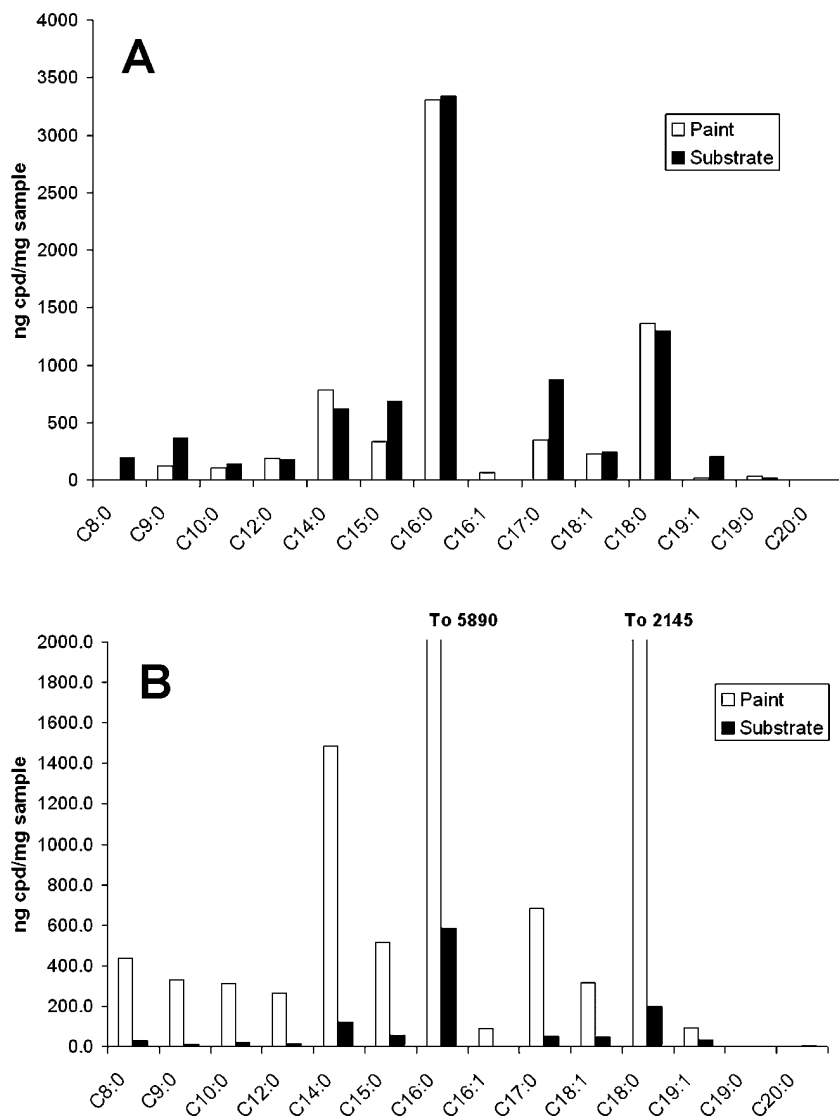


Figure 3. Graphs showing the comparative fatty acid composition of (A) Sample 5 and (B) Sample 7.

The compositions of the paint samples were dominated by saturated and unsaturated fatty acids ranging from C_{8:0} to C_{18:0}, as their methyl esters. The most common fatty acids identified were saturated C₉ and C₁₇, even-carbon chains from C₁₀ through C₁₈, and monounsaturated C₁₈. Nonanedioic acid, present as the dimethyl ester, was identified in both the paints and substrates of paint samples 7 and 8. Decanedioic acid, also as the dimethyl ester, was detected in both the

paint and substrate of paint sample 7. These compounds are formed from the decomposition of C₁₈ and C₂₀ fatty acids, respectively.

Fatty acids were also observed in blank runs, so a semi-quantitative analysis of each run was carried out using the mass of the internal standard. The mass of each compound was then corrected for the mass of sample used, and the blanks were subtracted from each sample. The corrected amount of each fatty acid derivative was plotted on a bar graph for comparison of the paint and substrate compositions. Figure 3a shows the fatty acid bar graph for sample 5; the graphs for samples 6 and 8 are generally identical. With a single analysis, no error bars can be drawn, but the general pattern of similarity between the fatty acid composition of the paint and substrate is readily observed. In the case of the paint and sample pair 7, a different trend is observed (Figure 3b). This may indicate that something like animal fat, now heavily degraded, might have been used as a binding medium by the artists of Cueva la Conga in the case of paint sample 7. In order to test this hypothesis, we compared the fatty acid composition of that sample to that of an animal fat prepared as a paint for another study in our laboratory several years ago.

We can only reliably say what the samples are not. It is impossible to test every possible binder, so positive identifications are not something that can be made definitively. Differences are more significant than similarities. For example, many more dicarboxylic acids were observed in the animal fat in large quantities, yet were not observed in any significant amount in paint 7.

Table IV. Ratios of fatty acids for distinguishing food residues (18) compared to animal fat standard and Cueva la Conga paint 7

<i>Ratio</i>	<i>Degraded fat from terrestrial mammals</i>	<i>Animal fat standard</i>	<i>Paint 7</i>	<i>Degraded fat from fish</i>
$(C_{15:0}+C_{17:0})/C_{18:0}$	<0.2	0.18	0.68	0.2–0.5
$C_{16:1}/C_{18:1}$	0.08–0.8	0.06	0.39	0.8–2.0
$C_{16:0}/C_{18:0}$	<7	1.95	3.16	8–12
$C_{12:0}/C_{14:0}$	<0.15	0.02	0.18	<0.15

Sometimes the relative amounts of different compounds can be informative about determining the source of fatty acids in archaeological materials. Eerkens (18) used the ratios between different fatty acids – specifically C_{12:0}, C_{14:0}, C_{15:0}, C_{16:0}, C_{17:0}, C_{16:1}, C_{18:1} and C_{18:0} – to classify food residues in pottery based on their sources using experimental archaeology, by cooking different materials in pots and then studying the composition of the total lipid extracts. Table IV shows Eerkens’ literature values for the different diagnostic ratios for degraded terrestrial mammal fat and fish oil; the observed ratios for our animal fat standard and paint 7 are shown for comparison.

The fatty acid ratios for paint 7 were not completely consistent with animal fat, although our animal fat standard was nearly consistent with the composition defined by Eerkins' study. This is further evidence that paint 7 does not likely contain degraded animal fat as a binder. For comparison, the composition of paint 7 is completely different from that of the fats in fish. We can unequivocally state, then, that fish oils were not used as binders in this paint. While it may be less satisfying to say what the composition does not correspond to, we can only confidently rule out substances that are significantly different.

For the other samples, the organic compounds in each pair of paint and substrate are overall generally consistent. This comparison is important because it indicates that the origin of these organics is unlikely to come from some binding medium. If the samples contain organic material that does not appear to originate from a paint binder, the question follows: then where does it come from? The other compounds observed in the chromatograms may provide some clues.

Benzoic acid was observed in all of the Cueva la Conga samples. One source of the benzoic acid may be soil humic and fulvic acids. Benzoic acid has been observed as a significant thermochemolysis product of fulvic acids (19), which are readily carried in water. Cueva la Conga is an active cave which is generally dry, although a ceiling drip was observed by Baker (1) during the rainy season. This dripping water within the cave may deposit fulvic acids on the limestone surfaces, or the fulvic acids may be derived from airborne soil particulate matter.

A great number of the fatty acids identified in our samples further support a humic or fulvic origin for most of the organic material observed. THM-GC-MS of the organic matter in natural waters from tropical climates has shown significant quantities of fatty acid methyl esters, with hexadecanoic acid and octadecanoic acid methyl esters predominating, and other monounsaturated and branched chain fatty acids also present (20).

The large number of long chain fatty acid methyl esters and the presence of phenolic compounds (like benzoic acid and methoxybenzene compounds) observed in our chromatograms is consistent with results obtained by others using pyrolysis with TMAH to characterize humic macromolecules. Patterns similar to the ones we have observed were found also by Martin et al. (19) and Chefetz et al. (21) in studies of humic acids extracted from soil. Fezzey and Armitage observed the same pattern in a residue associated with rock paintings at a cave in Idaho as well (12). It is likely that humic acids on the limestone walls of Cueva la Conga originate from the soils therein. Some of the cave walls were exceedingly dirty, as the damp walls readily collect the light, easily disturbed soil. Carbohydrates found in the samples are most likely derived from the humin, also a component of soil (19, 22).

Plasma-Chemical Oxidation and AMS Radiocarbon Dating Results

The results of the PCO-AMS radiocarbon dating are summarized in Table V. The charcoal samples (1–3) produced a strong “green” or “earthy” smell when pretreated. This comes from the presence of the compounds geosmin and 2-methylisoborneol, earthy or musty smelling organic compounds produced by many different microbes including cyanobacteria. Several pretreatments were

used on these samples to remove this contamination. THM-GC-MS analysis showed that these two odor compounds were present prior to pretreatment, but were not detectable afterward. Sample 4 was saved for future analysis, as it was not directly associated with a painting.

Table V. Radiocarbon dating results for Cueva la Conga samples (BP = before present, where present is defined by radiocarbon convention as 1950 A.D.). Calibrations were carried out with Calib 6.0 (online) (23)

<i>Sample</i>	<i>CAMS ID</i>	<i>Radiocarbon age, years BP</i>	<i>Calibrated age range (2σ range, % probabilities)</i>
Paint 1	142211	675 \pm 30	cal AD 1260- 1300 (94.3%) cal AD 1370-1380 (5.7%)
Paint 2	142210	345 \pm 45	cal AD 1400-1640 (95.4%)
Paint 3	142209	900 \pm 35	cal AD 1040-1210 (100%)
Paint 5 (untreated)	143515	modern	n/a
Paint 5	145948	390 \pm 30	cal AD 1440-1520 (72.8%) 1570-1630 (26.6%) 1559-1562 (0.6%)
Paint 9 (untreated)	143514	modern	n/a
Paint 9	145949	385 \pm 30	cal AD 1440-1520 (68.8%) 1570-1630 (29.9%) 1558-1564 (1.3%)

Radiocarbon dating of the untreated paint Samples 5 and 9 support the GC-MS results: only modern contamination was present on the surface of the samples. Because there was charcoal present in both of these samples, the plasma-treated material was removed from the plasma chamber, washed with the phosphate buffer, and re-processed for dating. Because of the contamination observed in the GC-MS, none of the other pigmented samples were subjected to plasma oxidation and radiocarbon dating. We have retained the samples, however, and if further analyses indicate that paint 7 in particular is a viable sample for dating, we will pursue that in the future.

The radiocarbon dates were calibrated using the online version of Calib 6.0 (23). The IntCal04 dataset for terrestrial samples was utilized for the calibration curve. Because all of the samples dated were charcoal, the $\delta^{13}\text{C}$ was presumed to be -25‰ . Calibrated dates with their associated 2σ ranges and percent probabilities are also shown in Table V. The cultural implications of these dates are described in detail elsewhere (2). These are the first radiocarbon dates for rock art in Nicaragua.

Conclusions

Radiocarbon dating of rock art is not a simple matter, because of the ubiquitous nature of organic material in the environment. However, when a full archaeological excavation is not practical at a rock art site, as was the case for Cueva la Conga, dating the paintings is one step in the process of placing the site into a chronological context. Because some of the Cueva la Conga images were created in charcoal, or contained charcoal, it was possible to obtain reliable radiocarbon dates for these paintings. The systematic collection of paint and substrate pairs in this case helped in fully understanding the nature of the organic composition of the samples prior to attempting radiocarbon dating. This conservative and comprehensive approach to characterizing and dating rock art is an ideal one that should be used in future studies when possible.

Acknowledgments

The authors thank all of the people and organizations that made the Cueva la Conga project possible. Funding was provided by the EMU Provost's Office, EMU Chemistry Department, and the Josephine Nevins Keal Faculty Development Fund. Pablo and Eunice Yoder provided gracious hospitality and organizational support in Waslala, Nicaragua. Dr. Daniel Fraser, Lourdes University, and Pablo, Kenny, and Nathan Yoder aided in the sample collection at Cueva la Conga. We gratefully acknowledge Dr. Caroline Cartwright, Ms. Maria Goodrich, Dr. Glenn Walker, and Dr. Tom Guilderson for their invaluable contributions to the project.

References

1. Baker, S.; Doty, G.; Kaufman, P.; Kaufman, K.; Yoder, P. *Ficha de Reporte de Sitio Arqueológico, Cueva la Conga*; Report on File at Museo Nacional de Nicaragua, Managua, 2006.
2. Baker, S.; Armitage, R. A. *Lat. Am. Antiq.* **2012** submitted.
3. Russ, J.; Hyman, M.; Shafer, H. J.; Rowe, M. W. *Nature* **1990**, *348*, 710–711.
4. Armitage, R. A.; Hyman, M.; Southon, J.; Barat, C.; Rowe, M. W. *Antiquity* **1997**, *71*, 715–719.
5. Armitage, R. A.; David, B.; Hyman, M.; Rowe, M. W.; Tuniz, C.; Lawson, E.; Jacobsen, G.; Hua, Q. *Rec. Aust. Mus.* **1998**, *50*, 285–292.
6. Hyman, M.; Sutherland, K.; Armitage, R. A.; Southon, J.; Rowe, M. W. *Rock Art Res.* **1999**, *16*, 75–88.
7. Rowe, M. W. *Anal. Chem.* **2009**, *81*, 1728.
8. Robinson, E.; Garnica, M.; Armitage, R. A.; Rowe, M. W. In *XX Simposio de Investigaciones Arqueológicas en Guatemala, 2006*; Laporte, J. P., Arroyo, B., Mejía, H., Eds.; Museo Nacional de Arqueología y Etnología: Guatemala, 2007; pp 1193-1212.
9. Livingston, A.; Robinson, E.; Armitage, R. A. *Int. J. Mass Spec.* **2009**, *284*, 142–151.
10. Spades, S.; Russ, J. *Archaeometry* **2005**, *47*, 115–126.

11. Hedges, R. E. M.; Ramsey, C. B.; VanKlinken, G. J.; Pettitt, P. B.; Nielsen-Marsh, C.; Etchegoyen, A.; FernandezNiello, J. O.; Boschini, M. T.; Llamazares, A. M. *Radiocarbon* **1998**, *40*, 35–44.
12. Fezzey, S.; Armitage, R. A. *J. Anal. Appl. Pyrolysis* **2006**, *77*, 102–110.
13. Saiz-Jimenez, C.; Hermosin, B. *J. Anal. Appl. Pyrolysis* **1999**, *49*, 349–357.
14. Mook, W. G.; Waterbolk, H. T. Radiocarbon Dating. *Handbooks for Archaeologists No. 3*; European Science Foundation: Strasbourg, 1985.
15. Cornell, R. M.; Schwertmann, U. *The Iron Oxides*; Wiley-VCH: Weinheim, 2003; p 463.
16. Zang, X.; Brown, J. C.; van Heemst, J. D. H.; Palumbo, A.; Hatcher, P. G. *J. Anal. Appl. Pyrolysis* **2001**, *61*, 181–193.
17. Fabbri, D.; Helleur, R. *Anal. Appl. Pyrolysis* **1999**, *49*, 277–293.
18. Eerkens, J. W. *Archaeometry* **2005**, *47*, 83–102.
19. Martin, F.; del Rio, J. C.; Gonzlilez-Vila, F. J.; Verdejo, T. *J. Anal. Appl. Pyrolysis* **1995**, *31*, 75–83.
20. Frazier, S. W.; Nowack, K. O.; Goins, K. M.; Cannon, F. S.; Kaplan, L. A.; Hatcher, P. G. *J. Anal. Appl. Pyrolysis* **2003**, *70*, 99–128.
21. Chefetz, B.; Chen, Y.; Clapp, C. E.; Hatcher, P. G. *J. Soil Sci. Soc. Am.* **2000**, *64*, 583–589.
22. Fabbri, D.; Chiavari, G.; Galletti, G. C. *J. Anal. Appl. Pyrolysis* **1996**, *37*, 161–172.
23. Stuiver, M.; Reimer, P. J. *Radiocarbon* **1993**, *35*, 215–230. Online version 6.0, <http://calib.qub.ac.uk/calib/>, accessed 05/09/2010.

Chapter 5

Laser Ablation-Inductively Coupled Plasma-Mass Spectrometry Analysis of Lower Pecos Rock Paints and Possible Pigment Sources

Jon Russ,^{*,1} Kaixuan Bu,² Jeff Hamrick,³ and James V. Cizdziel²

¹Department of Chemistry, Rhodes College, 2000 N. Parkway, Memphis, TN 38112

²Department of Chemistry and Biochemistry, University of Mississippi, 322 Coulter Hall, University, MS 38677

³Department of Mathematics and Computer Science, Rhodes College, 2000 N. Parkway, Memphis, TN 38112

*E-mail: russj@rhodes.edu

Chemical analyses of prehistoric rock paints from the Lower Pecos Region of southwestern Texas were undertaken using laser ablation-inductively coupled plasma-mass spectrometry. This technique allowed us to measure the chemical composition of the paint pigments with minimal interference from a natural rock coating that completely covers the ancient paints. We also analyzed samples representing potential sources of paint pigments, including iron-rich sandstones and quartzite from the study area and ten ochre samples from Arizona. Cluster analysis, principle component analysis and bivariate plots were used to compare the chemical compositions of the paint and pigment sources. The results indicate that limonite extracted from the sandstone was the most likely source for some of the pigments, while ochre was probably used as well.

Introduction

Studies of paleoart generally tend towards one of two strategies. The first can best be defined as iconography, in which motifs, themes, styles, placement, etc. are defined and used as comparison parameters. The second strategy is based on the physicochemical properties of the artifacts; in the case of pictographs, these properties usually include the chemical and mineral composition of the paints. Knowing the composition of the paint provides information on a variety of human activities and behaviors related to rock art production, such as how and where the paint materials were collected, how these substances were processed into paints, and the means by which the final product was applied to the rock surfaces. This can give direct evidence on the evolution and advancement of technologies used by prehistoric humans. Furthermore, the physicochemical characteristics of paints provide an independent means to compare and contrast assorted pictographs, one that is based on original paint recipes and not interpretations of the images (1).

We report here a study aimed at establishing the elemental composition of prehistoric rock paints from the Lower Pecos River region of southwestern Texas. Our objective was to determine whether there are chemical signatures in the paint that would allow us to identify the source(s) of the paint pigments and provide a means for comparing various pictographs. The Lower Pecos (Figure 1) contains one of the densest concentrations of rock art found anywhere, with more than 300 recognized rock art sites. The production of the rock art spans nearly 4000 years with the vast majority of the pictographs produced between 3000 and 4000 years ago. There were at least four different periods of pictograph production based on stylistic interpretations (2). Photographs and descriptions of the rock art can be found in a variety of publications (3–5).

A critical issue in analyzing ancient paints using current instrumental methods is that samples must be removed in order to perform most chemical analyses. Although there are a few techniques that can provide *in situ* analysis, for example portable X-ray fluorescence (XRF), most methods require samples to be brought into the laboratory. Bednarik (6) details the methods for collecting paint samples and the ethics of removing paint residues, mainly from the standpoint of direct dating of rock paints. Clearly, establishing the age of specific pictograms is important in terms of rock art studies, but developments and advances in analytical methods have emerged in the last several decades that allow paint chips or residues to be analyzed non-destructively, increasing the opportunity for multiple analyses to be performed in succession on a single sample (see for example, (7)). The requirements of a “multi-technique” study is that each method be capable of analyzing very small samples with negligible (or no) loss of material and that the integrity of the sample remains post-analysis (i.e., it is not ground into a powder or chemically pretreated). Presently there are a variety of methods that satisfy these requirements including X-ray diffraction (XRD), Fourier-transform Raman spectroscopy, Fourier-transform infrared spectroscopy (FTIR), particle induced X-ray emission (PIXE), optical microscopy, and microprobe microscopy, the latter in cases where the sample is not coated with a conductor. These techniques can be used in succession to provide distinct and overlapping information on the physicochemistry of the paints.

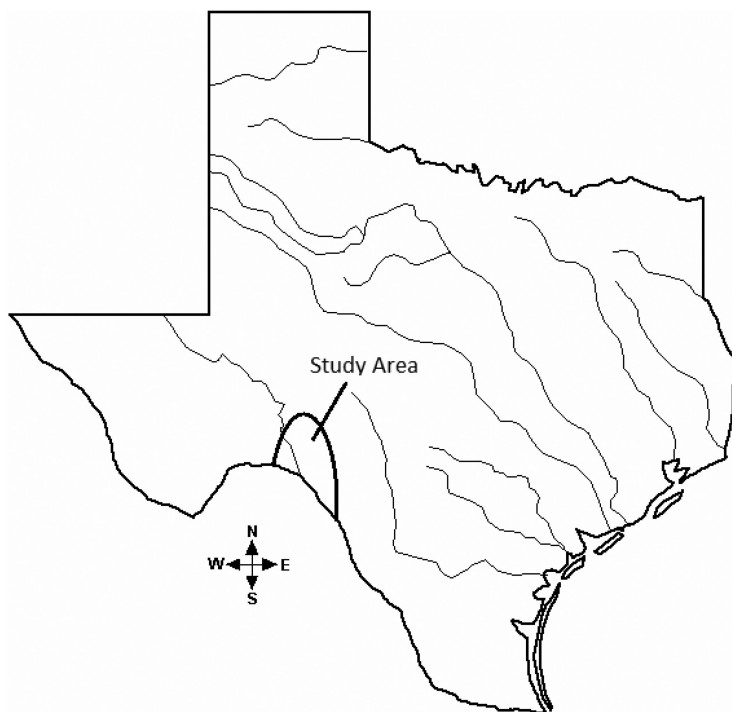


Figure 1. Map of Texas showing the approximate extent of the Lower Pecos Archaeological Region.

A relatively new method that fits the above criteria is laser ablation - inductively coupled plasma - mass spectrometry (LA-ICP-MS). This technique can be applied to very small samples (less than 1 mm² of surface area) with negligible sample loss—usually less than 1.0 μg of sample is removed. Post-analysis the sample is essentially pristine. Moreover, the method yields accurate quantitative data for most elements, including trace elements at the parts-per-billion (ng g⁻¹) concentration range. LA-ICP-MS has become increasingly important in the study of archaeological materials (8–10) and has been used successfully for analyzing prehistoric rock paints located in Spain (11).

Of particular importance in employing LA-ICP-MS for the analysis of ancient rock paints is that elemental concentrations can be monitored in real-time as the laser ablates through the sample surface and into lower strata. Because most ancient paints are incorporated within or covered by natural rock coatings this facet of the output provides a distinct advantage of being able to identify when data from the paint layer is being acquired.

The Physicochemistry of Lower Pecos Rock Paints

Lower Pecos pictographs have been studied extensively using scientific methods. The first analytical method applied to these artifacts was XRD by Zolensky in 1982 (12), where the mineral phases in the red, brown, orange and yellow pigments were determined to be iron-oxides, primarily Fe (II) and Fe (III) oxides, hydroxides, and hydrates (see also (13)). Iron oxides were also consistently present in black paints but with inclusions of manganese oxide/hydroxide minerals, mainly pyrolusite and manganite.

Paint samples from the Lower Pecos Region were the primary materials used in the original proof-of-concept research that led to the development of the plasma-chemical extraction technique for ^{14}C dating rock paint (14, 15). At least twenty-five individual Pecos River Style paint samples have since been radiocarbon dated using this technique, yielding data that demonstrated the viability of the plasma extraction method for isolating organic carbon for ^{14}C measurements. The results further established the period of production of the oldest and most extensive rock art style, the Pecos River Style, at between 3000-4000 years ago (16). The production of these artifacts coincides with a time period when the human population in the region was at a local maximum (2).

The pigments used in Lower Pecos rock paints are demonstrably inorganic. But the mineral pigments do not produce a substance that can be used as a paint when simply added to water, especially not a paint that can yield thin, continuous, vibrant lines that are characteristic of many of the Pecos River Style motifs (Figure 2). The pigments must have suspended in a more viscous substance, probably an oily or greasy material that would serve as a suspender as well as a vehicle to bind the pigments to the rock substrate (3). The presence of such an organic material is the basis for the ^{14}C analysis of the rock art. That elevated concentrations of organic matter do occur in the Lower Pecos pictograph paints has been demonstrated through the low-temperature oxygen plasma extractions of organic (reduced) carbon in paint samples. Paint samples yielded considerably more CO_2 during the experiments as compared to extracts taken from rock surfaces collected next to the painting (15).

The nature and source of the organic material used in Lower Pecos paints remains a mystery. It is generally assumed that animal fats or plant juices were used to prepare the paints. Reese et al. (17) attempted to identify the source of the organics using DNA extracted from the paints and amplified using PCR. This work initially indicated that there was animal DNA in the paint; however, these experiments were not reproducible (18). Extractions of lipids (focusing on bound and unbound fatty acids) from the ancient paints were also performed and analyzed using GC-MS (19). The results showed that the paint samples and non-painted surfaces next to paints have the same fatty acid compositions and concentrations. It stands to reason that these detected organic compounds were not those deliberately added to the paints, but instead the product of the organisms that grow naturally on the rock surfaces (which we address below). It is likely that any organic matter that was added to the paint mixture has polymerized over the past three to four millennia, and is no longer in the original molecular form.



Figure 2. Photograph of a Pecos Style pictograph (~ 1 m tall) where very fine lines of red and black paint were used to produce what appear to be wings, red paint that outlines the body, and individual toes. This suggests that some form of an organic substance was used to suspend the inorganic pigments. (see color insert)

All the extant rock paintings in the Lower Pecos region occur in dry rock shelters and under rock overhangs. The limestone surfaces in these environments, i.e., surfaces protected from rain and runoff, are completely covered with a natural rock coating composed almost entirely of calcium oxalate (20, 21). The pictograph paints are encapsulated within this oxalate-rich coating (Figure 3). Oxalate-rich rock coatings are common under rock overhangs world-wide, and occur on surfaces that also contain rock art in Australia (22), Africa (23), Spain (24) and Brazil (25).

The natural rock coating that occurs in Lower Pecos rock shelters is generally ~500 μm thick with micro-intrusions of gypsum from efflorescence and clay deposits, both of which occur on the surface and imbedded within the coating as observed using SEM-EDS (26, 27). There were also microstructures observed in the coating that resembled features observed in lichens (27), which are known to produce calcium oxalates. Hess et al. (28), however, demonstrated that at least five species of oxalate-producing bacteria (mainly *Bacillus*) occur on or

within the rock coating. Whether produced by lichen or bacteria, the oxalate is definitely biogenic and radiocarbon analyses of the coating indicate it was produced episodically during the middle and late Holocene (29).

The SEM analysis of paint samples showed that the paint layers were generally $\sim 100\ \mu\text{m}$ thick and discontinuous. In all cases the paint layers were completely covered by the oxalate coating and usually at the interface between the basal limestone and coating (20).

In summary, we can state unambiguously that the Lower Pecos rock paints were prepared primarily from iron oxides between 3000-4000 years ago and that these pigments are currently encapsulated within a naturally occurring, $500\ \mu\text{m}$ thick rock coating. The coating is mainly calcium oxalate with minor amounts of gypsum and clays incorporated within and on the surfaces of the coating.

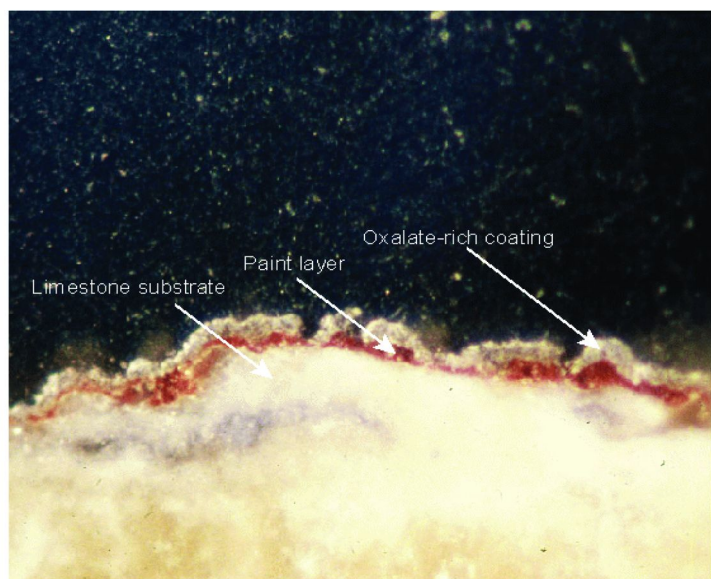


Figure 3. Optical photograph of a thin-sectioned paint sample showing the stratigraphy of the oxalate-rich coating, the paint layer, and the basal limestone. (see color insert)

Possible Sources of Pigments

Source(s) of Lower Pecos paint pigments have been speculated on for many decades. For example, Kirkland noted as far back as 1934 that a variety of local materials could have been used for Pecos River pigments including “limonite” (a native iron-rich sandstone) as well as other brown, red and orange stones common in the dry creek beds (3). The limonite pebbles are softer and easier to work with compared to the harder but more iron rich quartzite stones. The iron content of

the limonite sandstones is much too low to be used directly as a pigment, and so it would have been necessary to extract the iron-rich component from the sandstone. Ochre was also suggested as a possible pigment, a material that would not necessarily require preprocessing (3).

Turpin reported on two large pigment cakes, each weighing ~ 1 kg, that had been excavated from two Lower Pecos rock shelters (30). The nature of the cakes made it clear that if these were precursors to pictograph paints then some form of pre-processing of the pigments was used. Turpin (30) further noted that the most likely source of the pigment cakes were the local limonite stones, but that significant enrichment of the iron was necessary. She suggested that a similar technique, described by Lorblanchet et al. (31), for the production of Paleolithic paints in Europe was used by the Lower Pecos people to construct the pigment cakes. The extraction of the iron component involved grinding the pebbles and then putting the powder in water. The sandstone quartz would settle out and the iron-containing component would be suspended in the water to be isolated. The color of the material could be manipulated and enhanced by heating the iron extract to remove hydrates from the mineral matrix, creating different shades of red, yellow, orange and brown.

Another potential source of iron for the paint pigments could have been iron-rich quartzite stones, also common in dry creek beds in the region. Compared to the friable limonite sandstones the quartzite is considerably harder and much more difficult to grind into a powder, a process that would be necessary to produce the pigments.

Methods

Samples

We analyzed five different types of samples for this study: (a) Prehistoric paint chips from four sites in the Lower Pecos Region, (b) ochre from three sites in Arizona, (c) iron-rich sandstone (limonite) pebbles collected from dry creek beds in the Lower Pecos, (d) an iron-rich quartzite stone, and (e) samples of the oxalate-rich rock coating collected from non-painted surfaces in the rock shelters.

Prehistoric paints: Sixteen red paint samples from four different rock art sites were analyzed for this study. We obtained nine paint samples from five different areas inside site 41VV75. Most of the paints in the sampled surfaces appear to have merged into one amorphous montage, and so the individual pictographs could not be differentiated. We also analyzed six samples from 41VV576 collected from two different areas of what appeared to be the same pictograph. Two additional samples, one each from sites 41VV124 and 41VV127, were included in the study. All the paint samples were most likely from Pecos River Style paintings, and thus produced between 3000-4000 years ago.

Ochre: Ten ochre samples originally collected and analyzed using Instrumental Neutron Activation Analysis (INAA) by Popelka-Filcoff et al. (32), were included in this study. The samples were collected from three different geological formations in southern Arizona (Beehive Peak, Ragged Top and Rattlesnake Pass). The elemental signatures in the ochre were determined to be

site specific, thus demonstrating that elemental fingerprinting could be used for provenance studies of these ochre formations. For our analysis we prepared the samples by grinding them using an agate mortar and pestle and then pressing them into pellets using a pellet press under 12,000 psi for five minutes. We analyzed the pellets using XRF prior to the LA-ICP-MS analysis.

Iron-rich (limonite) sandstones: We prepared three samples from sandstone (limonite) pebbles collected from dry creek beds in the Lower Pecos region. The Munsell color of the original stones ranged from 10YR8/3 to 2.5YR6/6 and with a hardness of ~2 on the Mohs scale. The samples were prepared by emulating the method described by Lorblanchet et al. (31), which involved grinding the pebbles in an agate mortar and pestle and placing the powder in a beaker with deionized water. The heavier quartz was allowed to settle to the beaker bottom; then, the liquid phase with the limonite component decanted. The liquid was transferred to a watchglass and the water evaporated in a 100°C oven. The resulting powder was heated over a Bunsen burner for several hours to increase the redness, and then pressed into pellets as described above. The color of the pellets were significantly darker and redder (colors ranging from 5YR6/6 to 10R6/6) when compared to the original limonite pebbles. Moreover, the iron concentration increased from < 1% Fe in the pebbles to an average of 2.3% Fe in the pellets, as measured using XRF.

Iron-rich quartzite: There are a variety of different colored rocks in the dry creek beds throughout the study area, some potentially used as pigments (3). One that matches closely with the pigment color is a dark red quartzite with a Munsell color of 10R2.5/2. The iron content of the quartzite stone we analyzed was 3.4 % Fe and with a Mohs hardness of ~ 7. Chips of this stone were analyzed directly.

Oxalate coating: Since all paints are incorporated within the natural oxalate-rich rock coating we analyzed six individual samples collected from inside two of the rock shelters (41VV75 and 41VV576). We had five samples from site 41VV75 and one from sample site 41VV576; however, no samples from the other two sites (41VV224 and 41VV227) were available

LA-ICP-MS Instrumentation, Data Acquisition, and Data Reduction

The ICP-MS used was an X-Series 2 (Thermo-Fisher Scientific, Waltham, MA, USA). The instrument employs a quadrupole mass analyzer (filter) which provides fast scanning capability required for transient signals. Laser ablation was conducted using a UP-213 system (New Wave Research, Fremont, CA, USA). The UP-213 employs a frequency quintupled Nd:YAG laser with a resulting wavelength of 213 nm. Helium (0.8 L min⁻¹) was used as the cell carrier gas; argon (0.7 L min⁻¹) was added prior to entering the plasma. The LA-ICP-MS system was optimized for sensitivity and oxides prior to analysis using NIST glass reference materials (SRM 612). The instrumental settings for the LA-ICPMS analyses are summarized in Table 1. Briefly, the UP-213 was operated at 40% power (0.1 mJ), with a repetition rate of 2 Hz, and a spot size of 100 μm. Data was collected while performing spot shots at the surface of the rock samples. Each ablation lasted for about 3 minutes, including 20 seconds before the laser was fired to collect background levels (gas blank) and 60 seconds for preceding signal tail wash out. The ICP-MS was operated in peak jump mode. Raw

elemental intensities were processed using the X-Series software, where the data was reduced and concentrations were determined.

Table 1. LA-ICPMS instrument settings

<i>UP-213 system</i>	
Laser type	Nd-YAG
Wavelength	213 nm
Power	40 % (0.1 mJ)
Frequency	2 Hz
Carrier gas	He
Carrier gas flow	0.8 L min ⁻¹
Scan type	Spot
Spot size	100 μm
Duration per scan	~3 min
<i>Plasma</i>	
Cool gas flow	13.5 L min ⁻¹
Aux. gas flow	0.6 L min ⁻¹
Sample gas flow (Ar)	0.7 L min ⁻¹
Resolution	125
<i>Data Acquisition</i>	
Isotopes monitored	²⁴ Mg, ⁴⁴ Ca, ⁵¹ V, ⁵³ Cr, ⁵⁵ Mn, ⁵⁷ Fe, ⁵⁹ Co, ⁶⁶ Zn, ⁷⁵ As, ⁸² Se, ⁹⁰ Zr, ⁹⁵ Mo, ¹¹⁵ In, ¹²¹ Sb, ¹³⁹ La, ¹⁴⁶ Nd, ¹⁵³ Eu, ¹⁷⁵ Lu
Integration time	10 ms

Calcium was used as the internal standard for the analysis of the paint and coating samples because of the ubiquity of calcium oxalate in these samples (20). This is consistent with the Resano et al. (11) study of prehistoric paints from Spain, where Ca was also used as the internal standard. For the analysis of the ochre, sandstones and quartzite we used iron as the internal standard, using the concentration measured using XRF for each sample (see XRF section below). For quantification, we used a microanalytical carbonate standard (MACS-3) prepared by the USGS using a co-precipitation process in which trace and minor elements were mixed with the precipitate. A second carbonate material (GP-4, also from the USGS) was used for quality assurance purposes. The GP-4 material was used in a

proficiency testing program for microanalytical work. Both materials are available in pressed pellet form.

The relatively low laser power/frequency settings were selected to facilitate discrimination between the coating, paint and substrate during the ablation process, and to optimize the iron signal. This can be seen in Figure 4, where line scans represent the relative concentration of three elements: Ca, Fe and Mg. As the laser ablates through the rock coating, the Ca signal remains relatively level due to the dominate material being calcium oxalate. As the ablation proceeds into the paint layer, the Fe concentration increases dramatically due to the high concentration of iron oxides. Finally, as the laser penetrates through the paint it begins to interact with the limestone substrate, which contains relatively high Mg concentration, which is observed by the simultaneous decrease in Fe and increase in Mg. To determine the concentration of the elements of interest the signal from these elements were integrated over the area where the iron peak was observed.

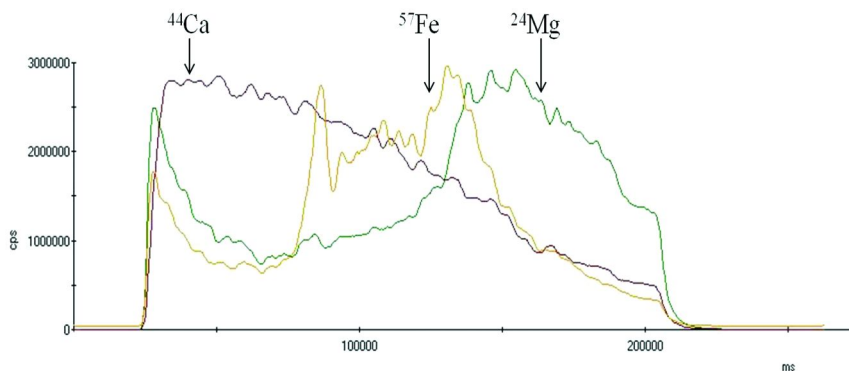


Figure 4. Typical elemental intensity variation during laser depth profiling. The rise in ^{57}Fe indicates ablation has reached a paint layer, and the rise in ^{24}Mg indicates the ablation has reached the limestone substrate layer.

We initially measured the concentrations of 37 elements in one red paint sample (75RP-34) and one coating sample (75-31) to determine which elements correlated with the Fe concentration using Pearson's correlation coefficients. Of the 36 elements, ten correlated positively with Fe ($r > 0.9$) in the paint sample (V, Cr, As, Zr, Mo, In, Sb, La, and Nd), whereas only Cr correlated with Fe in the coating. We selected the above elements for our analyses in subsequent measurements.

XRF

We analyzed the ochre, iron-rich quartzite, limonite pellets, and unmodified limonite pebbles using an Innov-X α -4000 AS X-ray fluorescence (XRF) spectrometer. Because the ablation process can result in varying amounts of sample reaching the plasma, an internal standard is used to compensate for fluctuating signals stemming from this mass transport process. For the paint layer, we used Fe as the internal standard; elemental signals measured by LA-ICP-MS were normalized to the Fe signal. The Fe concentration determined from the XRF analysis was used for quantification.

Results

Concentrations of the ten elements (V, Cr, Fe, As, Zr, Mo, In, Sb, La, and Nd) were measured in six rock coating samples, sixteen red paint samples, ten ochre samples, three limonite samples, and one quartzite sample using LA-ICP-MS (Appendix). All detectable elements from the XRF analysis are given in Appendix .

Chemistry of the Coating and Ancient Paints

A primary issue for obtaining reliable data from the paint analysis was the presence of each element of interest in the crust, i.e., the background. This was especially true for iron since it was the dominant element in the paint and the basis for the color. The iron concentrations of the rock coatings from site 41VV75 (5 samples) ranged from 0.0373% to 0.254% with an average of $0.13 \pm 0.10\%$. The average iron concentration in the eight red paint samples from site 41VV75 was $4.3 \pm 2.1\%$; therefore, on average, the coatings contribute 2.9% Fe (Table 2). At site 41VV576, the iron concentration in the one coating sample measured $0.82 \pm 0.34\%$ Fe, a value that is four times greater than the coating concentration at 41VV75.

The six paint samples from site 41VV576 contained $8.2 \pm 7.8\%$ Fe, and thus ten times greater than the average iron content of the coating from this site. The sample from site 41VV227 was $2.46 \pm 0.19\%$ Fe based on four repeat analyses of the one sample. Only one spot analysis of the single sample from site 41VV224 (out of four attempted) had a measured iron concentration significantly higher than the coatings from 41VV75 or 41VV576, a value of 2.6 % Fe, and so we used only this result.

Of the other eight elements included in the analyses, V, As, Mo and Sb had the lowest relative percentage in the crust compared to the paint, whereas, Cr, Zr, La and Nd had the highest relative percentages. Therefore, the former elements should more reliable in representing the composition of the paints, since they have the least relative contribution from the coating.

Table 2. Average concentration of the elements of interest in the coating and paint samples collected from two sites in the Lower Pecos (sites 41VV75 and 41VV576). Also shown are the relative proportions (%) of each element in the coating compared to the paint

<i>Element</i>	<i>Site 41VV75</i>			<i>Site 41VV576</i>		
	<i>Coating (ppm)</i>	<i>Paint (ppm)</i>	<i>Relative % coating/paint</i>	<i>Coating (ppm)</i>	<i>Paint (ppm)</i>	<i>Relative % coating/paint</i>
V	15.6	274	5.7	51.9	961	5.4
Cr	5.07	22.4	22.6	10.4	11.4	91.4
Fe	1252	42530	2.9	8200	77750	10.5
As	10.4	121	8.5	26.5	245	10.8
Zr	5.27	36.9	14.3	19.0	19.4	98.0
Mo	3.30	85.4	3.9	4.36	43.7	10.0
Sb	0.34	7.07	4.8	0.39	6.95	5.6
La	2.44	18.8	13.0	4.70	4.77	98.5
Nd	2.21	19.4	11.4	4.70	5.41	86.9

The cluster analysis further reveals that the paint composition from samples collected from different sites are often more similar as compared to paints collected from the same site. There is only one first order cluster consisting of paints from the sites (three samples from 41VV576), and one second order cluster also with three samples from a single site (41VV75), but the remainder of the first and second order clusters contain samples from a multiple sites.

Principle Component Analysis (PCA)

Additional comparisons between the paints and potential pigment sources were explored using PCA to determine which elements in our data set contributed most significantly to the variance in the data (Figure 6). From the plot, we ascertained that two principal components characterize approximately 75% of the variation in the elemental data. PC 1 is the dominant component, which is consistent in that most of the scored data variation lies along the x-axis (assigned to PC 1). The vectors indicate which chemical elements are responsible for most of PC 1; namely, the vectors most parallel to the x-axis. Hence PC 1 is mostly driven by the presence (or lack thereof) of Mo, La, Nd, and Zr. These elements make little, if any, contribution to PC 2.

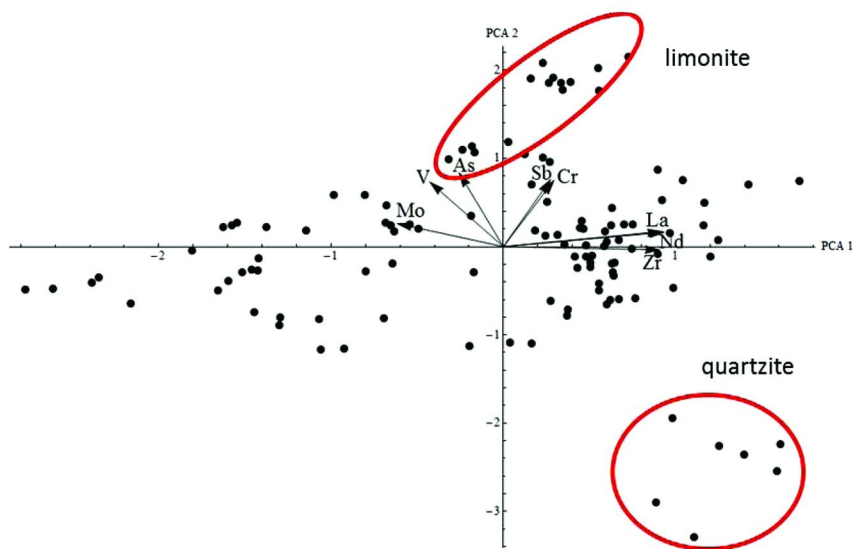


Figure 6. Principle component analysis (PCA) of PC 1 versus PC 2 showing which elements contribute most of the variance in the data, as expressed by the total chemical composition of the samples.

PC 2 is a much weaker factor, as indicated on this plot by the fact that few of the chemical elements are strongly parallel to the y-axis. However, most of the information driving PC 2 is provided by V, As, Sb, and Cr. Recall that vectors that are nearly parallel are redundant for purposes of the classification (for example, La, Nd, and Zr are highly correlated in the samples and they basically tell the same story about those samples). The elements Sb and Cr, similarly, provide nearly identical information, while V and As are the most interesting for purposes of adding new information to the analysis since they provide very different information than Sb and Cr.

Bivariate Plots

Based on the PCA we concluded that the elemental concentrations driving the variance in the data, and thus the most useful in associating the paints with particular pigment sources, were V, As, Sb and Cr. However, because Cr has a relatively high concentration in the coating compared to the paint we eliminated this element due to the expected interference.

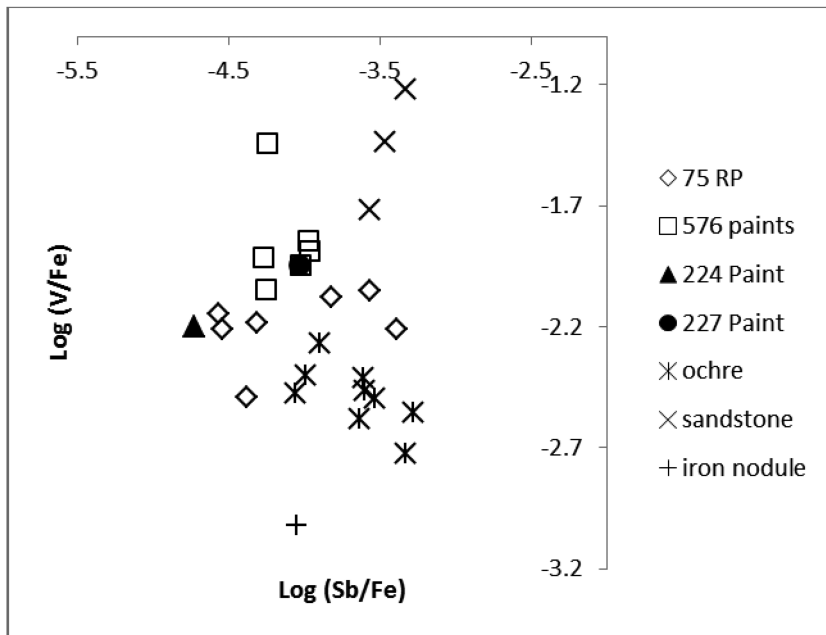


Figure 7. $\text{Log}_{10}(\text{Sb}/\text{Fe})$ versus $\text{Log}_{10}(\text{V}/\text{Fe})$ bivariate plot showing two dimensional relationships between the samples.

The two bivariate plots below demonstrate that the three potential sources of pigments are distinguishable based on the V, As and Sb concentrations (Figures 7 and 8). From these plots it is apparent that the paints are least similar to the iron-rich quartzite. In both graphs the paint data generally fall between the ochre and sandstone data. The As - V plot shows that there considerable overlap with the ochre and paint samples from 41VV75, and the paints from 41VV576 are more closely associated with the limonite in this plot (Figure 8).

Comparisons between the paint samples show that there is a chemical distinction between the V, As, and Sb content in samples from 41VV576 and 41VV75. The one paint sample from 31VV227 is chemically the same as those from 41VV576, while the single paint from 41VV224 is more closely related to the samples from 41VV75.

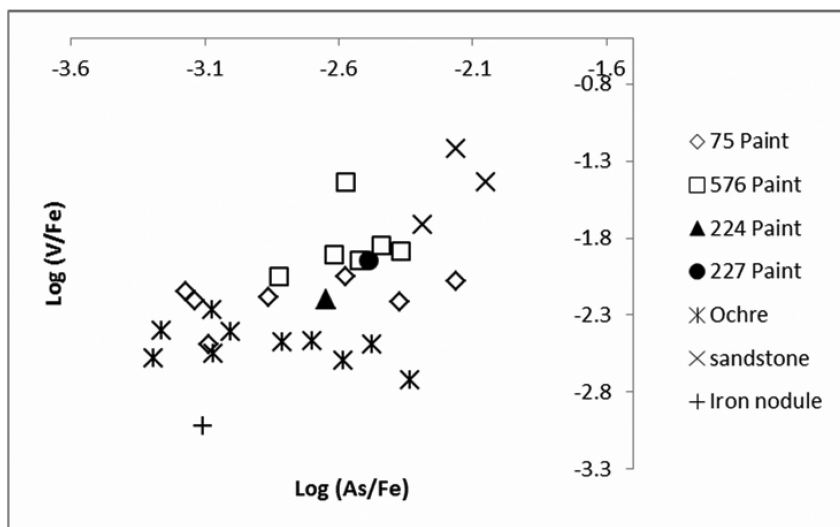


Figure 8. $\text{Log}_{10}(\text{As}/\text{Fe})$ versus $\text{Log}_{10}(\text{V}/\text{Fe})$ bivariate plot showing two dimensional relationships between the samples.

Discussion

LA-ICP-MS proved to be a useful technique for obtaining elemental data from samples containing prehistoric rock paints. The samples we studied remained essentially pristine post-analysis, with negligible amount of paint material removed and with no adverse effects to the sample integrity.

The application of the Ward's Method and bivariate plots consistently supported the hypothesis by Turpin (2) that the local iron-rich sandstones (limonite) was at least one source of the Lower Pecos paint pigments. This further indicates that the people that produced the paints were technologically advance enough to isolate the limonite from the sandstone and manipulate the color by dehydrating the iron (31). On the other hand, the local quartzite stone, despite having a much higher iron content than the sandstone and a native color similar to many of the paints, was not used in the production of the paints we studied. Finally, the chemical similarities between some of the paints and ochre samples from Arizona suggest that an analogous source was used in paint production.

Acknowledgments

The ICPMS used in this study was obtained through a NSF grant (Award #0923080). We thank Tristan Hill, Sydney Milton, Jaala Spencer for assistance with preliminary LA-ICP-MS analysis; David Jeter for help with the XRF analysis; and Chris Mouron for assistance with preliminary statistics. Part of this research was funded by a Rhodes Faculty Development Grant.

Table – Appendix 1. Elemental concentrations (ppm) of rock coatings, ochre, prehistoric paints, limonite, and an iron-rich quartzite (nodule)

Sample type	Sample Number	Elemental concentrations (ppm)									
		V	Cr	Fe	As	Zr	Mo	In	Sb	La	Nd
Rock Coatings	75C-31	25.37	0.562	866.7	16.28	2.018	13.34	0	0.049	1.624	1.462
		16.16	0.458	595.9	19.74	0.714	2.214	0	0.052	1.925	1.817
		22.51	0.374	500.3	-1.89	2.142	6.877	0	0.011	1.796	1.22
	75C-1-A	24.34	8.866	2890	22.74	30.81	2.714	0.004	1.864	6.006	6.427
		16.33	6.668	1300	17.7	3.076	2.018	0	0.315	2.656	2.235
		7.827	5.403	397	8.853	1.619	1.062	0	0.162	1.453	1.271
	75C-1-B	17.06	7.731	1845	17.57	8.39	2.474	0	0.465	3.463	3.217
		12.8	4.59	1038	10.75	3.382	3.005	0	0.436	1.897	1.704
		17.2	6.334	689.5	10.3	2.142	1.175	0.002	0.237	1.462	1.122
75C-1-C	19.18	9.39	1469	7.488	3.915	2.221	0	0.463	1.824	1.585	
	17.41	8.895	2762	6.683	8.751	2.77	0.001	0.418	4.459	4.389	
	21.52	9.48	3312	6.204	9.291	2.514	0.004	0.463	3.493	3.469	

Sample type	Sample Number	Elemental concentrations (ppm)									
		V	Cr	Fe	As	Zr	Mo	In	Sb	La	Nd
	75C-1-D	6.323	2.858	293.4	12.32	0.761	0.278	0	0.03	1.894	1.611
		2.763	0.787	173.9	10.86	0.288	2.499	0	0.024	0.863	0.369
		7.361	3.692	653.3	11.67	1.706	4.266	0.03	0.143	1.837	1.26
	576C-1-A	56.59	11.41	7829	28.07	16.77	5.634	0	0.711	5.048	5.572
		32.25	8.38	5042	15.3	9.893	2.577	0.003	0.168	4.578	4.324
		66.7	11.4	11720	36.22	30.3	4.88	0.059	0.29	4.462	4.209
<i>Red Paints</i>											
	75RP-34	167	1.904	26020	21.18	15.11	14.73	0	0.662	5.821	6.185
		85.94	1.257	14240	8.013	166	11.11	0	0.509	5.355	4.63
		130.3	1.839	22010	16.29	16.5	13.36	0	0.596	5.529	5.996
	75RP-42	178.3	91.48	72570	52.48	22.83	161.2	0.014	2.008	16.54	17.22
		194.6	105.2	49160	53.61	46.63	172.2	0.03	2.545	20.21	20.08
		94.38	43.45	23780	13.88	22.02	51.82	0	1.462	19.87	24.45

Continued on next page.

Table – Appendix 1. (Continued). Elemental concentrations (ppm) of rock coatings, ochre, prehistoric paints, limonite, and an iron-rich quartzite (nodule)

Sample type	Sample Number	Elemental concentrations (ppm)									
		V	Cr	Fe	As	Zr	Mo	In	Sb	La	Nd
75RP-3-A*		230.9	11.9	25640	68.92	10.95	128.5	0.004	7.183	9.574	10.64
		59.7	10.86	9890	22.71	11.25	26.41	0.006	1.804	7.909	8.016
		174.1	12.41	19680	51.84	15.23	82.52	0.004	5.012	8.18	7.882
75RP-3-B*		326.9	9.868	58860	248.1	39.82	58.2	0.007	22.99	4.374	5.398
		638.6	12.7	103800	430.4	24.5	102.7	0.005	42.53	8.127	9.117
		604	12.05	92770	409.2	24.99	86.52	0	37.71	8.806	8.538
75RP-4		198.2	16.26	29880	45.48	29.61	39.3	0.013	1.629	9.079	9.125
		473.9	18.63	73990	67.26	25.74	110.3	0.012	3.022	9.611	9.667
		97.4	15.72	13800	48.59	23.66	22.96	0.012	1.039	12.89	14.16
75RP-2-A*		385.9	43.62	53310	23.3	18.02	73.66	0.011	1.153	7.629	9.765
		237.1	3.156	34230	35.79	38.25	44.19	0.006	1.215	15.6	16.38
75RP-2-B*		487.6	9.871	44150	158.2	73.29	113.9	0	5.147	21.62	20.49

Sample type	Sample Number	Elemental concentrations (ppm)									
		V	Cr	Fe	As	Zr	Mo	In	Sb	La	Nd
		359	23.05	57380	728.8	117.9	149.4	0	11.9	177.3	179
		321.2	23.87	38550	75.85	40.39	80.68	0.029	4.128	24.71	25.01
	75RP-2-C*	159.4	13.22	21070	63.76	24.01	73.17	0.046	1.39	12.56	12.55
		157.4	17.78	21310	51.67	20.21	79.28	0.003	1.849	11.79	11.87
		529.1	15.51	72040	97.48	22.93	268.7	0.023	5.046	9.603	8.869
	576RP-3-A*	407.7	7.517	35940	67.17	11.71	36.67	0.002	2.283	4.33	4.858
		30.76	7.092	3950	16.22	22.56	4.008	0.004	0.067	3.975	4.667
		98.91	14.89	17180	5.483	28.58	5.661	0.017	0.706	7.432	8.782
		827.6	11.42	95520	161.4	12.67	92.38	0.007	5.197	4.142	4.687
	576RP-3-B*	819.4	32.23	22610	60.2	35.42	7.804	0.026	1.269	7.295	8.313
	576RP-3-C*	250.9	5.524	21220	54.31	6.578	6.195	0.001	1.271	2.189	2.452
		391.5	7.227	30160	77.85	13.83	9.119	0.001	1.763	2.886	3.41
		637.3	9.757	53030	119.2	21.46	14.3	0.002	2.549	3.25	3.671

Continued on next page.

Table – Appendix 1. (Continued). Elemental concentrations (ppm) of rock coatings, ochre, prehistoric paints, limonite, and an iron-rich quartzite (nodule)

Sample type	Sample Number	Elemental concentrations (ppm)									
		V	Cr	Fe	As	Zr	Mo	In	Sb	La	Nd
	576RP-5-A*	281.7	9.24	24730	127	11.16	8.267	0.01	2.213	4.516	4.835
		170.2	13.08	17100	86.8	15.36	5.211	0.025	1.133	6.184	10.44
		1284	11.43	92660	360.1	21.4	36.42	0.009	11.07	6.606	6.054
	576RP-5-B*	496.1	7.668	30290	149.1	9.26	16.53	0.01	3.199	3.353	3.394
		532.2	11.06	54020	177	18.11	23.33	0	4.772	6.202	6.984
		3449	12.93	228900	809	46.11	68.17	0.003	25.21	5.066	5.287
	576RP-5-C*	2480	9.987	210900	734.3	17.56	141.1	0	19.05	3.603	3.344
		1836	9.207	177200	543.7	15.31	138.7	0.012	16.88	3.933	3.982
		2345	13.06	206400	619.7	22.44	129.2	0.005	19.47	6.097	6.784
	224RP-3	77.04	12.48	7223	46.57	9.496	2.242	0	0.385	5.241	5.817
		65.93	7.052	4438	36.25	4.059	1.49	0	0.367	3.582	3.086
		166.8	9.668	26370	59.52	8.189	4.428	0	0.491	3.724	3.331

Sample type	Sample Number	Elemental concentrations (ppm)									
		V	Cr	Fe	As	Zr	Mo	In	Sb	La	Nd
		76.87	10.36	8874	50.79	10.91	2.062	0.003	0.446	4.415	4.778
	227RP-7	149.5	39.44	26140	203.5	60.72	37.28	0.067	6.887	42.42	45.47
		131.6	43.15	24060	107.5	433.5	34.53	0.102	6.105	55.8	64.07
		162.6	40.63	26130	181.9	46.14	36.17	0.166	8.059	35.03	41.87
		140.4	25.04	22150	97	41.62	12.73	0.036	5.365	26.64	27.88
<i>Ochre</i>											
	1031	17.77	3.732	18450 [†]	35.92	67.15	0.636	0.03	4.321	11.75	13.75
	Beehive Hill	29.29	8.006		89.88	36.56	1.141	0.064	5.199	56.47	49.56
		38.78	23.31		53.09	30.47	1.652	0.073	6.089	8.968	10.18
		44.52	6.996		104.5	220.2	3.235	0.114	13.37	150.8	166.1
		44.41	11.18		143.7	95.97	1.301	0.124	14.19	36.91	42.09
	1035	88.87	30.49	29138	45.01	113.2	1.776	0.141	2.368	33.69	33.53
	Beehive Hill	92.10	29.7		46.59	115	4.24	0.085	2.367	168.1	134.6
		88.52	26.12		54.73	102.5	3.634	0.136	3.093	28.51	35.4
		91.77	31.59		39.61	112.5	1.029	0.1	2.435	22.96	23.66

Continued on next page.

Table – Appendix 1. (Continued). Elemental concentrations (ppm) of rock coatings, ochre, prehistoric paints, limonite, and an iron-rich quartzite (nodule)

Sample type	Sample Number	Elemental concentrations (ppm)									
		V	Cr	Fe	As	Zr	Mo	In	Sb	La	Nd
		126.30	37.35		39.21	123.6	0.98	0.18	2.383	28.05	28.72
	1036	91.45	30.98	28972	85.8	104.7	1.429	0.085	8.094	31.81	33.79
	Beehive Hill	103.40	28.46		102.4	110.6	1.966	0.115	12.14	50.85	63.13
		94.46	30.12		94.55	105.3	1.052	0.098	7.64	35.08	35.06
		92.31	27.54		100.5	103	1.225	0.108	7.838	26.69	29.75
		82.33	33.14		103.2	103.7	1.157	0.19	6.456	24.62	25.72
	1037	106.30	46.87	30041	58.9	125.8	1.372	0.146	15.15	82.65	63.54
	Beehive Hill	98.10	39.2		58.9	95.08	0.91	0.104	4.842	38.16	33.33
		108.50	36.78		63.23	116.8	1.297	0.118	5.653	25.08	27.97
		99.00	35.13		58.92	92.96	1.31	0.092	6.25	20.61	22.46
		100.40	32.67		59.71	116.6	1.567	0.105	5.717	24.64	28.17
	1050	104.60	108.9	36780	26.11	34.37	1.925	0.19	17.99	15.33	29.24
	Ragged Top	102.80	97.19		27.06	30.14	1.971	0.176	18.87	15.07	25.27

Sample type	Sample Number	Elemental concentrations (ppm)									
		V	Cr	Fe	As	Zr	Mo	In	Sb	La	Nd
		107.50	79.99		40.15	39.03	1.686	0.162	22.43	23.53	33.76
		95.69	101.1		32.22	32.38	2.429	0.164	18.46	23.25	42.89
		103.50	255.3		30.96	48.82	3.252	0.153	18.7	31.49	46.96
	1046										
	Rattlesnake Pass	96.64	121.7	35074	22.42	354.6	4.055	0.11	6.065	12.93	16.13
		94.11	59.7		8.299	110.4	2.566	0.083	6.154	26.34	32.9
		95.66	120.1		25.41	62.4	2.261	0.13	7.054	20.74	24.83
		92.82	112.5		24.33	51.07	4.169	0.099	17.67	23.37	32.31
		79.81	29.69		9.003	44.89	1.101	0.075	3.359	9.37	11.25
	1043										
	Rattlesnake Pass	375.60	61.79	31322	57.84	626.9	5.961	0.226	6.185	134.2	175.6
		119.50	53.87		14.03	103.2	0.946	0.099	2.475	32.13	38.7
		90.49	45.19		15.05	321.8	2.041	0.101	4.384	26.49	48.05
		143.20	59.25		29.69	111.9	1.551	0.087	3.285	29.8	34.32
		116.50	35.23		15.4	124.1	0.968	0.057	3.228	22.55	24.86
	1044										
		117.50	30.24	25360	28.98	76.68	1.274	0.052	2.78	28.63	34.21

Continued on next page.

Table – Appendix 1. (Continued). Elemental concentrations (ppm) of rock coatings, ochre, prehistoric paints, limonite, and an iron-rich quartzite (nodule)

<i>Sample type</i>	<i>Sample Number</i>	<i>Elemental concentrations (ppm)</i>									
		<i>V</i>	<i>Cr</i>	<i>Fe</i>	<i>As</i>	<i>Zr</i>	<i>Mo</i>	<i>In</i>	<i>Sb</i>	<i>La</i>	<i>Nd</i>
Rattlesnake Pass		91.42	46.17		8.911	50.45	0.693	0.102	3.929	17.74	18.81
		94.53	46.29		16.3	100.7	0.906	0.08	15.85	45.16	48.81
		86.96	38.42		44.03	91.94	0.755	0.063	3.927	74.57	97.77
		100.00	39.04		27.78	115.3	0.781	0.094	4.279	32.56	34.6
1045		172.60	72.38	32324	22.39	210.5	4.33	0.162	7.14	26.74	34.29
Rattlesnake Pass		101.80	34.24		21.44	65.86	2.727	0.042	2.436	20.34	23.66
		114.70	34.65		8.916	54.35	1.056	0.053	1.446	13.96	14.73
		146.40	28.98		13.9	80.09	1.525	0.067	1.917	21.7	25.07
		122.10	30.16		18.45	80.36	1.669	0.081	2.022	21.34	25.84
1038		41.26	16.86	20684	48.01	44.77	0.961	0.045	3.023	14.94	16.9
Beehive Hill		41.50	18.09		69.48	133.4	1.598	0.049	3.225	12.81	14.52
		44.13	24.75		46.29	45.3	1.181	0.059	3.302	16.18	19.8
		77.65	152.7		53.56	82.58	4.163	0.065	3.945	10.15	11.26
		55.71	30.08		53.18	43.37	1.549	0.077	3.182	14.67	17.22

Sample type	Sample Number	Elemental concentrations (ppm)									
		V	Cr	Fe	As	Zr	Mo	In	Sb	La	Nd
<i>Sandstones</i>											
	SS 2	586.80	120.8	16387	158.9	40.26	9.91	0.071	5.625	25.05	24.19
		699.30	185.3		155.1	34.2	15.96	0.055	5.311	36.42	34.76
		578.00	123.5		135.1	43.33	8.946	0.075	5.5	29.89	27.13
		560.30	133.5		133.4	71.38	10.24	0.091	5.506	25.8	27.3
		561.20	129.5		144.5	46.73	10.05	0.091	6.006	30.23	28.65
	SS 3	632.60	82.34	31605	162.6	54.41	5.937	0.126	9.201	20.09	14.42
		631.30	102.8		161.5	69.23	6.38	0.105	8.399	28.45	21.11
		620.50	77.05		155.5	63.34	6.107	0.118	8.395	18.79	14.87
		552.50	63.7		164.9	51.32	6.186	0.102	8.099	15.59	11.47
		609.30	85.19		168.6	57.51	6.576	0.134	8.271	18.37	12.69
	SS 5	1136.00	88.21	19855	114.8	164.7	4.397	0.085	7.836	28.14	39.12
		1418.00	119.1		130.1	132.4	6.092	0.085	9.347	34.1	47.73
		912.00	72.7		136.7	102.2	5.038	0.07	9.703	22.24	29.3
		1116.00	85.09		149.4	115.9	5.173	0.079	8.693	24.66	34.07

Continued on next page.

Table – Appendix 1. (Continued). Elemental concentrations (ppm) of rock coatings, ochre, prehistoric paints, limonite, and an iron-rich quartzite (nodule)

Sample type	Sample Number	Elemental concentrations (ppm)									
		V	Cr	Fe	As	Zr	Mo	In	Sb	La	Nd
		1410.00	128.1		150.8	176.7	7.534	0.097	10.52	48.45	61.58
<i>Iron nodule</i>		25.05	0.513	33847	3.361	596.3	2.375	0.119	0.928	138.9	148.9
		32.94	0.681		1.015	377	2.015	0.188	1.007	29.75	31.7
		11.86	0.346		1.678	581.6	4.396	0.128	0.503	48.24	53.85
		34.30	0.39		8.392	408.5	1.977	0.154	1.021	95.96	104.4
		27.18	1.009		14.38	363.3	3.146	0.17	1.268	54.17	59.99
		32.63	0.193		10.02	804.5	3.049	0.173	1.108	188.5	202.8
		25.41	0.803		4.159	786.5	2.965	0.241	1.202	77.24	87.8

* Indicates aliquots where multiple samples were collected from the same spot on the shelter wall. † The Fe concentrations for ochre, sandstones and iron nodule were measured using XRF.

Table – Appendix 2. Elemental concentrations (ppm) of the pelletized ochre and limonite samples obtained using XRF

<i>Sample ID</i>	<i>Ti</i>	<i>Mn</i>	<i>Fe</i>	<i>Co</i>	<i>Cu</i>	<i>Zn</i>	<i>As</i>	<i>Pb</i>	<i>Rb</i>	<i>Sr</i>	<i>Zr</i>	<i>Mo</i>	<i>Sb</i>
Ochre 1031	1691	3933	18450	98	0	268	136	59	274	571	161	19	41
Ochre 1035	2728	3946	29138	402	23	126	48	33	260	109	192	12	0
Ochre 1036	2806	6678	28972	275	0	350	141	58	239	160	210	10	0
Ochre 1037	3060	4745	30041	422	32	139	62	40	236	174	308	5	0
Ochre 1038	1619	4595	20684	0	0	168	48	38	214	191	192	23	0
Ochre 1043	4700	1484	31322	283	46	59	17	30	160	1594	247	7	0
Ochre 1044	3426	2416	25360	350	0	74	11	35	140	872	255	7	0
Ochre 1045	5063	2409	32324	421	52	63	21	36	131	2080	217	14	0
Ochre 1046	5021	3560	35074	170	33	80	19	50	163	1059	271	25	0
Ochre 1050	4760	1073	36780	411	0	62	44	22	218	176	224	8	0
sandstone 2	481	0	16387	99	0	69	78	12	23	1398	55	54	0
sandstone 3	992	0	31605	503	49	138	184	18	24	1864	102	24	0
sandstone 5	447	0	19855	363	0	289	102	22	4	3865	104	28	0

References

1. Menu, M.; Walter, P. *Nucl. Instrum. Methods* **1992**, *B64*, 547–552.
2. Turpin, S. A. *American Indian Rock Art*; Proceedings of the International Rock Art Conference, San Antonio, TX, 1990; Vol. 16, pp 99–122.
3. Kirkland, F.; Newcomb, W. W. *The Rock Art of Texas Indians*; The University of Texas Press: Austin, TX, 1967; p 239.
4. Shafer, H. J.; Zintgraph, J. *Ancient Texans: Rock Art and Lifeways Along the Lower Pecos*; San Antonio Museum Association: San Antonio, TX, 1986; p 247.
5. Boyd, C. E. *Rock Art of the Lower Pecos*; Texas A&M University Press: College Station, TX, 2003; p 153.
6. Bednarik, R. G. *Rock Art Science: The Scientific Study of Paleoart*; Aryan Books International: New Delhi, India, 2007; pp 174–175.
7. Bonneau, A.; Pearce, D. G.; Pollard, A. M. *J. Archaeol. Sci.* **2012**, *39*, 287–294.
8. Speakman, R. J.; Neff, H. In *Laser Ablation-ICP-MS in Archaeological Research*; Speakman, R. J., Neff, H., Eds.; University of New Mexico: Albuquerque, NM, 2005; pp 1–14.
9. Guissani, B.; Monticelli, D.; Rampazzi, L. *Anal. Chim. Acta.* **2009**, *635*, 6–21.
10. Resano, M.; Garcia-Ruiz, E.; Vanhaecke, F. *Mass Spectrom. Rev.* **2010**, *29*, 55–78.
11. Resano, M.; Garcia-Ruiz, E.; Alloza, R.; Marzo, M. P.; Vandenabeele, P.; Vanhaecke, F. *Anal. Chem.* **2007**, *79*, 8947–8955.
12. Zolensky, M. In *Seminole Canyon: The Art and the Archeology*. Texas Archeological Survey Research Report No. 83; The University of Texas Press: Austin, TX, 1982; pp 277–284.
13. Hyman, M.; Turpin, S. A.; Zolensky, M. E. *Rock Art Res.* **1996**, *13*, 93–103.
14. Russ, J.; Hyman, M.; Shafer, H. J.; Rowe, M. W. *Nature* **1990**, *348*, 710–711.
15. Ilger, W.; Hyman, M.; Southon, J.; Rowe, M. W. *Radiocarbon* **1995**, *37*, 299–310.
16. Rowe, M. W. *Anal. Chem.* **2009**, *81*, 1728–1735.
17. Reese, R.; Hyman, M.; Rowe, M. W.; Derr, J. N.; Davis, S. K. *J. Archaeol. Sci.* **1996**, *23*, 269–277.
18. Mawk, E. J.; Hyman, M.; Rowe, M. W. *J. Archaeol. Sci.* **2002**, *29*, 301–306.
19. Spades, S.; Russ, J. *Archaeometry* **2005**, *47*, 115–126.
20. Russ, J.; Kaluarachchi, W. D.; Drummon, L.; Edwards, H. G. M. *Stud. Conserv.* **1999**, *44*, 91–103.
21. Russ, J.; Palma, R. L.; Loyd, D. H.; Farwell, D. W.; Edwards, H. G. M. *Geoarchaeology* **1995**, *10*, 43–63.
22. Watchman, A. *Rock Art Res.* **1990**, *7*, 44–50.
23. Mazel, A. D.; Watchman, A. L. *S. Afr. Humanit.* **2003**, *15*, 59–73.
24. Hernanz, A.; Gavira-Vallejo, J. M.; Ruiz-Lopez, J. F.; Edwards, H. G. M. *J. Raman Spectrosc.* **2008**, *39*, 972–984.

25. Steelman, K. L.; Rickman, R.; Rowe, M. W.; Boutton, T. W.; Russ, J.; Guidon, N. In *Archaeological Chemistry*; Jakes, K. A., Ed.; ACS Symposium Series 831; American Chemical Society: Washington, DC, 2002; pp 22–35.
26. Kaluarachchi, W.; M.S. Thesis, Sam Houston State University, Huntsville, TX, 1995.
27. Russ, J.; R. L. Palma, D. H.; Loyd, T. W.; Boutton, T. W.; Coy, M. A. *Quatern. Res.* **1996**, *46*, 27–36.
28. Hess, D.; Coker, D. J.; Loutsch, J. M.; Russ, J. *Geoarchaeology* **2008**, *23*, 3–11.
29. Russ, J.; Loyd, D.; Boutton, T. W. *Quatern. Int.* **2000**, *67*, 29–36.
30. Turpin, S. A. *J. South. Texas Archaeol. Soc.* **1997**, *24*, 34–37.
31. Lorblanchet, M.; Labeau, M.; Vernet, J.-L.; Fitte, P.; Valladas, H.; Cachier, H.; Arnold, M. *Rock Art Res.* **1990**, *7*, 4–20.
32. Popelka-Filcoff, R. S.; Miksa, E. J.; Roberston, J. D.; Glascock, M. D.; Wallace, H. *J. Archaeol. Sci.* **2008**, *35*, 752–762.

Chapter 6

Identification of Organic Dyes by Direct Analysis in Real Time-Time of Flight Mass Spectrometry

Jordyn Geiger,¹ Ruth Ann Armitage,^{*,1} and Cathy Selvius DeRoo²

¹Chemistry Department, Eastern Michigan University, 501 Mark Jefferson, Ypsilanti, MI 48197

²Conservation Department, Detroit Institute of Arts, 5200 Woodward Ave., Detroit, MI 48202

*E-mail: rarmitage@emich.edu

We report here further developments in identifying organic dye compounds in botanical materials and natural fiber textiles using direct analysis in real time-time of flight mass spectrometry (DART-TOF-MS). This method requires little to no sample preparation, and analyses are completed in less than one minute. Analyses were performed on dyed cotton fibers from *Traité des Matières Colorantes du Blanchiment et de la Teinture du Coton*, a late 19th century treatise on dye chemistry, mordants, and dyeing techniques. Sandalwood and turmeric dyes were readily identified in the 128-year old cotton fibers by DART-MS with no sample preparation. Simple in situ hydrolysis and derivatization have the potential to expand the applicability of DART-MS to other dye compounds, including those in cutch and quercitron.

Introduction

A shared attribute across cultures and throughout history is the use of plant extracts as colorants for the dyeing of textiles and the painting of objects. For example, a 7th century B.C.E. cuneiform tablet providing instructions for dyeing wool with madder and indigo to mimic the rare and expensive shellfish purple dyes speaks to the importance of plant-derived dyes in ancient cultures (*1*). Because of their inherent fragility and susceptibility to degradation, textiles are rare in

the archaeological record, and thus, as precious cultural heritage materials they require judicious sampling and analysis. Compounding the challenges presented by minute samples is the high tinting strength of most organic dyes, present only in nanogram to microgram quantities.

Very small samples containing miniscule quantities of dye require not only sensitive instrumental methods but also preparation methods which do not compromise the chemical integrity of the dyestuff in question. The oldest object to date in which the presence of madder has been detected, a 4000 year old painted Egyptian leather quiver, was analyzed using surface enhanced Raman spectroscopy (SERS) (2). While SERS provides both high sensitivity and requires only miniscule samples, the technique requires the preparation of colloids, hydrolysis pretreatment of the dye-mordant complex, and appropriate plasmon conditions for the Raman scattering effect to occur. High performance liquid chromatography (HPLC) is the more common method for identifying dyestuffs in historic textiles, though it, too, requires significant sample preparation in addition to often larger samples than are needed for SERS. Both diode array (DAD) (3–5), and mass spectrometry (MS) (6–10) detection methods have been used to identify dyes in historic and archaeological textiles.

An extensive review in 2010 described the many applications of spectroscopic methods to the characterization of organic dyes in cultural heritage materials (11). Several methods of direct mass spectrometry are described, including high resolution laser desorption-MS applications (both with and without a matrix) (12, 13). More recently, we reported on high resolution time of flight MS with direct analysis in real time (DART) ionization of indigoid, flavonoid, and anthraquinone dye materials (14). This method required no sample preparation, and possessed the requisite sensitivity to identify organic colorants in less than 1 minute. We report here on the extension of that work to the detection of curcuminoids from turmeric, pterocarpanes from sandalwood, flavonols from black oak, and catechins and tannins from cutch.

Cardon (1) provides an excellent review of the history and chemistry of natural dyes, which we summarize here. Turmeric, derived from the roots of *Curcuma longa*, has high tinting strength, but is not particularly light fast. The curcuminoids (Table I) collectively are known as Natural Yellow 3. Dyes derived from turmeric have long been an important part of Hindu culture, and the plant likely originates from India. Sandalwood, too, originates from India, and has been traded since medieval times, though its use in dyeing dates only to the 17th century. The colorants from sandalwood are considered insoluble, requiring an organic solvent for their use in dyeing. The santalins (A, B, and C) are the major colorants, though isoflavones, pterocarpanes, flavones, and aurones are also present. Quercitron, derived from the inner bark of the black oak (*Quercus velutina*), was introduced commercially in the late 18th century. The lemon yellow color obtained from quercitron derives primarily from quercitrin, the rhamnoside of the aglycone quercetin. Obtained from *Acacia catechu*, cutch and catechu are different preparations of the heartwood. The brown color of cutch comes primarily from tannins derived from the flavonol catechin.

Table I. Description of samples investigated

<i>Dye material</i>	<i>Colorant compound(s)</i>	<i>Dye Forms Analyzed</i>
Turmeric	Curcumin Demethoxycurcumin Bisdemethoxycurcumin	Powder, newly-dyed cotton, French cotton (<i>jaune de curcuma</i>)
Sandalwood	Santalin A Santalin B Pterocarpin Homopteroarpin	Powder, newly-dyed cotton, French cotton (<i>rouge au santal</i> and <i>brun au santal</i>)
Quercitron	Quercetin	Powder, powder + formic acid, newly-dyed cotton, French cotton (<i>jaune de quercitron</i>)
Cutch	Catechin Epicatechin	Powder, powder + formic acid, newly-dyed cotton, French cotton (light <i>cachou</i> , dark <i>cachou</i> , <i>et bois jaune</i> , <i>de Laval</i>)

Materials and Methods

Cotton standards from TestFabrics (either as skeins or woven textile) were dyed with and without alum mordant (15). Sandalwood was extracted in a minimal volume of absolute ethanol, and further prepared in deionized water as described by Cannon (15). All other dyes were prepared in deionized water. Turmeric was obtained from a local spice shop (By the Pound, Ann Arbor, Michigan). Sandalwood and cutch were obtained from Kremer Pigments (New York). Quercitron bark was obtained from Maiwa Supply (Vancouver, BC). Single fibers dyed with known colorants were obtained from *Traité des Matières Colorantes du Blanchiment et de la Teinture du Coton*, a late 19th century treatise on fiber, dye chemistry, mordants, and dyeing techniques that includes an appendix of dyed cotton skeins. These fibers were less than 0.5 cm in length and weighed approximately 1 mg.

Analyses were carried out on a JEOL AccuTOF mass spectrometer (JEOL USA, Peabody, MA) equipped with a DART ionization source (Ionsense, Saugus, MA). Samples were run in positive ion mode with helium as the DART gas at a flow rate of 2.5 L/min at 300 °C. Grid voltage was set at +350 V, with orifice 1 at 30 V and 120 °C. Orifice 2 and the ring lens voltage were both held at 5 V, and the peaks voltage was held at 1500 V. Each sample was calibrated by running PEG-600 in methanol during the acquisition.

Fibers were analyzed by placing them directly into the gap between the DART source and the mass spectrometer orifice using forceps. Dye solutions and powders, including finely ground botanical barks, were introduced on the closed end of a melting point capillary tube. To determine if acid hydrolysis affected the observed signal, quercitron bark and cutch were treated with a few microliters of 80% formic acid immediately prior to exposure to the DART source, directly on

the melting point capillary. Mass resolution of the AccuTOF was approximately 6000. Ions were observed at $M+H^+$ in positive mode; the DART ionization process has been described elsewhere (16, 17).

Results and Discussion

The primary colorant in turmeric, curcumin was observed in turmeric powder and freshly-dyed cotton as the protonated ion, at m/z 369.134 Da (Table II). Both demethoxy- and bisdemethoxycurcumin were also observed at the expected masses, (339.123 and 309.113 Da, respectively), at lower abundance. The 128-year-old French sample was a paler yellow color than the newly-dyed cotton. However, a peak at the exact mass of curcumin was observed at approximately 30% abundance. The other curcuminoids were also identified, at 12 and 16% abundances (Figure 1). No sample preparation was necessary.

Table II. Exact masses and expected DART-MS

<i>Colorant compound(s)</i>	<i>Formula</i>	<i>Exact mass (M^+), Da</i>	<i>Exact mass ($M+H^+$), Da</i>
Curcumin	$C_{21}H_{20}O_6$	368.126	369.134
Demethoxycurcumin	$C_{20}H_{18}O_5$	338.115	339.123
Bisdemethoxycurcumin	$C_{19}H_{16}O_4$	308.105	309.113
Santalin A	$C_{33}H_{26}O_{10}$	582.153	583.160
Santalin B	$C_{34}H_{28}O_{10}$	596.168	597.176
Pterocarpin	$C_{17}H_{14}O_5$	298.084	299.092
Homoptercarpin	$C_{17}H_{16}O_4$	284.105	285.113
Quercetin	$C_{15}H_{10}O_7$	302.043	303.050
Quercitrin	$C_{20}H_{21}O_{11}$	448.101	449.101
Catechin	$C_{15}H_{14}O_6$	290.079	291.087
Catechin gallate	$C_{22}H_{18}O_{10}$	442.090	443.098

Analysis of ground sandalwood bark showed no evidence of the santalins under these analytical conditions. However, both pterocarpin and homoptercarpin, also as $M+H^+$ ions, were readily observed in both the bark and the dye solution. The French treatise included two samples dyed with sandalwood: *rouge au santal* (sandalwood red) and *brun au santal* (sandalwood brown). The two pterocarpin compounds were observed in both French samples, in ratios similar to that of the raw sandalwood bark (Figure 2).

Quercetin was previously identified using DART-MS in textiles dyed with yellow onion skin (14). While the glycoside quercitrin reportedly predominates in the black oak bark, only the aglycone quercetin was observed in mass spectrum. However, cotton dyed with the bark extract yielded only a small signal (~9% abundance) for quercetin, similar to that observed in the *jaune de quercitron* sample from the French treatise (Figure 3). The low signal intensity is clear evidence of the tinting strength of this dye.

Others have utilized formic acid to extract dye colorants from fibers through acid hydrolysis for LC-MS studies (18). A fragment of quercitron bark was treated with a few drops of 80% formic acid, and introduced into the DART source, yielding a stronger signal for quercetin. This is most likely due to the hydrolysis of quercitrin to form the aglycone quercetin. Treating the quercitron-dyed cotton fibers with formic acid had no effect on the intensity of the quercetin signal.

The base peak from DART-MS analysis of the cutch powder was observed at m/z 291.084, which differs by 0.003 Da from the exact mass for protonated catechin. Cotton freshly-dyed with the Kremer cutch powder showed a small peak for protonated catechin only when the temperature of the DART gas was increased to 400 °C, resulting in significant charring of the fiber. The French treatise contained four different cutch-dyed cotton samples: a light khaki (*cachou*), dark brown (also labeled *cachou*), *cachou et bois jaune*, and *cachou de Laval*. Only the lightest color sample contained any indication of catechin in the mass spectrum, at low abundance and higher mass difference (~12 mDa) than observed for the standards. The primary colorant of old fustic (*bois jaune*, or yellow wood) is the flavonoid morin. The French sample dyed with cutch and old fustic contained neither catechin nor morin. Using *N*-methyl-*N*-trimethylsilyl-trifluoroacetamide (MSTFA), pure catechin gallate can be directly silylated in the DART source at 300°C, yielding a strong signal at 947.345 Da (R. Cody, personal communication, 2011). This in situ derivatization was reportedly simple, fast, and as such has significant potential for colorant compounds, including tannins, that have so far been difficult to ionize with DART.

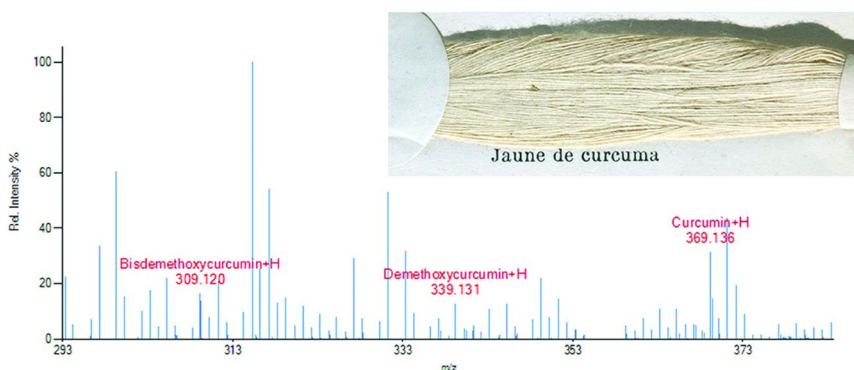


Figure 1. DART mass spectrum showing curcuminoids present in French textile.

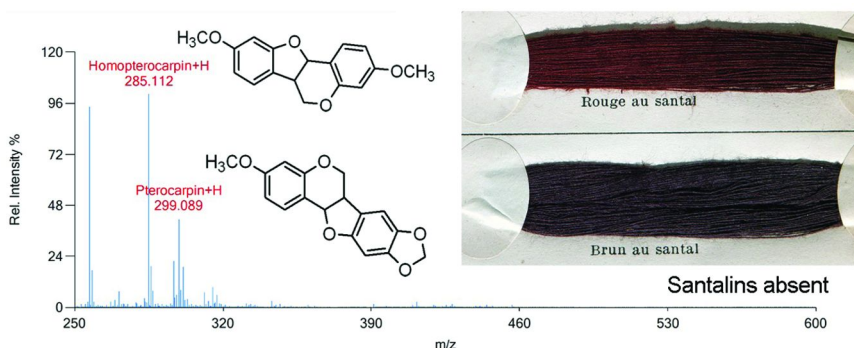


Figure 2. DART mass spectrum of sandalwood-dyed French cotton samples.

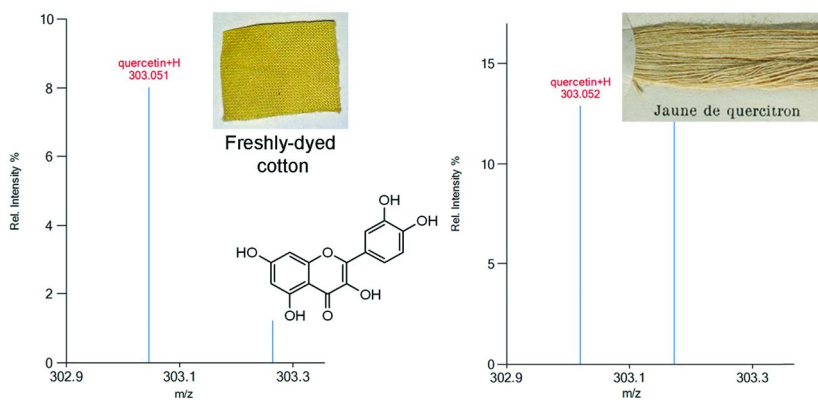


Figure 3. DART mass spectra of quercetin in cotton-dyed with quercitron bark.

Conclusions

DART-MS is a rapid and accurate method for identifying some organic colorants in textiles without any sample preparation. Of the samples investigated, turmeric and sandalwood were successfully identified without additional sample preparation. In situ acid hydrolysis increased the quercetin signal from quercitron bark, but had no effect on the dyed textile, possibly indicating that the textile did not contain significant quantities of the glycoside, quercitrin. In situ derivatization, particularly silylation, has potential for identifying tannins by DART-MS.

Acknowledgments

The authors gratefully acknowledge financial support from the National Science Foundation (Award MRI-R² #0959621), as well as the EMU Chemistry Department and Provost's Office. Thanks also to Robert Cody, JEOL U.S.A., for his help with the silylation of catechin gallate.

References

1. Cardon, D. *Natural Dyes: Sources, Tradition, Technology and Science*; Archetype: London, 2007.
2. Leona, M. *Proc. Natl. Acad. Sci. U.S.A.* **2009**, *106*, 14757–14762.
3. Wouters, J. *Stud. Conserv.* **1985**, *30*, 119–128.
4. Zhang, X.; Corrigan, K.; MacLaren, B.; Leveque, M.; Laursen, R. *Stud. Conserv.* **2007**, *52*, 211–220.
5. Vanden Berghe, I.; Gleba, M.; Mannering, U. *J. Archaeological Sci.* **2009**, *36*, 1910–1921.
6. Balakina, G. G.; Vasillev, V. G.; Karpova, E. V.; Mamatyuk, V. I. *Dyes Pigments* **2006**, *71*, 54–60.
7. Zhang, X.; Laursen, R. *Int. J. Mass Spectrom.* **2009**, *284*, 108–114.
8. Zhang, X.; Good, I.; Laursen, R. *J. Archaeol. Sci.* **2008**, *35*, 1095–1103.
9. Manhita, A.; Ferreira, V.; Vargas, H.; Ribeiro, I.; Candeias, A.; Teixeira, D.; Ferreira, T.; Dias, C. B. *Microchem. J.* **2011**, *98*, 82–90.
10. Mantzouris, D.; Karapanagiotis, I.; Valianou, L.; Panayiotou, C. *Anal. Bioanal. Chem.* **2011**, *399*, 3065–3079.
11. Degano, I.; Ribechini, E.; Modugno, F.; Colombini, M. P. *Appl. Spectrosc. Rev.* **2009**, *44*, 363–410.
12. Van Elslande, E.; Guérineau, V.; Thirioux, V.; Richard, G.; Richardin, P.; Laprèvote, O.; Hussler, G.; Walter, P. *Anal. Bioanal. Chem.* **2008**, *390*, 1873–1879.
13. Papageorgiou, V. P.; Mellidis, A. S.; Assimopoulou, A. N.; Tzarbopoulos, A. *J. Mass Spectrom.* **1998**, *33*, 89–91.
14. Selvius Deroo, C.; Armitage, R. A. *Anal. Chem.* **2011**, *83*, 6924–6928.
15. Cannon, J.; Cannon, M. *Dye plants and dyeing*; Timber: Portland, 1994.
16. Cody, R. B.; Laramée, J. A.; Durst, H. D. *Anal. Chem.* **2005**, *77*, 2297–2302.
17. McEwen, C. N.; Larsen, B. S. *J. Am. Soc. Mass Spectrom.* **2009**, *20*, 1518–1521.
18. Zhang, X.; Laursen, R. A. *Anal. Chem.* **2005**, *77*, 2022–2025.

Chapter 7

Characterizing Organic Residues on Ceramics by Direct Analysis in Real Time Time-of-Flight Mass Spectrometry

John Hopkins and Ruth Ann Armitage*

Chemistry Department, 501W Mark Jefferson,
Eastern Michigan University, Ypsilanti, MI 48197

*E-mail: rarmitage@emich.edu

Chemical analysis of residues on archaeological ceramics provides significant insights into how humans utilized food resources in the past. The methods most commonly used for these studies include GC-MS and LC-MS, which are both time consuming and expensive, but yield large amounts of diagnostic information. We report here developments in using direct analysis in real time mass spectrometry to identify the presence of biomarkers on ceramics. This technique, which requires little or no sample preparation and can be carried out in minutes, has the potential for screening large collections of ceramics for further study with other methods. Simulated sherds with a variety of food residues, including cacao, chilis, wine, olive oil, and *garum* were studied with and without burial and before and after standard field cleaning protocols. The results clearly show the importance of handling and storage of ceramics prior to any type of analysis.

Introduction

Organic residue analysis is a valuable tool for gaining insight into the history of human civilization. Identification of food residues can help the archeological community better understand the diet and trade of ancient cultures. These residues have been found to survive on or absorbed within the surface of ceramic vessels excavated from archaeological sites, and gas- or liquid chromatography - mass spectrometry are commonly used to characterize these residues (*1*). The chemical

identification of biomarkers on these ceramics can in turn aid in the identification of the food or beverage once contained within.

Biomarkers in archaeology are organic molecules that are characteristic of some botanical or animal product. Lipids are generally well preserved, and as such are the most widely studied of molecular markers found on ceramics (2, 3). Stable isotope mass spectrometry coupled to GC-MS is the method of choice for identification of the source of adsorbed lipids. Animal and plant fats can be distinguished by this method based on differences in isotopic ratios and the relative abundance of specific lipids (4). Amino acid composition is indicative of proteinaceous residues, such as *garum*, a popular Roman condiment made from fermented fish viscera and salt. The savory flavor of *garum* derives primarily from glutamate; Smirga et al. have identified *garum* on ceramics from Pompeii based partly on the high glutamic acid content of the residue (5).

Some botanicals have a single compound that is characteristic of that particular plant. Theobromine is a biomarker unique to *Theobroma cacao* in the Americas. Cacao beans were used by Mesoamerican cultures as an ingredient in ceremonial beverages (6), and residues of these beverages have been identified on ancient ceramics using HPLC or HPLC-MS (7–9). Fruits of *Capsicum annuum* have been an important food in what is now Mexico for approximately 8000 years, as indicated by the presence of chili pepper remains in Oaxacan pottery (10). We find no reports of chemical analysis of archaeological ceramics specifically for capsaicin, though Flamini et al. have examined fossilized fruits and votive offerings from Peru with HPLC to quantify capsaicinoids (11). Tartaric acid, a biomarker for grape products including wine and grape vinegar, has been found on amphorae using both FTIR and LC-MS/MS (12).

Existing methods of characterizing organic residues, such as GC or LC-MS are time intensive processes. These techniques require considerable sample preparation, such as organic solvent extraction, followed by filtration of the extract, and, for GC, derivatization (7, 9). Furthermore, the chromatographic aspect of these methods adds more time to the overall process, making each analysis a considerable investment of time and money. Contamination or degradation of the sample due to cleaning can further complicate the identification of the residues. A rapid method for screening potential samples for more rigorous analysis, such as those mentioned above, would facilitate residue characterization by removing contaminated or otherwise unpromising candidates from the pool of samples. Such an evaluation prior to LC or GC-MS would make analysis of ceramics of unknown identity a more practical undertaking. Ambient ionization mass spectrometry methods, such as direct analysis in real time mass spectrometry (DART-MS) and desorption electrospray ionization MS (DESI-MS) can be applied directly to ceramic surfaces, eliminating the need for chromatographic separation. DESI-MS has been used to identify proteins on simulated artifacts with minimal sample preparation (13). DART-MS is well suited to the identification of small molecules, such as the biomarkers already described. We report here on the use of DART-MS with minimal sample preparation in the detection of biomarkers within organic residues on ceramics.

Using residues created in the laboratory, we sought to answer three primary questions:

- Can the biomarker compounds be reliably identified after the residue has been applied to ceramic surface?
- Can residue biomarkers be identified after short-term burial (1 week – 6 months)?
- Does scrubbing the ceramics briefly with water remove or obscure residues?

Materials and Methods

Residues were prepared using the materials listed in Table 1 by placing approximately 15 mL of the material (dry or solid materials were prepared as a slurry in deionized water) in a shallow terra cotta ceramic dish and allowing the material to soak in for at least 24 hours. Terra cotta dishes were chosen because they were readily available in garden centers, and because the material absorbs liquids; they present a best case scenario for analysis. They were not cleaned or treated prior to use. Any liquid remaining was poured out, and the ceramic dish was left to dry at room temperature. Each ceramic dish, one for each residue and a control dish, was then broken into four or five pieces. Two pieces of each ceramic were buried within one week for up to six months. After excavation, one was briefly subjected to a standard field cleaning treatment for excavated pottery sherds: the buried ceramic pieces were allowed to dry, and were then placed together into a plastic container filled with tap water. Each was scrubbed briefly using a toothbrush to remove the majority of the soil, and then the wet ceramics were left to dry at room temperature. Of the remaining unburied pieces, one was left untreated, and the other was scrubbed as described. Scrubbed ceramics were left to dry overnight before further analysis.

Because of difficulties in placing the entire ceramic fragment into the gap between the DART ionization source and the mass spectrometer inlet, portions of the ceramic were removed for analysis. The exposed surface of the ceramic, near the rim where the residue was most concentrated, was abraded using a rotary grinding tool. The resulting powder (about 5 mg) was transferred to a small vial and combined with 10-15 μL of residue analysis grade methanol (Fisher) to form a paste.

Table 1. Description of samples investigated

<i>Food substance</i>	<i>Biomarker compounds</i>	<i>Ionization mode</i>
Chocolate	Theobromine Caffeine	Positive
Chili peppers	Capsaicin	Positive
Garum (fish sauce)	Pyroglutamic acid	Negative
Olive oil	Oleic acid Linoleic acid	Positive
Wine	Tartaric acid	Negative

Analyses were carried out on a JEOL AccuTOF mass spectrometer (JEOL USA, Peabody, MA) equipped with a DART ionization source (Ionsense, Saugus, MA). Samples were run in both positive and negative ion mode as appropriate with helium as the DART gas at a flow rate of 2.5 L/min at temperatures ranging from 200–400 °C. Grid voltage was set at +350 V (positive mode) and -530 V (negative mode), with orifice 1 at 30 V and 120 °C. Orifice 2 and the ring lens voltage were both held at 5 V, and the peaks voltage was held at 1500 V. Positive ion analyses were calibrated by running PEG-600 in methanol during the acquisition. PEG-600 provides poor calibrations in negative ion mode. A mixture of PEG and acids from fingerprints (including lactic, myristic, palmitic, oleic and stearic acids) was used for calibration of low molecular weight species in negative ion mode (R. Cody, pers. comm. 2011).

The ceramic/solvent pastes were introduced on the closed end of a melting point capillary tube by placing the tube directly into the gap between the DART source and the mass spectrometer orifice. Mass resolution of the AccuTOF was approximately 6000. Ions were observed at $M+H^+$ in positive mode and $M-H^-$ in negative mode; the DART ionization process has been described elsewhere (14, 15).

Results and Discussion

The expected DART-MS results are summarized in Table 2.

Cacao

The DART mass spectrum for the residue made from cocoa powder showed both theobromine (181.075 Da) and caffeine (195.088 Da). The cleaned ceramic sample showed little change in the theobromine and caffeine signal, and even after burial, clearly showed both compounds (Figure 1). While theobromine is a specific biomarker for cocoa, caffeine can come from other sources (e.g., coffee, tea, *yerba mate*) and cannot be used diagnostically for the presence of cacao beans.

Table 2. Exact masses and expected DART-MS results

<i>Biomarker compound(s)</i>	<i>Formula</i>	<i>Exact mass, Da</i>	<i>Ionization mode and expected ion</i>	<i>Expected DART mass, Da</i>
Theobromine	C ₇ H ₈ N ₄ O ₂	180.064	Positive, M+H ⁺	181.073
Caffeine	C ₈ H ₁₀ N ₄ O ₂	194.080	Positive, M+H ⁺	195.088
Capsaicin	C ₁₈ H ₂₇ NO ₃	305.199	Positive, M+H ⁺	306.207
Pyroglutamic acid	C ₅ H ₇ NO ₃	129.043	Negative, M-H ⁻	128.035
Oleic acid	C ₁₈ H ₃₄ O ₂	282.256	Positive, M+H ⁺	283.264
Linoleic acid	C ₁₈ H ₃₂ O ₂	280.240	Positive, M+H ⁺	281.248
Tartaric acid	C ₄ H ₆ O ₆	150.087	Negative, M-H ⁻	149.009

Chili Peppers

Capsaicin is a biomarker for the presence of chili peppers. Two sets of samples were made for chili peppers. The first set of samples were handled without gloves and stored in zip-top plastic bags, as archaeological samples typically are handled and stored. While capsaicin (306.207 Da) was clearly observed in the DART mass spectrum, the base peak was from erucamide (338.342 Da), the slip agent in zip-top plastic bags. Significant signal was also observed at 411.399 Da, arising from squalene in fingerprints. This sample (Figure 2, top) clearly illustrates the importance of handling and storage in residue analysis. The presence of these contaminants may mask the presence of residues: if the erucamide signal is strong, weaker signals from potentially diagnostic compounds may not be easily observed, and thus overlooked. The second set of chili pepper ceramic samples was buried and showed significant capsaicin signal after burial but before cleaning (Figure 2, bottom). No capsaicin signal was detected after cleaning.

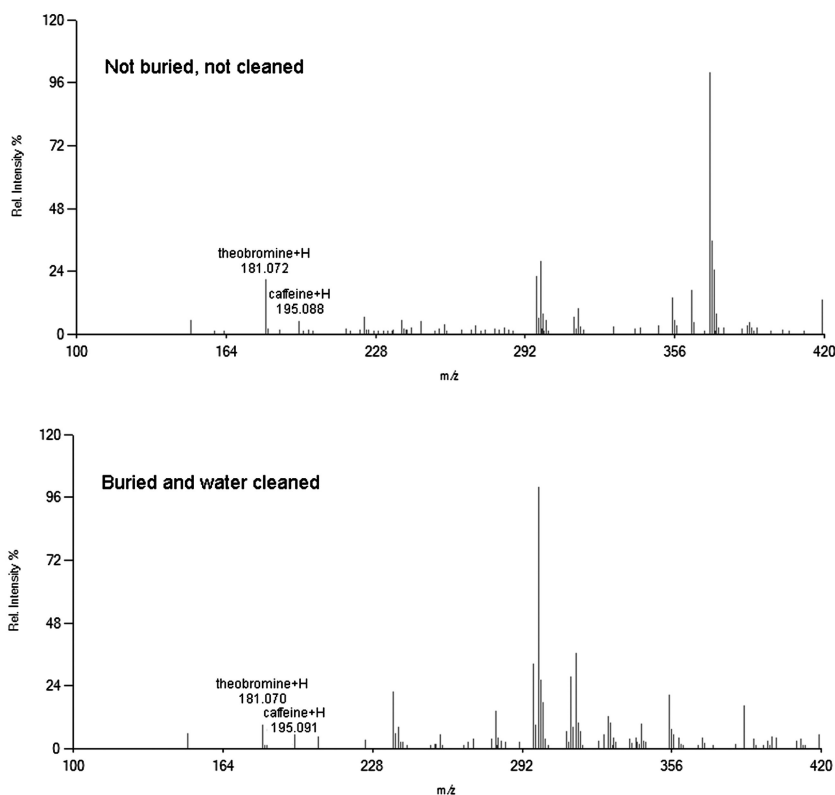


Figure 1. Theobromine and caffeine in mass spectra of ceramics containing cocoa residues.

Garum (Fish Sauce)

The Roman condiment *garum* has a modern equivalent in Asian fish sauces. *Colatura di alici*, or anchovy syrup is a modern Italian version of *garum*. Both are used to impart umami flavor to foods, and therefore are sources of glutamate. Negative ion DART-MS of neat fish sauce and anchovy syrup confirmed that the primary component is pyroglutamic acid, a cyclized form of glutamic acid. Pyroglutamic acid was observed as the M-H⁻ ion at m/z 128.032 Da, only 0.003 Da difference from the calculated exact mass (Figure 3). This was also observed for the *garum* residue on the ceramic, though the base peak was found to be leucine. The cleaning procedure removed most or all of the pyroglutamic acid, evidenced by the loss of signal in those samples. The buried ceramics also showed no evidence of the pyroglutamic acid. Other amino acids, including leucine, valine, and proline were also observed in significant quantities in the *garum* residue, and further study of the whole amino acid profile may provide further information about the preservation of the residue. In the future, we will compare the whole amino acid composition to that observed by Smriga et al. (5).

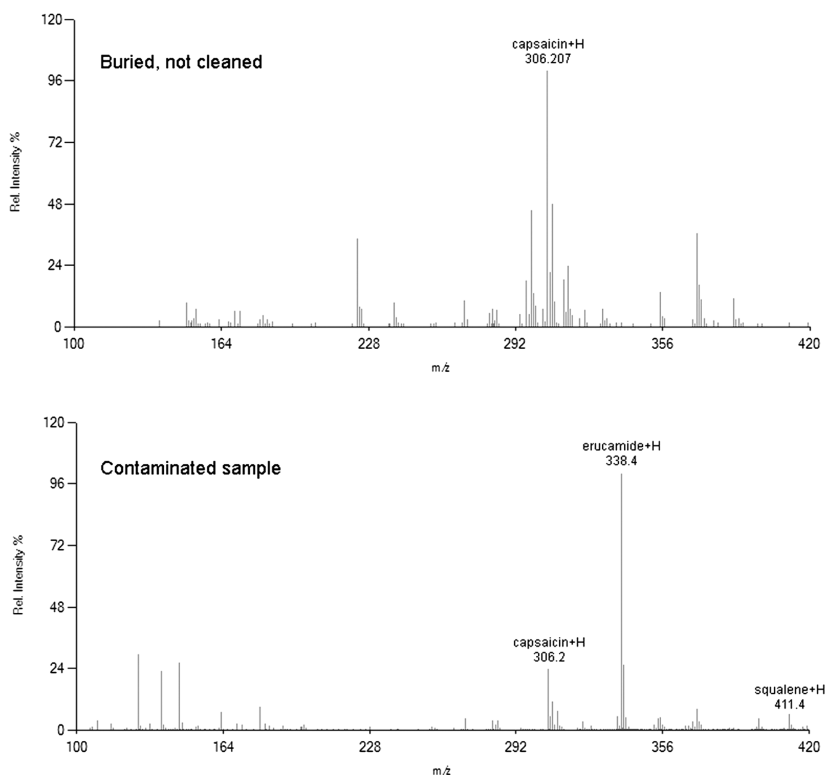


Figure 2. Capsaicin in mass spectra of ceramics with chili pepper residue.

Olive Oil

Olive oil does not have a single diagnostic biomarker, so the DART mass spectrum of the neat oil was compared to the residue. Oleic and linoleic acid, were the largest peaks observed in the extra virgin olive oil used in our study, which is consistent with previous DART studies of olive oil (16). As expected, this lipid residue was the best preserved, being clearly identifiable even after burial and cleaning (Figure 4). Significant improvement in the DART signal may be possible by using hexane rather than methanol to prepare the paste samples.

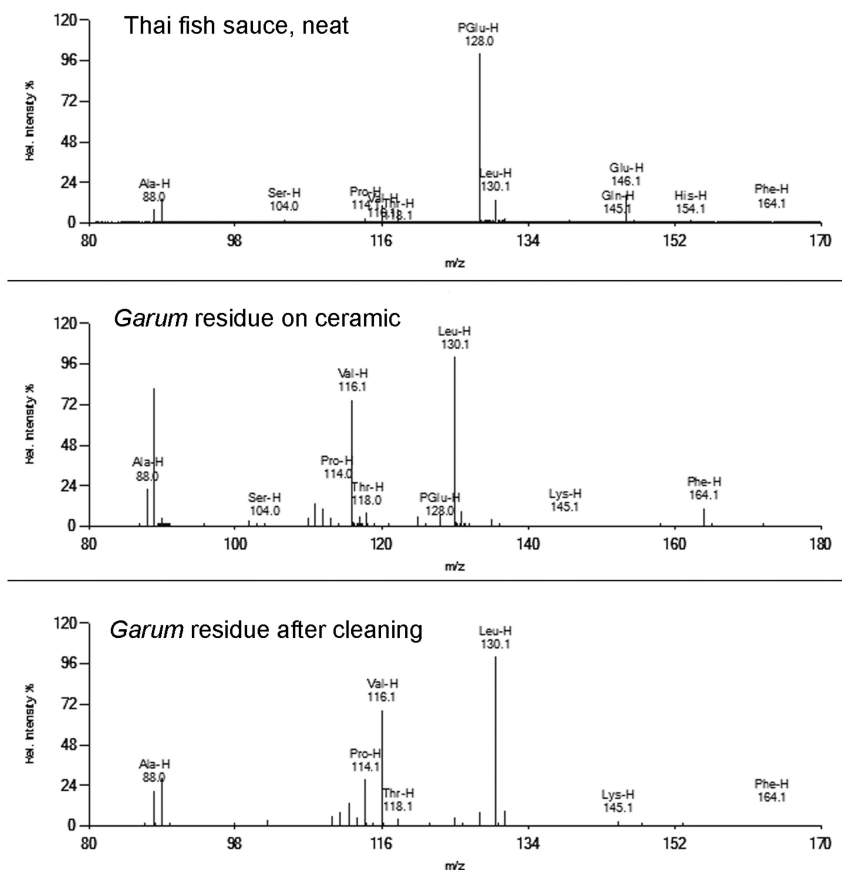


Figure 3. DART mass spectra for fish sauce (garum).

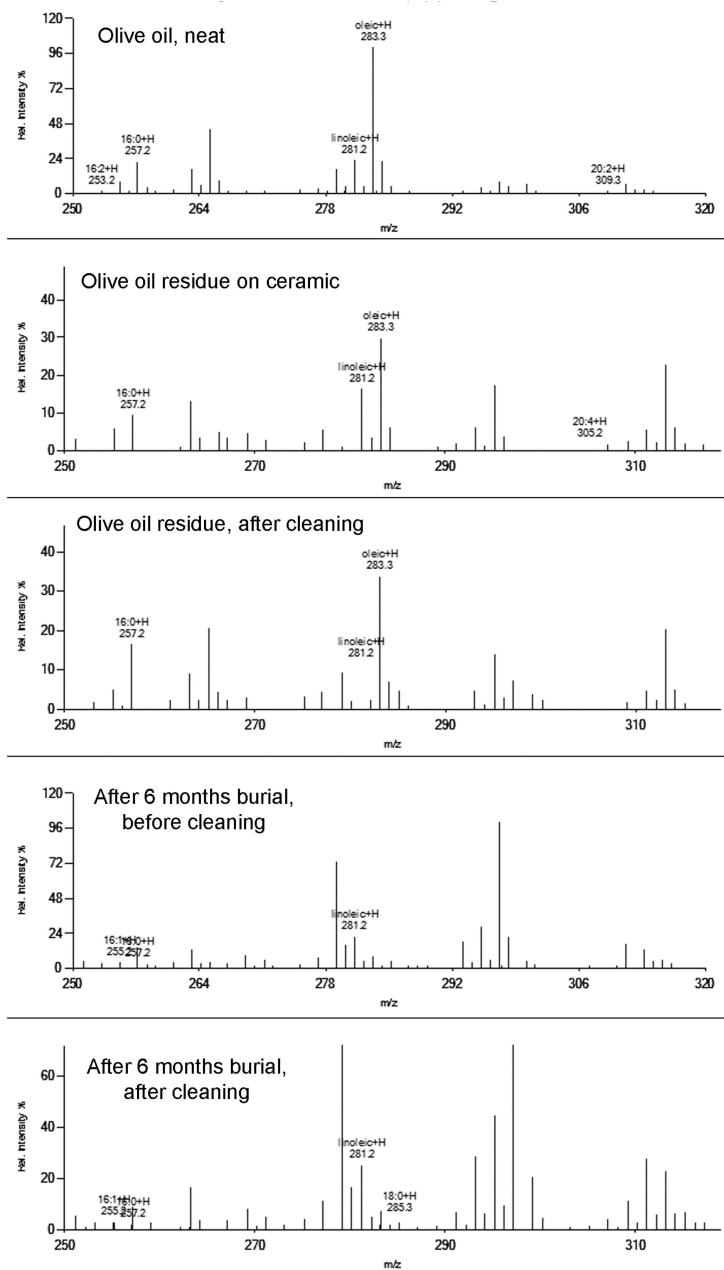


Figure 4. DART-MS of olive oil sherds, showing the effects of treatment on linoleic and oleic acids.

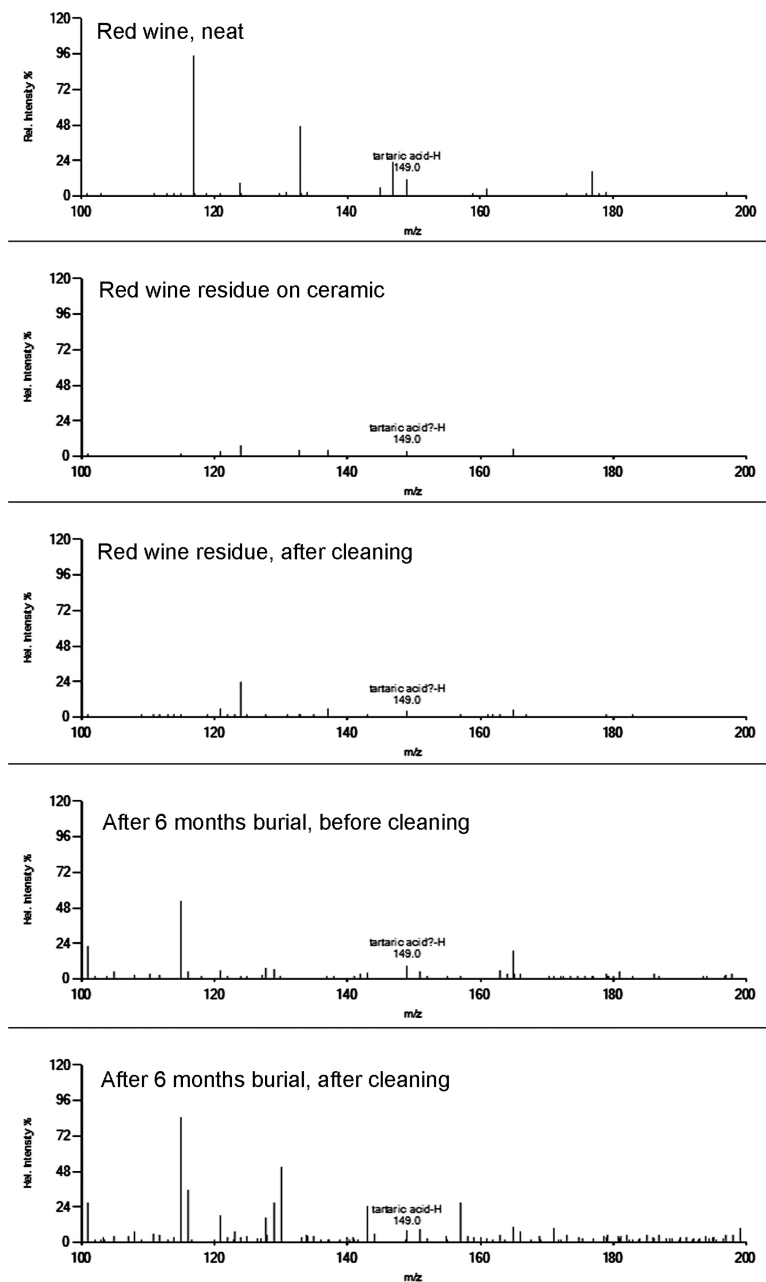


Figure 5. DART mass spectra of suspected tartaric acid in wine residues.

Wine

Wine remains a work in progress. Tartaric acid has so far been the most promising biomarker for wine, as polyphenols like malvidin (and the related syringic acid, which are also biomarkers for wine (17, 18) could not be detected under the DART conditions used in this study. However, calibration in this low mass range, as with pyroglutamic acid, has proven somewhat difficult. Pure tartaric acid solid yields a DART mass spectrum with the expected exact mass (149.009 Da). In neat wine samples, tartaric acid was identified at the correct mass, at about 10% relative abundance.

When the wine is applied to the ceramic, there is a peak in the mass spectrum at m/z 149.026, about 20 millimass units (mmu) different from the expected mass for tartaric acid (Figure 5). The AccuTOF mass spectrometer is expected have no more than 10 mmu difference. For the wine residue that was buried for six months prior to analysis, a peak was observed at m/z 149.015, within the expected uncertainty for tartaric acid. It remains unclear if we are truly seeing tartaric acid in all of the wine residues with a significant mass difference, or if the signal at 149.026 Da arises from a different component of the wine. Future studies will focus on understanding this problem and developing a method for identifying syringic acid rapidly by DART-MS.

Conclusions

Some biomarkers of food residues are readily identifiable on ceramics, regardless of exposure to a burial environment or cleaning. Olive oil was the most easily identifiable residue, as it is the most hydrophobic and therefore best preserved of the residues. Capsaicin is likely to be present in low concentrations and seems to be extremely sensitive to soil exposure. Tartaric acid as a marker for wine residues has shown that calibration in the mass range of interest is of utmost importance in DART-MS. Contaminants from handling ceramics without gloves and from storing sherds in plastic bags are readily observable by DART-MS; the method can at the very least be used for screening samples to determine those that are least contaminated and therefore best suited for further study.

Acknowledgments

The authors gratefully acknowledge financial support from the National Science Foundation (Award MRI-R2 #0959621), as well as the EMU Chemistry Department and Provost's Office. We also thank Laura Banducci, University of Michigan, for her guidance on how sherds are handled in the field, and EMU graduate Landrea Standfield for their help in the preliminary stages of this project. Thanks also to Robert Cody, JEOL USA for his advice and support.

References

1. Evershed, R. P. *Archaeometry* **2008**, *50*, 895–924.
2. Evershed, R. P. *World Archaeol.* **1993**, *25*, 74–93.
3. Evershed, R.; Dudd, S.; Copley, M.; Berstan, R.; Stott, A.; Mottram, H.; Buckley, S.; Crossman, Z. *Acc. Chem. Res.* **2002**, *35*, 660–668.
4. Steele, V. J.; Stern, B.; Stott, A. W. *Rapid Comm. Mass Spectrom.* **2010**, *24*, 3478–3484.
5. Smruga, M.; Mizukoshi, T.; Iwahata, D.; Eto, S.; Miyano, H.; Kimura, T.; Curtis, R. *J. Food Comp. Anal.* **2010**, *23*, 442–446.
6. Coe, S.; Coe, M. *The True History of Chocolate*; Thames and Hudson: New York, 1996; pp. 35–103.
7. Powis, T. G.; Cyphers, A.; Gaikwad, N. W.; Grivetti, L.; Cheong, K. *Proc. Natl. Acad. Sci. U.S.A.* **2011**, *108*, 8595–8600.
8. Crown, P. L.; Hurst, W. J. *Proc. Natl. Acad. Sci. U.S.A.* **2009**, *106*, 2110–2113.
9. Henderson, J. S.; Joyce, R. A.; Hall, G. R.; Hurst, W. J.; McGovern, P. E. *Proc. Natl. Acad. Sci. U.S.A.* **2007**, *104*, 18937–18940.
10. Perry, L.; Flannery, K. V. *Proc. Natl. Acad. Sci. U.S.A.* **2007**, *104*, 11905–11909.
11. Flamini, G.; Morelli, I.; Piacenza, L. *Phytochem. Anal.* **2003**, *14*, 325–327.
12. McGovern, P. E.; Mizorian, A.; Hall, G. R. *Proc. Natl. Acad. Sci. U.S.A.* **2009**, *106*, 7361–7366.
13. Heaton, K.; Solazzo, C.; Collins, M. J.; Thomas-Oates, J.; Bergstrom, E. T. *J. Archaeol. Sci.* **2009**, *36*, 2145–2154.
14. Cody, R. B.; Laram ee, J. A.; Durst, H. D. *Anal. Chem.* **2005**, *77*, 2297–2302.
15. McEwen, C. N.; Larsen, B. S. *J. Am. Soc. Mass Spectrom.* **2009**, *20*, 1518–1521.
16. Vaclavik, L.; Cajka, T.; Hrbek, V.; Hajslova, J. *Anal. Chim. Acta* **2009**, *645*, 56–63.
17. Guasch-Jane, M. R.; Ibern-Gomez, M.; Andres-Lacueva, C.; Jauregui, O.; Lamuela-Raventos, R. M. *Anal. Chem.* **2004**, *76*, 1672–1677.
18. Barnard, H.; Dooley, A. N.; Areshian, G.; Gasparyan, B.; Faull, K. F. *J. Archaeol. Sci.* **2011**, *38*, 977–984.

Chapter 8

New Developments in the “Nondestructive” Dating of Perishable Artifacts Using Plasma-Chemical Oxidation

Ruth Ann Armitage,^{*,1} Mary Ellen Ellis,¹ and Carolynne Merrell²

¹Chemistry Department, Eastern Michigan University, 501 Mark Jefferson,
Ypsilanti, MI 48197

²Archaeographics, 2090 N. Polk Ext., Moscow, ID 83843 U.S.A.

*E-mail: rarmitage@emich.edu

Fragile or perishable artifacts, including basketry, textiles, and netting, are rare in the archaeological record. Dating such objects must be undertaken with great care, as the process of radiocarbon analysis requires destructive sampling, cleaning, and combustion steps. We report here progression a minimally destructive, yet effective, sample pretreatment procedure for removing contaminants, followed by the application of plasma-chemical oxidation to prepare materials for accelerator mass spectrometric radiocarbon analysis. We have applied the new phosphate treatment to fragments from artifacts made from grasses and tree bark, excavated from a site in Idaho, and subjected the whole artifacts to plasma oxidation for comparison. Our results show that microsampling and pretreatment gives more reliable results with less damage to the artifacts.

Introduction

There are two processes in radiocarbon dating that combined are totally destructive. First is the harsh acid and/or base pretreatment(s) that are currently used to remove carbonates and oxalates, and humic acids from the burial environment respectively. A follow-up rinse with acid to prevent adsorption

of atmospheric carbon dioxide also contributes to loss of material during pretreatment. Finally, the conversion of the remaining organic matter to carbon dioxide for radiocarbon analysis is typically carried out via total combustion at high temperature.

Plasma-chemical oxidation (PCO), developed in the Rowe laboratory at Texas A&M University for direct dating of rock paintings, has been shown to also be a minimally-destructive method for preparing fragile artifacts like textiles and botanical specimens for radiocarbon dating (1, 2). Because the plasma conditions are gentle, carbonates and oxalates are not broken down to carbon dioxide, and thus do not need to be removed prior to treatment. These gentle conditions also are minimally destructive to the artifact itself, meaning the artifact is generally unaffected after sufficient carbon dioxide has been extracted for dating. Argon plasmas, while unreactive, can be used to remove surface- adsorbed gases as well.

Humic acids may permeate artifacts subjected to burial environments. This type of contamination is significant for the plasma-chemical oxidation method. Humic acids must be removed from artifacts prior to exposure to the plasma oxidation process. Standard pretreatment protocols used in radiocarbon dating, of which the acid-alkali-acid treatment is most common (3), are destructive, resulting in significant loss of sample during the process. A 1 M NaOH solution alone appears to be sufficient for removing humic acids from samples prepared with the PCO method (4, 5). Even this minimal treatment can be damaging to fragile artifacts.

To better understand the interplay between sample preparation, preservation, and reliable radiocarbon dating with the plasma oxidation method, we undertook a comparison study with two artifacts from a site in Idaho. These samples provided an opportunity to compare the radiocarbon dates obtained by direct plasma oxidation of whole, untreated artifacts to those for pretreated subsamples prepared either with plasma oxidation or complete combustion. In the course of this comparison, we applied the standard acid-alkali-acid treatments, base-only treatments, and a new, less harsh buffer treatment, and considered the affect of these treatments on the resulting radiocarbon ages.

Materials and Methods

All reagents were obtained from available stocks and were of ACS reagent grade or higher as indicated. Ultrapure water (18 M Ω , Barnstead NanoPure) was used for all aqueous solutions used in pretreatment. Glassware, filters, and aluminum foil were cleaned of all organic matter prior to use by baking overnight at 500 °C in a muffle furnace.

Artifacts from Little Lost River Cave, Idaho

Little Lost River Cave no. 1 (10BT1) is a deep, low-roofed limestone solution cave in the Lemhi Mountains of central Idaho overlooking the Snake River Plain (6–8). The archaeological site was brought to the attention of several faculty members at the Idaho State College by Albert Whiting, a local artifact

hunter. The site was originally excavated in 1954 by researchers from the museum at the College over the course of only three days. A single 5' x 5' test pit was dug to a depth of ~100 cm. The excavators described three naturally-occurring stratigraphic layers in the test pit. Layers 2 and 3 yielded a number of perishable artifacts including cordage and basketry as well as lithics. After this initial study, some 30 years passed before the site was again investigated. Surface surveys showed that, particularly at the entrance to the cave, some pothunting activity had occurred during the interim. A new test pit was dug in 1990; a more detailed stratigraphic record resulted from the 1990 excavation, one that cannot be exactly correlated to the simpler record from 1954. Layer C in 1990 contained the majority of the artifacts and so may relate to Layer 2 from 1954. Both studies describe the presence of red and yellow pictographs underlying a shiny black coating.

Two artifacts from Layer 2 of the 1954 excavation were selected for further analysis (Figure 1). Specimen no. 23 is a knotted ring of shredded juniper bark, measuring about 80 cm in diameter. Animal hair, later identified as from an antelope, was found associated with this artifact. Specimen no. 13 is a knot tied in a fragment of reed. Ethnographic studies, along with the images depicted in the pictographs and the abundance of antelope faunal remains at the site suggest that Little Lost River Cave may once have been used by an antelope shaman or charmer. It has been suggested that the juniper ring may have represented a corral into which the shaman sought to charm the herd, represented by the associated hair (9); however, this remains a hypothesis that cannot be tested. An uncalibrated radiocarbon date of 3900 ± 100 yrs. BP was obtained on a fragment of charcoal from a hearth in Layer C of the 1990 excavation at 10BT1. Radiocarbon dates of the selected artifacts were sought to further place in time the human activity at the site.

Direct “nondestructive” dating using the plasma chemical oxidation process was initially planned for these fragile artifacts. In shipping, small fragments of the reed and bark broke off from the artifacts. We chose to use the fragments to compare the direct dating of the whole artifacts to standard methods requiring destructive pretreatment and combustion, as well as to plasma oxidation after chemical pretreatments to remove contamination from the burial environment

Direct Plasma Oxidation of Whole Artifacts

To evaluate direct “nondestructive” dating of whole artifacts, the juniper ring and knotted reed artifacts were placed entirely within the plasma chamber. Samples are inserted under a positive flow of ultra-high purity (99.999%) argon to minimize the chance that atmospheric aerosols will enter the reaction chamber, and then sealed with a copper-gasketed flange.

The plasma chamber was maintained at a vacuum pressure of $\sim 10^{-7}$ Torr under a heat lamp for at least 24 hours prior to further processing. Vacuum integrity checks (VIC) prior to plasma oxidation indicated that no significant leaks were present in the system. We assume, as a worst case scenario, that all pressure increase during the 60-min arises from carbon dioxide; as long as the pressure increase corresponds to less than the contamination background in the

accelerator mass spectrometer (typically 0.5-1 $\mu\text{g C}$), the increase is considered inconsequential. Oxygen gas for plasma oxidation was of research grade (99.999+ %).



Figure 1. The two artifacts from Little Lost River Cave, Idaho. Top: Ring made from juniper bark. Bottom: Reed stems tied together.

The oxygen plasma has been shown to react with organic carbon at a sufficiently low temperature (~150 °C) that any inorganic oxalates and carbonates present are unaffected, thus eliminating the need for an initial acid wash. The whole artifacts were exposed to short duration, low power (20-40 W) oxygen plasmas to minimize the chances of damage occurring. The reed artifact was oxidized three times, with the products of each plasma sealed off for dating. The juniper ring was initially exposed to a short plasma to remove surface contamination, the product of which was not saved. The ring was exposed to three additional oxidation plasmas.

Animal hair has a high surface area, and cannot be dated nondestructively. Some of the antelope hair that was associated with the juniper ring artifact was selected for dating. The hair was rinsed thoroughly with water to remove surface contamination, dried, and exposed to plasma treatment at high RF power. While the hair at first appeared unchanged after plasma treatment, upon removing the sample from the chamber, it was found to have been completely ashed.

The carbon dioxide products from the plasmas were collected by cooling a glass finger on the plasma system with liquid nitrogen. The glass tube was then sealed off and sent to the Center for Accelerator Mass Spectrometry at Lawrence Livermore National Laboratory for radiocarbon analysis. The plasma conditions for the direct oxidation of the artifacts are listed in Table I.

Table I. Pretreatment and plasma conditions for direct plasma oxidation

<i>Sample name</i>	<i>Pretreatment</i>	<i>Plasma conditions</i>	$\mu\text{g C}$
Ring, fraction 1	40 W O ₂ plasma, 5 min	40 W, 4 min	100
Ring, fraction 2	n/a	40 W, 10 min	230
Ring, fraction 3	n/a	30 W, 7 min	170
Reed, fraction 1	none	40 W, 10 min	210
Reed, fraction 2	n/a	40 W, 5 min	100
Reed, fraction 3	n/a	20 W, 12 min	100
Antelope hair	Water, 15 min	1000 W, 45 min	460

Pretreatment Protocol for Artifact Fragments

Small fragments of reed and bark were observed in the foil packaging along with the two artifacts when they arrived in our laboratory. These fragments were subjected to chemical pretreatments prior to radiocarbon dating to compare the results to those obtained by directly oxidizing the whole artifacts. The standard acid-alkali-acid (AAA) treatment consisted of a wash with 1 M HCl to remove carbonates, followed by a wash with 1 M NaOH to remove humic acid, after which samples were reacidified to prevent adsorption of atmospheric carbon dioxide (3).

The alternative, less destructive treatment involved use of a pH 8 buffer solution of Na_2HPO_4 and NaH_2PO_4 with a phosphate ion concentration of 1 M. Previous studies with phosphate solutions have been shown to be effective in removing humic acids from soils and charcoals (10, 11).

The reed and bark fragments were placed in 1 mL microcentrifuge tubes, to which was added 1 mL of the corresponding wash solution. In acid wash steps, the samples were examined under 20x magnification to look for evidence of carbonate decomposition, as bubbles of CO_2 . The sealed tubes were placed in an ultrasonic bath at $60 \pm 5^\circ\text{C}$ for one hour. The vials were then centrifuged to separate the samples from the solution. If the NaOH or phosphate solutions had any yellow color present, this indicated the presence of humic acid contamination. In these cases, the base/phosphate wash was repeated. Following each wash, the solution was removed with a Pasteur pipet and saved for future analysis. After the final wash step, samples were combined with deionized water, vortexed, and vacuum filtered through binder-free borosilicate glass filters. At least three funnel volumes (about 3 mL) of DI water were used for a final rinse. Samples were dried on the filter wrapped in aluminum foil in an oven at 100°C overnight, then stored in a desiccator until plasma processing. Samples subjected to AAA pretreatment were sent directly to LLNL-CAMS for combustion and ^{14}C analysis.

Plasma-Chemical Oxidation Procedure

The phosphate-treated samples were removed from their filters when dry. The organic material was placed into a clean glass dish. The sample and the dish were then placed directly into the plasma-chemical oxidation chamber. Plasma treatment followed the oxidation procedure described above. The conditions are summarized in Table II. The resulting carbon dioxide was collected and sent for radiocarbon dating at LLNL-CAMS.

Table II. Pretreatment and plasma oxidation conditions for fragments of bark and reed artifacts

<i>Sample name</i>	<i>Pretreatment</i>	<i>Plasma conditions</i>	<i>$\mu\text{g C}$</i>
Juniper ring fragment	AAA	None- combusted	n/a
Juniper ring fragment	1x phosphate	40 W , 30 min	100
Reed fragment	1x phosphate	40 W, 19 min	50
Reed fragment	AAA	None- combusted	n/a

Results and Discussion

Direct Oxidation of Whole Artifacts

Plasma oxidation of whole artifacts cannot, based on our observations, be deemed “nondestructive” to the objects, as can be clearly observed in Figures 2 and 3. The plasma oxidation reaction occurs at the sample surfaces. Only the surfaces exposed to the plasma react, and thus only that material is collected for radiocarbon dating. When a portion of the sample is exposed on all sides to the plasma, as seen in the thin portions of the artifacts in Figures 1 and 2, the sample is likely to char or ash.

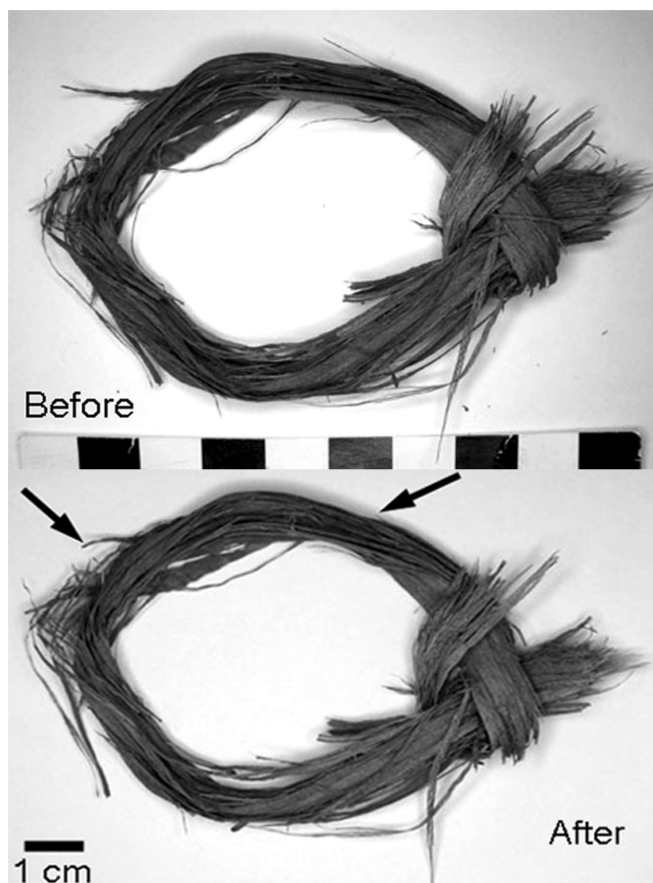


Figure 2. Juniper ring before and after plasma oxidation. Arrows note where significant damage occurred. Color difference is due primarily to ash coating on surface of artifact after plasma oxidation.

The radiocarbon dates obtained from the direct plasma oxidation of the whole artifacts are summarized in Table III. The first fraction of reaction products from the juniper ring was not dated. It was instead sent for $\delta^{13}\text{C}$ analysis to correct the dates for carbon isotope fractionation. The resulting $\delta^{13}\text{C}$ of -24.69% was consistent with the expected -25% for wood (12). Two dates were obtained from the second and third direct plasmas on the juniper ring. These dates were statistically indistinguishable from each other.

The antelope hair that was found on top of the juniper ring *in situ* during the excavations at Little Lost River Cave was found to be of the same radiocarbon age as the ring, indicating that the hair and ring were contemporaneous, though any cultural association or ritual use cannot be confirmed based solely on the dates.

The products obtained from the first plasma on the reed artifact were radiocarbon dated to 1615 ± 40 years BP. Unfortunately, the products from the second plasma carried out on the reed artifact “did not run well at all on the ion source” (T. Guilderson, personal communication 6/2007) at LLNL-CAMS, and no date was obtained. The third fraction was sent for $\delta^{13}\text{C}$ analysis; the resulting -29.73% is generally consistent with values measured for grass stems such as wheat straw ($-27 \pm 2\%$) (13, 14).

Table III. Radiocarbon results for direct plasma oxidation of whole artifacts from Little Lost River Cave

CAMS ID	Sample name	Pretreatment	^{14}C date (uncalibrated years BP)
n/a	Ring, fraction 1	5 min, 40 W O_2 plasma	Not dated $\delta^{13}\text{C} = -24.69\%$
134005	Ring, fraction 2	n/a	4550 ± 40
134006	Ring, fraction 3	n/a	4520 ± 50
132754	Antelope hair	Water, 15 min	4500 ± 35
132755	Reed, fraction 1	none	1615 ± 40
134005	Reed, fraction 2	n/a	No date obtained (see text)
n/a	Reed, fraction 3	n/a	Not dated $\delta^{13}\text{C} = -29.73\%$

Dating of Cleaned Fragments from Artifacts

The radiocarbon dates obtained on the pretreated fragments from the two artifacts are summarized in Table IV. Little damage was incurred to the fragments from even the harsh pretreatments; some bleaching of color occurred, but little of the sample was lost. Because the fragments were mostly flat, the plasma treatment was not significantly destructive either. After plasma oxidation, the fragments were removed from the plasma chamber and saved for future study.

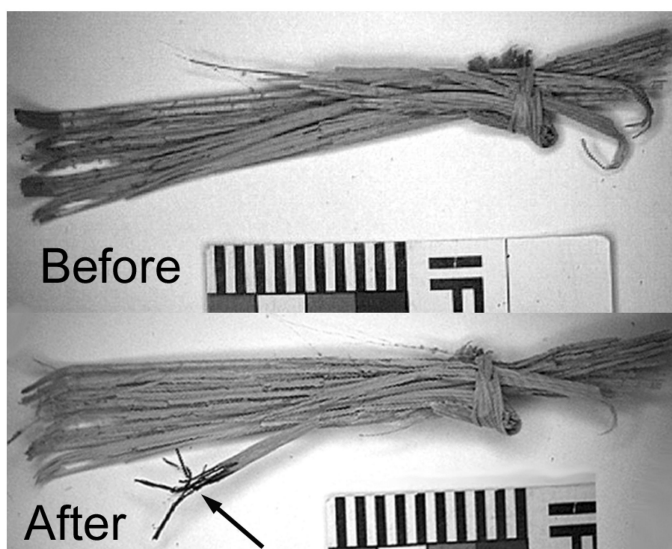


Figure 3. Reed artifact before and after plasma treatment. Arrow marks significant charring; color difference is due to ashing of surface during plasma oxidation.

Table IV. Radiocarbon results for pretreated fragments of the artifacts from Little Lost River Cave

CAMS ID	Sample name	Pretreatment	^{14}C date (uncalibrated years BP)
127362	Ring fragment	AAA	4460 \pm 30
140319	Ring fragment	pH 8 phosphate buffer (1x)	4460 \pm 80
134007	Reed fragment	pH 8 phosphate buffer (1x)	1100 \pm 110
134008	Reed fragment	AAA	1180 \pm 80

The juniper ring fragments prepared with two different methods – AAA/combustion and phosphate buffer/plasma oxidation – yielded the same radiocarbon age of 4460 years BP, with differences only in the uncertainty. Smaller samples generally have larger uncertainties. Because AAA/combustion is the standard method of preparing samples for AMS dating, this date is considered the “best” age for the juniper ring. In the case of the juniper ring, all of the radiocarbon dates obtained are indistinguishable at the 95% confidence limit, yielding a pooled mean age of 4465 \pm 8 years BP ($T=6.139907$, $\chi^2=7.81$). The consistency of these dates is illustrated in Figure 4.

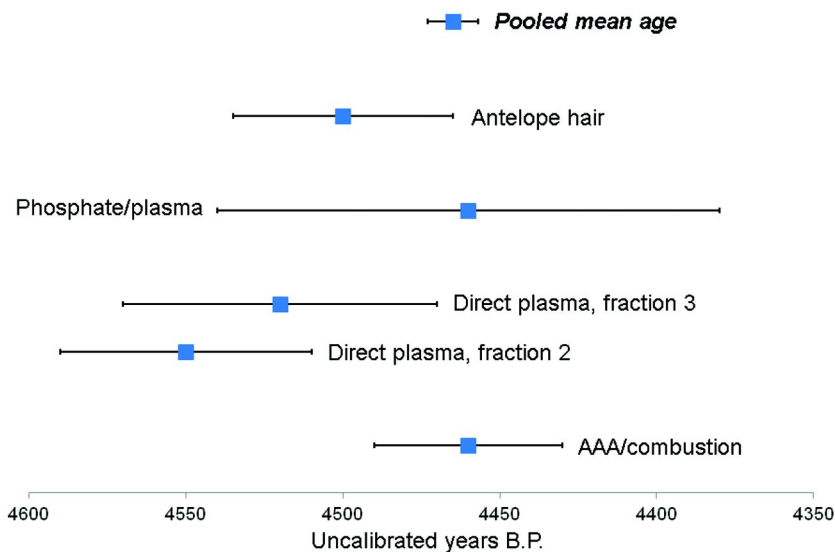


Figure 4. Summary of radiocarbon dates for juniper ring from Little Lost River Cave, Idaho.

The fragments of the reed artifact prepared with the AAA/combustion and phosphate buffer/plasma oxidation yielded dates that were statistically indistinguishable at the 95% confidence level ($T = 0.345954$, $\chi^2 = 3.84$). Again, the AAA/combustion age can be considered the most reliable age for the reed artifact. The direct plasma oxidation yielded an age nearly 500 years older than the AAA/combustion process. This is likely due to the presence of humic acid contamination at the surface of the artifact. A radiocarbon age for the second fraction of plasma products, which was not available due to a problem at LLNL-CAMS, would have provided sufficient information to test this hypothesis. If the second fraction had yielded an age consistent with that of the AAA/combustion process, we could state with some confidence that surface contamination was the cause of the earlier date for the first fraction. The range of radiocarbon ages obtained for the reed artifact is illustrated in Figure 5. The pooled age of the reed artifact, based only on the cleaned samples, is 1150 ± 65 years BP.

The efficacy of the phosphate treatment is supported by gas chromatography-mass spectrometry analysis of textile samples contaminated intentionally with humic acids. Linen and wool were soaked in a saturated solution of an 11,000-year-old humic acid standard, dried, and aliquots were removed for thermally assisted hydrolysis/methylation GC-MS. After two washes with phosphate buffer, marker compounds for humic acids (substituted methoxybenzenes) decreased to the level observed after a single ABA treatment (15).

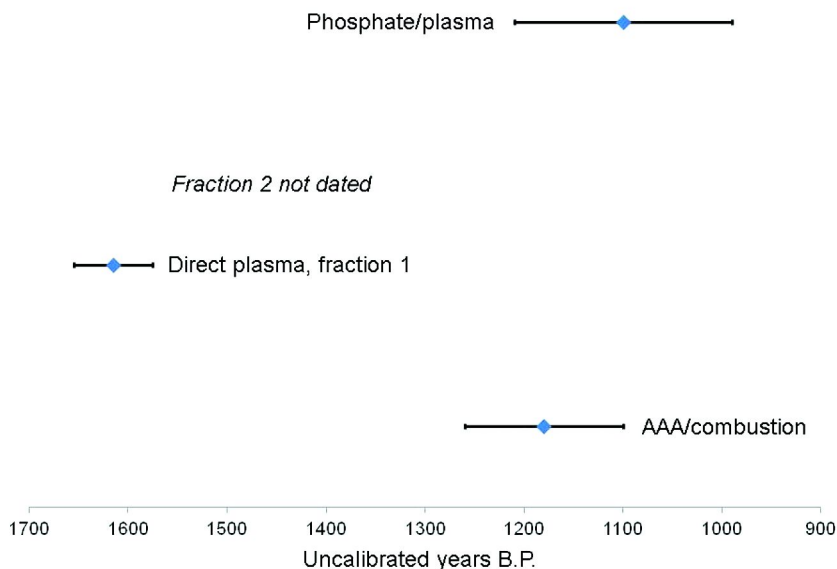


Figure 5. Summary of radiocarbon dates obtained on reed artifact from Little Lost River Cave, Idaho.

Because of the damage incurred to the artifacts, and the problem of surface contamination, we will not pursue further use of direct plasma oxidation of whole artifacts. Only a small sample of the material is needed for the plasma oxidation and AMS radiocarbon dating. Rather than risking the entire artifact, we will in the future use the fragments that form incidentally during handling of fragile artifacts. Dating these incidental fragments after chemical pretreatment is both more conservative, and more likely to provide a meaningful radiocarbon age.

Conclusions

Phosphate buffer at pH 8 is an effective alternative to the standard AAA pretreatment when samples are dated using the plasma-chemical oxidation method to prepare samples for AMS dating. Radiocarbon dates obtained on AAA-treated and combusted samples are statistically indistinguishable from those obtained on phosphate-treated and plasma-oxidized samples. Direct application of plasma oxidation to three-dimensional artifacts can result in charring and ashing of the materials and is not always nondestructive.

Acknowledgments

The authors thank Marvin Rowe, Texas A&M University (emeritus), and Tom Guilderson (Lawrence Livermore National Laboratory) for their support of this project. Funding was provided by the EMU Chemistry Department Sellers Fund and the EMU Provost's Office (through a Faculty Research Fellowship for RAA). EMU students Deidre Hardemon and Joslyn Kirkland also participated projects associated with the work presented here.

References

1. Steelman, K. L.; Rowe, M. W. In *Archaeological Chemistry: Materials, Methods, and Meaning*; Jakes, K., Ed.; SCS Symposium Series 831; American Chemical Society: Washington, DC, 2002; pp 8–21.
2. Steelman, K. L.; Rowe, M. W.; Turpin, S. A.; Guilderson, T.; Nightengale, L. *American Antiquity* **2004**, *69*, 741–750.
3. Mook, W. G.; Waterbolk, H. T. *Radiocarbon Dating (Handbooks for Archaeologists)*, No. 3; European Science Foundation: Strasbourg, 1985.
4. Armitage, R. A. Ph.D. dissertation, Texas A&M University, College Station, TX, 1998.
5. Pace, M. F. N.; Hyman, M.; Rowe, M. W.; Southon, J. R. *American Indian Rock Art* **2000**, *24*, 95–102.
6. Fichter, E.; Hopkins, M.; Isotoff, A.; Liljeblad, S.; Lyman, R. A.; Strawn, M.; Taylor, E. *Exploratory Excavations in Little Lost River Cave; No. 1 A Progress Report*; Idaho State College, Pocatello, ID, Unpublished report, 1954.
7. Gruhn, R.; Bryan, A. *Report on a Test Excavation at Little Lost River Cave No. 1 (10BT1) in 1990*; Report on Cultural Resource Permit ID-I-27727; Bureau of Land Management: Idaho Falls, ID, October, 1990.
8. Butler, B. R. In *When Did the Shoshoni Begin to Occupy Southern Idaho? Essays on Late Prehistoric Cultural Remains From the Upper Snake and Salmon River Country*; Occasional Papers of the Idaho Museum of Natural History: 1981; Vol. 32, pp 4–17.
9. Merrell, C.; Armitage, R. A. *Dances with Antelopes: Exploring the Possible Use of an Idaho Cave by an Antelope Shaman*, Book of Abstracts, 73rd Annual Meeting of the Society for American Archaeology, Vancouver, BC, 2008.
10. Tatzber, M.; Stemmer, M.; Spiegel, H.; Katzlberger, C.; Haberhauer, G.; Mentler, A.; Gerzabek, M. H. *J. Plant Nutr. Soil Sci.* **2007**, *170*, 522–529.
11. Valladas, H. *Meas. Sci. Technol.* **2003**, *14*, 1487–1492.
12. Bowman, S. *Radiocarbon Dating*; British Museum Press: London, 1990; p 23.
13. Gupta, S. K.; Polach, H. A. *Radiocarbon Dating Practices at ANU*; ANU Radiocarbon Dating laboratory, Research School of Pacific Studies: Canberra, 1985; p 114.
14. Aitken, M. J. *Science-based Dating in Archaeology*; Longman: London, 1990.
15. Hardemon, D.; Armitage, R. A. Determining the Efficacy of Non-Destructive Pre-Treatment Methods on Known Age Textile Samples by Gas Chromatography-Mass Spectrometry Analysis. Presented at the Pittsburgh Conference on Analytical Chemistry and Applied Spectroscopy, Orlando, FL, March 2010; Paper 510-1P.

Chapter 9

The Roles of Chemistry and Culture in the Origins and Legacy of Crucible Damascus Steel Blades

Ann Feuerbach*

Anthropology Department, Hofstra University, Davison Hall 200,
Hempstead, NY 11549

*E-mail: AnnFeuerbach@gmail.com

Crucible damascus steel blades are used to illustrate various ways in which multidisciplinary collaborations and research have helped to answer a variety of ethical and scholarly problems. Rather than focusing on a single collaborative effort, this paper illustrates the benefits of collaboration between specialists with different sets of expertise and identifies areas which would benefit from future collaborative research.

Introduction

When treating, examining or studying material culture, collaboration between scholars and scientists from diverse disciplines is useful for focusing research questions, developing ethical procedures, and for extracting scientific, artistic, historical, and cultural information about the objects (*I*). Whether it is considered a utilitarian object or a sacred work of art, material culture is the result of humans' observations and interactions with the natural world. It offers a glimpse into the past and it is the foundation on which the future will be built. This paper illustrates how multidisciplinary research and collaborations have helped to solve ethical problems and answer research questions regarding the origins, manufacture, treatment, and legacy of crucible damascus steel blades. The overall intent is to increase awareness of the complexity of material culture studies and suggest areas in need of further collaborative research.

Today, the science of chemistry can be used to help answer questions about the material characteristics of an object. We can "reverse engineer" objects to understand their technology and we are able to determine the chemical elements

they contain in order to discover the raw materials and perhaps provenance. We can also subject the objects to hardness, flexibility, and strength tests to indicate how they may have performed their intended function. However, chemistry itself does not tell us about the people who first invented, made, traded, bought, used, and disposed of these objects (2). To answer these questions, we need a different group of specialists including archaeologists, historians, ethnographers, and artisans, to name but a few. Only by combining information from different sources can we truly begin to understand material culture in its proper historical and socio-cultural context. This information will help determine what questions to ask and what evidence to preserve for future generations.

Crucible Damascus Steel Blades

There are four different types of steels that are referred to as Damascus or Damascene. The first type is created by pattern welding iron and steel strips together. The second type involves using wax and acid to preferentially etch a deliberately designed pattern onto the blade's surface. The third type is created by inlaying one metal into another. The fourth is made using crucible damascus steel, and this type is sometimes referred to as watered steel, Indian "wootz", a derivation of the word pulad. All of these types of Damascus steels have a long history of production. Despite the name, there is no evidence indicating that any of these steels were made in Damascus, Syria. However, as Damascus was a large trading center, it is likely that, at some point in history, one or more of these types of blades were sold in the city. The term crucible damascus steel, with a lowercase "d" in damascus, is used here to break the association with the Syrian city and to differentiate it from the other types of so-called Damascus steels and crucible steels.

Crucible damascus steel is a particular type of ferrous technology and its production seems to be limited to regions of Central Asia (3), India (4) and Sri Lanka (5). The earliest evidence of its manufacture dates from the 3rd century CE and the traditional technology died out during the 1800's. The process involves charging the crucible with an iron rich substance, such as pieces of an iron bloom or scrap iron, along with a carbon-rich substance, such as charcoal, plant matter or cast iron. The crucible and its contents are then heated to approximately 2500 °F, which facilitates carbon diffusion into the iron, thus creating steel. During the process the steel becomes liquid, and then during cooling, it solidifies inside the crucible. The resulting product is a comparatively homogenous steel ingot that is virtually slag free. The ingot's shape will reflect the crucible's internal cavity on the bottom and sides. The top will exhibit evidence of shrinkage, or it will be raised as a result of the steel's surface tension when it was liquid. Because the crucible charge and solidification rate can vary greatly, these ingots can have differing carbon contents, elemental compositions, and microstructures. Additionally, when it is being shaped into a blade or other object, the ingot can be subjected to different temperatures and forging techniques. Due to all of these variables, the resulting pattern will be unique to that object.

It is the steel's specific microstructure that can result in the blade exhibiting a pattern after an etchant is applied to its surface. Generally, crucible damascus steel blades come in two forms: hypoeutectoid (below 0.8% C) or hypereutectoid (above 0.8% C). There are historical examples of both types of patterned blades (6). In hypoeutectoid steels the pattern is formed by ferrite-pearlite banding (7), whereas in the hypereutectoid steels the pattern is formed by the alignment of cementite in either a ferritic or pearlitic matrix (8). Some crucible steel patterns are said to resemble water, hence the term watered steel. In Islamic lands, the water pattern was highly desired because it was a particularly important symbol representing the Waters of Paradise (9). Just as a blade could simultaneously save a life while taking a life, water symbolized both life (clear sweet water) and death (dark brackish water). In Islamic poetry, to drink the water of the sword was to die and begin everlasting life in Paradise. The blade was the means by which a warrior would transmute from this life to the next. Thus, the water pattern on a blade was a very significant symbol of life, death, rebirth, and a constant reminder that dying in battle would result in being reborn into Paradise.

The fact that not all crucible damascus steels will exhibit a pattern when etched causes a number of problems. The pattern is not the only important feature of the blade. The fact that it was made of crucible damascus steel is significant because it narrows the provenance for the steel's production to a limited number of possible locations. However, if the blade does not exhibit the pattern, determining that it is indeed crucible damascus steel, rather than ordinary steel, requires metallographic analysis. This may or may not be allowed depending on the museum's policy. While there have been numerous studies addressing the cause of the pattern, more research is necessary to better understand the possible variables. Once the variables are better understood, it may be possible to determine provenance, and perhaps age. Nevertheless, for centuries crucible damascus steel blades were said to be the best available. Not only did they often exhibit the much sought-after decorative pattern—a virtual hallmark of quality—but they were also said to retain a sharp edge and have the ability to bend without damage. It is this reputation that has caused so many people to want to be a part of its history.

Over the centuries crucible damascus steel blades have meant different things to different people. To the ingot maker, the blacksmith, sword polisher and the scabbard maker it represented their livelihood. To the warrior, the blade was the means of life and death; to the archaeologist and curator, it is a prized piece of history; to the scientist, it is an object of study; and to the conservator, it is an object to preserve for future generations. The remainder of this paper endeavors to illustrate various ways in which multidisciplinary research has helped to solve some of crucible damascus steel's various ethical and scholarly problems.

Ethics

As noted above, the most notable characteristic feature of many crucible damascus steel blades is their decorative surface pattern. Based on stylistic attributes, it is presumed that there are many such objects in collections that once

exhibited the characteristic pattern. However, the decorative etched surface was removed due to over-cleaning, possibly in the 18th century when shiny armor was in fashion. The result is objects that appear as though they were made of ordinary steel, and not crucible damascus steel. Since this steel is a specific technology that suggests provenance, and because the pattern is an important decorative and symbolic feature of the object, the fact that it is made of crucible steel needs to be recognized and documented in order for the object to be correctly understood.

The UKIC's (The United Kingdom Institute for Conservation) Guidance for Conservation Practice states, "It is unethical to modify or conceal the original nature of an object through restoration". By not renewing the pattern, the curator or conservator is "concealing the nature of the object" which, according to the UKIC guideline, is unethical. However, the traditional process of etching literally dissolves part of the steel, modifying its surface and perhaps increases the risk of corrosion. Thus, the problem is to find an acceptable method to use on objects in museums that would not only reveal the pattern, but would also prevent further deterioration, be cost effective, and have minimum health and safety risks. Without satisfying all these requirements, one could not hope to persuade conservators and/or curators to undertake the treatment to reinstate the pattern.

Wills and Metcalf (10) discuss some of the issues they encountered when deciding whether or not to reinstate the pattern on a Mughal saddle axe. After consulting the Victoria and Albert Museum's Conservation Department Ethics Checklist and consultation with V&A curators and senior conservators, Sikh military experts, and specialists from other museums, they decided that they should reveal the pattern. Their argument concluded that "the intrinsic value of the object to the original owners lay as much in the material from which it was made as in its form. Because the watering was not visible, the axe was not 'readable' as the high status object it was, and so to return the surface to its intended finish would increase understanding of it (10). In addition, they felt, "The bright polished surface is now considered a bad old conservation treatment, and etching would be a reversal of this treatment" (10). After collaboration, the decision was made to re-etch the blade to reveal its true physical and symbolic nature.

Origins

There are other complex yet intriguing questions that the study of crucible damascus steel poses, such as: how might the early producers have perceived or rationalized the materials and methods they used? To help answer these questions, the distant ancestor of both chemistry and crucible damascus steel—alchemy—needed to be investigated. Both of their origins lie in the distant past with people's quest for understanding and manipulating the natural world. If we want to begin to understand the origins of chemistry, technology and material culture, we might want to consult religious scholars first.

The relationship between science, art and history has been discussed by Cyril Stanley Smith in his many essays (11). He reminds his readers how the division between these topics is misleading and how it was not necessarily the need or desire

for tools, but the need for new materials and methods for creative expression that spurred technology. Indeed, decorative clay figurines, as well as copper and iron jewelry, pre-date utilitarian ceramic vessels and metal weapons. Albert Einstein (12) also stated that “All religions, arts, and sciences are branches of the same tree”. Initially this statement might seem to be a paradox, but each of these topics is concerned with the act of creation, and when viewed from a history of technology point of view, they are all inextricably linked. How far removed is the art of the blacksmith from the science of the engineer? It is a matter of materials, approach, and scale. It is easy to forget that for the majority of our existence as humans, all arts and crafts were based on religious beliefs, not founded in what is called “science”, today. Both religion and science are fundamentally belief systems, cosmologies or worldviews, used to explain and predict how the natural world will behave under certain circumstances. It is the root of Einstein’s tree we are seeking when we look for the origins of technology.

A most important, yet overlooked source for understanding the origins of alchemy and metallurgy comes from the field of religious studies; M. Eliade’s *The Forge and the Crucible: the Origins and Structures of Alchemy*. Eliade primarily examined Chinese, Indian, and Babylonian myths, rites and symbols to better understand the origins and the “spiritual adventure” which occurred when people first realized they could transform what nature provided into something else. Eliade concluded that it was not the quest to counterfeit gold but rather “...it was probably the old conception of the Earth-Mother, bearer of embryo-ores, which crystallized faith in artificial transmutation (that is, operated in a laboratory)...It was the encounter with the symbolisms, myths and techniques of the miners, smelters and smiths which probably gave rise to the first alchemical operations” (13). If we want to better understand ancient technology and the origins of chemistry, rather than strictly looking at materials and techniques, specialists with knowledge of the culture’s beliefs, rituals and traditions should also be consulted.

In the past, and in some cultures today, it was believed that rocks, ores and metals are living organisms that are born, grow, have likes and dislikes, and could even marry, have offspring, die and be reborn (14). This is very different than the way modern science views these materials. These inorganic materials were genderized and considered to be either male or female, depending on their traits. Eliade offers numerous examples of the sexualizing of minerals and tools in many societies worldwide. He also found that in many of these early cultures the word for cave, mining gallery and womb are the same. They are the places that human, animal or mineral embryos matured and took their form. It was believed that the ores would eventually develop into metals inside the earth, and then rise to the surface, if they were given enough time. It was the job of the miner to retrieve the embryonic-ore from the “Earth-Mother”. While it was the smelter’s job to speed up this reproductive process and assist with the birth of the metal, it was the job of the smith to shape the metal, as a parent helps shape a child into an adult.

Many of the common themes that Eliade discusses, particularly that minerals, ores and metals are alive, have genders, and that their characteristics or properties can be transferred to their offspring, still remain in Islamic cosmology many millenniums later (15). In the production of crucible damascus steel, the Islamic historian Al-Beruni also refers to the mixing of soft “female” iron and hard “male”

iron in the crucible (16) and the result is a product that will contain characteristics of each parent. In current scientific thought, the “reason” for mixing the two types of iron would be to produce a product with a carbon content somewhere between the two; there is nothing more to it than the practical explanation of the physical process. However, in light of the information from religious studies, it is evident that the process of combining these materials had much more symbolic and cognitive associations than just being a practical application. Another symbolic reference to birth and rebirth is the shape of the crucible damascus steel ingot, which is referred to as “egg” shaped in Islamic texts, and contemporary archaeological evidence supports this (17). In many cultures the egg symbolizes not only fertility, but also life and rebirth, just as the water pattern on the blade represents rebirth in Paradise. Thus, not only did the crucible damascus steel blade assist in the transmutation from this life to the next, the ingredients used to produce the blade also contained elements which carried similar symbolism. The frequency of these reoccurring themes and symbols, in relation to crucible damascus steel production and products, makes it unlikely that these are just coincidences. Recognition of these aspects offers additional dimensions to appreciate when considering the raw materials, technology, and products.

While the cognitive aspects surrounding the origin of both alchemy and crucible damascus steel may never be known for certain, it is evident that they share the same roots. Indeed, when questioning why a certain material or method may have been used, along with the scientific evidence it would be beneficial to collaborate with scholars with knowledge of the culture’s belief systems. Only then can we begin to suggest the possible intentions and rational of the producers and consumers, who were, after all, from a very different culture.

Legacy

We now jump centuries ahead to investigate the legacy and contributions of crucible damascus steel blades to chemistry. As stated above, the blades had a reputation for quality, and it was this reputation that has caused numerous scientists to attempt to recreate the steel and understand the mechanisms that led to this status. In the 1800’s, scientists including Jean Robert Bréant from France, Michael Faraday and Henry Wilkinson from England, and Pavel P. Anosov from Russia, studied crucible damascus steel in earnest to discover the “secret” of its strength. There are two major scientific developments that resulted from their study of blades and wootz ingots from India. In 1831, Anosov was the first metallurgist to use a microscope to study the metallurgical structure of his samples (18). This is three years before Sorby, who is usually credited for being the first (19). The second is the discovery of alloy steels by Bréant and Faraday. For the most part, from the late 1800’s until the later part of the 1900’s, steel research concentrated on alloys and other aspects of steel production, such as stainless steel, rather than crucible damascus steel replication.

Research resumed in earnest in the 1980’s with research conducted by Sherby and Wadsworth who discovered a way of replicating the crucible damascus steel pattern using steel casting and modern methods of high temperature rolling of

steel (20). Next, research that combined traditional blacksmith techniques with state-of-the-art scientific analysis were conducted primarily by John Verhoeven and Al Pendray (21). Through their investigations they discovered the role that trace elements play in the alignment of cementite and the necessity of cyclical forging in the production of the pattern in hypereutectoid blades (21). M. Reibold *et al* (22) studied crucible damascus steel objects and discovered carbon nanotubes in the steel which they concluded may account for the blades' apparent high quality cutting edge. Furthermore, a recent study by Nikolai Kobasko (23), resulted in what he suggests may be a new explanation for the formation of cementite. This research is inspiring new techniques for improving the continuous casting of high quality steels. In addition to these laboratory investigations, there are numerous blacksmiths around the world who continue to learn about the steel, experiment with different materials and methods, and teach its production, using new and old techniques, to the next generation of smiths. Crucible damascus steel research, experimentation, and practice appear to be continuing well into the future.

Crucible Damascus Steel Kard: A Case Study

The following case study of a crucible damascus steel blade illustrates the amount of information that can be learned about an object by using information from different disciplines. The bladed object of this study is known as a kard (Figure 1). Art historians describe the kard as a “straight, single-edged pointed knife, worn on the left side” (24). This blade is from a private collection and was initially included in an analytical study conducted by Verhoeven and Peterson (25). They concluded that the blade is composed of high carbon steel and has significant amounts of trace elements including vanadium and manganese which promote the alignment of the cementite and help produce the microstructure and resulting water-like pattern.



Figure 1. 18th century Persian Kard. (see color insert)

The owner graciously allowed this author to further study the kard to identify other technological, art historical and cultural aspects associated with its “life history”. A summary of the technology of the kard is as follows: the entire length of the kard is 14 inches long and 1¼ inches at the widest part. It has a superb water pattern including what is called a 40 steps or Mohammad’s ladder pattern. The “steps” are made by engraving or forging a perpendicular line in the steel to create the ladder effect. The blade has a Type C bolster with sloping cheeks, according to Zeller and Rohrer’s bolster classification (26). There is a slight raised midrib

along the spine of the blade, sloping to the edge. On the blade's spine, near the join with the bolster, there is a raised floral design. The tang runs virtually the entire length of the handle and exhibits an arabesque pattern along the handle strap. The pattern also appears on the blade and includes an inscription. The pattern is made using the inlaid koftgari method, also called damascene inlay, which involves chiseling out the design and then inlaying gold into the recessed areas. However, in some parts of the design, the gold is missing (Figure 2). The handle is made of ivory and its crystalline structure strongly suggests that it is walrus ivory.



Figure 2. Detail of the Koftgari inscription and pattern.

The kard is typically a Persian knife and used in various areas which had a Persian influence. It is probable that this kard was made in a workshop in Isfahan during the 1700 CE, or perhaps even earlier. The style of the blade is strikingly similar to a group of daggers discussed by Allan and Gilmore (27), particularly dagger A.8 in the Tanavoli collection, and one in the Khahili collection, apart from the fact that the decoration on the Tanavoli blade has only chiseled decoration, whereas this one has a chiseled leaf pattern on the spine as well as koftgari. The open arabesque design is also not dissimilar to the work on the body armour of the Tanavoli collection (28). Therefore, by consulting art historical sources and comparing the style and technique to known pieces, a place and date can be suggested.

As for the method of distribution and use, kards were worn hanging from the belts of rulers and were often given as gifts. The “40 steps” or “Mohammad’s ladder pattern” is symbolic of heaven and the 40 virgins waiting in the afterlife for the warrior who dies in battle. As discussed above, the water pattern represents the Waters of Paradise, and this symbolism would not have been lost on the original patron. While this kard would have been fully functional as a utilitarian object,

the lack of wear, the intricate goldwork and decorative features suggest that it was likely a prestigious gift to be admired rather than used. Furthermore, walrus handles were highly prized, particularly those which exhibited the crystalline pattern. Walrus ivory was traded a great distance into Islamic lands from the Arctic north, and was greatly sought after because it wears well with time and produces handles that are smooth to the touch and less prone to slipping. The long distance trade further indicates the wealth of the purchaser.

The area of *koftgari* poses some interesting questions. On other kards, the name of the maker, or owner, is often inscribed. The inscription was translated by Prof. Haideh Sahim of Hofstra University. The inscription is in Farsi, which further supports the Persian provenance, but what it says is not altogether clear. On close examination of the inscription, there is a chiseled area where the gold has been lost. However, this may have been a mistake on the part of the engraver rather than a loss of material. According to Sahim, if the engraved area was filled with gold, the inscription would not make sense. It was expected to be a proper name, as on other similar kards, but as it stands it appears to read “Allah” which, of course, may be a religious reference. However, according to Allan and Gilmore (29), there was a swordmaker in Isfahan called “Asad Allah” so perhaps this is a maker mark. Apart from the proposed date and place of manufacture, nothing else about the history of this kard is known. For its more recent history, however, it was sold by a dealer in antique arms to a collector. How it came into the hands of this dealer is not known. It now resides in the southern part of America as part of a well-cared-for collection.

When we looked beyond the technology, we learned much more about the object. Questions that the research endeavored to help answer included: when and where was the blade likely to have been made? Who may have made it? Why might it have been made? To help answer these questions, the expertise of specialist scholars was sought, either through their published works or through personal communication. The study resulted in learning more about the culture in which the kard was made and used—in addition to the materials of which it is made.

Conclusion

There is more to the study of material culture than chemical analysis and preservation of the physical object. Material culture contains clues about the people and their culture. The investigation into crucible damascus steel not only offers insight into the past, but also illustrates how the study of past technologies can inspire the development of new technologies. Material culture helps people understand and take control of the world around them, literally and figuratively. To fully understand objects, we must understand their physical components as well as cognitive associations, and to achieve this, collaborative research is necessary. Above all, material culture studies remind us that we are guardians of the past, yet we can only control what we do in the present, and we must always consider the future.

References

1. Kirby, J. In *Art Technology - Sources and Methods*; Kroustallis, S., Townsend, J. H., Bruquetas, E. C., Stijnman, A., Moya, M., Eds.; ATSR Publication 2; Archetype Publications: London, U.K., 2008; p 7.
2. Schiffer, M. B.; Skibo *J. Am. Antiq.* **1997**, *62*, 27–50.
3. Feuerbach, A. *JOM* **2006**, *58*, 48–50.
4. Srinivasan, Sh.; Griffiths, D. Crucible Steel in South India-Preliminary Investigations on Crucibles from Some Newly Identified Sites. *Materials Issues in Art and Archaeology V*; Druzik, J. R., Merkel, J. F., Stewart, J., Vandiver, P. B., Eds.; Materials Research Society; Pittsburgh, PA, 1997; pp 111–125.
5. Wayman, M.; Juleff, G. *Hist. Metall.* **1999**, *33*, 26–42.
6. Sachse, M. *Damascus Steel: Myth, History, Technology, Applications*; Wirtschaftsverk: N.W. Verl. Fur Neue Wiss: Germany, 1994.
7. Samuels, L. E. *Optical Microscopy of Carbon Steels*; American Society of Metals: Washington, DC, 1980.
8. Verhoeven, J; Pendray, A.; Gibson, E. D. *Mater Charact.* **1996**, *37*, 9–22.
9. Alexander, D. G. *Metrop. Mus. J.* **1983**, *18*, 97–109.
10. Wills, S.; Metcalf, S. *V&A Conserv. J.* **1999**, *31*, 10–13.
11. Smith, C. S. *A Search for Structure: Selected Essays on Science, Art and History*; Society for the History of Technology; MIT Press: Cambridge: 1982.
12. Einstein, A. *Out of My Later Years*; Open Road: New York, 1956; p 9.
13. Eliade, M. *The Forge and the Crucible: The Origins and Structures of Alchemy*; Harper: New York, 1971; p 148.
14. Eliade, M. *The Forge and the Crucible: The Origins and Structures of Alchemy*; Harper: New York, 1971; p 151.
15. Nasr, S. H. *An Introduction to Islamic Cosmological Doctrines: Conceptions of Nature and Methods Used for its Study by the Ikhwān al-afā, al-Bīrūnī, and Ibn Sīnā*; State University of New York Press: New York, 1993; p 91.
16. Said, H. M. *Al-Beruni's Book on Mineralogy: The Book Most Comprehensive In Knowledge On Precious Stones*; Pakistan Hijra Council: Islamabad, 1989.
17. Feuerbach, A. Ph.D Thesis. Institute of Archaeology, University College London, London, U.K., 2002.
18. Bogachev, I. N. *Pavel Petrovich Anosov and the Secret of Damascus Steel*; Mashgiz Publishers: Moscow, 1952.
19. Smith, C. S. *Sources for the History of the Science of Steel 1532-1786*; Society for the History of Technology; MIT Press: Cambridge, MA, 1968; p 218.
20. Wadsworth, J.; Sherby, O. D. *Science* **1982**, *22*, 328–330.
21. Verhoeven, J.; Pendray, A. H.; Berge, P. *Mater Charact.* **1993**, *30*, 187–200.
22. Reibold, M.; Paufler, P.; Levin, A. A.; Kochmann, W.; Pätzke, N.; Meyer, D. *C. Physics and Engineering of New Materials*; Springer: New York, 2009; Vol. 127, pp 305–310.
23. Kobasko, N. In *Proceedings of the 8th WSEAS International Conference on Fluid Mechanics*; WSEAS: 2011, pp 81–86.

24. Allan, J.; Gilmore, B. *Persian Steel: The Tanavoli Collection*; Oxford University Press: Oxford, 2000; p 146.
25. Verhoeven, J. D.; Peterson, D. T. *Mater. Charact.* **1992**, *29*, 335–341.
26. Khorasani, M. M. *Arms and Armor from Iran: The Bronze Age to the End of the Qajar Period*; Legat-Verlag: Germany, 2006; p 232.
27. Allan, J.; Gilmore, B. *Persian Steel: The Tanavoli Collection*; Oxford University Press: Oxford, 2000; pp 150–153.
28. Allan, J.; Gilmore, B. *Persian Steel: The Tanavoli Collection*; Oxford University Press: Oxford, 2000; pp 134–137.
29. Allan, J.; Gilmore, B. *Persian Steel: The Tanavoli Collection*; Oxford University Press: Oxford, 2000.

Chapter 10

Elemental Composition of a Series of Medieval Korean Coinage via Energy-Dispersive X-ray Fluorescence Spectrometry

**Danielle M. Garshott, Elizabeth MacDonald, Stephanie Spohn,
Hana Attar, Jennifer Shango, Irice Ellis, Meghann N. Murray,
and Mark A. Benvenuto***

**Department of Chemistry & Biochemistry, University of Detroit Mercy,
4001 W. McNichols Road, Detroit, MI 48221**

***E-mail: benvenma@udmercy.edu**

Eighty-five small coins, presumed Korean, were analyzed via energy dispersive X-ray fluorescence spectrometry and examined for copper, zinc, tin, lead, iron, nickel, cobalt, arsenic, antimony, bismuth, gold, platinum, palladium, and silver. The compositions of the eighty-five coins consistently were copper with lead, or zinc as the second most common element, and a mixture comprised of the remaining metals at trace levels. The characters on the seven subsets of coins analyzed indicate that these coins are, indeed, Korean, but due to their distinctly different chemical compositions, they were most likely manufactured in a variety of locations, and in several cases are neither brass nor bronze.

Introduction

The use of energy dispersive X-ray fluorescence (EDXRF) has become a reliable tool in the analysis of ancient and medieval metals, and has gained a position alongside other analytical techniques in determining compositional make-up of a variety of objects from past cultures (1–8). Curiously however, there appears to have been no published EDXRF studies of traditional Korean coinage, although there are some established references to the cataloguing of Korean coinage (9–12). Thus, this study adds depth to the understanding of the elemental composition of coins cast on the Korean peninsula, may shed light on whether techniques were shared between Korean and Chinese foundrymen and mint workers, and further indicates that such compositions can be determined in a non-destructive manner.

Korean coinage has a centuries-long history that appears to those illiterate in the characters of Oriental writing systems to be parallel to that of Chinese coinage (9). Traditional Korean coins appear to be made of brass, are round, and have a central, square hole (2, 10, 11). Both sides, the obverse and reverse, bear traditional characters.

For the purposes of this research, the side bearing the characters of the dynastic name is considered the obverse. The markings on the obverse side of the coin are read in a specific sequence: top, bottom, right, left. On the reverse side of the coin from one to four characters are found. These characters are specific to the mint and denote the value of that particular coin (9).

Traditionally produced Korean coins, like many ancient and medieval coins, were not die cut as modern coinage is. Metals were melted in crucibles, and the molten metal was poured into hand crafted molds. Typically the coins were cast in what is known as a “coin tree.” The coins’ square-shaped hole was utilized after coins were broken off the branches of the tree, when they were placed on a square rod and buffed along the edge to remove the sprue remaining after being broken from the coin tree. The square shape prevented the coins from rotating during the sprue removal process.

The eighty-five coins analyzed vary slightly in size, weight and markings. The weight of the coins ranged from roughly 2.50 g to no more than 5.40 g. There are significant differences in the style of characters that appear on the reverse of the coins. Based on these character differences, each coin was placed into one of seven subsets.

Experimental Methods

Coins 1-85 are denoted by subsets: KA, KB, KC, KD, KE, KF and Kmisc in all of the following figures. All eighty-five samples were placed in a sonicating hot water, non-corrosive soap bath for two hours to remove dirt and surface residue. They were then rinsed with distilled water and wiped dry immediately with a Kimwipe. They were then visually examined to ensure they were free of surface corrosion and oxidation. If needed, they were cleaned with a common toothbrush, and, if foreign matter or material still adhered to any portion of the surfaces, the process was repeated.

After cleaning, each coin's obverse and reverse characters were examined to determine each sample's place in a designated subset, and to determine that a bare metal surface would be exposed to the X-ray beam.

While cleaning the surfaces of cultural heritage objects can be frowned upon, there were other issues to consider. The entire data set is composed of coins that are visibly corrosion free; the cleaning was to remove any foreign contaminants on the surfaces. EDXRF is a technique that analyzes roughly a 100 μm depth below the surface; thus a clean, corrosion-free surface was imperative for the collection of accurate and reproducible data. Ultrasonic cleaning is a procedure commonly used for the elemental analysis of old coins (13), and the use of a mild soap in this study provided a minimal "alteration" of the object compared to polishing, cross-sectioning, or the use of organic solvents for cleaning.

The coins were then analyzed via energy dispersive X-ray fluorescence on a Kevex Spectrace QuanX spectrometer for the following elements: copper, zinc, tin, lead, iron, nickel, cobalt, arsenic, antimony, bismuth, gold, platinum, palladium, and silver. Excitation conditions for each sample were as follows: 20 kV, 0.10 mA, 100 second count $K_{\alpha,\beta}$ for iron, cobalt, nickel, copper, zinc, arsenic, platinum, gold, bismuth, and lead, followed by 45 kV, 0.72 mA, 60 second count, L lines, for palladium, silver, tin, and antimony, using a rhodium target X-ray tube. Pure elemental standards and fundamental parameter software, purchased from Spectrace (Thermo Fisher Scientific), were utilized for daily calibration. A copper standard sample disk was run each day before the subset samples.

Results and Discussion, Chemical Compositions

The coins are believed to have been manufactured during the period from 1806 – 1897, and are identified in subsets and Mandel numbers (9) as follows: KA, Treasury Department (#13.2A); KB, Pyongan Provincial Office (#47.8); KC, Military Training Command (#28.6); KD, Pyongan Provincial Office with different characters than subset KB (#47.5); KE, Treasury Department with different characters than subset KA (#13.19); KF, unable to be identified using existing references, and not identifiable as similar to subsets KA through KE; and Kmisc, two samples that could not be identified by reverse characters.

The chemical composition of each subset, inclusive of major and minor elements, is represented using bar graphs in Figures 1–6. In the majority of instances, copper is shown to be the major element present, although there are some samples in which it is not. Interestingly, in the majority of cases, lead is by far the second element in abundance, and not zinc or tin. The addition of lead to numerous metal alloys lowers the melting temperature of the alloy; and indeed, the presence of so much lead in some of these coins may indicate that the foundrymen had this knowledge. As well, since lead is sparingly soluble in copper, there may be surface enrichment of lead in these samples that is manifested by elevated percentages of this metal. It is not inconceivable though that the ores from which tin and zinc were smelted had been either interchanged with or confused with lead ores.

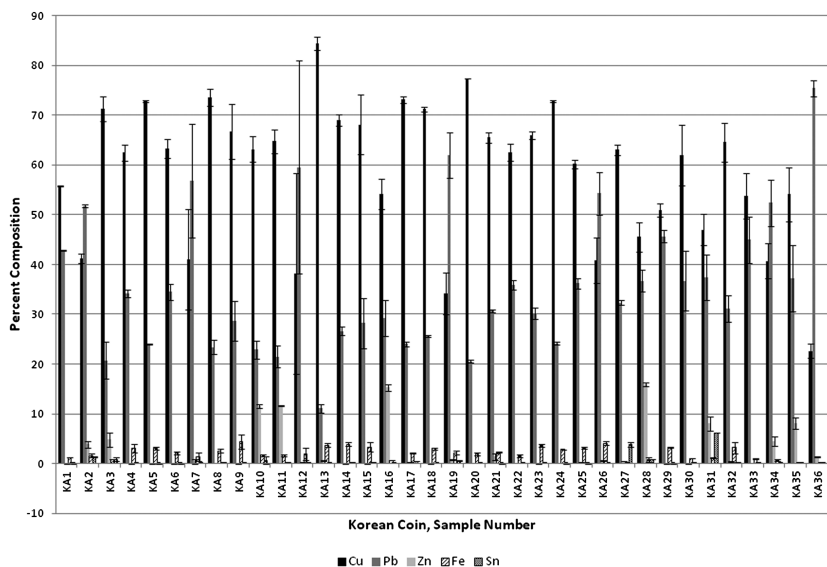


Figure 1. Composition of KA.

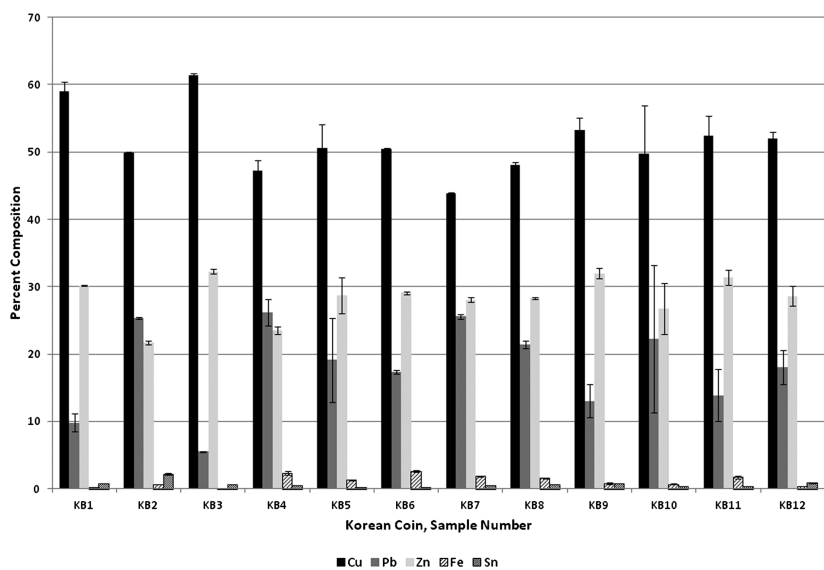


Figure 2. Composition of KB.

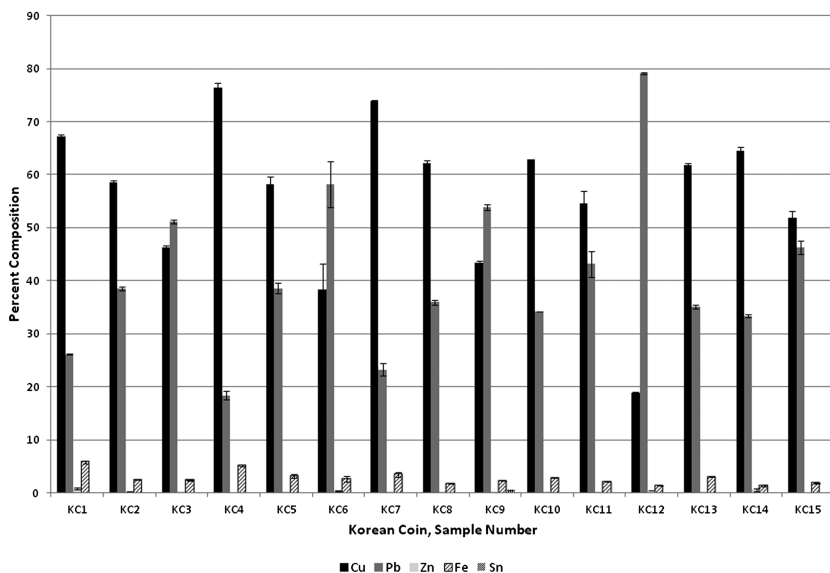


Figure 3. Composition of KC.

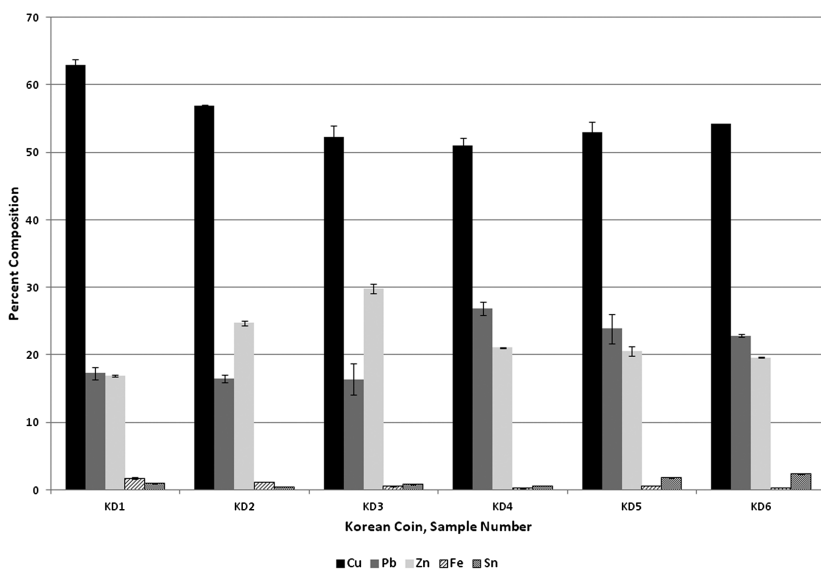


Figure 4. Composition of KD.

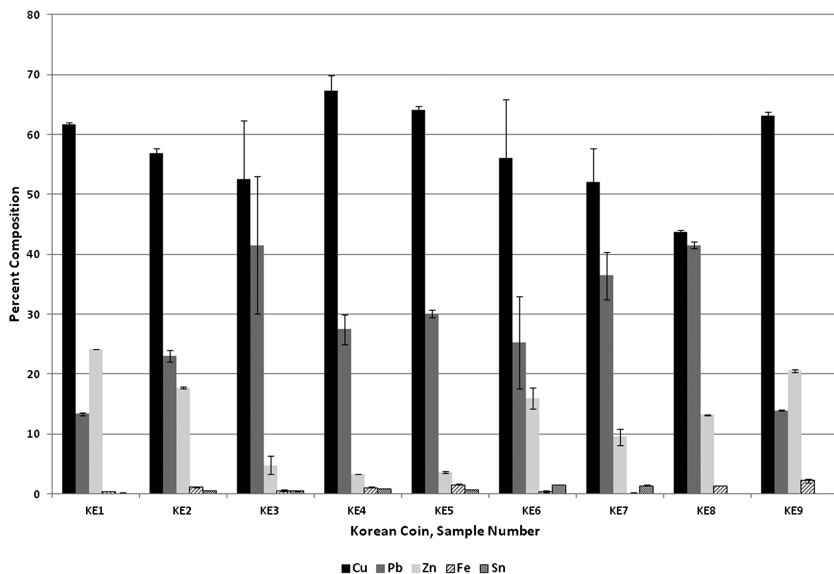


Figure 5. Composition of KE.

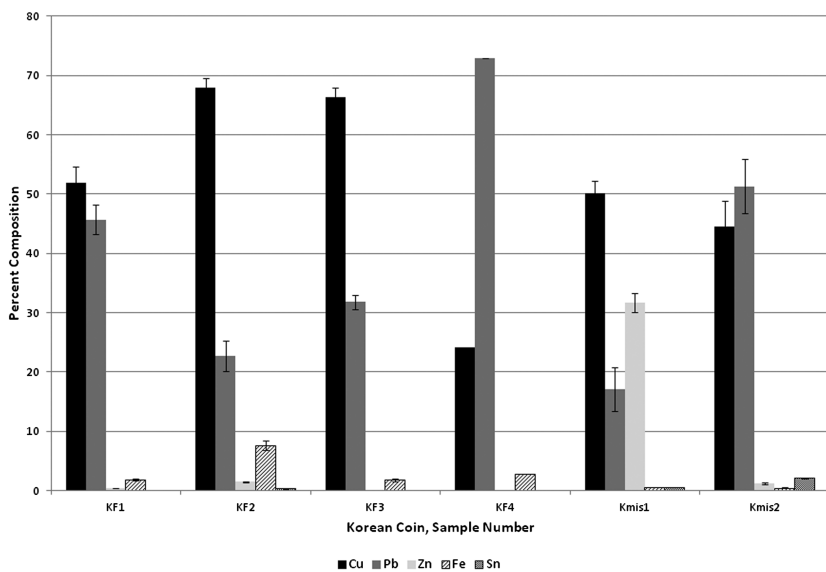


Figure 6. Composition of KF.

In an effort to understand the data in greater detail, each subset has been re-graphed, still as bar graphs, but with copper and lead compared in one display, and

zinc, iron, and tin in another. Thus, the most abundant two elements are compared directly with each other, and the next three elements in abundance are similarly examined. This is shown in Figures 7–18.

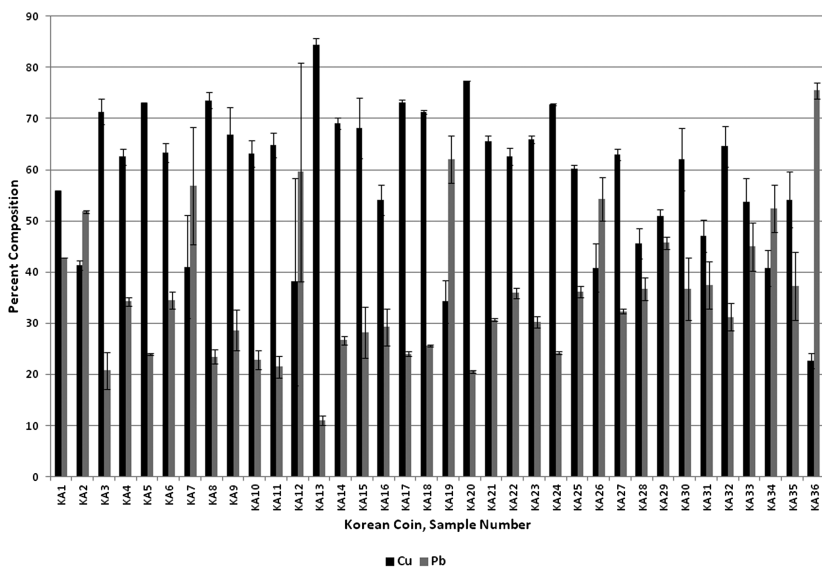


Figure 7. KA, Cu and Pb.

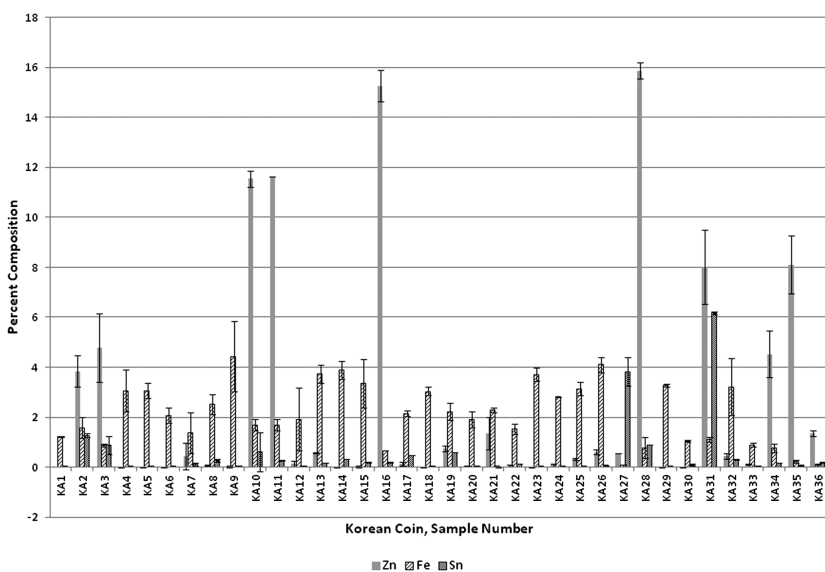


Figure 8. KA, Zn, Fe, and Sn.

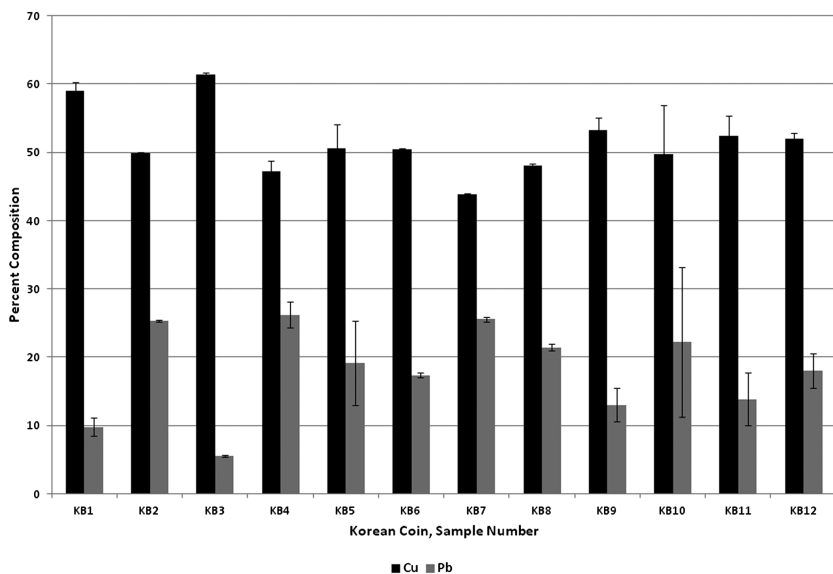


Figure 9. KB, Cu and Pb

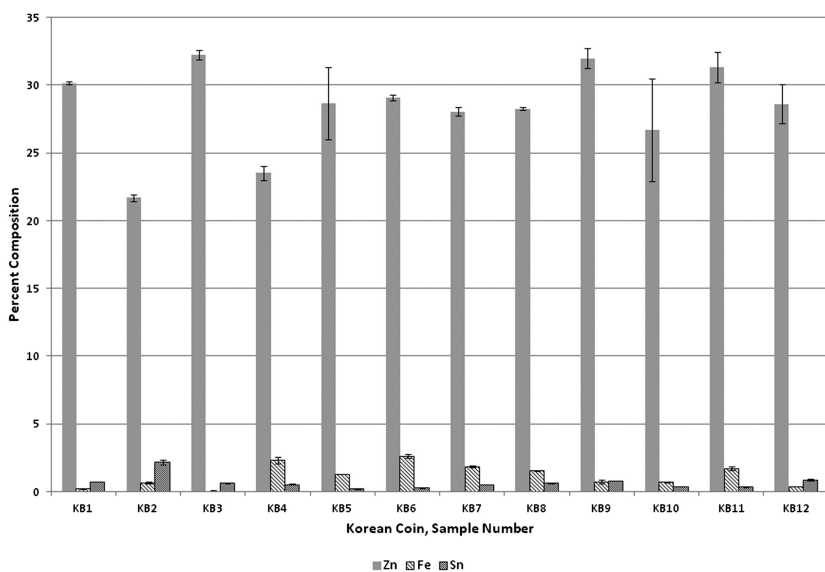


Figure 10. KB, Zn, Fe, and Sn.

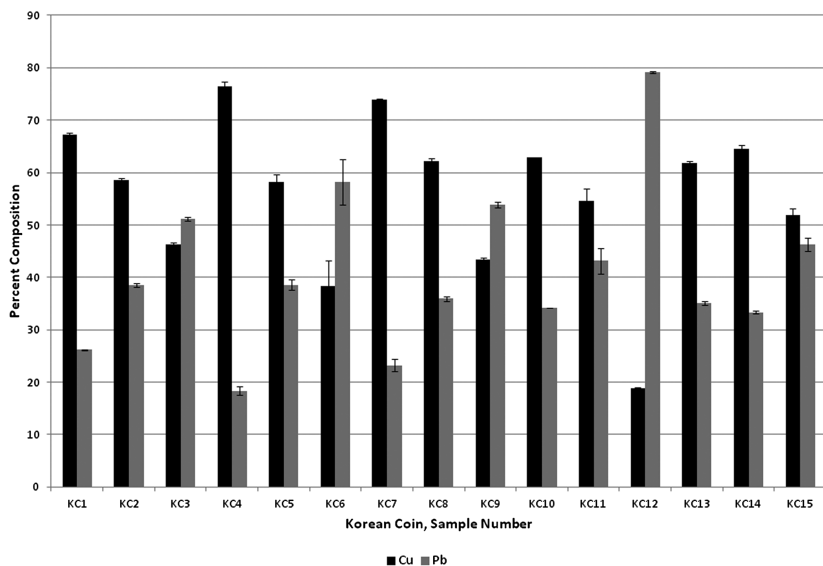


Figure 11. KC, Cu and Pb.

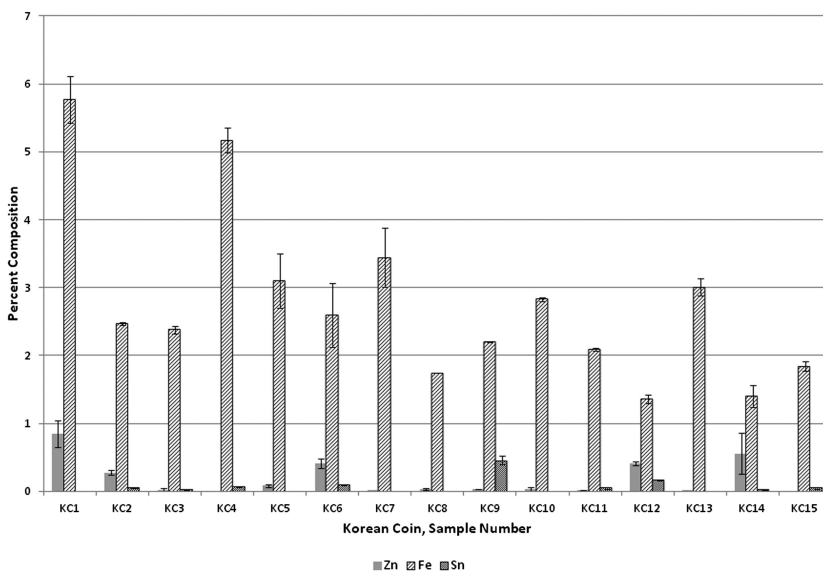


Figure 12. KC, Zn, Fe, and Sn.

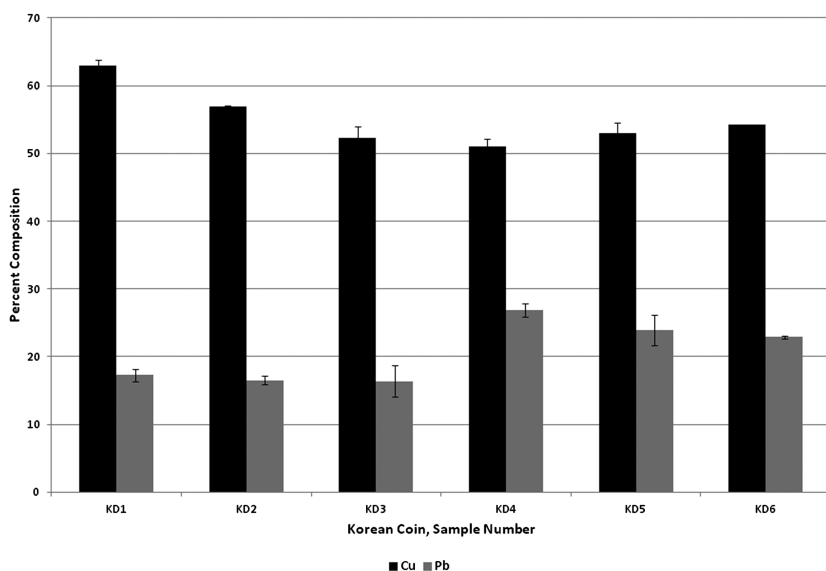


Figure 13. KD, Cu and Pb.

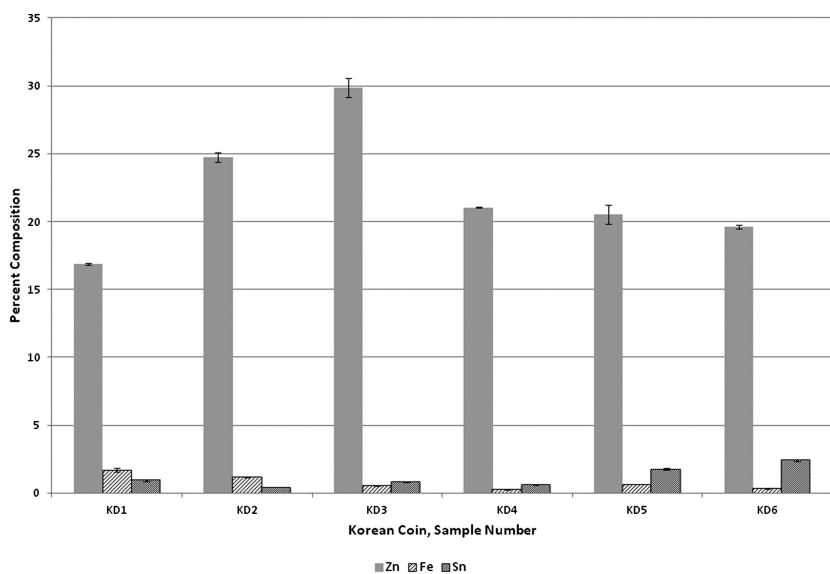


Figure 14. KD, Zn, Fe, and Sn.

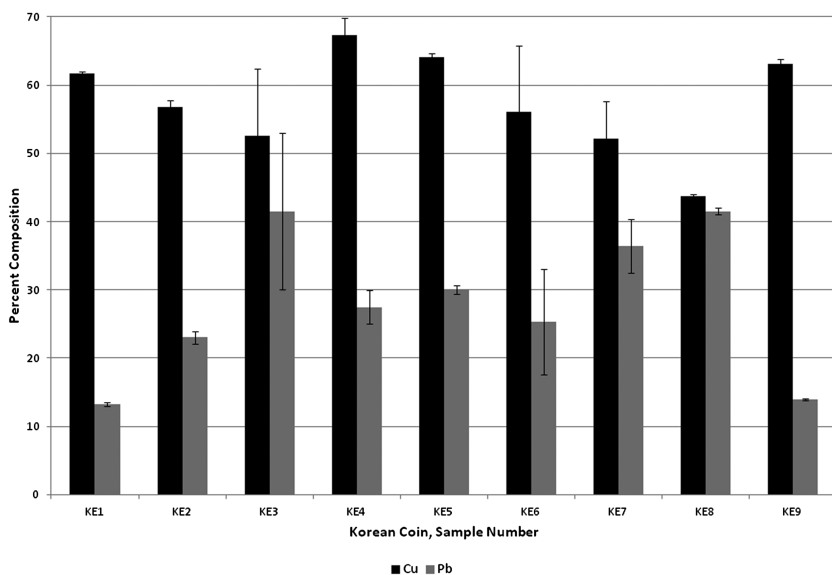


Figure 15. KE, Cu and Pb.

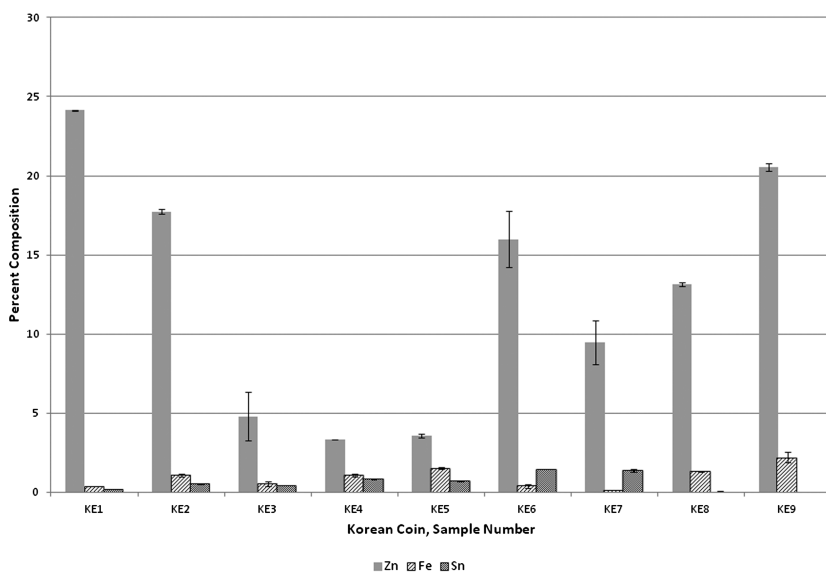


Figure 16. KE, Zn, Fe, and Sn.

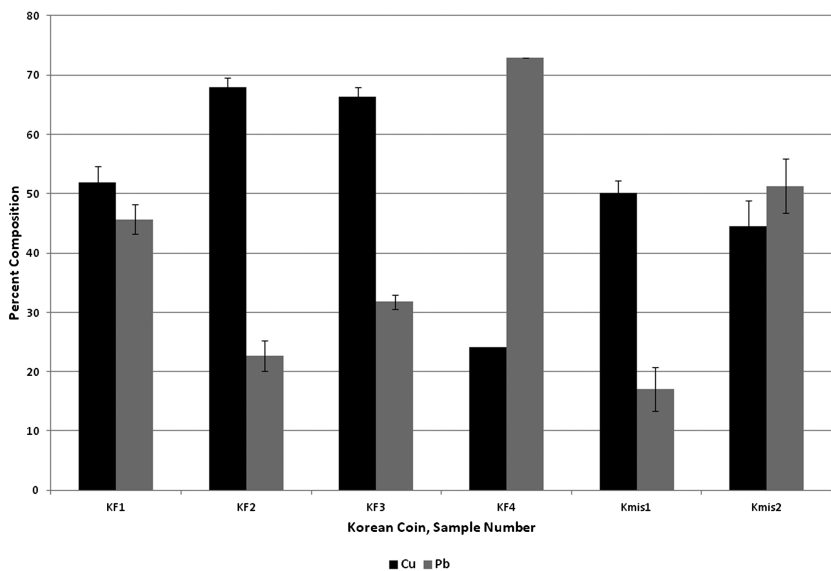


Figure 17. KF, Cu and Pb.

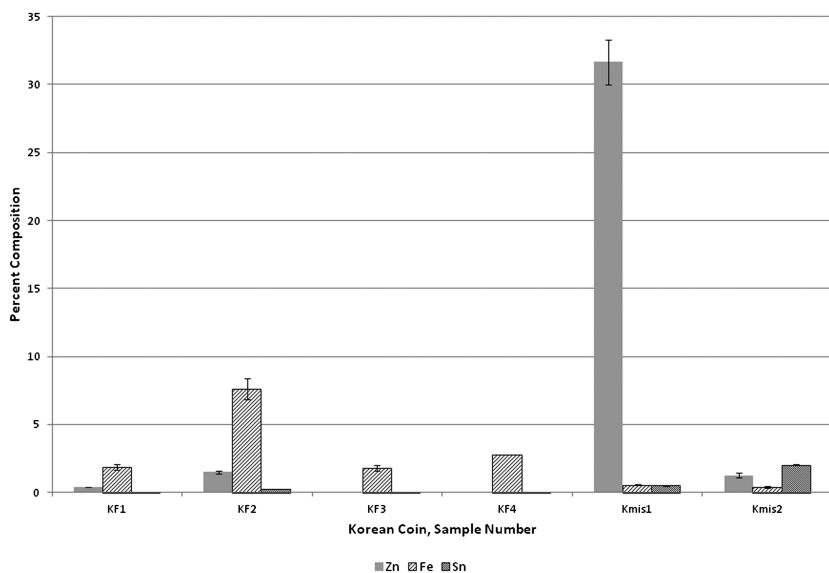


Figure 18. KF, Zn, Fe, and Sn.

This re-graphing illustrates more clearly the samples in which copper is actually the second most abundant element when compared to lead. In all of the 85 coin sample set, KA7, KA19, KA26, KA36, KC3, KC6, KC9, KC12, KF4, and Kmisc2 are the only examples in which copper is second in abundance to lead. It is noteworthy that those coins of the Pyongan Provincial Office never rise to this level of lead, and that graphically they appear to be more uniform in the composition of these two, major elements.

Interestingly, the KE subset also contains no examples in which there is more lead than copper, although KE7 and KE8 are very close. Since this is one of two subsets that are both from the Treasury Department, one can speculate that there was some form of division within the Department's production operations, or that the two subsets were perhaps made at different times, or using different ores.

The KB and KD subset do not contain any examples in which there is more lead than copper. Also, each set shows what appears to be the consistent presence of zinc in the coins, in some cases to percentages higher than that of lead. This may imply that better control was exercised in the production of a proper, brass coinage at the Pyongan Provincial Office, or that certain ores and ore sources were consistently available there.

The sample KC12 has an amazingly high percentage of lead, and low percentage of copper. This single sample is actually one of the most extreme outliers in all of the series, dwarfing all but two other samples in the percentage of lead. While this may be due in part to surface enrichment of lead based on its low solubility in copper or in copper alloys, it may be high for other reasons, such as its traditionally lower cost when compared to copper. One can speculate as to why the alloy of such outliers is so rich in a metal that should not, in theory, be present at all, but unfortunately EDXRF does not provide a reason why this is so.

The KF and Kmisc subsets are a difficult group from which to draw conclusions, in part because the subsets are so small, and in part simply because the characters are so worn over time. However, it is interesting to note that Kmisc1 has an elemental profile very similar to the KB and KD subsets, and that the Kmisc2 sample is close in profile to those samples in KA and KC in which lead was the predominant element.

In all cases, iron was graphed, and compared to the other minor elements, but a pattern never seems to appear for this element. The reason for this may be that small amounts of iron are present in any of the other ores, or that small amounts of iron end up in coins poured from molten alloys that have been melted in iron crucibles.

In a further step that was taken to derive greater understanding from the data, the entire set of 85 coins was graphed in a rather traditional x-y scatter plot, but with what we believe is the unique approach of graphing copper exclusively on the x-axis, and the combination of copper and some second element on the y-axis. These graphs, shown in Figures 19–22, require some explanation.

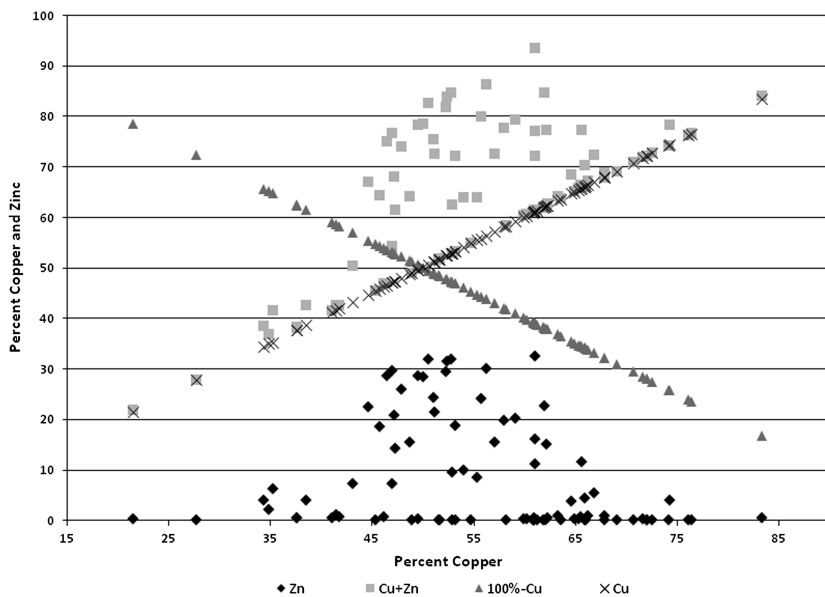


Figure 19. Cu and Zn.

Using Figure 19 as an example, one can observe an “X pattern” which is formed by the points representing ascending amounts of copper as one of the diagonals, and the descending amounts from 100% of all elements minus copper as the other. For Figure 19, the y-axis is the combination of copper and zinc, and thus, if the coins were simply a binary mixture of the two elements, the Cu+Zn points would make a straight line across the top of the graph, at the 100% line. Also, the Zn points would constitute the descending line. On the other hand, if there were almost no zinc in the samples, the Cu+Zn points would form a line that essentially mirrored the ascending Cu points. Clearly though, this is not the case, since the Cu+Zn points occupy an area between the ascending Cu points, and the 100% line. This then indicates the presence of other elements in the samples.

Figure 20 illustrates this phenomenon a second time, but with tin as the second element in relation to copper. Here the Sn+Cu points do almost mirror the Cu points, indicating that there is very little tin in any of the samples.

The third such figure, Figure 21, repeats this graphical representation, but now with iron as the second element. Once again, iron shows up almost atop the ascending copper line, indicating that while there is some iron present in many of the coins, it is never present in large amounts.

Finally, Figure 2 illustrates graphically the comparison between copper and lead. There are several samples in which the Cu+Pb points lie between the ascending copper line and the 100% top line, but there are also a large number of Cu+Pb points that are very close to the 100% line. This shows that numerous samples are essentially a binary alloy of copper and lead, with only small amounts

of all the other elements combined. Our experience is such that it is rare to find a set of copper-based objects that are so high in lead, although it is not unheard of (14).

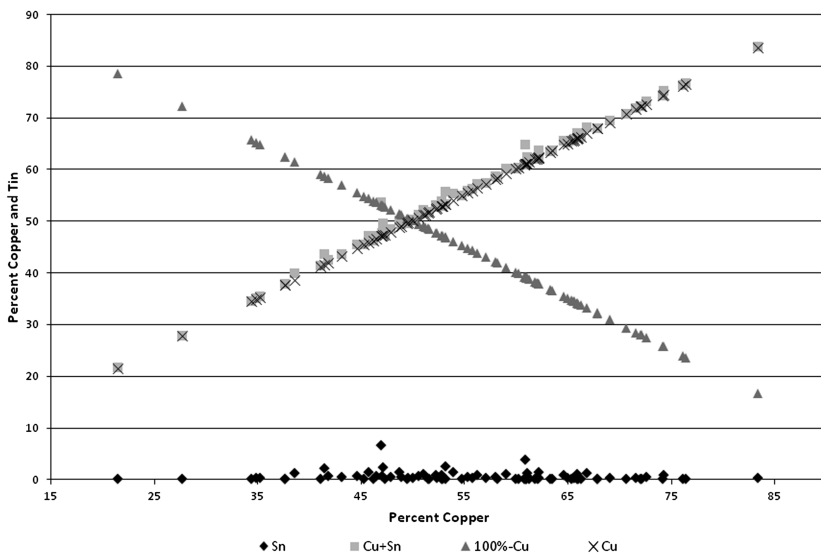


Figure 20. Cu and Sn.

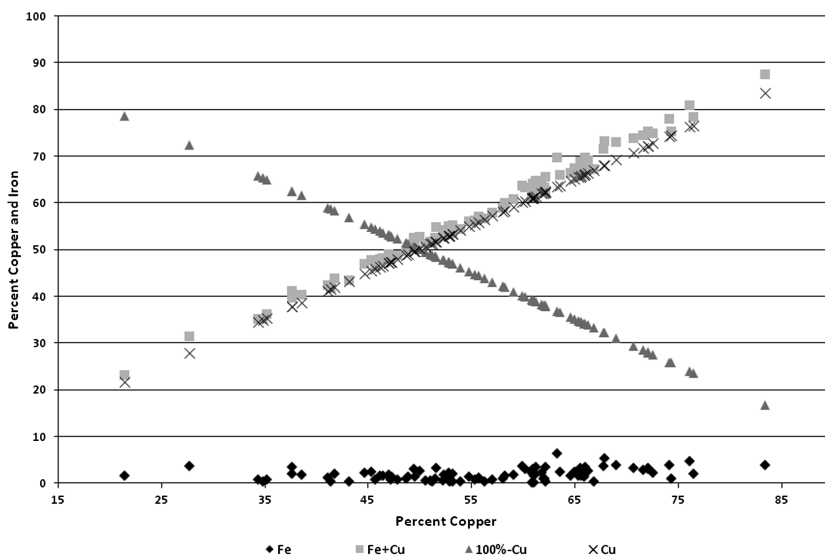


Figure 21. Cu and Fe.

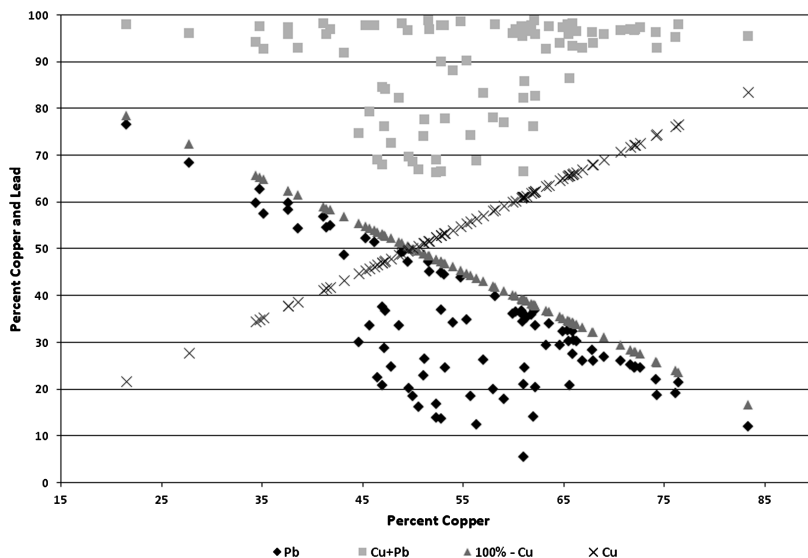


Figure 22. Cu and Pb.

Finally, while the Experimental Methods section, above, lists several other elements for which an EDXRF examination was conducted, those elements did not appear in any of the samples in statistically significant amounts, and therefore were not graphed.

Conclusions

While copper appears to be the element present in the greatest amount in the majority of the coins, it does not always reach 50%, meaning that several of the samples are heavily alloyed. The term “brass” indicates an alloy of copper and zinc, and the term “bronze” indicates one of copper and tin, yet neither of these is an apt description of this entire set of coins. The KB and KD subsets may be properly called brass, but leaded brass would be a more descriptive term. In the cases of the other four subsets, it is more fitting to call them leaded copper.

The wide differences in the amounts of copper and lead, as well as zinc, in the various subsets give credence to the belief that the coins were produced at several different locations. It also appears that there may have been stricter control of the coining operations at the Pyongan Provincial Office than there was at either the Treasury department or at the Military Training Command.

Finally, the overall composition of these coins is not widely different from those produced in China or Annam at roughly the same time, (15, 16) indicating that there may have been significant exchange of ideas and techniques among those who worked in the foundries of the different countries.

Acknowledgments

Technical support from Bill Jambard and Randy Cohn at Thermo Fischer Scientific was greatly appreciated. This research would not have been possible without the continuing financial support of the University of Detroit Mercy Department of Chemistry & Biochemistry.

References

1. Jenkins, R. *X-ray Fluorescence Spectrometry*, 2nd ed.; Wiley-Interscience Publication, John Wiley & Sons, Inc.: New York, 1999; Volume 152; pp 53–73.
2. Bendall, C.; Wigg-Wolf, D.; Lahaye, Y.; Von Kaenel, H.; Brey, G. *Archaeometry* **2009**, *51*, 598–625.
3. Weeks, L.; Keall, E.; Pashley, V.; Evans, J.; Stock, S. *Archaeometry* **2009**, *51*, 576–597.
4. Dussubieux, L.; Deraisme, A.; Frot, G.; Stevenson, C.; Creech, A.; Bienvenu, Y. *Archaeometry* **2008**, *50*, 643–657.
5. Deraisme, A.; Barrandon, J. *Archaeometry* **2008**, *50*, 835–854.
6. Hoppner, B.; Bartelheim, M.; Huijsmans, M.; Krauss, R.; Martinek, K.; Pernicks, E.; Schwab, R. *Archaeometry* **2005**, *47*, 293–315.
7. Giunlia-Mair, A. *Archaeometry* **2005**, *47*, 275–292.
8. Pryce, T.; Bassiakos, Y.; Catapotis, M.; Doonan, R. *Archaeometry* **2007**, *49*, 543–557.
9. Mandel, E. J. *Cast Coinage of Korea*; Western Publishing Company, Inc.: Racine, WI, 1972; pp 13–16.
10. Gardner, C. J. *China Branch R. Asiat. Soc.* **1892-93**, XXVII.
11. Craig, A. *The Coins of Korea and an Outline of Early Chinese Coinages*; Ishi Press: Berkley, CA, 1955.
12. Mandel, E. *Cast Coinage of Korea*; Western Publishing Company, Inc.: Racine, Wisconsin, 1972.
13. Linke, R.; Schreiner, M.; Demortier, G.; Alram, M.; Winter, H. In *Comprehensive Analytical Chemistry XLII*; Janssens, K., Van Grieken, R., Eds.; Elsevier: Amsterdam, 2004; pp 605–633.
14. Kuntz, M.; Ferguson, J.; Iduma, V.; Kuzava, R.; Benvenuto, M. *Am. J. Undergrad. Res.* **2002**, *1*, 29–37.
15. Atallah, P.; Kuntz, M.; Kuzava, R.; Ferguson, J.; Iduma, V.; Benvenuto, M. *AJN Second Series* **2004-05**, 231–257.
16. Gaines, T.; McGrath, E.; Iduma, V.; Kuzava, R.; Frederick, S.; Benvenuto, M. A. Chemical Compositions of Chinese Coins of Emperor Ch'ien Lung (Qian Long) and Annamese Coins of Emperor Thanh Thai via Energy Dispersive X-ray Fluorescence. In *Archaeological Chemistry: Materials, Methods, and Meaning*; Jakes, K. A., Ed.; ACS Symposium Series 831; American Chemical Society: Washington, DC, 2002; pp 231–244.

Chapter 11

Chemical Composition of a Series of Siamese Bullet Coins: A Search for Contemporary Counterfeits

Danielle M. Garshott, Elizabeth MacDonald, Meghann N. Murray,
and Mark A. Benvenuto*

Department of Chemistry & Biochemistry, University of Detroit Mercy,
4001 W. McNichols Road, Detroit, MI 48221

*E-mail: benvenma@udmercy.edu

Fifteen small bullet coins, presumed to be of Siamese manufacture, were analyzed via energy dispersive X-ray fluorescence spectrometry and examined for the following elements: copper, zinc, tin, lead, iron, nickel, cobalt, arsenic, antimony, bismuth, gold, platinum, palladium, and silver. The compositions of the bullet coins were then compared to a single Siamese bullet coin that is known to be authentic. The fifteen bullet coins in the set varied slightly in size, but were comparable in look, size, shape, and weight to the one sample of known provenance. There are significant differences in the markings that appear on the fifteen bullet coins when compared to the one of known provenance and to others pictured in established references, and the elemental composition of the fifteen is strikingly different from that of the known, authentic example.

Introduction

Silver and gold lumps (generally referred to by historians and numismatists as bullet money) have been a medium of exchange in Siam (modern Thailand) since medieval times (*1*) but appear never to have been studied in any serious manner in terms of metallic and elemental composition. Bullet money was demonetized on October 28, 1904 but could be exchanged for flat coins until October 26, 1905. This date was later extended to July 24, 1908. Bullet money had thus lasted as

a medium of exchange for more than 600 years (1). To manufacture pieces of bullet money, molten silver (90 to 95% fine silver) was poured into a wooden form and shaped into an elliptical bar, then hammered into a round shape. Nearly all bullet money is marked by a die stamp. The exception was one type that was hand-carved, representing the dynasty. Commemorative, presentation, and private bullet coins all are known to exist (1, 2).

Examples of the bullet coins examined in this study are shown in Figure 1. Examples 1 to 3 are from the set thought to be contemporary counterfeits, while the one labeled 16, in the lower right of Figure 1, is the example of known provenance. It can be seen that they are all of roughly the same shape and size, although the markings differ. The markings on the first three appear to cover more of the surface of each bullet coin. The markings on number 16 appear to be more localized.

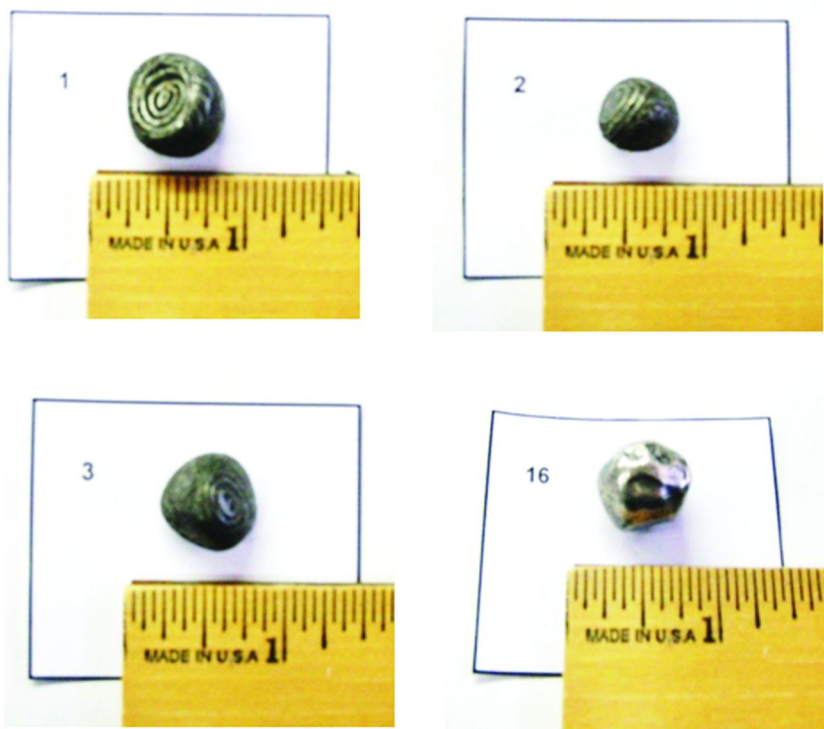


Figure 1. Three examples of contemporary counterfeits, and known Siamese bullet coin.

Fifteen small bullet coins presumed to be Siamese and presumed to be manufactured in Thailand, along with one authentic bullet coin, sometimes called a “Baht Thailand bullet coin,” of established provenance, were analyzed via energy dispersive X-ray fluorescence spectrometry and examined for copper, zinc, tin, lead, iron, nickel, cobalt, arsenic, antimony, bismuth, gold, platinum,

palladium, and silver. While there are notable differences in the markings that appear on the fifteen individual coins when compared to the authentic Siamese bullet coin, the authentic piece, the Baht Thailand bullet coin, is not significantly larger in size or mass (in grams) than the set of fifteen.

This study is designed to determine the elemental composition of these bullet coins, to compare the composition of the set of fifteen to that of an authentic Siamese bullet coin, and thus to help establish whether these fifteen are authentic or contemporary counterfeits. Additionally, this study is intended to deepen the awareness of a rather unexamined aspect of Siamese monetary history.

Experimental Methods

Bullet coins 1-15 (denoted Sib1-Sib15 in the six figures) were purchased for this study, and bullet coin 16 (Sib16) was in the personal collection of the corresponding author (3). All sixteen bullet coins were placed in a sonicating hot water, non-corrosive soap bath for a total of two hours to remove any surface dirt and residue. They were then rinsed with distilled water and wiped dry immediately with a Kimwipe.

After this preparation, each bullet coin was examined to ensure that the point of exposure to the X-ray beam was clean and free of any surface irregularities or oxidation. The bullets were then examined via energy dispersive X-ray fluorescence on a Kevex Spectrace Quanx spectrometer for the following elements: copper, zinc, tin, lead, iron, nickel, cobalt, arsenic, antimony, bismuth, gold, platinum, palladium, and silver. Excitation conditions for each sample were as follows: 20 kV, 0.10 mA, 100 second count $K_{\alpha,\beta}$ for iron, cobalt, nickel, copper, zinc, arsenic, platinum, gold, bismuth, and lead, followed by 45 kV, 0.72 mA, 60 second count, L lines, for palladium, silver, tin, and antimony, using a rhodium target X-ray tube. Pure elemental standards and fundamental software, purchased from Spectrace (now Thermo Fisher Scientific), were utilized in determining all elemental concentrations. A copper standard sample disk was run each day before the samples as a calibration. Samples were run a minimum of three times each.

Results and Discussion, Chemical Compositions

Figure 2 shows graphically the percentage by weight of copper in each of the fifteen bullet coins. Since this project was approached with the idea that based on their irregular markings the fifteen coins may not be genuine, and possibly not made of silver, it is logical to assume they are made from some less expensive metal. Copper is one metal that appears always to be cheaper than silver, and it is one that when alloyed with others does not retain the distinctive copper color. The most obvious example in circulating coinage today within the United States is the five-cent piece, or nickel, which is 75% copper and only 25% nickel, yet which has no copper color to it. As well, we have examined several other series of ancient or medieval coins containing copper, and have found the characteristic copper color is not present when coins and objects are heavily alloyed (4-7). Clearly, this set of fifteen coins is almost devoid of copper.

Figure 3 shows graphically the iron present within the set of fifteen bullet coins. While iron is not a particularly expensive metal, it was surprising to find that these coins essentially are iron, and that all other elements are at trace levels in comparison. Also, it is noteworthy to see the rather large difference from the high to the low data point concerning this element. It suggests that the person or persons who made this set used more than one metal source, or that this set is composed of samples from several different batches of iron.

Since genuine Siamese bullet coins are made from silver, Figure 4 shows the element in these fifteen coins. Clearly, silver is only a trace element within the set. The silver is actually so low that one can surmise it is nothing more than a contaminant. Taking data from different positions on each bullet did not give uniform readings amounts of silver, although this did give values within the range of those reported in the figure, implying that the coins were not silver plated after being formed.

Figures 5 – 7 are bar graphs illustrating the amount of antimony, tin, and zinc in the coins respectively. These three elements are routinely seen in objects that are copper-based and alloyed (4–7), and again, the initial thought was that this set of bullet coins may have significant amounts of copper in them. However, it is evident that, with only one exception, these three elements are present in no more than trace amounts. The exception is the element tin in Sib1, which is omitted from the graph in Figure 6, because at 0.834% it would skew the graph to an extent that the differences in the other fourteen pieces would no longer be noticeable.

The fifteen bullet coins were also examined for other trace elements because of the presence of such elements in iron ores, as well as silver ores. None of the elements beyond those discussed above were present in any of the samples in high enough amount to be perceived as significant.

The actual, silver Siamese bullet coin, Sib16, against which the fifteen in the set were compared has had its elemental composition displayed separately in Table I. The reason this single sample was not included in the previous six graphs is simply that its composition is so markedly different that it would have eliminated a wealth of detail in the graphs as they are presented. For example, Sib16 is well over 90% silver, while the fifteen are not even near 1%. Similarly, Sib16 has no iron in it that is even statistically significant at the lower limit that the EDXRF spectrometer can read. The set of fifteen has iron percentages that are all significantly above 98%. Even the copper percentage of Sib16 is much higher than the set of 15. In short, this coin of known provenance is completely different than those of Sib1 to Sib15.

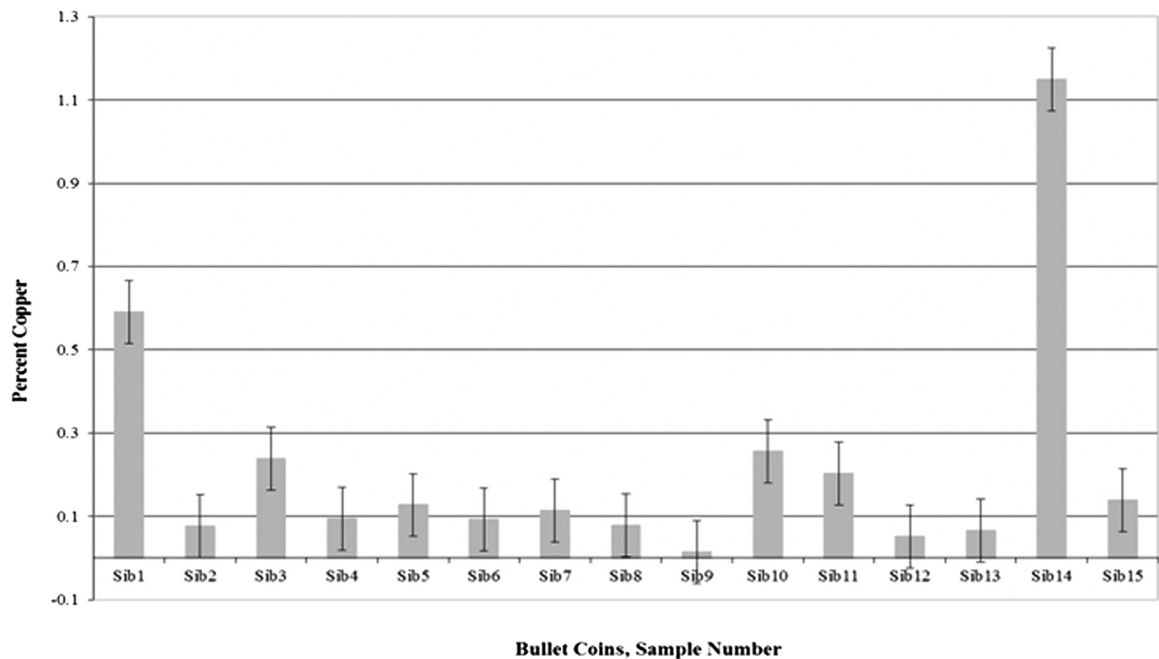


Figure 2. Copper in Sib1–Sib15.

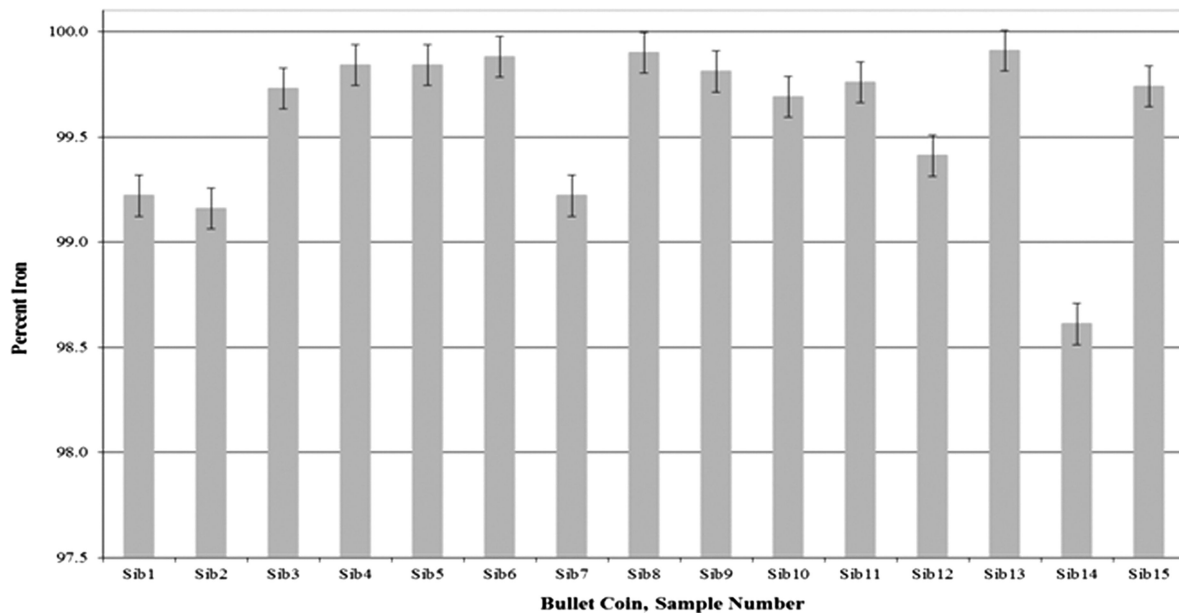


Figure 3. Iron in Sib1–Sib 15.

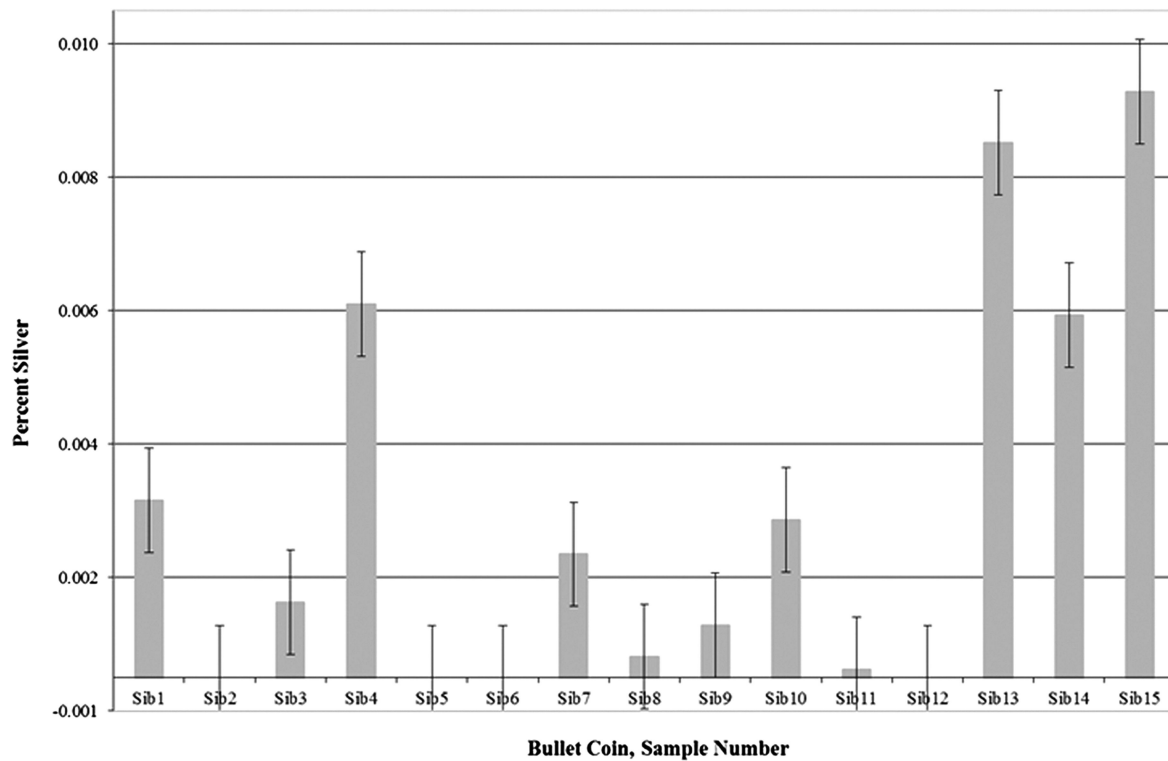


Figure 4. Silver in Sib1–Sib 15.

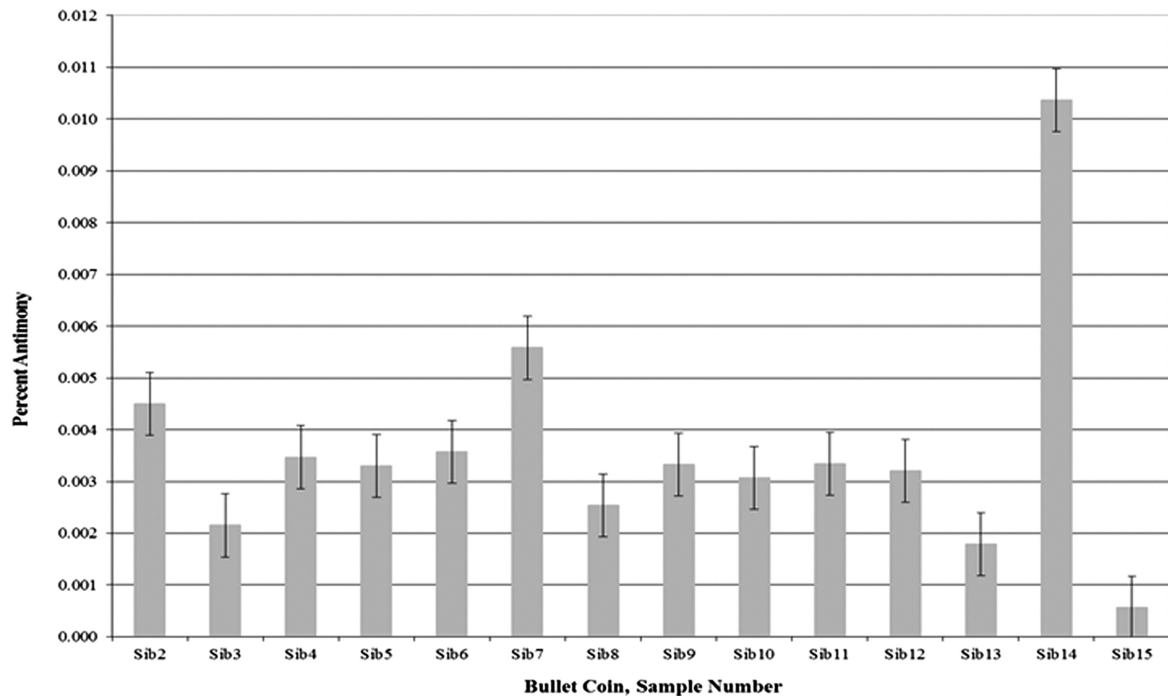


Figure 5. Antimony in Sib1-Sib15.

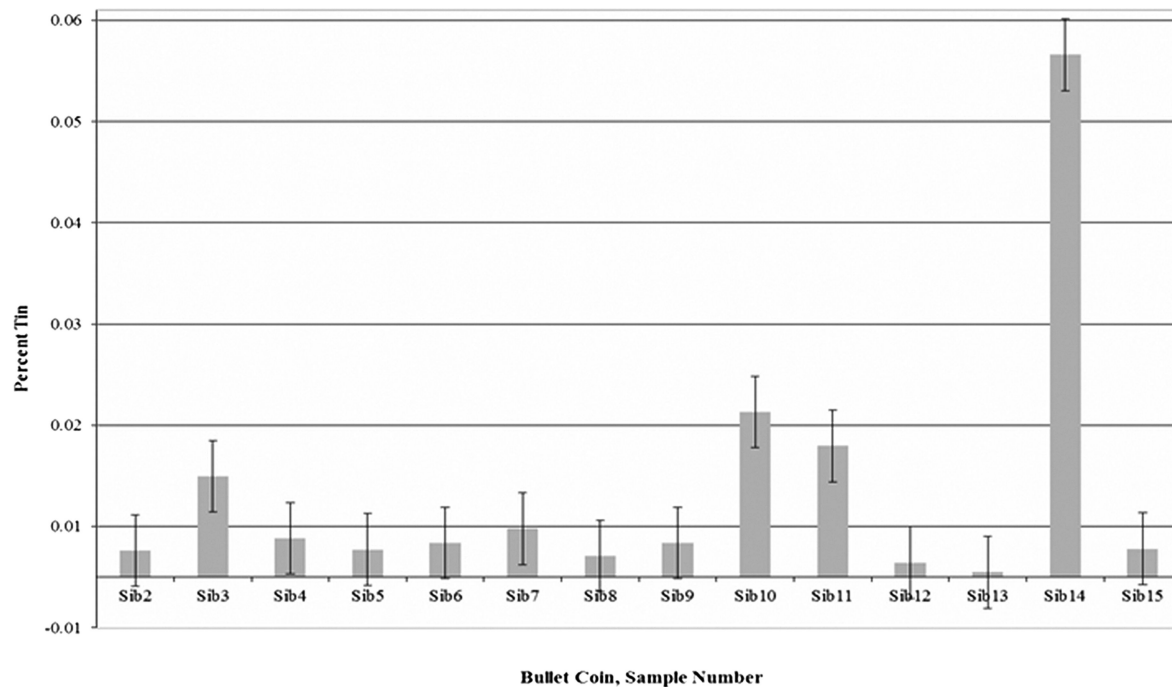


Figure 6. Tin in Sib1–Sib15.

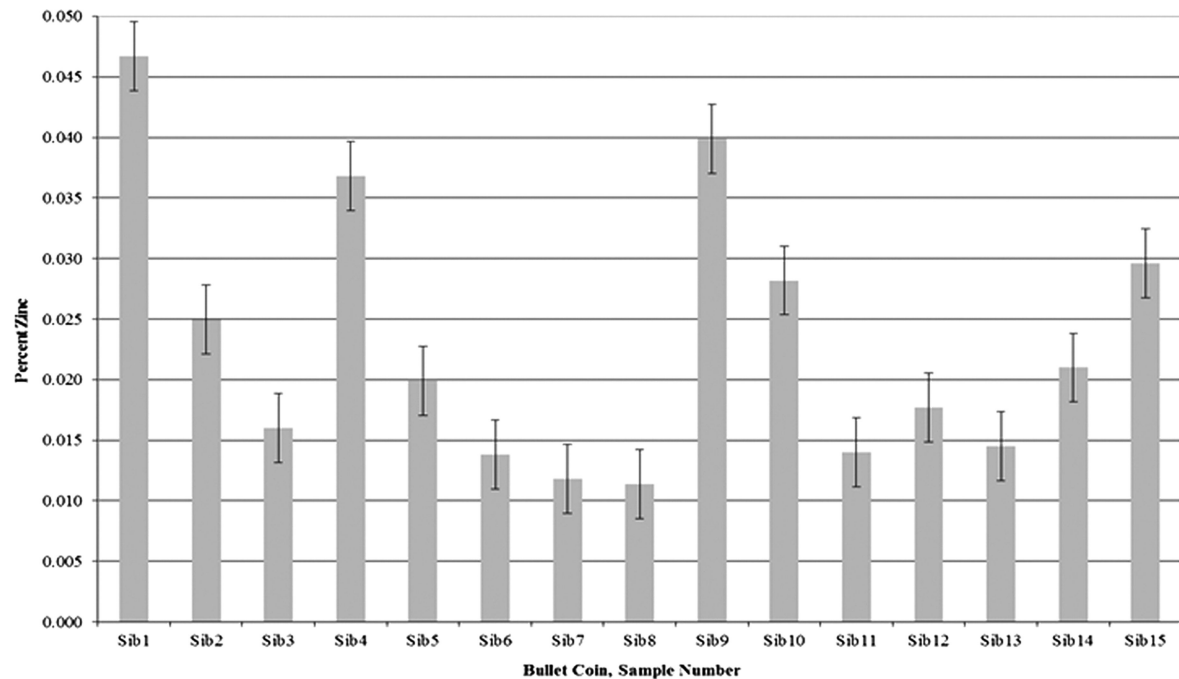


Figure 7. Zinc in Sib1–Sib15.

Table I. Major elemental composition of authentic Baht Thailand bullet coin

<i>Element</i>	<i>Average Percent Composition</i>	<i>Standard Deviation</i>
Silver	93.99	0.1300
Copper	4.879	0.0120
Lead	1.349	0.0081
Gold	0.089	0.0033
Antimony	0.042	0.0043

Conclusions

Despite the size and weight of these fifteen bullet coins being close to that of a known example, their markings are different, and their elemental composition is decidedly different from that of known, officially-produced, silver, Siamese bullet coins. This set of coins is almost entirely iron. Since silver Siamese bullet coins were demonetized early in the 20th century (*1*), it seems logical to conclude that these are contemporary counterfeits, meaning counterfeits made at a time contemporary to the use of genuine Siamese bullet coins.

While this set of fifteen samples are counterfeit, these bullet coins remain culturally interesting objects of study themselves, and the trace metal composition of these contemporary counterfeit coins may aid future researchers in determining their geographical source, trade routes, and/or intended use.

Acknowledgments

This research would not have been possible without the continuing financial support of the University of the Detroit Mercy Department of Chemistry & Biochemistry.

References

1. Opitz, C. J. *An Ethnographic Study of Traditional Money*; First Impressions Printing, Inc.: Ocala, FL, 2000; pp 92–97.
2. Ridgeway, W. *The Origin of Metallic Currency and Weight Standards*; Cambridge University Press: Boston, MA, 1892; pp 28–29.
3. M. Benvenuto purchased the authentic piece from a numismatics shop in Mannheim, West Germany when stationed there as a lieutenant in the United States Army in the mid-1980s. It has been in his personal collection since then.
4. Gaines, T.; McGrath, E.; Iduma, V.; Kuzava, R.; Frederick, S.; Benvenuto, M. A. Chemical Compositions of Chinese Coins of Emperor Ch'ien Lung (Qian Long) and Annamese Coins of Emperor Thanh Thai via Energy

Dispersive X-ray Fluorescence. In *Archaeological Chemistry: Materials, Methods, and Meaning*; Jakes, K. A., Ed.; ACS Symposium Series 831; American Chemical Society: Washington, DC, 2002; pp 231–244.

5. Atallah, P.; Kuntz, M.; Kuzava, R.; Ferguson, J.; Iduma, V.; Benvenuto, M. *Am. J. Numismatics* **2004/5**, 16–17, 231–257.
6. Kuntz, M.; Ferguson, J.; Iduma, V.; Kuzava, R.; Benvenuto, M. *Am. J. Undergrad. Res.* **2002**, 1, 29–37.
7. Misner, J.; Boats, J. J.; Benvenuto, M. A. Chemical Composition of Song Dynasty, Chinese, Copper-Based Coins via Energy Dispersive X-ray Fluorescence. In *Archaeological Chemistry: Analytical Techniques and Archaeological Interpretation*; Glascock, M., Ed.; ACS Symposium Series 968; American Chemical Society: Washington, DC, 2007; pp 231–45.

Chapter 12

Analysis of the “Archaic Mark” Codex

A Collaborative Study in Authentication

Joseph G. Barabe,^{*1} Abigail B. Quandt,² and Margaret M. Mitchell³

¹McCrone Associates, 850 Pasquinelli Drive, Westmont, IL 60559

²The Walters Art Museum, 600 North Charles Street, Baltimore MD 21201

³The University of Chicago, 1025 E. 58th Street, Chicago, IL 60637

*E-mail: jbarabe@mccrone.com

The forger’s strategy is straightforward: convince the person with the power (usually with the money) to accept the piece and pay the price. For most, this means keeping it simple, using materials and techniques that will convince on a superficial level but not invite scrutiny. The analyst evaluating the authenticity of the object must sift through the available evidence with the goal of uncovering just those methods and materials that are consistent with an artist or an age (suggesting authenticity) or inconsistent, indicating non-authenticity. An authentication study may be seen, then, as a contest between the two competing strategies of willful forger and the disinterested analyst. With highly complex objects, a team of experts may be called upon to collaborate in the study. This paper will focus on the analysis of a particularly complex work, the “Archaic Mark” codex, which was reputed to be a manuscript version of the Gospel of Mark possibly created in the 14th century but suspected to be a fake. The analytical team consisted of curatorial and conservation staff at the University of Chicago Library Special Collections, a New Testament scholar, a prominent manuscript conservator/codicologist, and a microscopist. The multidisciplinary approach was especially fruitful, not only proving the item false but illuminating the forger’s methods and overall strategy as well.

Introduction

In January 2008, Dr. Alice Schreyer, Director of Special Collections at the Regenstein Library of the University of Chicago formed a committee to determine, once and for all, the authenticity of an important Greek New Testament manuscript in the Goodspeed Manuscript Collection, University of Chicago ms 972, also known as the “Archaic Mark” (1). This manuscript is also known as Nestle-Aland ms 2427. Over the years, many scholars had questioned its authenticity on both textual history and material constituents’ grounds. McCrone Associates was invited to meet with the committee and to develop an analytical plan to address the question through materials analysis. During this meeting, I had the opportunity to briefly examine this piece and some of the critical literature that the committee had gathered together.

One of the scholars present at that meeting was Dr. Margaret M. Mitchell, who had studied the text critically and is one of the co-authors of this paper (See **Forger’s Textual Source**). A scholar not present at this meeting, but who took a special professional interest in the manuscript, was Ms. Abigail B. Quandt, Head of Book and Paper Conservation at the Walters Art Museum in Baltimore MD, and an expert in medieval codices; Ms. Quandt has been conserving the Archimedes Palimpsest for many years, and her interest in the “Archaic Mark” stems partly from her research on the working methods of forgers of ancient manuscripts, especially those of Greek provenance. Ms. Quandt’s elucidation of the forger’s techniques added greatly to our understanding of this artifact. (See **Codicological Analysis**.)

Much of this material was previously published in the journal *Novum Testamentum* (Brill), and is published here with Brill’s kind permission. In that publication, the emphasis was on clarifying the status of the “Archaic Mark” so that it would no longer be considered an early textual witness in the field of New Testament studies (2).

The “Archaic Mark”

The “Archaic Mark” is a small, handwritten manuscript of the full Greek text of the Gospel of Mark, consisting of 44 folios 11.5 x 8.5 cm, each page containing 20 - 25 lines of text. It contains 17 miniatures - a large author portrait on folio 1 verso, and sixteen narrative scenes - in addition to a Byzantine-style headpiece and decorated initials within the text. Figure 1 is a photograph of the evangelist’s portrait on folio 1 verso, and folio 2 recto, the first page of text with the illuminated headpiece. (Digital images of all the folios of the “Archaic Mark” and its binding may be found at: <http://goodspeed.lib.uchicago.edu>. Accessed April 9, 2012.)



Figure 1. Photograph of the “Archaic Mark,” folios 1 verso, with evangelist’s portrait and first page of text with illumination.

Provenance and Early History

The manuscript was originally found in the possession of John Askitopoulos, an Athenian collector and antiquities dealer, after his death in 1917. In about 1926, it was seen and noted by art historians Andre Xyngopoulos and Sirarpie Der Nersessian (3). The codex was sent to Dr. E. J. Goodspeed in 1937, and purchased by the University of Chicago Library in 1941. Because the textual readings are surprisingly so close to those in the very early *Codex Vaticanus*, it was named the “Archaic Mark.” It was considered by some prominent New Testament scholars to be an early textual witness of the Gospel of Mark and, therefore, of great philological interest. In 1945, Professor Ernest Cadman Colwell said that its text perhaps contained “the text of the Gospel of Mark in a more primitive form than any other known manuscript,” (4) and as recently as 1982, Kurt and Barbara Aland declared the work a Category One Witness “...von sehr hohem textkritischen Wert,” (of very high text-critical value) (5). All Greek New Testament scholars and translators depend on the Nestle-Aland edition of the Greek New Testament, now in its 27th edition, in which the “Archaic Mark” is classified as Nestle-Aland ms 2427, and was listed as “XIV century?” (6).

Previous Examinations

The codex had undergone two previous exploratory investigations, but neither was brought to a final conclusion. These initial analyses were significant in that they raised a number of important questions.

21

Archais Mark
University of Chicago Manuscript 972
(meas. bottom up; left in)

11/11/71 Green sample h. 3.1 cm; w. 6.3 cm

mostly blue
& yellow

deep blue - isotropic (n_x 1.66) 7-10 μm
amorphous shapes in medium
pale yellow particles - anisot. 1 μm
Corbiref. due to anisot. white beneath

first order white - 5-20 μm
some particles have fairly high biref.
related to medium?

? green (or pale white) particles 0.5-1 μm

red particles - a few, appear to be
deep red-rose biref.

a few large black particles -
bones charcoal

much medium visible, eggwhite?

Red border h. 4.0 cm; w. 3.25 cm

eggwhite
transparent, clear biref. material

rose red particles 10 μm particles
0.5-1 μm
clustered on surface of above

much eggwhite - like medium visible

Figure 2. Page from conservator Marigene Butler's handwritten notes.

In 1971 – 1972, Marigene H. Butler, Conservation Microscopist at the Art Institute of Chicago, performed a polarized light microscopy examination of a number of paint samples from the manuscript. She was able to describe a number of materials and, most importantly, noted possible consolidation treatments to stabilize flaking paint, which she dated to approximately 1900. She also noted that the particle sizes of the pigments were very small. However, due to a lack of resources, she was unable to complete her analyses at that time, and she issued no formal report (7). Figure 2 is a sample of a page from her notebook. At the time that Mrs. Butler was doing her analysis, she was unaware that the two most important pigments in the miniatures were among those most difficult to identify with polarized light microscopy alone, that is, without further instrumental analysis.

In 1989, an article by Orna et al. on ten different Byzantine and Armenian codices, included an examination of the blue paint in the miniatures in the “Archaic Mark” (8). They were surprised to see an infrared band indicating the presence of Prussian blue, a pigment first available in the 18th century (Figure 3) (9). In their seminal paper, they stated: “Replicate spectra of blue pigments removed from different locations in ms 972 indicate that the average frequency of this band is $2083 \pm 6 \text{ cm}^{-1}$. The ubiquitousness of an iron blue in this manuscript raises doubts about the authenticity of this manuscript.” Also, the question of possible restoration of the paint layer – in the form of consolidation and/or retouching of losses - remained.

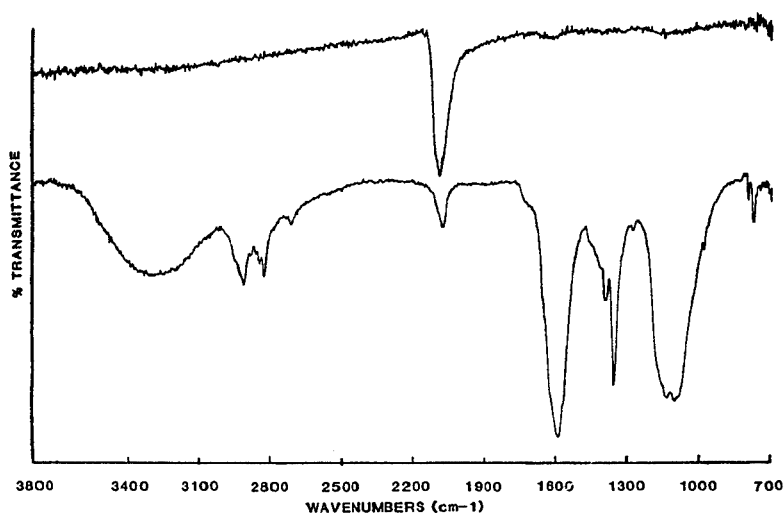


Figure 3. Spectrum demonstrating presence of Prussian blue in Orna et al. study of the “Archaic Mark.”





Figure 4. (A) White light photograph of portrait of the evangelist Mark on folio 1 verso. Dark robes include several shades of blue; (B) Photomacrograph of portrait of the evangelist Mark on folio 1 verso, original magnification 7.5X. Severe losses allowed for sampling with little cosmetic impact; (C) Ultraviolet fluorescence photograph of portrait of the evangelist Mark on folio 1 verso. Bright areas include zinc-containing pigments.

Examination and Photography

On 13 February 2008, the manuscript was hand carried to McCrone's laboratory for examination, photography and sampling, under the watchful eyes of conservator Christine McCarthy. In our white light examinations, we noted that folio 1 verso (Figure 4A), the portrait of the evangelist Mark, had extensive paint losses, so we chose to begin our sampling on that page. The robes provided clear access to several shades of blue, and both white and off-white were present. Figure 4B is a photomacrograph of the sampling site for the flesh-colored paint. Each of the sample sites was photographed under the stereomicroscope.

Examination of the document with long-wave ultraviolet at 365 nm (UVA) also proved fruitful: the whites fluoresced brightly, so we suspected that the white pigment might be zinc white, a relatively modern pigment. We also noted that the gold background of the miniatures seemed to have a translucent coating that fluoresced a dull orange. Figure 4C is a UV fluorescence photograph of folio 1 verso; note the bright areas.

Samples of paint and ink were taken with an extremely sharp tungsten needle. A small amount of parchment was taken from dog-eared corners for carbon dating of the substrate. The paint and ink samples were analyzed with polarized light microscopy (PLM), microchemical tests, elemental analysis by energy dispersive X-ray spectrometry (EDS in the SEM), infrared (FTIR) spectroscopy, and X-ray diffraction (XRD).

Paint Analysis

We examined several blue paints ranging from light to dark. The primary blue colorant was identified as Prussian blue, confirming the earlier analyses by Professor Orna and her colleagues. PLM and SEM/EDS data were suggestive, and infrared spectroscopy was definitive. Figure 5 is the FTIR spectrum of a medium blue from the evangelist's robe; note the prominent band at 2090 cm^{-1} due to the nitrile stretching of Prussian blue. Although this band is at 2085 cm^{-1} in the reference spectrum of Prussian blue, minor shifts in this absorption band are normal, and this is considered a good match. The blue paint sample locations were carefully examined for any evidence of retouching, but none was found.

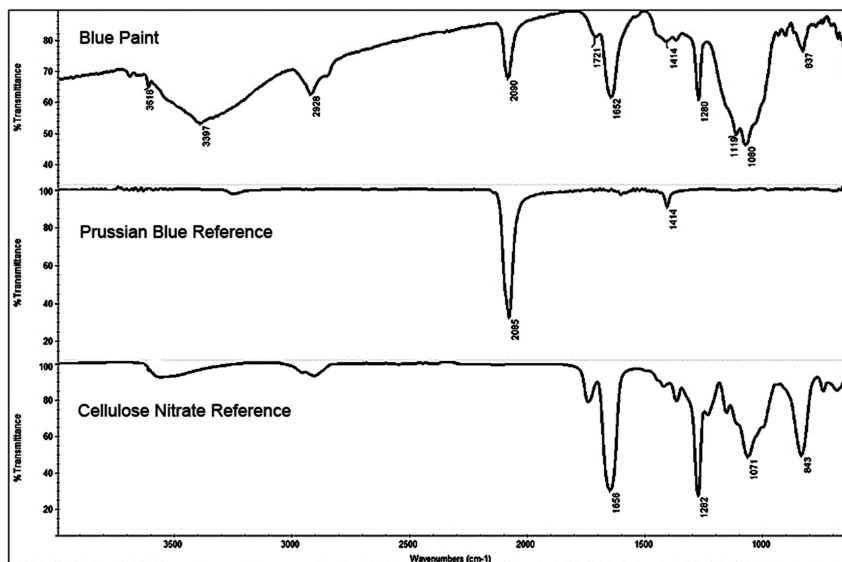


Figure 5. FTIR spectrum of blue paint from blue robe (top), with reference spectra of Prussian blue (middle), and cellulose nitrate (bottom).

In addition to showing the presence of Prussian blue, the spectrum is also consistent with that of cellulose nitrate (Figure 5C). Cellulose nitrate was only found as a clear coating over the paint of the miniatures, and, while we are unable to rule it out as having been applied by the forger, it makes more sense that it was used later as a consolidant, in an effort to prevent or arrest the flaking of the paint.

One of the two opaque white pigments identified in the miniatures is zinc white, or zinc oxide; it was found in only limited areas, such as the white book, folio 1 verso. Zinc white was suggested by PLM and the paint's fluorescence characteristics, and confirmed with SEM/EDS (Figure 6). Zinc white was first suggested for use as an artists' pigment in 1780 and was commercially available by 1825 (10). It, too, was taken only from areas that were clearly original.

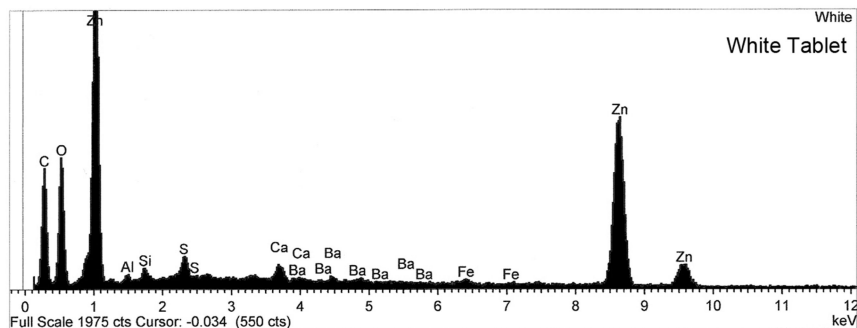


Figure 6. EDS spectrum of white paint, confirming the presence of zinc white pigment, zinc oxide.

A second opaque white pigment was identified as lithopone, which was found in many more of the samples. Lithopone represents a more difficult analytical problem. It is manufactured by coprecipitating and calcining a mixture of zinc sulfate and barium sulfide, resulting in a physical solid mixture of zinc sulfide and barium sulfate (11). The resulting material is microscopically very similar to conventional, nodular zinc oxide. The elemental composition as determined by EDS would be consistent with a mixture of zinc white and blanc fixe (synthetic barium sulfate) as well as lithopone, so that, if only these two analytical methods are available, it would be difficult to distinguish between the two pigment compositions. However, as zinc sulfide is present as one of the components of lithopone, its detection is confirmatory for lithopone. And, because lithopone's date of first availability (1874) (12) is considerably later than that of zinc white, it is important to be able to distinguish the two with confidence.

Figure 7A is the EDS spectrum of Sample 1, cream, indicating the presence of zinc, barium, sulfur and oxygen in proportions consistent with either a mix of zinc white and barium sulfate as separate pigments, or lithopone. Figure 7B is the X-ray diffraction pattern for the same sample; it identifies the specific crystal phases present in the sample, which turns out to be relatively complex. It identifies zinc sulfide in two different crystal forms, as zinc sulfide and wurtzite – this confirms the presence of lithopone – but also indicates the presence of barium sulfate (expected) and also calcium sulfate and quartz. Raman spectroscopy could also have been used to identify zinc sulfide, but XRD provided a more complex body of information.

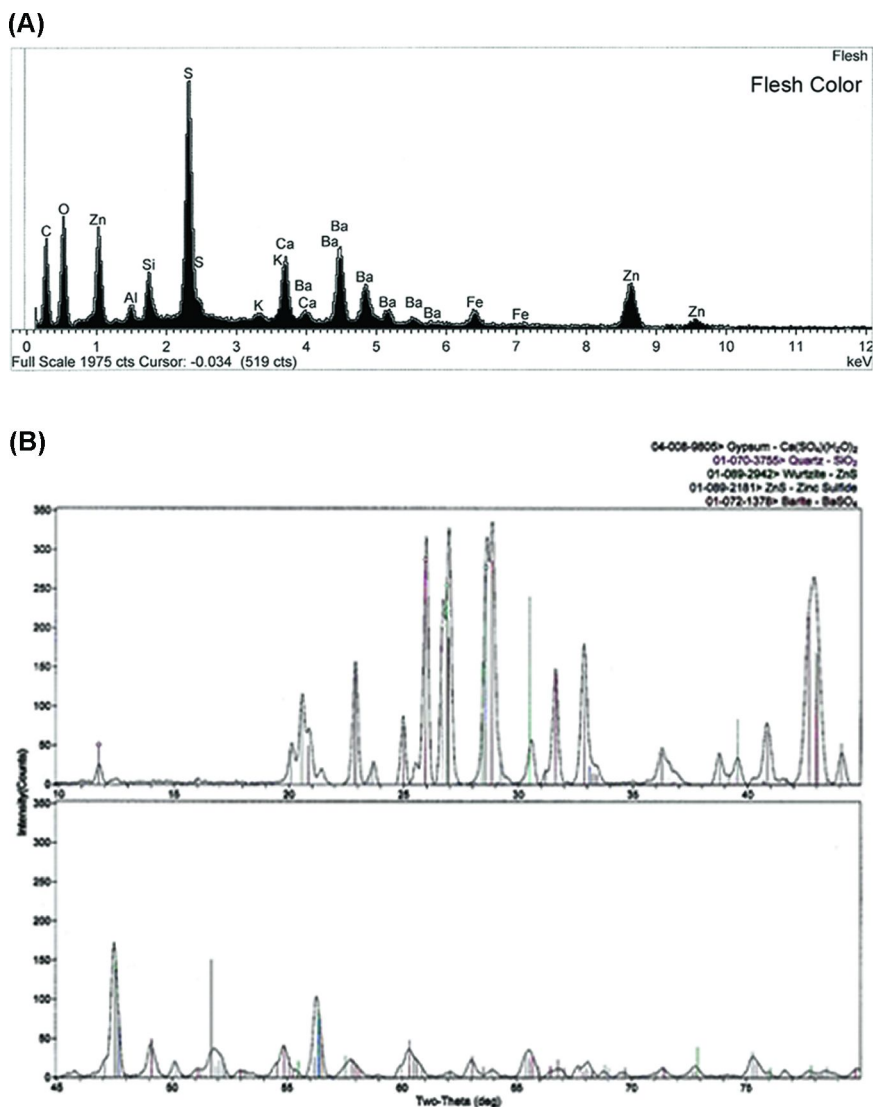


Figure 7. (A) EDS spectrum of flesh color. The presence of zinc, barium and sulfur suggests the possibility of lithopone; (B) X-ray diffraction pattern indicating the presence of several crystalline compounds including gypsum, quartz, barite and two forms of zinc sulfide. Zinc sulfide confirms the presence of lithopone.

The brown-black paint found in the miniatures will be discussed with the inks. The gold background was identified as, indeed, gold leaf.

Ink and Brown-Black Paint Analysis

Brown-black ink was originally sampled from two text areas and one of the miniatures, and several other samples were taken during a later examination. Additionally, in order to investigate the order in which the ink and coatings were placed on the substrate, an entire cross section was taken from an ink line using a 0.5 mm punch (Figure 8A). Removal of a sample of this size is not routine and was only performed after consultation with the Library team. In the end, it was decided that the information to be gained warranted the cosmetic damage to the folio. The sampling site was chosen by the team to minimize loss of information, and the letter chosen remains readable. This sample was mounted for imaging both with light microscopy (Figure 8B) and scanning electron microscopy (Figure 8C) by microscopist Carol Injerd. For the latter, the sample was mounted onto conductive carbon tape and lightly plasma-coated with carbon so that the sample would be sufficiently conductive to be imaged in the scanning electron microscope. Both images were helpful in determining the relative locations of the ink with respect to the parchment substrate and a glossy coating on the parchment surface. In Figure 8C, we attempted to isolate the ink from the transparent coating by colorizing the transparent coating layer, which was determined to be over the parchment and under the ink. Colorization of scanning electron micrographs is an illustrative, not a forensic technique, used to demonstrate structural continuities when tonal differences are subtle.

Identifying the colorants in the inks and the black paints was one of the most challenging tasks in this analysis. In the cross section, the EDS spectrum of the bulk ink (Figure 8D) is clearly carbonaceous, with little inorganic material, and, most important, no evidence for an iron gall component. However, the evidence for a traditional carbon black ink was not strong. Microscopically, the brown material consists of relatively large, transparent particles more consistent with Van Dyke brown pigment, and we have tentatively identified it as such, but while the evidence is suggestive, it is by no means definitive. The (probable) Van Dyke brown is present in a likely attempt on the part of the forger to imitate the brown tone of oxidized, centuries-old iron gall ink. Some of the particles analyzed in the ink are elementally consistent with iron gall ink, so an admixture of this material is also a distinct possibility.

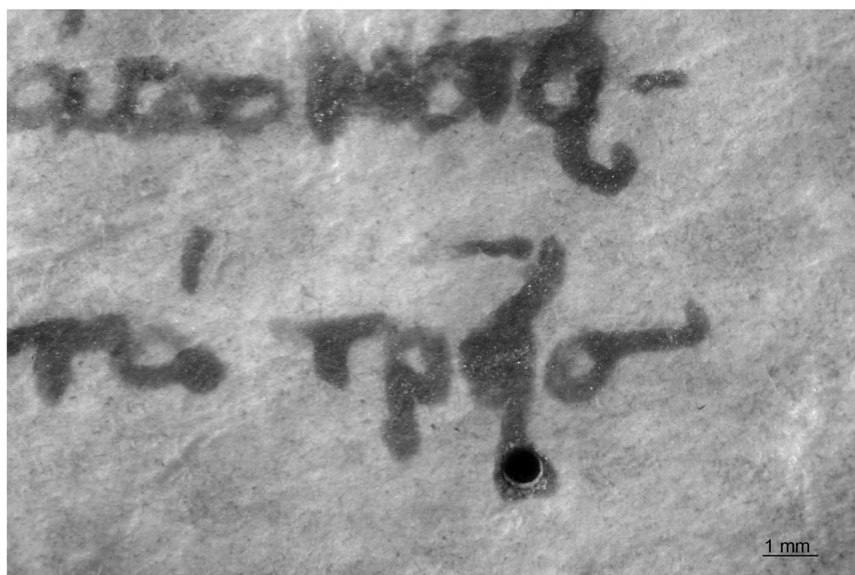
The brown-black paint in the miniatures shares some characteristics with the text ink, but also includes an iron-manganese component with a complement of other inorganic materials (clays, silicas) suggesting the presence of an umber (Figure 9). UMBER-like particles are also found in some of the text ink samples (Figure 10), and it is likely that both the illumination and writing inks include these same components.

Paint and Ink Binding Media

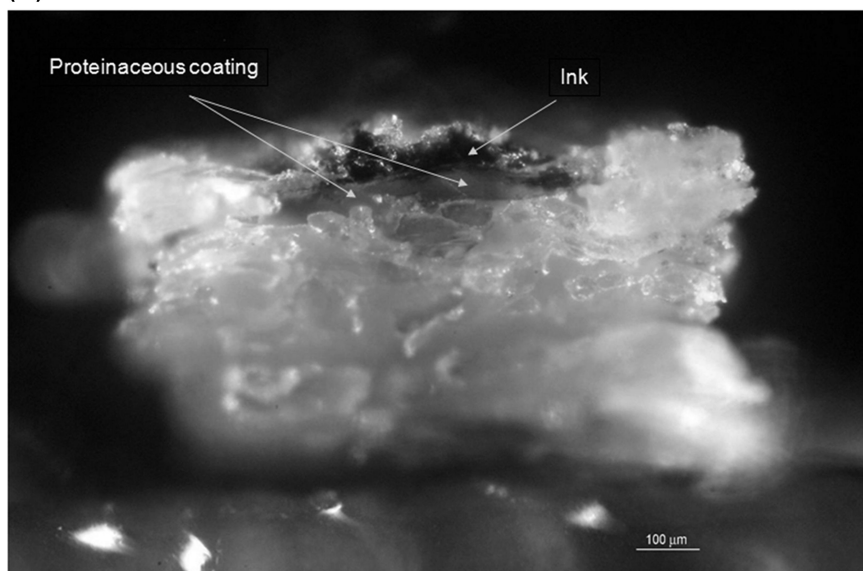
Although infrared spectroscopy of the “as is” sample is usually sufficient to identify at least the general class of binding medium in paints and inks, we often find it useful to separate components with the use of solvents. Figure 11 (top) is the FTIR spectrum of a green paint. The water extract (middle spectrum) is more

distinctive, and allows us to identify the water-soluble fraction as a gum (bottom spectrum).

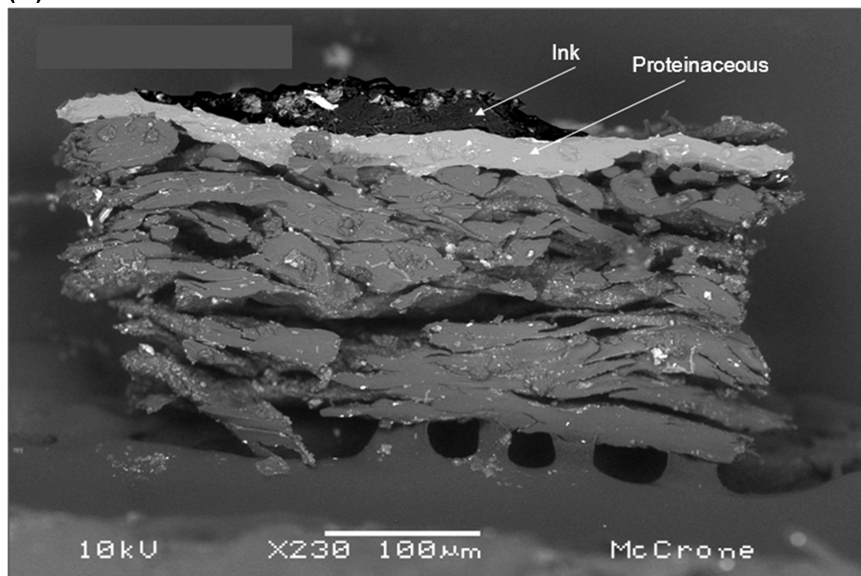
(A)



(B)



(C)



(D)

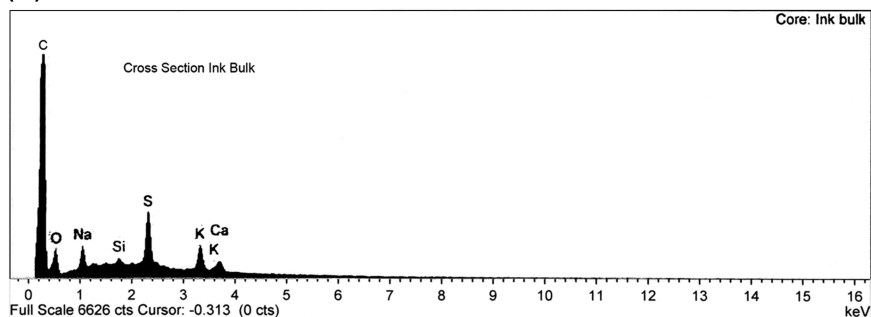


Figure 8. (A) Photomicrograph of text area from which cross section was taken, original magnification 7.5X; (B) Photomicrograph of ink on parchment cross section showing ink over clear proteinaceous coating. Original magnification 200X; (C) Scanning electron micrograph in backscattered mode of ink on parchment cross section. Image has been enhanced to show ink layer (dark) and proteinaceous coating (light). Original magnification 230X; (D) EDS spectrum of ink from ink line cross section.

Gold Leaf Coating

The gold leaf was also found to be coated with a gum and possibly other materials, as indicated by the orange fluorescence under long wave ultraviolet illumination. In addition to transparent material, a number pigments were also identified in the coating; these include zinc white, iron earths, calcium sulfate, an unidentified organic red lake pigment, and traces of a blue pigment, most likely synthetic ultramarine blue.

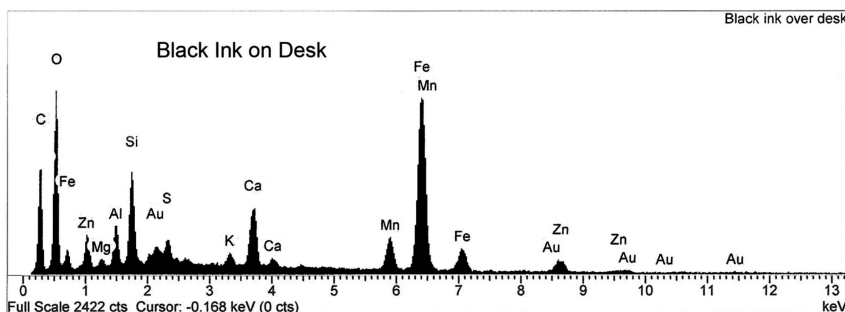


Figure 9. EDS spectrum of black paint on desk.

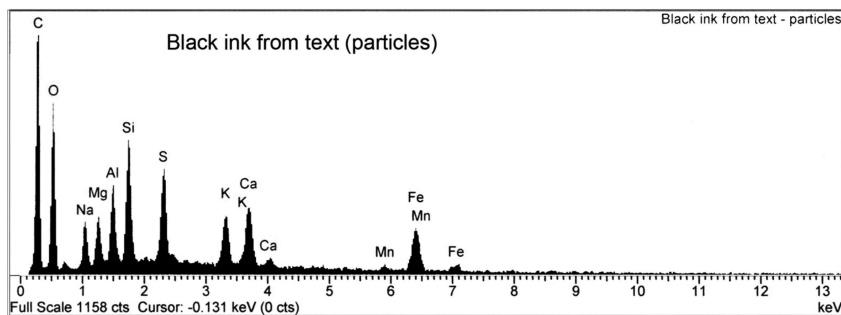


Figure 10. EDS spectrum of ink from text.

Parchment Coatings

In our examinations of the parchment, we noted that there was a glossy, transparent coating over each of the pages; it appeared that the writing rested on that surface. We were able to take small samples from the surface with a modified double edged razor blade. FTIR analysis indicated that the material was proteinaceous, and PLM examination confirmed that the sample was coating material only, not the parchment itself, which is also proteinaceous. Common protein media and coating materials include egg white, gelatin and casein. For a number of reasons, we concluded that the most likely material would be gelatin,

although it should be emphasized that this conclusion is suggestive rather than confirmed. This coating is discussed in more detail below.

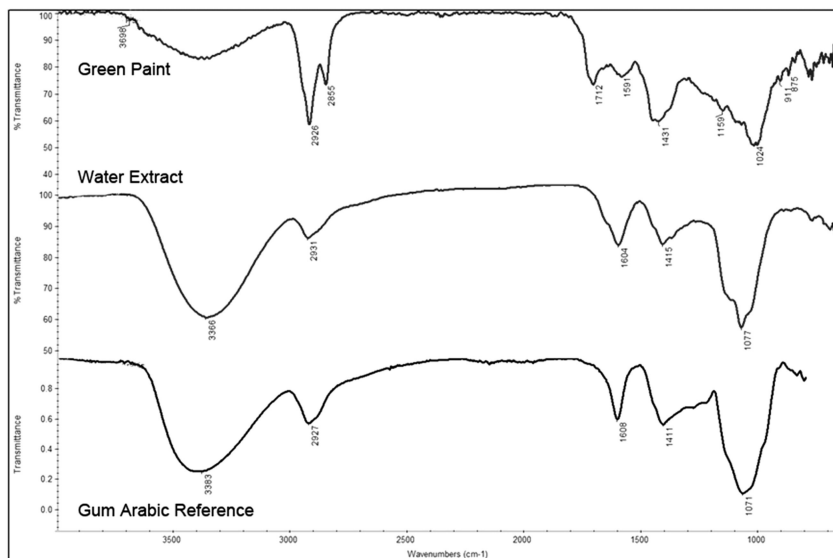


Figure 11. FTIR spectra of from green paint (top), a water extract of the paint (middle) and a gum Arabic reference (bottom).

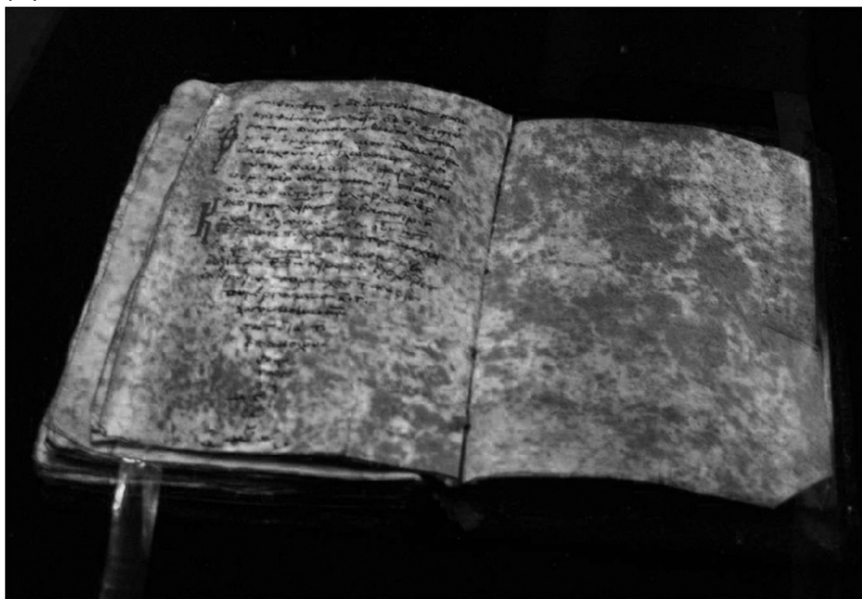
In addition to the clear, glossy coating, there is also a yellow and brown coating material that is present in irregular splotches on all folios. To both the naked eye and with ultraviolet fluorescence (Figure 12A), this material looks much like foxing, brown spots often found on paper (not parchment) that are caused by fungal growth and/or the presence of iron impurities. A few starch grains (probably corn starch) were visible with PLM, and the iodine microchemical test for starch was positive. Figure 12B, top, is the FTIR spectrum of the yellow and brown material. The water extract (middle) provided a much better spectrum, which confirmed the presence of starch (bottom spectrum).

The Parchment: Carbon Dating

During our initial discussions with the Special Collections team, we requested that they identify sufficient parchment material for carbon dating, suggesting that some of the dog-eared corners might be suitable candidates. They identified several, and we chose three; these provided us with eleven milligrams, the recommended amount for parchment. The samples were wrapped in aluminum foil and sent to the University of Arizona AMS Facility for carbon dating. Their report is included as Table I. They dated the parchment provided them between 1485 and 1631 at 1 sigma, 68 % confidence, or between 1461 and 1640 at 2 sigma, 95% confidence. It is not known if the gelatin coating was removed in

the cleaning prior to processing the parchment. If present, it would likely have resulted in a slightly later date. However, the weight percent of carbon in the coating with respect to the parchment substrate would be small.

(A)



(B)

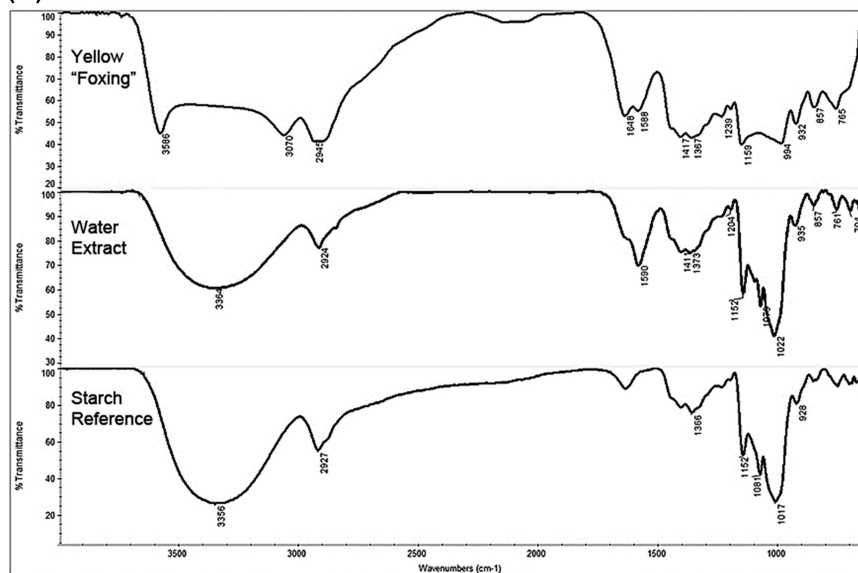


Figure 12. (A) Ultraviolet fluorescence photograph of inner pages with imitation fungal stains; (B) FTIR spectra of yellow stain (top), a water extract of the material (middle) and a starch reference (bottom).

Table I. Carbon dating report table from the University of Arizona AMS facility

Date no.	AA - 79900
Sample no.	Parchment, MA46422-15
$\delta^{13}\text{C}$:	-13.1%
Fraction of modern carbon:	0.9579 \pm 0.0046
Uncalibrated Radiocarbon Age:	345 \pm 38 years before present
Calibrated Age Ranges:	1485-1631 AD (1 sigma, 68% confidence) 1461-1640 AD (2 sigma, 95% confidence)

Codicological Analysis

Although the materials analyses as described above were sufficient to prove the relative modernity of the work, they were insufficient to demonstrate its codicological inconsistencies or the strategies of the forger. Ms. Quandt's analyses proved invaluable in this regard.

The skins, mid-16th century as confirmed with carbon dating, were prepared as per medieval practice and therefore had the correct look and feel, which was necessary in order to convince potential modern buyers, who would generally be aware of modern creation. The parchment was likely obtained from older documents with writing on one or both sides, which then had to be thoroughly removed in order to avoid detection. This may explain the pronounced surface abrasion seen on all the folios. In addition to scraping with a knife, the parchment may also have been sanded to even out the nap on both sides.

In order to smooth the surfaces that had been roughed up by the scraping the sheets were coated with a material identified as being proteinaceous. Byzantine scribes typically applied a coating to the blank parchment that was made by combining egg white with an emulsifying agent prepared from flax seed broth (13). While traditional manuscript coatings are shiny and clear, and form a thin, hard film on the substrate, the coating on the "Archaic Mark" is yellow and relatively thick, and has penetrated into the napped surface of the parchment. The yellow color, plus the degree of puckering and creasing in the parchment folios, suggests the use of a warm solution of gelatin or hide glue for the coating.

The edges of the folios have most likely been darkened with ink in an attempt to imitate the appearance of many Byzantine manuscripts whose edges are blackened and gelatinized from exposure to the soot and heat of a fire.

In addition to the shiny proteinaceous coating, there is also an irregular speckled coating on all the folios; this is visible in both white light and with ultraviolet fluorescence, and has the appearance of foxing or some other type of fungal growth. These splotches were identified as starch. Foxing spots are brown in color, yet are only found on paper, not parchment. If intended to

resemble the mold stains often seen on Byzantine manuscripts, the color of these splotches is wrong: mold stains on parchment are usually purple to red, and associated with localized degradation of the support. The stains on the folios of the “Archaic Mark” vary from yellow to orange to brown and there is no evidence of degradation of the parchment. Like the clear coating, this speckled layer also appears to rest under the text, although the precise sequence is difficult to determine.

The forger ruled the parchment in a manner similar to that of a Byzantine scribe, but with a number of differences, including at least one major mistake: a bifolio (Fols. 17-24) had been ruled twice, in two separate directions. Whether this was due to sloppiness or a lack of available material is unknown.

Usual scribal practice was to copy the text first, leaving room for the miniatures which were then painted in later. In the “Archaic Mark,” the sequence is reversed and, as a result, the writing is often cramped, and appears occasionally to overlap the borders of the miniatures.

Byzantine illuminators would often apply their gold leaf ground to the entire image area and then paint the figural and architectural elements on top of the gold. While this method was adopted for the smaller miniatures of the “Archaic Mark,” the gold leaf was applied to only the background areas of the larger miniatures, probably after first sketching in the overall composition. Unlike the Byzantine artists the forger applied a pale orange-yellow coating over the gold leaf, possibly to hide possible imperfections in the gilding or to give the gold a warmer, “older” look. This coating consists of a transparent gum tinted with a variety of pigments. A dull orange fluorescence under UV suggests the addition of a resinous component to the coating, although this could not be confirmed by FTIR.

The paint in the miniatures of the “Archaic Mark” is heavily cracked and cupped, and there are numerous losses. Paint losses are not abnormal in authentic Byzantine illuminated manuscripts which, because of flaking that occurred early on, were often retouched by their owners within 50-100 years of their manufacture. The miniatures were carefully examined for signs of restoration, which would be obvious at high magnifications; none were found. When Marigene Butler, painting conservator, examined the manuscript in 1972, she noted some possible consolidation treatments that may have been undertaken in an attempt to arrest the flaking.

A clear, shiny layer over the paint of the miniatures, but not over the gold ground, was identified as cellulose nitrate. If the miniatures were indeed consolidated, cellulose nitrate would have been a reasonable choice in the early 20th century (14). It is difficult to imagine why a forger would have treated the miniatures with this material unless the cracking and flaking began almost immediately after the codex was created.

The ink includes a possible iron gall component and a brown pigment, most likely Van Dyke brown, in a gum binding medium. Iron gall ink, as it ages, tends to become lighter and browner, so the brown pigment may have been used to imitate this natural occurrence. Gum is the usual binding medium for iron gall ink.

The manner in which the gold and sometimes red initials are applied is often sloppy and haphazard, including the frequent repetition of letters at the beginning

of a line of text. Normal Byzantine practice was to first write the initial in red ink, and then overlay it with gold leaf, thus warming the color of the gold and providing the initial with more bulk. Contrarily, the forger began with the same brown-black ink used for the text, resulting in a somewhat dirty appearance to the initials, which is emphasized by his failure to burnish the gold leaf.

The binding does not appear to be the work of a professional (or even amateur) bookbinder, but rather that of a forger attempting to create an ancient-looking binding. Instead of using a new piece of leather the forger took a heavily worn blind stamped cover from a larger book and cut it down for his cover and pastedowns (15). If pastedowns were used at all in Byzantine bindings they would be parchment and not leather. Perhaps leather was used here in order to better hide the relatively new wooden boards, which are light in tone. Additionally, the cut-outs around the cord lacings are non-traditional, and one bifolium in the manuscript was sewn into the book reversed. In summary, the forger, while a skilled painter, was not a competent scribe or bookbinder, and the manner in which the codex was created reinforces the conclusion that the book is a relatively modern forgery.

The Forger's Textual Source

While this publication is primarily concerned with the chemical and physical analyses of the materials used in the construction of the manuscript, it must be noted that the codex's potential value had been thought to lie not in its virtues as a museum-quality example of historical book production or book-binding (which it is not), but that the text is present in what appears to be a particularly ancient form (hence its name) and thus of importance to New Testament scholars attempting to reconstruct the earliest readings of the first-century work. Most striking of all is the closeness of the text of ms 2427 to Codex Vaticanus, a major fourth-century Greek codex. Suspicions about ms 2427 being "too good to be true" had arisen very early after it came to the attention of scholars in the 1940s. In 1947, Robert P. Casey commented, "It is to be hoped that in the forthcoming edition a chapter may be written by an *advocatus diaboli* who would do his best to prove that the codex was a manufacture of the nineteenth century, executed by a workman with the skill and limitations of a Simonides [the famous forger], familiar with Lachmann's edition and the modern Greek Bible, and thinking in Greek (16)..." A full analysis of the text had been planned and begun by University of Chicago professors Edgar Johnson Goodspeed, Ernest Cadman Colwell and Allen Wikgren, but it was never completed. In 2006, Margaret Mitchell and Patricia Duncan published a list of corrected and supplemented readings of the codex, with readings facilitated by zoomable digital images of the codex, which were posted online at the Goodspeed Manuscript Collection website of the University of Chicago Libraries Special Collections Research Center. In that article, they recommended a comprehensive study of the codex, including a full materials analysis, a codicological study and a careful examination of the textual readings (17).

The first significant discussion following that call to action was provided by Stephen C. Carlson, a doctoral student at Duke University, who proposed in a paper at the Society of Biblical Literature meeting, that the scribe of the “Archaic Mark” used Philipp Buttmann’s 1860 edition of the Greek New Testament (18) as his exemplar. Carlson announced that, through keen detective work, he had found that ms 2427 follows the readings of Philipp Buttmann’s 1860 edition, even when it departs from the readings of Codex Vaticanus (81 of 85 times). Further research in the history of printed editions of the Greek New Testament has reconfirmed and refined Carlson’s proposal by demonstrating that the source of these readings was not Cardinal Mai’s famously flawed edition (as Carlson had assumed) but Buttmann’s use, in the first edition of his Greek New Testament, of earlier collations of the famous codex Vaticanus made in the late 18th and 19th centuries. In tell-tale fashion, ms 2427 reproduces errors that were corrected in the flurry of collations of Codex Vaticanus in the years 1857-1867, but those correct readings had been unavailable to Buttmann when he published his *first* edition in 1856. In multiple cases the correct readings of Vaticanus are to be found in an appendix of addenda et corrigenda of Buttmann’s later editions (1860 and beyond), but the appendix, with these superior readings, appears to have been completely ignored by the forger.

Combined chemical, codicological and text-critical analyses have confirmed the conclusion that ms 2427 is a late 19th or early 20th century counterfeit. Within the field of New Testament scholarship, the removal of ms 2427 from the list of important early textual witnesses was an occurrence of singular significance. The manuscript is no longer a valuable witness for the ancient Greek text (and hence will not be included in the *Novum Testamentum Graece* 28th edition, now in process), but it will continue to provide scholars insight into the techniques employed in the late 19th and 20th century to fashion counterfeit Byzantine Greek manuscripts.

References

1. Dr. Alice Schreyer’s “Archaic Mark” Committee members included Dr. Daniel Meyer (Associate Director, Special Collections, and University Archivist), Ms. Patti Gibbons (Preservation Manager, Special Collections), Ms. Christine McCarthy, (Head of Conservation, University of Chicago Library, now at Yale University), Ms. Ann Lindsey (Head of Conservation, University of Chicago Library), Ms. Judith Dartt (Digital Specialist, Special Collections), Dr. Beth Bidlack (Bibliographer for Religion and Philosophy, University of Chicago Library), and Dr. Margaret M. Mitchell (Professor of New Testament and Early Christian Literature at the University of Chicago Divinity School).
2. Mitchell, M. M.; Barabe, J. G.; Quandt, A. B. *Novum Testamentum* **2010**, *52*, 101–133.
3. Mitchell, M. M.; Duncan, P. A. *Novum Testamentum* **2006**, *48*, 1–35.
4. Colwell, E. C. *The Emory University Quarterly* **1945**, *75*, 65–75.

5. Aland, K.; Aland, B. *Der Text des Neuen Testaments: Einführung in die wissenschaftlichen Ausgaben sowie in Theorie und Praxis der modernen Textkritik*; Deutsche Bibelgesellschaft: Stuttgart, 1982; p 163.
6. In *Novum Testamentum Graece*, 27th ed.; Nestle, E., Aland, K.; Eds.; Deutsche Bibelgesellschaft: Stuttgart, 1986; p 711.
7. Robert W. Allison summarized Butler's handwritten notes in a report on file at the University of Chicago's Special Collections, "Report on the study of the "Archaic Mark" (ms 972) under the Stereomicroscope and Polarizing Microscope."
8. Orna, M. V.; Lang, P. L.; Katon, J. E.; Mathews, T. F; Nelson, R. S. In *Archaeological Chemistry IV*; Allen, R. O., Ed.; Advances in Chemistry Series 220; Washington, DC: American Chemical Society, 1989; pp 265–288
9. Berrie, B. H. Prussian Blue. In *Artists' Pigments: A Handbook of Their History and Characteristics*; Fitzhugh, E. W., Ed.; Oxford University Press: New York, 1997; Vol. 3, p 192.
10. Kühn, H. Zinc White. In *Artists' Pigments: A Handbook of Their History and Characteristics*; Feller, R. L., Ed.; Oxford University Press: New York, 1986; Vol. 1, pp 170–171.
11. Clausen, H.; Issel, M.; Cremer, M. Zinc Sulfide Pigments. In *Industrial Inorganic Pigments*, 2nd ed.; Weinheim, G. B., Ed.; Wiley-VCH: Weinheim, 1998; p 71.
12. Uebele, C. L. Lithopone White. In *Paint Making and Color Grinding: A Practical Treatise for Paint Manufacturers and Factory Managers*; The Painters Magazine: New York, 1913; Chapter IV, pp 51–67.
13. Abt, J.; Fusco, M. A. *J. Am. Instit. Conserv.* **1989**, 28 (2), 61–66.
14. A French restoration manual from 1890 by Ris-Paquot describes the use of cellulose nitrate or collodion for preserving valuable paper documents. See Ellis, M. H. *J. Am. Inst. Conserv.* **1996**, 35(3), 239–254.
15. Harold Willoughby of the University of Chicago identified the pattern of the stamps on the cover as "Greek-monastic in origin" (cited in R. W. Allison, "Report on the study of the "Archaic Mark" (ms 972) under the Stereomicroscope and Polarizing Microscope," 4).
16. Shepherd, M. H., Jr.; Johnson, S. J. *The Journal of Religion* **1947**, 27, 148–9.
17. Mitchell, M. M.; Duncan, P. A. *Novum Testamentum* **2006**, 48, 1–35.

Chapter 13

Developing a Community of Science and Art Scholars

Patricia Hill^{*1} and Deberah Simon²

¹Department of Chemistry, Caputo Hall, P.O. Box 1002,
Millersville University, Millersville, PA 17551

²Department of Chemistry, Hall of Science, Whitman College,
345 Boyer Avenue, Walla Walla, WA 99362

*E-mail: pat.hill@millersville.edu

This chapter documents the 20-plus year development of a groundswell of innovative practice that integrates chemistry and art in college classrooms, research labs, and faculty professional development activities. It also provides a plan for sustaining and expanding such activities in the future and fostering collaborations between chemists, materials scientists, and professionals entrusted with the care of cultural heritage materials.

Introduction

Where do innovative ideas come from and how does a “movement” develop? What contributes to the transformation of science education for both the future professional and for the average citizen? The National Science Foundation (NSF) has struggled with these questions for decades and has willingly risked putting public monies on the line to support innovative efforts to improve science education from elementary school through college and beyond. NSF funding has also consistently provided needed research infrastructure to topnotch academic and public facilities around the country. Enhancing collaboration, whether in education or research, has been a top priority for all NSF funding programs. This chapter hopes to illustrate how the confluence of a number of NSF-sponsored events and programs has led to a valuable mindset and critical mass of players that can make a substantial impact on both education and research in the fields of cultural heritage materials, materials science, and science education.

Early Chemistry and Art Efforts

Conservators and others interested in the preservation, restoration and authentication of works of art, cultural materials, and historical artifacts share a 60-year tradition of organizations and publications dedicated to the study of art and artifacts. The International Institute for Conservation of Historic and Artistic Works (IIC), founded in 1950, provides research-based articles by conservators and conservation scientists worldwide in *Studies in Conservation*. The American Institute for Conservation of Historic and Artistic Works (AIC), founded in 1972, has grown to include over 3,500 members comprising conservators, educators, scientists, art historians, students, and other conservation enthusiasts organized into 10 specialty groups. The Foundation of the AIC (FAIC) has supported conservation education, research, and outreach activities that increase understanding of our global cultural heritage and since 2001 has created a strong professional development program for conservators that strives to support a range of educational programs, in order to elevate the status of conservation in the eyes of the public.

In the late 1970s to early 1980s there was little crossover between the average chemistry professor in academia and the world of conservation. However, a few notable pioneers began to venture into the world of artists' materials and archaeological artifacts and publish papers and books targeted to fellow chemists (1–8). In April of 1980, *The Journal of Chemical Education (JCE)* brought the topic of chemistry and art to a wider audience of educators when it published a special section on “Chemistry in Art” under the Secondary School Chemistry section (9). A year later “The Chemistry of Art — A Sequel” (10) appeared. The articles in these two issues, covering topics from the chemistry and physics of colors and colorants to the chemistry of ceramics, textiles, and metals used in art objects, were also published by JCE in two monographs. At about the same time, Sister Mary Virginia Orna developed a chemistry and art course for non-science majors at the College of New Rochelle and published a textbook designed to accompany the course (11). Also in the late 1980s several other publications appeared both in the US and abroad that were targeted to a broader audience than just the conservation community (12–18).

In the early 1990s, inspired by these publications and convinced that teaching chemistry to undergraduates, especially non-science majors, focusing on the chemistry of materials used in art would prove successful, one of the authors (Hill) and Michael Henchman, professor of chemistry at Brandeis University, independently developed and taught chemistry and art courses designed specifically for liberal arts students (19, 20). The courses were essentially materials science courses on the fabrication, examination, conservation, and authentication of artifacts. Twenty years later the demand for these courses remains high and a myriad of other courses has appeared in institutes of higher education across the country and around the world.

This 20-year period has witnessed a significant transformation in the use of chemistry and art in undergraduate education. What began as an interesting topic for high school teachers to engage students has ignited the development of a widespread community of college and university faculty working with museums, historical societies, archaeologists, and conservation scientists. A common goal of this community is to bring transformative education to undergraduates and engage students and faculty in authentic research with and service to those whose profession is to understand, protect and preserve cultural heritage materials. This chapter provides one perspective on how this movement developed, the role the NSF played, and what the future may hold.

Joining Forces To Ignite a Movement

In February 1995, the National Science Foundation and the US Department of Education held a joint conference, *Joining Forces: Spreading Successful Strategies*, in Washington, D.C. It was at this conference that Patricia Hill met Michael Henschman whose poster described the course he had developed using his NSF DUE grant #92-54291 “Developing a science course for non-scientists on the chemistry of art”. This course, additionally, teaches scientific literacy to undergraduates in the humanities. Everyone is familiar with art. By demonstrating how science can increase one’s understanding and appreciation of art, science is shown to play a unique role that cannot be ignored. Multi-media presentations of works of art illustrate the insights that science can bring to art. His project was one attempt to remedy the lack of suitable chemistry and art textbooks and usable scientific data for use in teaching by developing multimedia in-depth art conservation case studies and introduction of chemical microscopy laboratory activities.

One goal of the *Joining Forces* conference was to stimulate “scale up” of educational reform with the hope that participants would “return home with new insights and new energy to move the reform agenda ahead”. Several briefing papers, made available to conference participants, and conference sessions articulated the many challenges to implementing reform of traditional curricula or teaching approaches (21, 22). Undaunted by the formidable barriers to educational reform, Hill and Henschman quickly “joined forces” and in the summers of 1996 and 1997 jointly facilitated a 3-day short course on Chemistry and Art for the NSF-funded Chautauqua Program. Almost 50 college and university physical science faculty from across the country participated in these two short courses and it was due to the enthusiasm and interest of faculty in teaching across the disciplines of chemistry and art, that the following year Hill submitted and was awarded a Division of Undergraduate Education NSF grant (DUE-9752769) to continue to provide professional development around the theme of chemistry and art for college and high school teachers.

Chemistry and Art Professional Development Workshops

The project, *Undergraduate Faculty Workshop for the Integration of Chemistry and Art into Liberal Arts, Chemistry and Teacher Curricula*, funded four six-day intensive workshops for college, university, and high school teachers of both chemistry and art. The workshops, held at Millersville University of Pennsylvania during the summers of 1998-2000, brought together 75 educators to learn how to integrate the teaching of chemistry and art in the college and high school curriculum. From the very beginning, the philosophy of Hill and Henchman was to develop leadership among the workshop participants, inviting those participants who had incorporated lectures, assignments and lab activities into their teaching to return to subsequent workshops and act as “mentors” to new participants and “co-facilitators” for the workshop itself. By the end of the grant project in 2000, a small network of educators interested in integrating art and science topics into their teaching and curricula had begun, with one third of workshop participants developing and teaching courses specifically linking chemistry and art for either non-science majors at the college level, college chemistry, engineering or materials science students, or high school chemistry and physics students. Another third of participants utilized workshop materials and activities in the courses they regularly taught. Both workshop facilitators and participants began to actively disseminate ideas and workshop materials via established national conferences (American Chemical Society, Biennial Conference on Chemical Education, National Science Teachers Association, Geological Society of America) as well as through more regional and local outreach teacher education programs.

The Center for Workshops in the Chemical Sciences (CWCS)

As a result of dissemination efforts from the initial NSF-DUE grant, the workshop facilitators were contacted in 2001 by Dr. Jerry Smith of Georgia State University, to continue to offer a chemistry and art workshop for college chemistry faculty as part of an NSF Course, Curriculum, and Laboratory Improvement National Dissemination (CCLI-ND) project. The project titled *A Series of Workshops in the Chemical Sciences* (CCLI-ND# 0089417 and 0341138) established the Center for Workshops in the Chemical Sciences (CWCS) in 2001. From its inception, the CWCS program has thus far organized some 113 workshops on over 25 different chemical science topics. The Chemistry and Art workshop, one of the most popular and over enrolled, was first offered under the auspices of CWCS in the summer of 2002 at Millersville University. Since then, 11 introductory level chemistry and art workshops for college and university faculty have taken place, each accommodating 20 participants. In addition, an advanced workshop focusing on chemical analysis in the conservation of cultural heritage objects has been developed and offered twice to alumni of the introductory level workshop. A unique characteristic of chemistry and art

workshops is that they include five days of intensive learning, including extensive hands-on activities (lectures, laboratory work, computer activities, field trips, etc.). In addition, participants are provided with sets of tested curricular materials, books, articles, and supplies that can be immediately incorporated into their own instructional activities upon return to their home institutions. The aim of the workshop has been to: (i) augment and upgrade faculty expertise in the chemistry of artists' materials, art history, and conservation science methods and ethics; (ii) explore these topics in a pedagogical framework suitable for the implementation of workshop materials into the undergraduate curriculum for science and non-science majors; (iii) illustrate the integration of chemistry with other fields, exposing participants to new or emerging fields of applied research, and (iv) create networking opportunities for participants.

The popularity of these chemistry and art workshops can be gauged by the fact that they are chronically oversubscribed with long waiting lists. As of this writing, a critical mass of well over 300 educators, primarily chemists but with a smattering of physicists, geologists, biologists, mathematicians, conservators, and artists, have participated in one or more of these workshops. Workshop participants have actively used and adapted workshop materials in their teaching, developed undergraduate research projects which integrate chemistry and art, and developed innovative honors courses, first year courses, winter term courses or study abroad courses for their students. In addition numerous chemistry faculty have taken sabbatical leave opportunities to work with conservators and in museum laboratories to develop their knowledge and skills working with art objects and artifacts. Research activities of these educators and their students are appearing in well-known scholarly journals.

Towards a Community of Scholars

From detailed self-evaluation of CWCS workshops and follow up with workshop participants, it has become apparent that making major impacts on the quality of teaching and learning in science education requires a different approach than simply providing workshops. Although workshops provide faculty with valuable networking opportunities (23–25), exposure to new topics and skills (23, 26–29), and renewed dedication to maintaining high standards in the classroom (23, 27, 30), there are considerable challenges to engaging faculty members in professional development activities, especially those related to undergraduate instruction. It can be difficult for faculty members, especially those at community colleges and smaller 4-year institutions, to find the time, motivation and money to attend meetings and workshops (27, 31). Upon return to the home institution, workshop attendees can face numerous institutional barriers, including resistance to changes in the curriculum and lack of availability of load reduction to facilitate curriculum development (27, 31), as well as a sense of isolation if the faculty member is the only one from that institution to attend the workshop.

To begin to address some of these issues, the focus for CWCS workshops has shifted toward the formation of “communities of scholars” around workshop topics. NSF funding has been renewed for the project, now called *Chemistry Coalitions, Workshops, and Communities of Scholars (cCWCS)* (TUES Type 3 Project #1022899). Today the chemistry and art community of scholars is focused on fostering and sustaining collaboration, coalition and scholarly growth among educators, students, and conservation professionals by:

- Extending the membership in the community beyond those who have attended the chemistry and art workshop to include: faculty and students at universities, two- and four-year colleges; staff and educators in museums; conservators and conservation scientists; and members of other related professional organizations (e.g. AIC, IIC)
- Developing and sharing best research and education practices among a wide range of professionals and educators
- Equipping community members to become leaders who have impact beyond their own teaching or classrooms
- Providing resources to aid collaborative projects, proposal writing, networking and dissemination of activities to broad audiences.

The graphic presented in Figure 1 illustrates the evolution of the CWCS model from the traditional view of workshops on the left to the current cCWCS model of “community of scholars” on the right.

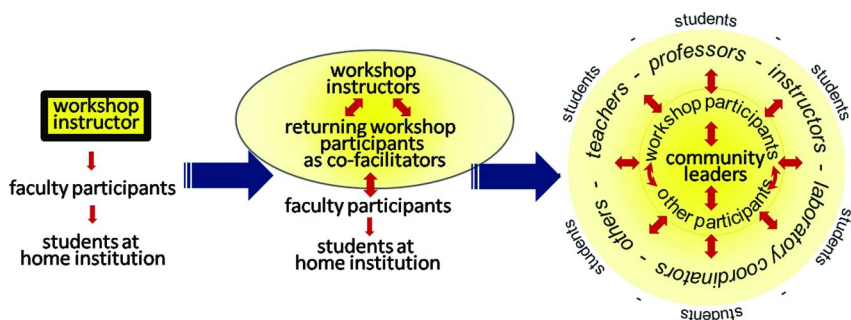


Figure 1. Evolution of community of scholars model. Courtesy of cCWCS.

The development of scholarly communities combines several components from the cyclic model for the relationship between knowledge production and improvement of practice in undergraduate Science, Technology, Engineering, and Mathematics (STEM) education. To develop self-sustaining communities – new ideas and products feed back into the communities in a variety of

ways – via subsequent workshops, collaborative research projects, web and videoconferences; the products are disseminated more broadly via a community website, at national symposia and through publication. The community grows in number through these activities and dissemination efforts, and in depth through evolving partnerships. The cycle repeats, with spin-off of new products and new opportunities for faculty and student development.

Recently, concerted efforts have focused on building a cadre of workshop alumni who present talks and co-facilitate half-day workshops at national and regional meetings such as the American Chemical Society (ACS), the Biennial Conference on Chemical Education (BCCE), the Pittsburgh Conference (PittCon) and the AIC conference, and who also serve as mentors to new workshop participants. cCWCS has supported the development of these faculty through partial travel grants to present their curricular innovations. Community members actively consult with and visit the home institutions of workshop alumni, speak with their classes, aid them in planning course activities, put them in touch with nationally and internationally known figures and resources, and write supporting documentation for faculty promotion and tenure reviews. In turn, workshop alumni have contributed exciting new ideas, laboratory activities, and course and curricular innovations to the workshop programs. The Advanced Chemistry and Art workshop relies on the expertise and creativity of workshop alumni to deliver high quality information and tested laboratory activities readily applicable to undergraduate teaching and research. The introductory chemistry and art workshop is now held at various home institutions of workshop alumni in order to make workshops more accessible nationally and build coalitions with various levels of institutions from 2-year community colleges to small liberal arts colleges to major universities.

Virtual Chemistry and Art Community

The most recent product of the chemistry and art scholarly community is the development of a website that will specifically meet the needs of community members. It will offer a repository of resources for content and pedagogy, online discussion boards, remote access to instrumentation, opportunities for collaborative projects, and a means of dissemination of research findings. It will be guided in design and implementation and maintained by a Leadership Council composed of interested community members. It will be highly interactive and will be continuously updated based upon the input and needs of the chemistry and art community. A collaboration between the Research and Technical Studies Group (RATS) of the AIC and cCWCS Chemistry and Art Leadership Council will provide an interactive map, accessible to registered website users, designed to match conservators and museum staff in need of technical assistance with chemists having interest and appropriate research skills and/or instrumentation. This website is nearing completion and will be launched in the spring of 2012 (32). The banner for the website is shown in Figure 2.

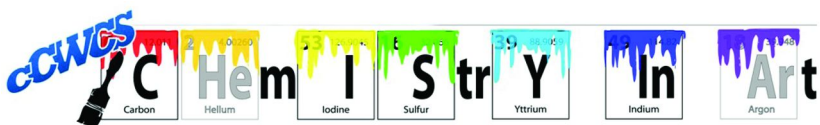


Figure 2. Web banner and logo for cCWCS Chemistry and Art Virtual Community. Designed by Jessica Gerlach. Courtesy of cCWCS.

Impact on Undergraduate Teaching and Personal Career

The effectiveness of this multi-pronged model can be illustrated by the impact on one participant's career in the years since attending one of the weeklong CWCS workshops in 2004. The participant, an instructor at a small liberal arts college, enrolled with the goal of finding a few additional topics for her general chemistry laboratory courses. After completing the intensive workshop, however, the scope of possibilities was significantly expanded, and work began on implementing a full course at her home institution. The validation provided by the workshop's NSF imprimatur proved crucial in shepherding the idea through the administrative process. A semester-long non-science majors chemistry of art class was implemented in the fall of 2007.

The strength of the cCWCS community of scholars approach is the enveloping support offered by the community. Unlike the typical post-workshop atmosphere of isolation and uncertainty, participants leave with a concrete, easily accessed support system in place. Ample classroom materials and, more importantly, the practical expertise and encouragement of seasoned colleagues are readily available. This expertise was called on repeatedly and was crucial to the success of the course.

The course proved to be very popular (enrolled to the maximum, with an extensive waiting list), and students from the general chemistry classes began clamoring for access to the same topics. In response, more than half of the laboratory experiences in the general chemistry class were changed to chemistry of art topics. In all instances, the rigor of the assignments was maintained, and, in several instances, increased. This change of focus has had an impact on nearly 200 students every semester. Lasting student engagement in these real-world topics is reflected not only in positive evaluations, but also in unsolicited emails from alumni, both non-science majors and chemistry majors, several years after the class.

Unlike the traditional trajectory of professional development where the effect is linear, short-lived and single-peaked, this topic engenders a nonlinear, branched effect that affects every aspect of one's professional life. The results are invaluable in career advancement, and invigorating in personal satisfaction and growth. In addition to the transformation of the classroom, the instructor has become a co-facilitator of the cCWCS workshops, hosting two at her home institution, and is an active presenter on the chemistry of art at regional and national conferences.

Coming full circle, she is an active member of the very group that supported her early efforts, providing immediate and ongoing expertise to those who are themselves in the early stages of implementation.

One of the most rewarding aspects of belonging to this community of scholars is the opportunity for collaborations between chemists and practicing artists. As word spread about the chemistry of art class, local artists began to inquire about technical issues. Rather than analyzing existing pieces of art, the intersection of chemistry and art has taken place during, or before, the creation of the artwork. Current projects include a collaboration between the instructor and an artist on glass fusing and etching techniques, a jewelry artist on an issue with metal casting alloys and sculpture investment degassing, and the city council on the implementation of a large-scale glass recycling project that would involve the creation of art from waste glass.

These intersections of chemistry and art are far from being confined to individuals who reside in proximity to large museums and research institutions. The nature of the community of scholars is such that an interested colleague is always available. And the broad range of areas of expertise means that nearly any potential problem is met with enthusiastic ideas for collaboration and exploration that enrich everyone involved.

NSF Research Funding in Cultural Heritage Science

In 2009, NSF and the Andrew W. Mellon Foundation co-sponsored a workshop “to explore the basic scientific questions relating to cultural heritage materials; define priorities for research; frame promising research initiatives that can be implemented in the near and long term; and enhance cross-disciplinary collaborations among scientists in cultural heritage institutions and their peers in academic, national, and industrial laboratories” (33, 34). The workshop and its report (35), resulted in a new NSF program, *Chemistry and Materials Research in Cultural Heritage Science (CHS)*, which solicits collaborative 3-year proposals in chemistry and materials science among researchers in US museums and academic institutions that aim to address grand challenges in the field of science of cultural heritage. The program strongly encourages the formation of new collaborations and requires that the proposed projects also involve undergraduate students, graduate students and postdoctoral research associates. The program also encourages the development and use of cyber infrastructure to increase the level of synergy of the proposed projects.

This new initiative and the interest developed among noted conservation researchers, chemists, and materials scientists such as Marco Leona at the Metropolitan Museum of Art, Paul Whitmore of the Conservation Research Center of Carnegie Mellon University, and Janice Carlson of the Winterthur Museum, and many others involved in the planning and review of the NSF-Mellon workshop are the result of the synergy between efforts on many fronts. This chapter has attempted to describe some of the factors which have led to today’s interest in the establishment of firm collaborations among scientists, educators, and professionals entrusted with the care of cultural heritage materials.

Conclusions

When the NSF-Mellon Foundation workshop took place in 2009, several members of the organizing committee, contributing authors, and reviewers were aware of, had worked with, or were themselves participants in the chemistry and art workshops sponsored by NSF. In fact a white paper report by Whitmore (35) cited not only Henchman's and Hill's courses and NSF grants but also the CWCS chemistry and art workshop series. The paper went on to state that: "As a result of these efforts, courses on Art and Chemistry are being introduced in colleges and universities across the country, demonstrating the general interest and appeal the field of conservation has for students, and the possibility of engaging students who might not otherwise study scientific subjects". Several chapter authors of this ACS book have also been participants and/or facilitators in cCWCS chemistry and art workshops. Their commitment to research, education, and professional development of themselves and their colleagues, along with similar commitment of many other educators, scientists, and conservators across the country, is a driving force that will foster and sustain this growing chemistry and art community for years to come.

References

1. Orna, M. V. *J. Chem. Educ.* **1978**, *55*, 478.
2. Orna, M. V. *Color Res. Appl.* **1978** (Winter), *3*, 189.
3. Orna, M. V. *J. Chem. Educ.* **1980**, *57*, 256–67.
4. Orna, M. V.; Low, M. J. D.; Baer, N. S. *Stud. Conserv.* **1980**, *25*, 53.
5. Orna, M. V.; Mathews, T. F. *Stud. Conserv.* **1981**, *26*, 57.
6. Orna, M. V. *Today's Chemist* **1991**, *4* (6), 20–24.
7. *Archaeological Chemistry III*; Lambert, J. B., Ed; American Chemical Society: Washington, DC, 1984.
8. Brill, T. B. *Light, Its Interaction with Art and Antiquities*; Plenum Press: New York, 1980.
9. The Chemistry of Art. *J. Chem. Educ.* **1980**, *57*, 255–282.
10. The Chemistry of Art — A Sequel. *J. Chem. Educ.* **1980**, *58*, 290–330.
11. Orna, M. V.; Goodstein, M. P. *Chemistry and Artists' Colors*, 3rd ed.; Spaulding Press: Wallingford, CT, 1990.
12. Greenberg, B. *J. Chem. Educ.* **1988**, *65*, 148–150.
13. Bomford, D.; Kirby, J.; Leighton, J.; Roy, A. *Art in the Making: Impressionism*; National Gallery (London) Publications Limited: London, 1990.
14. Bomford, D.; Brown, C.; Roy, A. *Art in the Making: Rembrandt*; National Gallery (London) Publications Limited: London, 1991.
15. Salters Advanced Chemistry Course, <http://www.york.ac.uk/org/seg/salters/chemistry/index.html> (accessed March 1, 2012).
16. Bull, D.; Plesters, J. *The Feast of the Gods: Conservation, Examination, and Interpretation, Studies in the History of Art*; University Press of New England: Hanover, 1990.

17. Mills, J. S.; White, R. *The Organic Chemistry of Museum Objects*; Butterworth-Heinemann: Oxford, 1987.
18. Shulman, K. *Anatomy of a Restoration: The Brancacci Chapel*; Walker & Company: New York, 1991.
19. Henchman, M. *J. Chem. Educ.* **1994**, *71*, 670.
20. Hill, P. S. *Book of Abstracts*; 14th Biennial Conference on Chemical Education, Clemson University, Clemson, SC, August 4-8, 1996; W-AM-SY-N-4.
21. Klein, S. P.; McArthur, D. J.; Stecher, B. M. In *Joining Forces: Spreading Successful Strategies*; National Science Foundation and U.S. Department of Education Invitational Conference, Washington, DC, February 23-25, 1995.
22. Millar, S. B. In *Joining Forces: Spreading Successful Strategies Conference*; National Science Foundation and U.S. Department of Education Invitational Conference, Washington, DC, February 23-25, 1995.
23. Frick, L.; Kapp, C. *Teach. Learn. Forum* **2006**, 1–13.
24. Aiken, R.; Ingargiola, G.; Wilson, J.; Kumar, D.; Thomas, R. *SIGCSE Bull.* **1996**, *28*, 3–7.
25. Bland, C. J.; Risbey, K. R. *Eff. Pract. Acad. Leaders* **2006**, *1*, 1–15.
26. Latchem, C.; Odabasi, F. H.; Kabakci, I. *Turk. Online J. Ed. Technol.* **2006**, *5*, 20–26.
27. Marder, C.; McCullough, J.; Perakis, S. *SRI Int.* **2001**, 141.
28. Centra, J. A. *J. Higher Ed.* **1978**, *49*, 151–162.
29. Kreber, C.; Brook, P. *Int. J. Acad. Dev.* **2001**, *6*, 96–108.
30. Fahrenholtz, W. G.; Bieniek, R. J.; Graham, S. W. “Multi-Campus New Faculty Development to Improve the Culture of Teaching,” *Proceedings of the American Society of Engineering Education Annual Conference*, Nashville, TN, June 22-25, 2003.
31. Moeini, H. *Proceedings of World Conference on Educational Multimedia, Hypermedia and Telecommunications*; AACE: Chesapeake, VA, 2007; pp 2418–2425.
32. cCWCS Chemistry in Art Community of Scholars, www.chemistryinart.org.
33. Chemistry and Materials Research at the Interface between Science and Art. A jointly sponsored workshop between The National Science Foundation and The Andrew W. Mellon Foundation, July 6-7, 2009, <http://mac.mellon.org/NSF-MellonWorkshop> (accessed March 1, 2012).
34. Program Guidelines: Chemistry and Materials Research in Cultural Heritage Science(CHS), http://www.nsf.gov/funding/pgm_summ.jsp?pims_id=503478 (accessed March 1, 2012).
35. Whitmore, P. M. *Conservation Science Research: Activities, Needs, and Funding Opportunities, A Report to the National Science Foundation*, July 26, 2005, [http://mac.mellon.org/NSF-MellonWorkshop/Whitmore White paper.pdf](http://mac.mellon.org/NSF-MellonWorkshop/Whitmore%20White%20paper.pdf) (accessed March 1, 2012).

Chapter 14

The Chemistry of Artists' Pigments: An Immersive Learning Course

Patricia L. Lang*

Department of Chemistry, Ball State University,
2000 West University Avenue, Muncie, IN 47306

*E-mail: plang@bsu.edu

A course was designed to bridge the interface of art and science by helping students develop an understanding of light and the color of objects, the structural features of pigment molecules, the preparation, types, and properties of classical and medieval artists' pigments used on manuscripts, paintings, and other artifacts, and the use of the modern analytical instrumentation used to study the chemical composition of art materials. Students experienced an immersive learning experience as they applied their knowledge to the analysis of paints on a late 15th c. polychrome wood sculpture *Male Saint* housed in the David Owsley Museum of Art at Ball State University.

Introduction

Art majors and chemistry majors in the same chemistry course? Equal numbers of students were brought together in the spring of 2009, when "The Chemistry of Artists' Pigments" was taught by the author. The planned student learning outcomes centered on understanding the basic scientific concepts of the nature of light and color, what structural features of a compound are needed to make it colored, the types of compounds that were used by the ancients and by medieval artists, and the theory and operation of modern analytical instrumentation used to determine the composition of paints. Yet learning the theory of artists' colors was only a means to get to the course objective -- which was to have the students *experience* the analytical work that a conservation scientist might perform. The class would undertake an examination of the paint materials on a late Gothic, early Renaissance polychrome wood sculpture called

Male Saint, 2007.004.002, housed in the David Owsley Museum of Art at Ball State University. Further, students would communicate their findings both orally and in writing to professionals in the art and science community.

Male Saint, a 1450 German sculpture from the circle of Hans Multscher discussed more thoroughly elsewhere (1), was chosen because the author has some expertise in the infrared spectroscopy of medieval pigments and because this period has some of the most chemically interesting pigments used by artists. Few other periods were known to use reds extracted from beetles (2, 3). Further, the museum director was interested in knowing if the sculpture had been repainted, and, if so, in what areas, in order to consider and plan future conservation measures.

At Ball State University, a cross-disciplinary, collaborative student project (art and chemistry majors), having a community partner (David Owsley Museum of Art) with outcomes that impact this partner, and with a tangible product (a report, presentation, and published manuscript) are critical elements of an immersive learning course. The students' experience allowed them to apply the scientific method to answer the question, "What are the paints and pigments used on *Male Saint*?" In completing the course, the students truly had a valuable immersive experience that affected how they each thought about their discipline.

Progression of Chemistry Topics

It is often difficult to imagine how one can bring a varied group of students along to the "same place" intellectually in such a short time, given the comprehensive and cumulative nature of chemistry. In order to achieve the goals above in a 15-week course with senior chemistry students side-by-side with those with only minimum science backgrounds, a very focused coverage of topics were chosen.

Since the students would be using spectroscopic methods, understanding how light interacts with matter was a primary goal. Consequently, the first material introduced was the concepts of light as wave and particle, its characteristic frequency, wavelength, and velocity, and the electromagnetic spectrum. In terms of understanding matter, the components of the atom are essential introductory material, along with atomic energy states and how light can be absorbed or emitted to effect transitions. The simplest form of spectroscopy was then introduced, and the theory of how to interpret spectral curves and how a spectrometer worked was taught. Students made Prussian blue and a tempura paint in the lab and then obtained visible spectral curves of their product and the potassium ferrocyanide reactant. The above topics were covered in the first exam.

The lecture material for the next exam included the concepts of chemical symbols and formulas with an emphasis on inorganic compounds, since many pigments are minerals. Each class member was assigned five pigments used in medieval art, and as homework students looked up historical information about the pigment and their properties. During class the students organized the pigments into a table according to color that included name, chemical formula, source (animal, vegetable, or mineral), and use. This table was to serve as an

important resource for the class when the analysis of the sculpture began. The topics of atomic orbitals, electronic configuration, and covalent and ionic bonding were included in this exam along with conjugation in organic compounds, simple molecular orbital theory, charge-transfer theory, and crystal splitting. Additionally, the class was introduced to limewood sculpture and the materials used in its production (4).

The last formal lecture topics covered included the basic theory and operation of the infrared spectrometer and the scanning electron microscope with energy dispersive x-ray (SEM/EDS) detection. Instead of including this topic in exam material, the students were expected to summarize how the instruments worked in their final presentation and written report.

Details of Course Structure and Delivery

The syllabus outline is shown in Table I. The chapters listed are those found in the text by Orna and Goodstein (5). The first seven weeks of the course was more theory-heavy as preparation for the analysis of *Male Saint*. When possible, hands-on activities (shaded in the table) were included to help solidify and apply chemical principles (6). The class was scheduled as two weekly meetings of 90 minutes each to allow for lab activities which were held in an organic or instrumentation laboratory. Also, in-class worksheets were completed at the end of most lectures. Chemistry and art students were paired in both activities, so that the more chemically experienced could assist the less experienced. Nonetheless, during this period of the course, traditional lecture methods were used in a standard classroom setting. Under supervision of the instructor, the students collected samples from *Male Saint* (See Figure 1) in Week 4 of the course. They met the Director of the David Owsley Museum of Art, Mr. Peter F. Blume, who provided background on the piece and who arranged for a viewing of the sculpture under ultra-violet light. Students photographed all sampled areas of the sculpture and kept records in their lab notebooks.

From Weeks 8-12 there were only five formal classroom meetings, two which included a lecture on infrared theory and instrumentation, and a lecture on scanning electron microscopy and energy dispersive x-ray spectroscopy. The remaining three formal class meetings were teleconference presentations from experts in the field, two lectures from Professor of Chemistry and Scientist-in-Residence, Dr. Mary Virginia Orna at the College of New Rochelle, and one from Senior Conservation Scientist, Dr. Beth Price from the Philadelphia Museum of Art. Three additional field trips were scheduled, one to a nearby analytical lab for SEM/EDS analysis, one to the geology department for microscopic examination consultation, and one for additional sampling from the sculpture.

During the rest of the scheduled class time, the students worked on the pigment analysis performed in the author's research space and/or in the instrumentation lab. Students collected infrared spectral data and found and examined reference data. They each learned how to operate the infrared spectrometer, to make infrared assignments, and to make spectral comparisons. Using the table they constructed in class summarizing the types and formulas

of medieval pigments and chemical composition, they learned what absorptions would be associated with particular functional groups found in the paint materials. Although the details of the experiments are provided in a different publication (1), a key feature was the use of the universal attenuated total reflectance accessory with a diamond element on an infrared spectrometer. The instrumentation was sensitive, easy-to-use, and provided the student with selective, molecular information.



Figure 1. Students assist in collection of samples from Male Saint. (see color insert)

In Week 13, students started on the Power Point presentation of their scientific findings. The class was held in a computer laboratory designed for teamwork, where each chemist/artist pair was assigned a particular section of the presentation to construct. One team was assigned to format and compile the sections, and another team volunteered to be the presenters. During the last week of class, students presented their work to Dr. Orna (who travelled from New York to hear the presentation), Mr. Blume, the class, and members of the Department of Chemistry.

The final exam was submission of a written report that could be given to the Museum Director and that could be converted to a manuscript at a later date. The class fulfilled this task by converting their presentation into a scientific document format.

Table I. Outline of Class Lecture Topics and Activities (bold)

<i>Week</i>	<i>Lecture Topic/Activity</i>
1	Light and EM spectrum- Chapter 1 (5)
	Inside the atom-Chapter 7 (5)
2	Experiment 1: Synthesis of Prussian blue and tempura (6)
	Reflection, transmission, absorption -Chapter 9 (5)
3	Spectral curves, the spectrometer -Chapter 10 (5)
	Experiment 2: Visible spectra of Prussian blue and $KFe(CN)_3$ (6)
4	Exam 1: 100 pt. short answer, essay, matching
	Collection of samples from <i>Male Saint</i>
5	Chemistry shorthand - symbols, formulas -Chapter 13 (5)
	Medieval artists' pigments -Chapter 18 (5)
6	IR data collection on <i>Male Saint</i> samples
	Electronic configuration, bonding-Chapter 15 and 16 (5)
7	Limewood, gesso, binders (4)
	Exam 2: 100 pt. short answer, essay, matching
8	IR spectroscopy theory and instrumentation, Handouts
	IR data collection on <i>Male Saint</i> samples
9	Teleconference: Chemical Analysis of Ancient and Medieval Art, I
	IR data collection on <i>Male Saint</i> samples
10	Electron microscope/ EDS instrumentation, Handouts
	IR data collection on <i>Male Saint</i> samples/data interpretation
11	Teleconference: Chemical Analysis of Ancient and Medieval Art, II
	IR data collection on <i>Male Saint</i> samples/data interpretation
12	Field trip to SEM/EDS instrument
	IR data collection on <i>Male Saint</i> samples/data interpretation
13	Teleconference: Chemical Analysis in the Conservation of Art
	Data interpretation/Preparation of presentation
14	Preparation of presentation
	Preparation of presentation
15	Presentation to Dr. Orna, Mr. Blume, and chemistry department
	Preparation of written report

The final grade was determined by attendance and in-class activities (43%), exams (43%), and the student presentation and written report (14%). The presentation and written report was given less weight because it was a class project, rather than an individual or small team project. The in-class activities were graded individually or in a team of two.

Student Learning Outcomes

The average exam score for the art majors was 80% versus 89% for the chemistry majors. Given the nature of the material, these results are neither surprising nor disappointing. They indicate that students with minimum chemistry background can do well in the course. A larger percentage of the grade could have been awarded to the report and presentation since those assignments were a major part of the course in terms of time spent. However, students took this assignment very seriously, probably because an expert art analyst flew 1600 miles round-trip just to listen to the class presentation. Thus, it was observation of the instructor that each class member had a personal stake in ensuring that the quality of the presentation was high, and that its scientific content was sound. Since the report was submitted to the art museum and to be used as a template for a future publication, students invested in that activity as well.

As indicated previously, an art major was always paired with a chemistry major during non-lecture activities. My observations were that the students shared their knowledge and gained a richer experience because of it; all students “bought into” the mission of discovery, and they were excited, determined, and conscientious about their analysis. The art major learned how to present a scientific paper as well as to write one, and while the chemistry student had previous experience with experimental reports, the practical applications of applying chemistry to art analysis was very novel to them. Further, chemistry students had not thought about color in the same way as they were required to in this course, and many had never thought about the composition of paints. What each student got out of the course was a way to view their discipline and skills in a different light.

Those familiar with the pedagogy of service-learning (7–9) can recognize the positive student outcomes described above. In the same way, the analysis of *Male Saint* provided the students with a genuine task and an authentic audience, and from my observations the activity increased their motivation and confidence to learn and apply chemical principles (7).

How Can an Immersive Learning Course Fit into the Curriculum?

The author had tremendous flexibility in developing the course, since it was a “dream course” that she was invited to teach. Consequently, it was not bound by course enrollment minimums (this class had only six students) or curriculum constraints, and it had a small budget associated with it that allowed for travel and course materials. However, an immersive learning course described above

could regularly be incorporated into a department's core curriculum or offered as an elective for a larger group. In fact, Professor Uffelman at Washington and Lee University has used a very similar approach to "teaching science in art" since 1998 (10) and provides a fairly comprehensive list of resources.

The essential factors to consider for implantation of an immersive learning course in art or cultural heritage object analysis are:

- The size of the class
- The availability and nature of the art work or object(s)
- The availability of the instrumentation or technique
- The expertise of the faculty member
- The background of the students
- The tangible product

First, in order to adapt this immersive learning course to a larger section of 20 students, the management of the second half of the course would be altered. One could limit the size of the group that is performing the instrumental analysis to a team of four; then using a teaching assistant, one could have the remaining students (the 16 left) begin work on their presentation and written report starting at week 7, while a smaller group of 4 goes to the instrument for data collection. Five teams of 4 students should be able to participate in least two sessions on the instrument used for analysis. The presentation and report that the students produce may have more background information and fewer analytical results, and, obviously, the larger the class, the less immersive the experience.

Secondly, a partner who needs and wants the analysis has to be identified. University art museums, and/or archaeology, chemistry and anthropology departments are excellent resources to find collaborators. Although one does not have to think locally, it is a good place to start.

Next, although the attenuated total reflectance infrared spectroscopy provided the key to getting complex results in this study quickly, the author would urge the faculty to find a project that capitalizes on the instructor's expertise and uses instrumentation that yields meaningful data for the analysis of the object under study. X-ray fluorescence and X-ray radiography are techniques used effectively in interdisciplinary courses (10). Additionally, polarizing light microscopic analysis could be the sole technique used, and it can allow for the identification of many pigments (11), given the experience and training of the instructor. Microscopic techniques also have the advantage of being able to be taught to a relatively large number of students if one has access to a standard microscopy lab found in geology departments.

How would the course change if taught to all chemistry majors? My sense would be to keep the same course content but only increase the level of difficulty required from the student. For instructors interested in introducing art and science to larger numbers of primarily non-majors, the reader is referred to the chapters in this monograph by Gaquere-Parker and Parker who share valuable insights from chemistry of art courses they have taught and by Hill who elaborates on her twenty years of practice in integrating chemistry and art.

The class presentation and report “products” which can be viewed at https://ilocker.bsu.edu/users/plang/WORLD_SHARED/ were not typical of those required in introductory chemistry courses, as the level of scientific language, scientific format, and scientific accuracy were expected to be on the level of a beginning master’s student. In fact, the presentation was at a high enough quality that the author had only to adapt it minimally to present at the Art in Chemistry Symposium at the 42nd Meeting of the American Chemistry Central Region in the summer 2011. The students’ report was relatively easy to convert into a manuscript which is also published in this monograph (*I*). The class members serve as co-authors because each contributed significantly to the results.

The author encourages teachers to look for opportunities to offer immersive experiences in their curriculum, as it allows the student to experience the learning, the process of discovery, and the collaboration that scientists who work in the art and archaeology fields experience.

Acknowledgments



Figure 2. The 2009 Chemistry of Artists’ Pigments Class.

The author would like to gratefully acknowledge the Ball State University Office of the Provost for funding this course. She would also like to thank Mr. Peter F. Blume, Director of the David Owsley Museum at Ball State, the BSU Teleplex for their assistance in teleconferencing, Dr. Mary Virginia Orna and Dr.

Beth Price for their valuable time and expertise, Michael Kutis, BSU Geology Technician for assistance in microscopic analysis, and Mr. Robert Galyen, formerly of TAWAS, Inc. for SEM/EDS sampling.

The author would also like to thank the class members, R. Carey, M. Coffey, R. Hamilton (The Artists) and A. Klein, S. Leary, and R. Short (The Chemists) in Figure 2, who made this one of the most enjoyable courses she has ever taught.

References

1. Lang, P. L.; Leary, S. P.; Carey, R. F.; Coffey, M. N.; Hamilton, R. E.; Klein, A. N.; Short, R. T.; Kovac, P. A. The Spectroscopic Analysis of Paints Removed from a Polychrome Wood Sculpture of *Male Saint*. In *Collaborative Endeavors in the Chemical Analysis of Art and Cultural Heritage Materials*; Lang, P. L., Armitage, R. A., Eds.; ACS Symposium Series 1103; American Chemical Society: Washington, DC, 2012; Chapter 17.
2. Lang, P. L.; Orna, M. V.; Richwine, L. J.; Mathews, T. F.; Nelson, R. S. *Microchem. J.* **1992**, *46*, 234–248.
3. Lang, P. L.; Keifer, C. D.; Juenemann, J. C.; Tran, K. V.; Peters, S. M.; Huth, N. M.; Joyaux, A. G. *Microchem. J.* **2003**, *74*, 33–46.
4. Baxandall, M. *The Limewood Sculptors of Renaissance Germany*; Yale University Press: New Haven, CT, 1980.
5. Orna, M. V.; Goodstein, M. P. *Chemistry and Artists' Colors*, 2nd ed.; ChemSource, Inc.: New Rochelle, NY, 1998.
6. Sagarin, K. L. <http://www.elmhurst.edu/~ksagarin/color/lab3-F10.pdf> (accessed Feb. 19, 2012.)
7. Esson, J. M.; Stevens-Truss, R.; Thomas, A. *J. Chem. Ed.* **2005**, *82* (8), 1168–1173.
8. Kesner, L.; Eyring, E. M. *J. Chem. Ed.* **1999**, *76* (7), 920–923.
9. Draper, A. J. *J. Chem. Ed.* **2004**, *81* (2), 221–224.
10. Uffelman, E. S. *J. Chem. Ed.* **2007**, *84* (10), 1617–1624.
11. McCrone, W. C. *J. IIC-CG* **1981**, *7* (1-2), 11–34.

Chapter 15

Bridging the Gap of Art and Chemistry at the Introductory Level

Anne Gaquere-Parker^{*,1} and Cass D. Parker²

¹Chemistry Department, University of West Georgia, 1601 Maple Street,
Carrollton, GA 30118

²Chemistry Department, Clark Atlanta University, 223 J.P. Brawley Drive,
Atlanta, GA 30314

*E-mail: agaquere@westga.edu

In institutions where non-science majors are required to enroll in a science course, especially chemistry, it may be difficult to capture their attention and keep them interested in the topic. A number of different approaches have been used to capture their attention and to achieve this goal. For instance topics such as forensics, food chemistry or green chemistry have been used as the descriptive title to bring students into the classroom and provide the vital connection of chemistry content. The authors attended an NSF-sponsored CWCS workshop in 2006, led by Drs. Patricia Hill and Michael Henchman which provided resources to teach a chemistry course for non-science majors with the emphasis in art as the attractor and the chemistry content connection. Based on the general content from the workshop and an expansion of the topic matter a non-science majors course has been created and taught at the University of West Georgia ever since. This paper provides an overview of the topics and some of the contents covered in the Chemistry of Art course at the University of West Georgia.

Background

Creativity is a fundamental precept of art and science! Yet, for a number of people they are viewed and promoted incongruously with no commonality. However creativity in art has led artists to seek out the same in science to add

to their palette colors and materials that will sustain and capture that creativity. Chemistry of Art is an introductory course that links that creativity of colors and materials to the basic chemistry behind it. As opposed to the traditional approach, this course shows that chemistry is intricately linked to art and in some cases the ultimate basis for what we enjoy in an artist's works.

Discussion

The background of students in chemistry for non-science majors' course is usually very diverse; it ranges from students who had many science courses in high school, including AP chemistry sometimes to students who only had a general physical or biological science course. The class size ranging from 25 students during the summer semester up to 75 during the fall semester as well as the disparity in the students' prior knowledge are true issues and they make it difficult to keep all of them interested at the same time. One solution to the latter problem is to broach topics in a nontraditional approach opposed to the traditional taught in high school. The authors thus chose to cover specific topics among the large variety available for such a course. However, with the increasing number of articles, presentations and symposia on the topics of art and chemistry an instructor can tailor a course according to their audience (1, 2).

Elements, Properties, and Bohr's Atomic Model

In Chemistry of Art the topic of elements and their properties are introduced from the standpoint of materials used in the production of an art piece. A description of the elements found in the periodic table can be linked to the elements found in jewelry, pigments and alloys and why they were chosen because of those properties. Copper is present in metallic alloys such as bronze and brass and also in green and blue pigments such as malachite and azurite. In some cases a historical event or archeological find is used in the introduction. For instance, mercury is present in the red pigment called vermilion widely present in the frescos found in Pompeii, Italy. Discussing the fate of Pompeii is always of great interest to all students regardless of their personal background or chosen field and it keeps them engaged in the course. When one considers the large variety of pigments available in the artist's palette, one quickly finds an ample source that allows the instructor to introduce and discuss chemical formulas, ionic and covalent bonds, oxidation states and nomenclature of common polyatomic anions. When discussing Bohr's atomic model the traditional flame test experiment can be described in testing for metals present in a material, as shown in Figure 1. Naturally, students are informed that this kind of destructive test is not used for the identification of artistic or historical objects.



Figure 1. Flame test.

However a more unusual example linking color and metallic ions can be seen in stained glasses. The Sainte Chapelle built in Paris 1245, shown in Figure 2 or the work of Chagall in the Cathedral of Chartres can be used as examples to introduce the topic of metal ions, electronic structure, electron transition and electromagnetic radiation absorption to give rise to colors. The understanding of materials and their electronic properties gives students a link to the importance of chemistry in producing stained glasses and the research required to manipulate the chemistry to produce them.

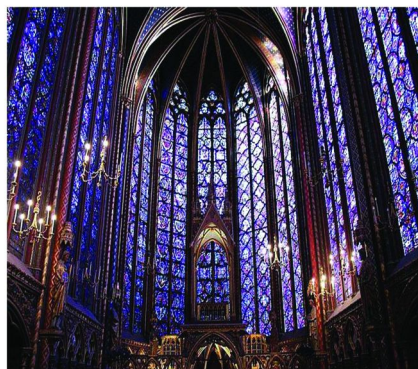


Figure 2. Stained glass, Sainte Chapelle, Paris, France.

Acids and Bases Chemistry

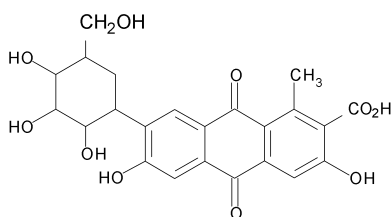
Another important topic covered in a chemistry course is the one related to acids and bases. Of course, color indicators are a classic example that can be used to introduce the topic in addition to more unusual examples such as the action of acids on metals, the destruction and preservation of statues and paper or the nature of acidic and basic organic dyes that have been used in the production of masterpieces of art. The introduction of dyes as opposed to pigments allows students to separate organic and inorganic chemistry into distinct

fields of chemistry. The various acid or base functional groups found in dyes can begin the discussion of organic materials and their chemical properties, color and permanence. The study of dyes provide students a perspective of how an understanding of chemical behavior and structure over time led to a much more diverse range of colors used by an artist. Student are made aware that many dyes were first produced without any thought about their chemical structure.

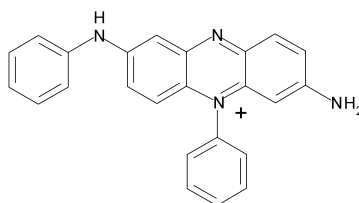
Organic Chemistry

As organic and inorganic chemistry has been introduced to students through the topic of acids and bases additional selected topics in organic chemistry are also taught in this course for non science majors. The subject matter of organic chemistry puts every student on the same level since it is very rare any incoming freshman has had any organic chemistry prior to taking this course. In addition to the acid and base functional groups, additional organic chemical groups can be described in a simple manner. Details about geometry and hybridization of the atoms are not necessary in such an introductory course. The primary goal is to introduce students to what functional groups are present in common materials to the artist or non-artist palette and uses. Acetone, ethyl acetate, and terpene derivatives to cite only a few examples are described since they are commonly found in the painter's studio as paint removers or thinners.

Dyes, used in the manufacture of the organic colorants for the artist's palette, also can serve as a great source for teaching organic functional groups. Historically they have been extracted from plants, like the red obtained from the madder root or from bugs such as the red from the cochineal bug, as shown in Figure 3.a. Dyes are also synthesized in the chemistry laboratory, like the famous historical landmark: the mauveine dye, as shown in Figure 3.b.



3.a. Cochineal dye



3.b. Mauveine

Figure 3. Molecular structure of organic dyes: (a) cochineal red and (b) mauveine.

Perkins' synthesis of mauveine leads to a discussion on the history of organic chemistry, which includes Wohler's urea synthesis and its significance for organic chemists. The description of organic dyes also includes a discussion

on chromophore and auxochrome groups. Students in this course are also taught an introduction to spectroscopy as described later in this chapter. UV-vis spectroscopy is used to show the effect of acids, bases, oxidizers and reducing agents on dyes and how that chemical change impacts the structure resulting in a change in the absorption spectra and ultimately to their observations of the material (3).

Carbohydrate and protein chemistry are also introduced in this course. Encaustics are produced using beeswax as a binder which may also contain residual sugars and honey. This discussion brings to bear the importance of understanding the functional groups contained in carbohydrates and so the structures of mono, disaccharides and polysaccharides are studied. In addition, the chemical composition of cellulose is provided to aid the discussion on wooden sculptures and cotton canvasses and textiles. Some knowledge of protein chemistry is also provided since ancient glues were prepared from animal hides. We introduce students to the use of milk as a reported paint binder and textiles made from silk that have been used as art supports. In addition to natural polymers being described as significant aspect and contributor to art as described in this course, synthetic ones are also introduced. Indeed modern paintings may use acrylic-based paint and modern sculptures may contain plastic materials. The introduction to plastics is also used to show the difference between thermoset and thermoplastic polymers, their uses and preparation.

The last major family of biomolecules covered in the course is the lipid family. Lipid binders are the most widely used. We begin with the use of animal fats used in cave paintings, beeswax, as mentioned earlier, used in Egyptian and Greek encaustics, egg tempera as the preferred media for painting up to the 15th century and finally drying oils. Examples of each media are included in the introduction followed by a chemical description of saturated and unsaturated fatty acids and their properties to explain the difference between drying and non-drying oils to the students such that the oxidation process that occurs when oil paints dry can be shown.

Spectroscopy

The topics described above represent two thirds of the material presented to the students during this one-semester introductory course. The remaining third of the course is dedicated to spectroscopy. Now that the students have a background in chemistry related to the different classes of materials that can be found in a piece of artwork, ranging from metals to wood to egg and milk, they are prepared to learn about the technical analysis of works of art. UV- vis spectroscopy is presented which provides a review of auxochrome and chromophore groups. This also leads to a student understanding of how colors are viewed differently. Students are presented with information that shows the variations in the spectra due to the modification of chemical structure as the result of pH or dilution effects, as shown in Figure 4.

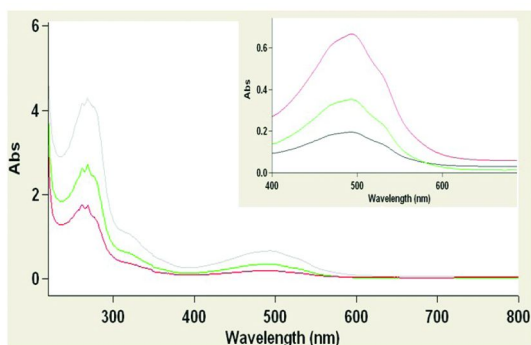


Figure 4. UV-vis spectra showing the effect of dilution on the cochineal red dye.

The use of dating techniques such as carbon dating provides a review on isotopes and atomic structure. A broader discussion on balancing nuclear equations, radioactivity, half-life and safety issues follows. Thermoluminescence is also presented as a technique to date ceramics. Although the topic is not covered in depth, it allows for a discussion on crystal lattices.

Infra-red spectroscopy is also covered and provides a great review of the organic functional groups learned earlier in the class (4). Basic knowledge is given to the students who are then able to differentiate between the spectra of molecules containing common functional groups and recognize the specific peaks associated with them, as shown in Figure 5.

More sophisticated instrumentation is also discussed in this course. For instance students learn about x-ray spectroscopy. X-ray spectroscopy encompasses a wide range of techniques which can be connected to the technical analysis of the works of the cultural heritage (5). X-ray diffraction allows the instructor to discuss crystal lattices as would be noted during the discussion of inorganic materials. Bragg's equation is presented to the students although no actual calculation used in crystallography is performed. However this allows for an introductory discussion in mineralogy and gemology. X-ray fluorescence and laser ablation coupled with inductively coupled plasma spectroscopy are also shown which allow for a review on atomic structure. Examples of varying elemental compositions in coins or in pottery are given. The importance of knowing the exact chemical composition of an artifact is emphasized as it can help archeologists establish ancient trade routes or forensics scientists detect fakes and forgeries (6).

Finally gas and liquid chromatography coupled with mass spectrometry (LCMS or GCMS) is introduced to the students. These techniques are largely used in the technical analysis of works of art (7). The analysis of paint binders for instance can be done by GCMS whereas dye analysis is carried out using LCMS. The spectra shown to the students allow for a review of molecular structure of organic compounds, as shown in Figure 6.

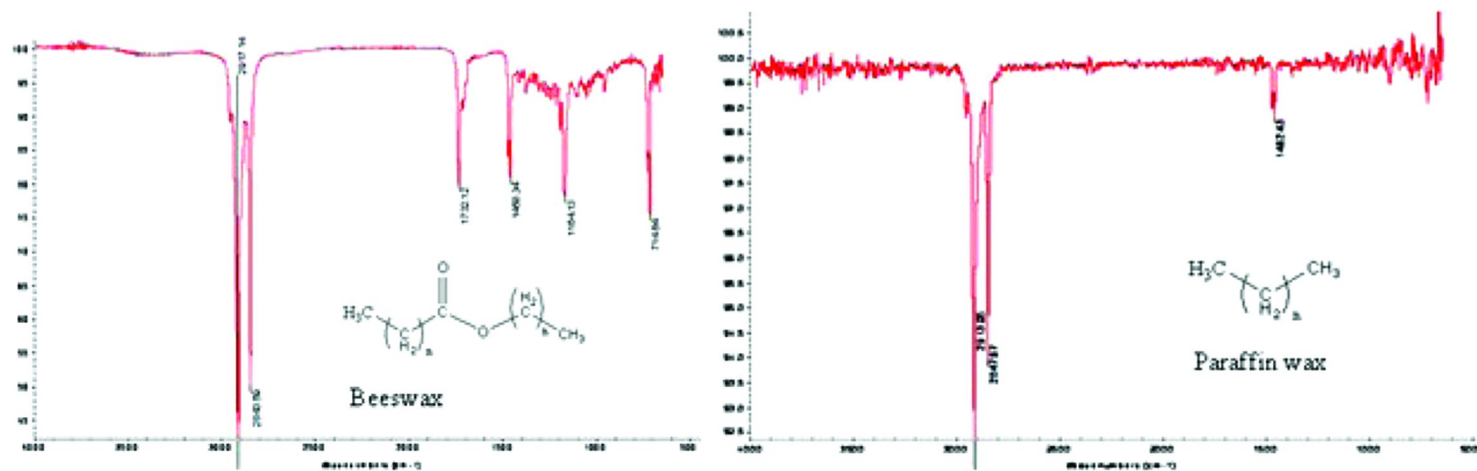


Figure 5. IR spectra of beeswax and paraffin wax.

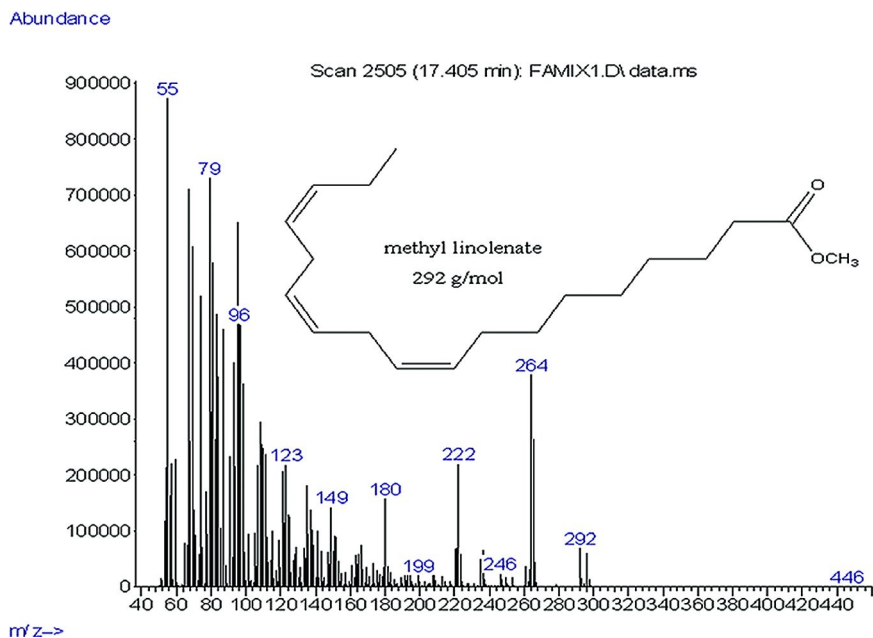


Figure 6. Mass spectrum of methyl linoleate.

With the appropriate set of data, the students can determine if the binder used in a given example was egg or oil-based and also identify an unknown dye by matching its mass spectrum with a known substance.

Conclusion

This introductory chemistry course, aimed specifically at art majors, allows the students to see the connection between chemistry and the technical analysis of works of art and more generally of the cultural heritage. Students from all backgrounds benefit working with real-life applications of chemistry and by keeping the students excited with cross-disciplinary examples. Two reflective examples of comments written by students at the end of the semester are cited here to show how they embraced the course: “*The course is very interesting and mind opening*” and “*This was a very interesting course and unlike any other course I have ever taken regarding the material*”. It is especially noteworthy to receive such positive comments from the students enrolled in this course, since they are all non-science majors and mainly freshmen.

References

1. Uffelman, E. S. *J. Chem. Ed.* **2007**, *84* (10), 1617–1624.
2. Uffelman, E. S.; Alty, L. T.; Fuchs, R. W.; Sturdy, L. F.; Bowman, D. S.; Lemon, A. M.; Malachosky, E. W. Abstracts of Papers, 241st ACS National Meeting and Exposition, Anaheim, CA, United States, March 27-31, 2011; CHED-98.
3. Hill, P. S. *The Molecular Basis of Color and Form: Chemistry in Art, Laboratory Manual*; Millersville University, Millersville, PA, unpublished.
4. Derrick, M.; Stulik, D.; Landry, J. *Infrared Spectroscopy in Conservation Science*; The Getty Conservation Institute: Los Angeles, CA, 1999.
5. Uda, M.; Demortier, G.; Nakai, I. *X-rays for Archeology*; Springer: Dordrecht, The Netherlands, 2005.
6. Bradley, D.; Creagh, D. *Physical Techniques in the Study of Art, Archeology and Cultural Heritage*, 1st ed.; Elsevier: New York, 2006.
7. Mills, J. S.; White, R. *The Organic Chemistry of Museum Objects*, 2nd ed.; Butterworth-Heinemann: Woburn, MA, 1999.

Chapter 16

Technical Examination of Cultural Heritage Objects Associated with George Washington

Erich Stuart Uffelmann,^{*1} Ronald W. Fuchs II,² Patricia A. Hobbs,² Lauren F. Sturdy,¹ Danielle S. Bowman,² and Derek A. G. Barisas¹

¹Department of Chemistry, Washington and Lee University,
Lexington, VA 24450

²University Collections of Art and History, Washington and Lee University,
Lexington, VA 24450

*E-mail: uffelmane@wlu.edu

Several genuine pieces of George Washington's Society of the Cincinnati porcelain, as well as a piece with later decoration, were examined by handheld XRF spectroscopy to determine if diagnostic chemical markers were present. The green enamel of the authentic porcelain was copper; the green enamel of the piece with later decoration was chromium. George Washington's Charles Willson Peale portrait of the Marquis de Lafayette was examined by handheld XRF, InGaAs digital IR photography, and UV-induced visible fluorescence to determine the condition of the painting and its chemical attributes. A period copy of Gilbert Stuart's Lansdowne Portrait of George Washington was examined by handheld XRF, InGaAs digital IR photography, and UV-induced visible fluorescence to determine the condition of the painting and to attempt to contribute basic knowledge that might assist in its proper attribution.

Introduction

Washington and Lee University is fortunate to possess several cultural heritage objects that belonged to George Washington or that are closely associated with him. The NSF recently funded a non-destructive instrumentation grant at W&L that has allowed us to undertake studies of our paintings, ceramics and porcelain, and archaeological objects. To initiate these projects, we were

particularly eager to study our Washington-related materials and to incorporate undergraduate researchers into those studies. We report here our findings concerning Washington's porcelain decorated with the insignia of the Society of the Cincinnati (and a piece with later decoration, almost certainly done with the intent to deceive), Washington's Charles Willson Peale portrait of the Marquis de Lafayette, and a mysterious contemporaneous copy of Gilbert Stuart's famous Washington Lansdowne Portrait. This chapter will discuss each of these topics sequentially.

George Washington's Society of the Cincinnati Porcelain

Background

The Chinese export porcelain service decorated with the badge of the Society of the Cincinnati is arguably the most significant group of antique porcelain with an American provenance in existence. Made in 1784, it was commissioned by the first American merchant to go to China and was owned first by George Washington and later by Robert E. Lee. The dishes from the Cincinnati service commemorate the American Revolution and the values that underpinned it, are tangible evidence of the United States' entrance into global trade, and are witnesses to the Civil War and the nation's subsequent re-unification afterwards. They have been bought, sold, gifted, confiscated, restituted, curated, and studied. They have also been copied, most likely with the intent to deceive.

Understanding how and when these pieces with later decoration were made helps us better understand the Cincinnati service, its significance, and its history, and determining how to differentiate between the genuine and the spurious helps us avoid mistaking the copies for the genuine examples.

The Society of the Cincinnati is an organization of Revolutionary War officers that was founded in 1783 to perpetuate, in the words of its charter, "the mutual friendships which have been formed under the pressure of common danger" (1, 2). It was named after Lucius Quinctius Cincinnatus, a Roman military leader from the fifth century B.C.E. Cincinnatus was a farmer who was appointed military dictator to defend Rome against invasion. After victory, he relinquished his power and returned to his farm. Cincinnatus was seen by many as the model of the selfless patriot who served his country without expectation of reward. George Washington was seen by many as the embodiment of what Cincinnatus represented, and was called "The Cincinnatus of the West." Washington also served as the Society's first President General.

The porcelain decorated with the badge of the Society was commissioned by Samuel Shaw, a member of the Society of the Cincinnati and a China Trade merchant. Shaw was the supercargo, or chief merchant in charge of buying and selling a ship's cargo, of the *Empress of China*, the first American ship to go to China. She departed New York on February 22, 1784, and arrived in Guangzhou (then known as Canton) in China on August 28, 1784.

While in China, Shaw commissioned the porcelain, selecting a stock pattern decorated with what is known today as the Fitzhugh border, which is an elaborate design painted in underglaze blue. The border would have been painted on the

porcelain in Jingdezhen, the city in south-central China where the porcelain was made. The porcelain would then have been sent to Canton, where further decoration, such as coats of arms, initials, or other personal devices, would be applied in overglaze enamels to the blank sides or center of each piece. This would have been done through merchants like Yam Shingqua, “China Ware Merchant at Canton,” who advertised, circa 1800, “All sorts of Chinaware, Arms etc., Painted on the most reasonable Terms” (3).

Shaw provided the porcelain painter with drawings of the badge and a figure of Fame, and he complained in his journal about the frustrations he had in communicating his exact wishes; “he (the painter) was allowed to be the most eminent of his profession, but after repeated trials, was unable to combine the figures with the least propriety; though there was not one of them which singly he could not copy with the greatest exactness. I could therefore have my wishes gratified only in part” (4). This reflects the difficulty European and American merchants had in dealing with their Chinese counterparts; neither spoke much, if any, of each other’s language, and there was an equal lack of understanding of each other’s culture and design traditions.

The design that Shaw was only partly satisfied with consisted of a winged female personification of Fame holding the badge of the Society, which is an eagle with a shield on its breast. The badge was designed by Major Pierre-Charles L’Enfant, the Frenchman who was the Continental Army’s chief engineer and who, among other things, designed the layout of the new federal capital of Washington D.C.

Once completed, the Cincinnati service was brought to America and offered for sale. It was purchased by Henry (Light-Horse Harry) Lee III, a Revolutionary War officer, on behalf of George Washington, in 1786. According to the receipt dated August 7, 1786, the service consisted of 302 pieces, including dinner and tea wares, and cost \$150, an enormous sum at the time (5).

Washington used the service in the presidential mansions in New York and Philadelphia and at Mount Vernon. Washington’s choice of the service was probably more than just sentimental; as the first president, Washington was very aware that he was setting the standard for the office, and by using dishes decorated with a symbol associated with Cincinnatus, a citizen who served his nation without wish for reward or permanent power, he was sending a signal that he was a leader who was not establishing an hereditary monarchy.

Washington died in 1799 and the Cincinnati service passed to his wife, Martha. Upon her death, in 1802, she left “the sett of Cincinnati tea and table China” to her grandson, George Washington Parke Custis. He kept it at Arlington, the house he built overlooking the nation’s capital. Following his death in 1857, the service, along with Arlington and other Washington heirlooms, passed to his daughter, Mary Anna Randolph Custis, and her husband, Robert E. Lee (6).

In May of 1861, shortly after Robert E. Lee resigned from the U.S. Army to fight for the Confederacy, Mary Lee left Arlington. She took with her some of the Washington heirlooms she had inherited, but much remained in the house, including the Cincinnati service, which “was carefully put away & nailed up in boxes in the cellar” (7).

Arlington was confiscated by the U.S. government, as was the Cincinnati service and other Washington pieces, which were transported to the U.S. Patent Office, where they were displayed. They were later transferred to the Smithsonian, and were ultimately returned to the Lee family in 1901, supposedly upon the orders of President William McKinley himself. The return of the Lee's property came at a time when the country was working to reunite the nation as it entered a new century (8).

During the 20th century the service was dispersed and pieces are now found in numerous public collections, including Mount Vernon, the Smithsonian, the Winterthur Museum, the White House, the Metropolitan Museum of Art, Stratford Hall, and the Reeves Center at W&L. Others remain in private hands.

Pieces of the Cincinnati service do periodically come on the market and have made consistently high prices due to their rarity and historical importance. Primarily because of their high value, later copies of the Cincinnati service have been made. There exists at least one group thought to date to the late-1970s or early 1980s. Approximately half a dozen pieces are known, and are in fact genuine pieces of Chinese export porcelain made about 1785, but the figure of Fame holding the Cincinnati badge is modern.



Figure 1. Authentic Society of the Cincinnati plate. Made in China, about 1785. Reeves Center, Gift of the Thompson Family (R1995.3.1.3). Courtesy of the Reeves Center, Washington and Lee University. (see color insert)

Though it is not known who made these pieces, they probably come from a partial dinner service of export porcelain that sold at Christie's in London in 1975 (9). Traditional connoisseurship analysis showed that this service was comprised of genuine pieces of Chinese export porcelain made about 1785. The service consisted entirely of blanks; pieces that had the underglaze blue border applied when made, but which had never had any overglaze enamel decoration applied. It would have been relatively easy to add the figure of Fame and the Cincinnati eagle to the pieces, transforming them from mundane antiques of minimal value to significant objects of tremendous value.

Traditional connoisseurship techniques do reveal a difference between the genuine and spurious decoration; comparison between pieces with impeccable provenances (Figures 1 and 3) and questionable pieces (Figures 2 and 4) show visual differences between the figures of Fame; most noticeably in the later Fame's overall tan skin as opposed to the blushes of pink found on the genuine article. At least one of the pieces with later decoration also has patches of gray staining on the reverse. This staining probably resulted from the refiring that fixed the new enamel decoration to the glaze of the old plate.



Figure 2. Plate with later decoration. Made in China, about 1785; decorated about 1980. Reeves Center, Museum Purchase (R2004.7.1). Courtesy of the Reeves Center, Washington and Lee University. (see color insert)



Figure 3. Detail of plate with authentic decoration. (see color insert)



Figure 4. Detail of plate with later decoration. (see color insert)

pXRF Analysis

The previous two chapters in this volume have already briefly discussed approaches to conservation and the pros and cons of handheld (portable) X-ray fluorescence spectroscopy (pXRF) as a tool for analyzing cultural heritage objects (10, 11). Each spectrum in the porcelain analysis, unless noted otherwise, was collected for 180 seconds with a Bruker Handheld Tracer III-SD Portable XRF Analyzer operating under a vacuum of approximately 20 Torr, with a rhodium anode target producing X-rays with voltage and current conditions of 40 kV

and 11 μ m, respectively (note that as a consequence, each spectrum shows a prominent set of rhodium lines produced by the X-ray tube and not the target area of the object). The element assignments were made using the Bruker Artax 7.2.1.1 software, but comprehensive tables of XRF lines are readily available in common sources (12). The spectra were obtained by undergraduate researchers under close curatorial supervision. After we acquired our data, Mueller and Mass reported an excellent similar study of authentic and spurious Society of the Cincinnati porcelain, and the authors provided a concise history of the later pieces (13). Our results confirm and extend those that recently appeared. We examined four plates and one soup plate out of our eight authentic pieces of the service, and we examined one piece with later decoration. The five authentic pieces all produced very similar spectra, and so only one spectrum from each color area is presented below. Note that some of the elemental lines observed in each spectrum are not from the sample (11, 14–17).

The white background (Figure 5) of the genuine plate shows an elemental signature typical of Chinese export porcelain from this time period. Because the plate with the later decoration is a modified authentic late 18th century piece of Chinese export porcelain, its white background spectrum is very similar. Not surprisingly, the blue border of the authentic plate (Figure 6) shows prominent cobalt lines; cobalt was a typical blue colorant of the period. The plate, with its authentic blue border, shows a similar spectrum. The brown wing of Fame on the authentic plate (Figure 7) provided a spectrum in which manganese was the probable source of the brown coloration; the much higher lead signal is caused by lead being used as a flux in the decoration. The plate gave a similar spectrum, even though the wing was a 20th century addition. Pink colors in porcelain are frequently produced using colloidal gold. The tinting power of the colloidal gold is such that it is very difficult to detect. A 3600 second accumulation run on the authentic plate (Figure 8) was required in order to have any confidence that gold was present.

We anticipated the key measurement would be of the green dress. Copper was typically the source of green pigmentation in porcelain prior to 1800, while chromium, which was first discovered by Vauquelin in 1797 (18), was used as a green colorant for ceramics by 1802 at the Sèvres factory in France (19). The authentic green dress (Figure 9) shows a strong copper peak, while the green dress (Figure 10) shows a prominent chromium peak. Overlaying the spectra and zooming in on the region where elements chromium through zinc fluoresce X-rays (Figure 11), reveals that, in addition to the presence of chromium instead of copper in the green dress, the green dress also exhibits prominent cobalt lines (unambiguously distinguished from Fe by curve fitting) and a significant zinc signal.

Clearly, beyond curatorial observations which can distinguish authentic and later reproductions of Society of the Cincinnati Chinese export porcelain, these particular pieces can be instantly identified by their telltale chromium signature. The presence of chromium found through pXRF analysis thus provides definite proof of what has been suspected by simple visual analysis---that this group of pieces has later, non-authentic decoration.

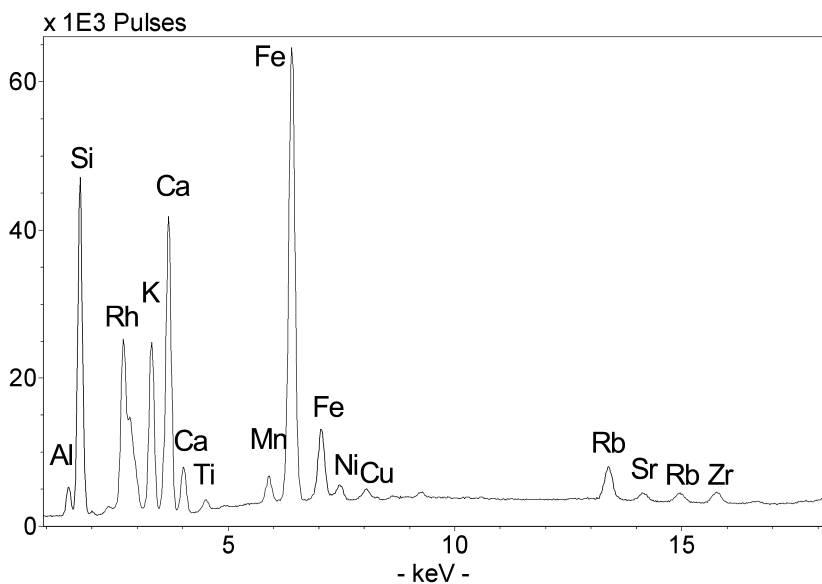


Figure 5. Society of the Cincinnati porcelain, white background (1995-3-1-3).

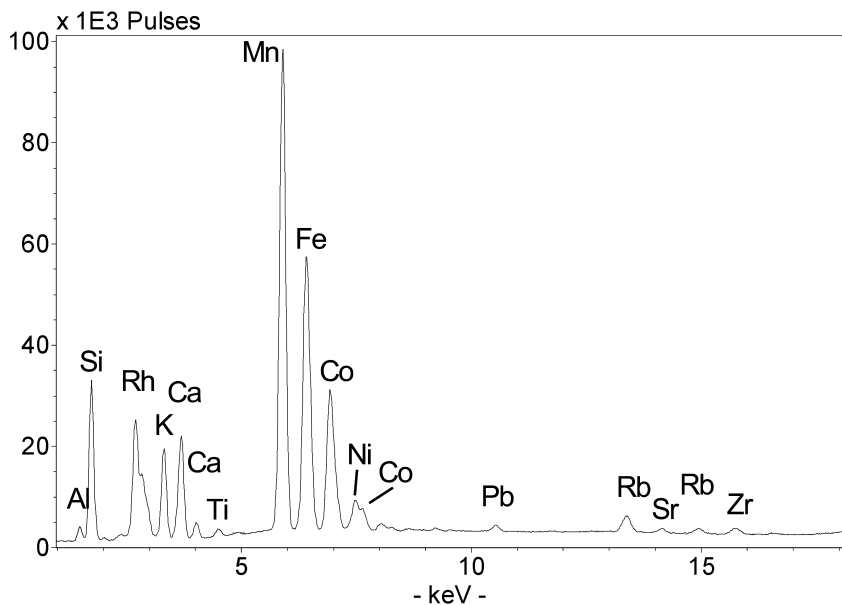


Figure 6. Society of the Cincinnati porcelain, blue border (1995-3-1-3).

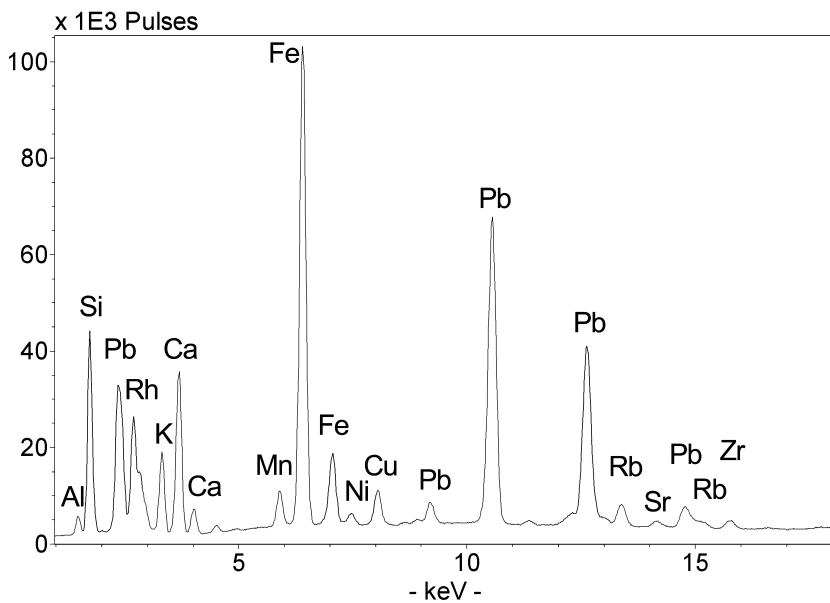


Figure 7. Society of the Cincinnati porcelain, brown wing (1995-3-1-3).

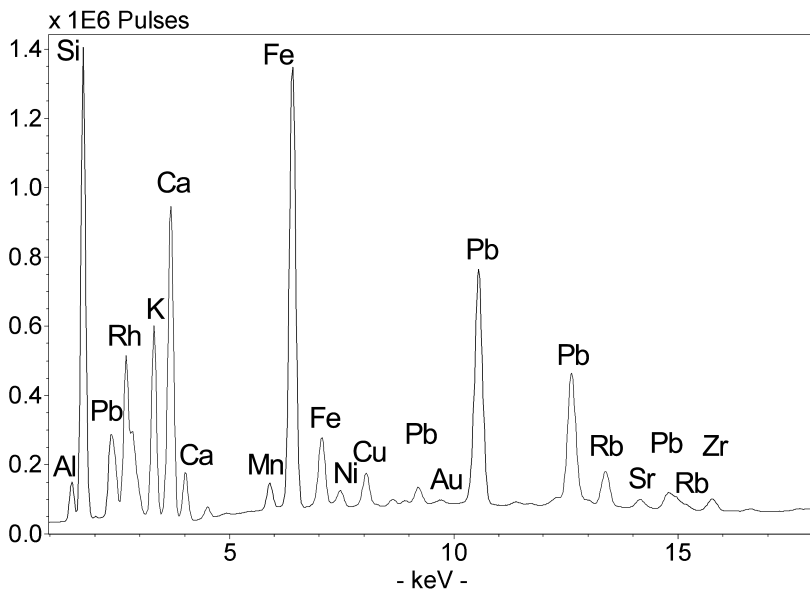


Figure 8. Society of the Cincinnati porcelain, pink sash (3600 s accumulation) (1995-3-1-3).

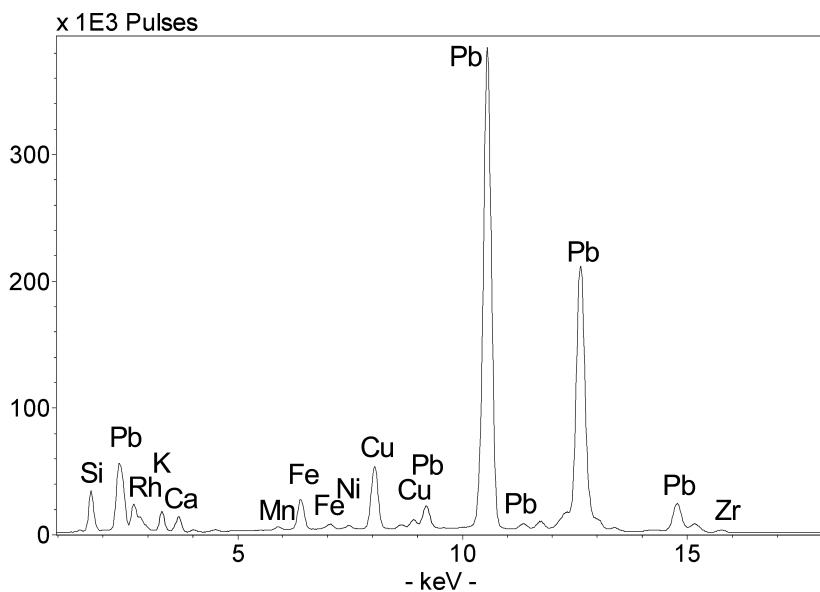


Figure 9. Society of the Cincinnati porcelain, green dress (1995-3-1-3).

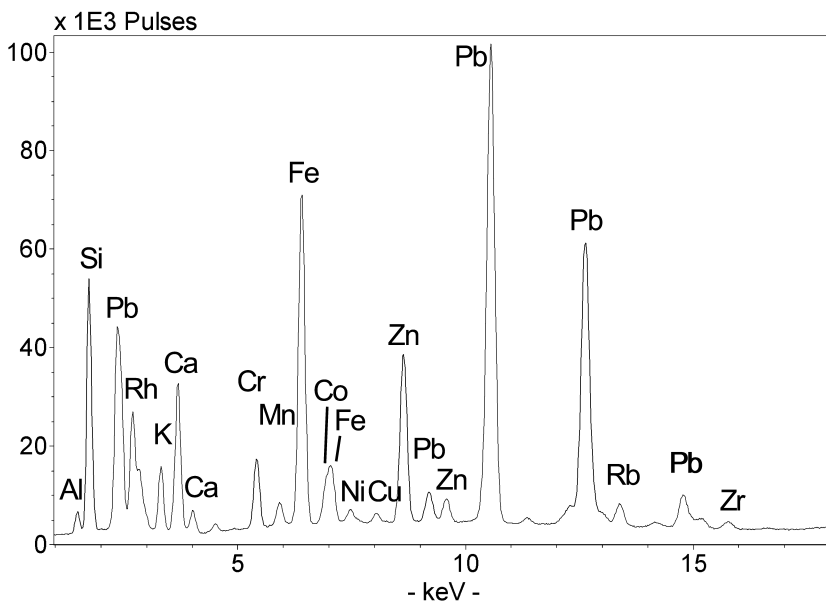


Figure 10. Design, green dress (2004-7-1).

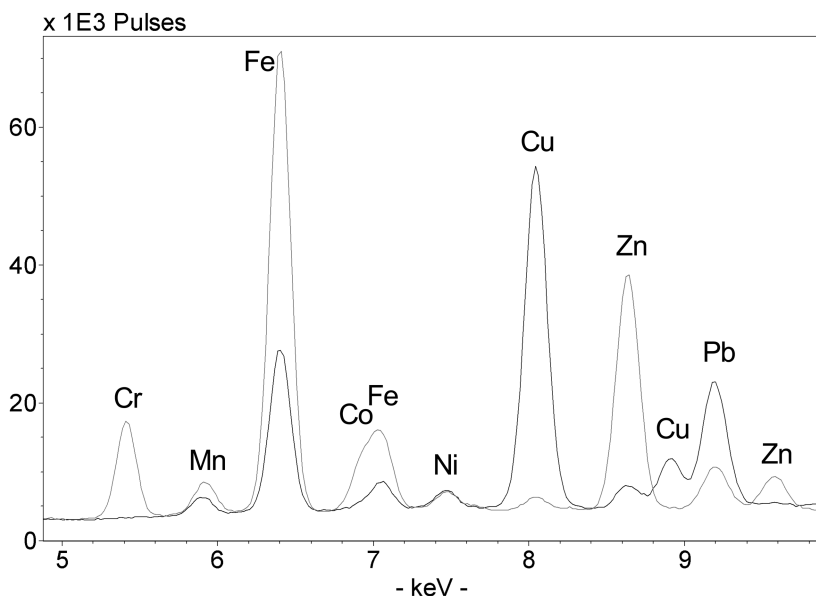


Figure 11. Overlaid spectra of the design (gray) and the authentic design (black) of the green dress. Note the differences in Cr, Co, Cu, and Zn signals.

Washington's Charles Willson Peale Portrait of *The Marquis de Lafayette*

Charles Willson Peale

Charles Willson Peale (1741-1827) was one of America's preeminent portrait painters and patriarch of an artistic family (20, 21). Born in Maryland and apprenticed as a youth to a saddle-maker, Peale had an aptitude for drawing and painting. He studied briefly with portrait painters John Hesselius and John Singleton Copley before painting portraits in Annapolis, MD. In 1767, a supportive group of wealthy Maryland patrons sent him to London to study with noted American painter Benjamin West. Peale returned to Maryland in 1769 and travelled throughout the middle colonies to paint socially and politically prominent families. This included a portrait in 1772 of George Washington, commissioned by his wife Martha.

In 1776, Peale moved his family to Philadelphia, became involved with politics, and fought with the Pennsylvania militia during the Revolutionary War. During the War, Peale carried his paints with him and painted miniatures of Continental Army officers. These became studies for larger portraits that Peale produced after the war and which became the nucleus of a gallery of art and natural history that he established in Philadelphia in 1782.

Peale is significant as a portrait painter, but he also pursued interests in natural history and science. A noted inventor, agricultural reformer, museum director, and a founder of the Pennsylvania Academy of Fine Arts, Peale was an example of American Enlightenment.

The Portrait

In 1777, General George Washington was introduced to the young Gilbert du Motier, Marquis de Lafayette, a French aristocrat who at sixteen became an officer in the French army. At the age of nineteen, he set sail to fight against England in the cause of American liberty. Very quickly, Lafayette earned Washington's respect and affection as both a soldier and a friend. He became Washington's aide-de-camp and later a Major General in the Continental Army. Their personal bond was as close as that of a father and son.

Sometime in 1778 or 1779, Washington commissioned the first American portrait of Lafayette from Charles Willson Peale, who was working in Philadelphia at the time. The artist, the only American painter to do a life portrait of Lafayette (22), began the painting, possibly during the three weeks that Lafayette spent in Philadelphia in October 1778 before Congress granted him a leave of absence on October 21 (23).

Lafayette returned to France in early 1779. While in France, he negotiated and secured financial aid for Washington's army and persuaded France to enter the war against Great Britain. This pivotal event strengthened ties of friendship between America and France, made Lafayette the symbol of this alliance, and helped lead the American forces to victory at Yorktown against Lord Cornwallis in 1781.

Peale's portrait of Lafayette wearing his Continental Army uniform (Figure 12) is signed and dated 1779, but the painting remained unfinished for more than a year after Lafayette's departure. Peale often dated a painting from the time of its beginning, or receipt of commission, rather than its completion (24). Although Lafayette was again able to sit for the portrait after his return to America in April 1780, Peale continued to delay completion of the painting, in part because he had to move his home and studio (25). By December, Washington was impatient and wrote to Peale, "I persuade my self you will embrace the oppertunity [sic] of the Marquis de la Fayette's visit to Philadelphia to give the picture of him the finishing touches. You may not have another oppertunity [sic], and I wish for its completion." Peale continued to work on the portrait, making major changes to the background (26, 27). In addition, he painted a bust-length copy of the portrait for his museum (28), which is now in the collection of the Independence National Historical Park (29). Lafayette also ordered two smaller versions of the portrait as gifts to James Duane, a representative to the Continental Congress from New York (30), and to "Light-Horse Harry" Lee, a fellow soldier and another young friend of Washington. This latter painting was done by Peale's assistant and nephew, Charles Peale Polk (22). Peale finally sent the original three-quarter length portrait of Lafayette to Mount Vernon in 1781.

According to a probate inventory taken after Washington's death in 1799, the portrait hung in a second-floor bedroom, which was used by Lafayette during his visit in 1784. The portrait remained at Mount Vernon during Martha Washington's

life and was inherited by her grandson, George Washington Parke Custis, who displayed it in his home, Arlington, along with other Washington memorabilia. After Custis' death in 1857, his only surviving child, Mary Anna Randolph Custis, who had married Robert E. Lee in 1831, inherited the house and its contents. In 1861, as Federal troops approached Arlington, Mrs. Lee packed this painting and others she inherited from her father, and sent them for safe-keeping to another Custis plantation in Virginia called Ravensworth.



Figure 12. The Marquis de Lafayette, by Charles Willson Peale, 1779. Oil on canvas; H – 48.5” x W - 40”. Washington-Custis-Lee Collection of Portraits, Washington and Lee University (U1897.1.2). Signed and dated lower left (on edge of table): C. W. Peale, Pinx. 1779. Courtesy of Washington and Lee University. (see color insert)

After the end of the Civil War, the Lees moved to Lexington, where Robert E. Lee became president of Washington College. He arranged for the return of the portraits to the family, but during their transport to Lexington, the paintings were damaged when the packet boat carrying them sank. The portraits, including that of Lafayette, fortunately were retrieved and sent to Baltimore for restoration (31).

Lee died in October, 1870. In January, 1871, the college was renamed Washington and Lee University, and George Washington Custis Lee, Lee's oldest son, succeeded his father as president. This enabled his mother to remain in the president's house, along with the portrait collection. After Mrs. Lee's death in 1873, Custis inherited the two Peale portraits of George Washington and the Marquis de Lafayette, and upon his retirement in 1897, he donated them to the University. W&L collections records indicate that the Lafayette portrait was cleaned and varnished in 1900 by Herbert Welsh of Philadelphia. It was cleaned again in 1922 by Arthur Dawson and conserved in 1970 by Russell J. Quandt, paintings conservator at Winterthur.

Analysis

While on recent loan to Mount Vernon, the painting was surveyed extensively under UV illumination to detect areas of different fluorescence, indicating retouched areas, and many were noted. This was not a surprise, given the history of the painting (particularly the accident it experienced in boat transport). Russell J. Quandt's conservation treatment report of January 29, 1970 in W&L's object files was useful for examining the painting. The painting was photographed in many areas using a Goodrich InGaAs IR camera sensitive in the 900-1700 nm region of the IR spectrum. The IR photos were useful for clarifying some areas of the composition and confirming areas of retouching or inpainting detected by UV fluorescence. However, no underdrawings were detected (32, 33).

Given the airtight provenance of the painting, the pXRF analysis of the painting revealed elements consistent with pigments of the period (34), except, of course, in areas of recent retouching or inpainting. Spectra were acquired by an undergraduate researcher under the close supervision of Mount Vernon's curatorial and conservation staff; instrument parameters and methods were those reported for the Society of the Cincinnati porcelain (*vide supra*). All of the spectra show the presence of lead from lead white and calcium probably from either chalk (most likely) or gypsum. The spectrum of the gold sword hilt (Figure 13) showed such a strong Fe signal that one or more of the yellow iron oxide pigments is almost certainly present (35, 36). In contrast, Lafayette's yellow pants, at the conclusion of 180 seconds of accumulation, appeared to contain antimony, and so a 2700 second run was used to confirm that suspicion (Figure 14). This points to Peale's use of lead antimonate yellow (Naples yellow) (36, 37). The UV-induced visible fluorescence, IR camera, and 1970 treatment report all confirmed that conservation treatment had been performed on Washington's proper left hand, and this was confirmed by the pXRF observation of titanium (Figure 15), which is almost certainly present as one of the titanium dioxide whites, pigments that typically appear only after around 1920 (36, 38). Peale achieved the red of the curtain and of the lips (Figure 17) via different (and typical for the time) means.

The pXRF spectrum of the red curtain (Figure 16) shows a strong signal for iron, strongly indicating the presence of red iron oxide pigment (35, 36), and a weak signal for mercury, strongly suggesting the presence of vermilion, HgS, pigment (36, 39). On the other hand, the pXRF spectrum of the red lips (Figure 17) shows a much weaker signal for iron (at an intensity level not necessarily associated with the lip pigmentation, but potentially with the lower paint layers and/or as an artifact from the instrument's stainless steel components) and a much stronger signal for mercury; artists frequently used vermilion as one of their principal skin coloration pigments.

Finally, the black collar was interesting, because there were several black pigments artists could choose during Peale's working period (36, 40). Bone black or ivory black was prepared by roasting bone or horn materials in an oxygen-deprived environment, degrading the collagen protein on the hydroxyapatite substrate. Hydroxyapatite, $\text{Ca}_{10}(\text{PO}_4)_6(\text{OH})_2$, obviously contains both calcium and phosphorous, but calcium is present throughout the painting because of the likely canvas preparation involving chalk and hide glue, so a finding of phosphorous is necessary to support the presence of bone black or ivory black. Other carbon-based black pigments are much less likely to have high concentrations of phosphorous (40). The pXRF spectrum of the black collar (Figure 18) did show a clear phosphorous signal.

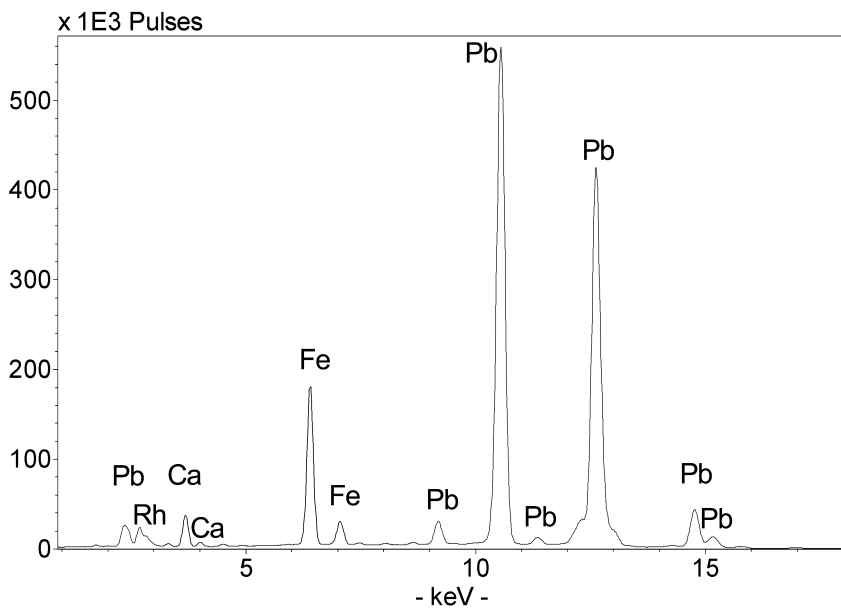


Figure 13. Lafayette's gold sword hilt.

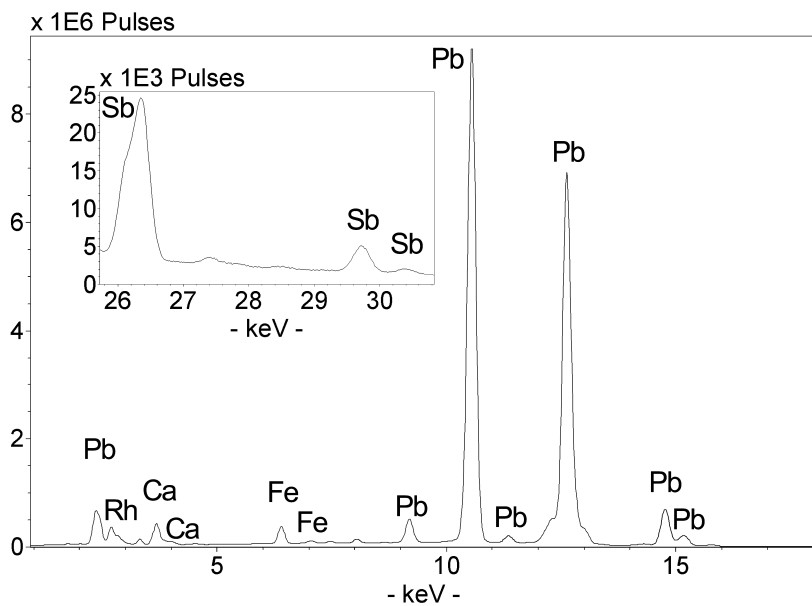


Figure 14. Lafayette's yellow pants (2700 s accumulation).

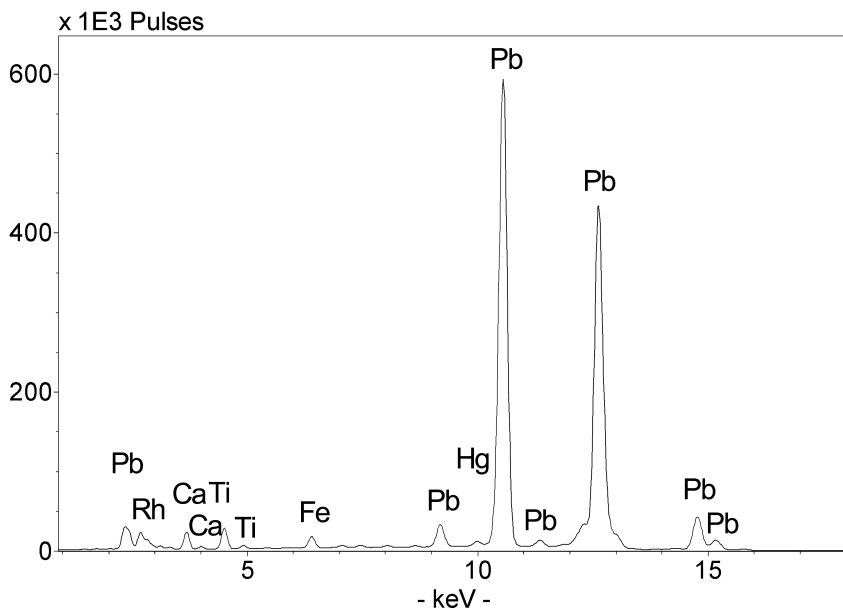


Figure 15. Lafayette retouched area of the proper left hand.

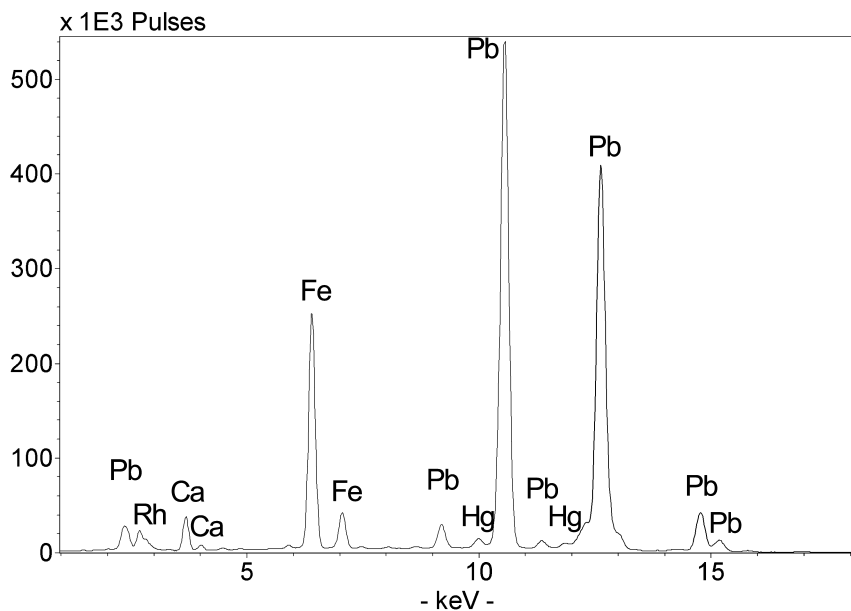


Figure 16. Lafayette red curtain.

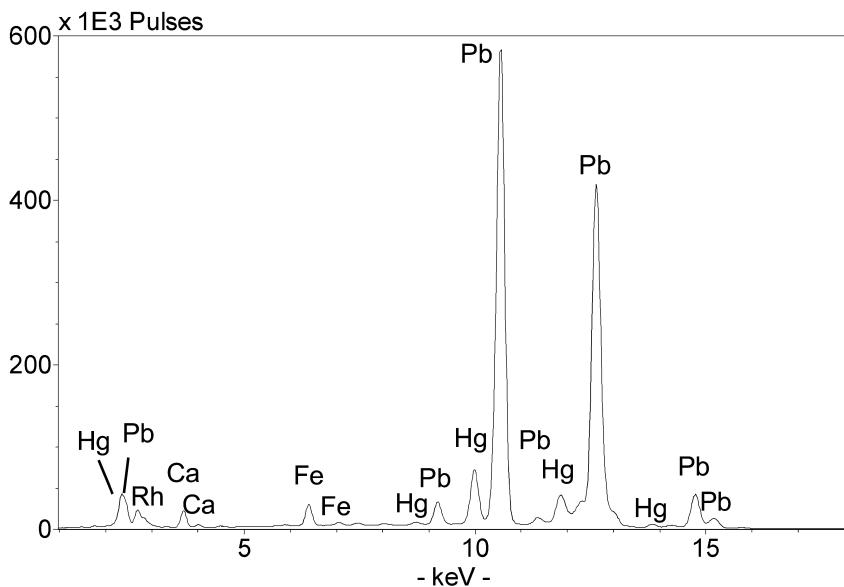


Figure 17. Lafayette red lips.

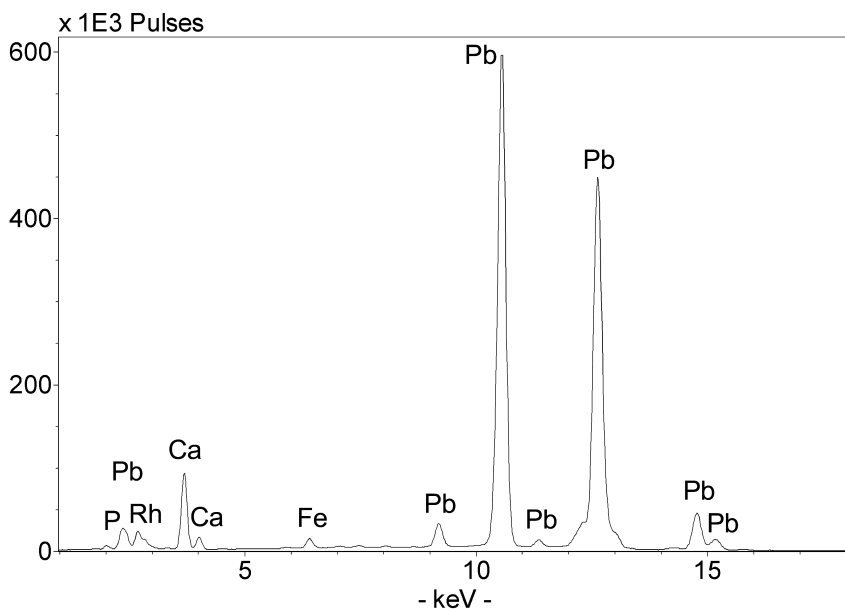


Figure 18. Lafayette black collar.

Copy of Gilbert Stuart's Lansdowne Portrait

During summer 2011, one of Washington and Lee University's several paintings of George Washington returned to campus after a long-term loan to the Westervelt Warner Museum of American Art. The return of this very large (H: 94" x W: 59") full-length portrait, which is usually inaccessibly displayed, afforded a rare opportunity to get close enough to the painting to examine it scientifically in some detail.

The painting (Figure 19) depicts George Washington wearing a black velvet suit, posed as an orator with his right arm outstretched over a gilt table. His left hand holds a sheathed ceremonial sword. This painting is one of several versions that exist of the ambitious and iconic portrait by Gilbert Stuart of George Washington, first President of the United States, known as the "Lansdowne type" (41–44). We hoped with our analysis to provide data that might one day help point to a correct attribution for W&L's painting, in the context of growing scholarship and investigations.



Figure 19. George Washington (Lansdowne Portrait), after Gilbert Stuart, ca. 1800. Oil on canvas.; H - 94" x W - 59. Gift of the David Warner Foundation (U1980.1.1). Courtesy of Washington and Lee University. (see color insert)

Background

Gilbert Stuart (1755-1828) was a preeminent American portrait painter of the late 18th and early 19th centuries. He studied with Benjamin West in London for five years and quickly became a successful portraitist in his own right. However, Stuart lived extravagantly and in 1787 fled from his English creditors to paint in Ireland. In 1793, he returned to New York with a plan to paint the first President of the United States in order to earn money from the replicas he would make of his own paintings (a replica is a copy or reproduction of a work of art by the original artist).

With a letter of introduction from John Jay, who had posed while in England for a portrait by the artist, Stuart was able to meet Washington and arrange for the president to sit for him. The first portrait of Washington in which he faces right was completed in 1795; Stuart made about a dozen replicas of the painting. It became known as the “Vaughan type,” named after Samuel Vaughan of England, whose replica of the original was reproduced as an engraving in 1796 and was widely published. A second sitting was arranged through Martha Washington, who commissioned a pair of portraits of herself and her husband, which were to be hung in Mount Vernon after the President’s retirement. These portraits, begun by the spring of 1796, were never completed or delivered. Stuart retained them to use as models to fill the many orders he was receiving for portraits of George Washington. Stuart completed at least 70 replicas of this painting during his lifetime; he believed the likeness was more successful than his earlier “Vaughan type” portrait. This 1796 portrait version in which Washington faces left has become known as the “Athenaeum type” because the Boston Athenaeum acquired the unfinished original paintings after Stuart’s death. Washington and Lee University owns one of these replicas, which Dr. W. Newton Mercer of New Orleans gave to the institution in 1874. The Athenaeum portrait is also the source of the iconic image of Washington on the U.S. one-dollar bill. [More information on Washington portraits by Stuart is available from several sources (41, 43–45).]

Gilbert Stuart also planned to paint a full-length portrait of Washington and received a commission for one early in 1796 from William Petty, the first Marquis of Lansdowne. Lord Lansdowne was a British supporter of the American cause and noted patron of literature and the arts. Washington sat for this portrait in April towards the end of his presidency, but for only one session, during which time Stuart completed the head. This was standard practice for the period, when an artist would complete a portrait in the studio, using one or more live surrogate models for a standing figure. The pose and general tenor of the painting is based on engravings of European state portraits in Stuart’s collection, but the artist changed the iconography to reflect the ideals of the new American republic (41, 42, 44).

Senator and Mrs. William Bingham of Philadelphia purchased this painting as a gift to Lord Lansdowne and also ordered a replica for their country home, coincidentally named “Lansdowne” by a former owner. The portrait that was sent to the Marquis of Lansdowne in November 1796 and received in March 1797 is universally recognized as by Gilbert Stuart’s hand. [It is worth noting, in the context of the first part of this chapter on the Society of the Cincinnati porcelain, that Lord Lansdowne was highly pleased with the painting, and displayed it in his

large library, where there was also on display an ancient Roman marble statue of Cincinnatus tying on his sandal (42).] The painting is now in the collection of the National Portrait Gallery, Smithsonian Institution, acquired as a gift to the nation in 2001 through the generosity of the Donald W. Reynolds Foundation.

The portrait was much admired and Stuart received orders for as many as one hundred copies, a fact that impressed Robert Gilmor of Baltimore, who visited Stuart in 1797. In his journal, Gilmor, who became one of America's pioneer art collectors, wrote, "This circumstance is unique in the history of painting, that the portrait of one man should be sought after in such a degree as to be copied by the original artist such a number of times and for such an amount" (42).

Margaret Christman states in her essay about the Lansdowne portrait, "However many orders for copies of the Lansdowne Stuart actually received, it is inconceivable that the number was more than one hundred. Equally incredulous is the notion that Stuart – who was easily bored by details beyond the face – could bring himself to replicate the elaborate full-length in any great numbers" (42). Indeed, in 1817 Stuart stated that he made only one replica entirely by himself; for all others he used assistants to complete the majority of each painting, other than the face and possibly the hands (41).

Although the Pennsylvania Academy's full length is signed, Stuart's Washington portraits are generally unsigned, and the artist did not keep clear records about the originals and his copies of them. This makes definitive attribution difficult. The original Lansdowne portrait, now owned by the National Portrait Gallery, and two replicas are indisputably by Gilbert Stuart. Senator Bingham bequeathed his replica to the Pennsylvania Academy of Fine Arts. The third undisputed copy by Stuart's hand was commissioned by William Constable, a New York merchant, and now is in the collection of the Brooklyn Museum of Art (43, 44).

A fourth copy of the Lansdowne portrait, which hangs in the White House also has been attributed to Stuart, but is the subject of much controversy. It was purchased in 1800 on behalf of the government as part of the furnishings for the executive mansion. This is the portrait Dolly Madison famously saved as the British burned Washington in August 1814 (42).

However, within two years of purchase, the authorship of the portrait was under dispute. In 1802, Stuart himself denied painting it. Some scholars believe that he did so as way of denying that he had sold the painting twice, once to Charles Cotesworth Pinckney, newly appointed minister to France, and again to Gardner Baker. Others assert that he may have been embarrassed about the inferior quality of his replica, which may have been hurriedly painted in order to accompany Pinckney to France (46).

Further fuel was added to this controversy in 1834 when William Dunlap wrote in *The History of the Rise and Progress of the Arts of Design in the United States* that Stuart accused William Winstanley, a minor English landscape artist who was hired to ship the painting in 1800 to Washington (D.C.), of keeping the original and forging a copy that actually was delivered to the White House (46).

There are several known copies (as opposed to replicas) of the Lansdowne portrait by noted artists, including Thomas Sully, G.P.A. Healy, H.F. Prime, and James Frothingham. Because of the anecdotal connection of Winstanley to the

White House portrait, three other copies have been attributed to him. One is now in a private collection, purchased at auction after the Art Institute of Chicago deaccessioned the painting in 1997, when it was no longer considered to be by Gilbert Stuart. The other two are in the collections of Catholic University and Washington and Lee University (W&L) (44). The attribution to Winstanley, however, remains questionable because very little is known or well documented about the artist and his work in the United States. In fact, the attribution is based primarily on William Dunlap's 1834 book, in which he states that Stuart, who had died six years earlier, accused Winstanley of painting six copies of the Lansdowne portrait. His source, however, was unidentified (46).

Washington and Lee's version of the Lansdowne portrait is most significant for its provenance. In 1959, Duncan Emrich, a historian who was then working with the U.S. Information Service in India, saw the portrait in the Calcutta home of H.C. Mallik. Mallik's grandfather, also H.C. Mallik, had purchased the painting at auction around 1896 from the family of Ramdoolal Dey, an 18th century Indian mogul. While in Calcutta, Emrich conducted research in the Indian National Library and located a pamphlet that recorded a lecture on "... the Life of Ramdoolal Dey, the Bengalee Millionaire" delivered in 1868 by Grish Chunder Ghose at Hooghly College. Ghose, who had interviewed relatives of Ramdoolal Dey and had access to his firm's papers, stated that American merchants of the East India trade, whom he named and who hailed from New England, New York and Philadelphia, commissioned the painting as a gift to Bengali mogul Ramdoolal Dey "as a mark of their esteem and affection... Such a distinction was never before or afterwards conferred on a Bengalee by the merchants of America or any other continent" (47). According to Ghose, Dey received the painting in 1801. Emrich's notes, a copy of which are in the files of Washington and Lee University, record that the portrait was "painted not later than 1799 and possibly earlier, it was shipped by sailing vessel as a gift - 'a token of esteem' - to Ramdoolal Dey in Calcutta, where it arrived in the year 1801" (48).

A shrewd businessman, Ramdoolal Dey (1752-1825) recognized the value of befriending American ship captains and merchants who sailed to India and China after gaining independence from Great Britain. Advancing credit to the Americans and judiciously buying cargo helped Dey's business grow, but the benefits were mutual; the Americans prospered. In gratitude, one American merchant named his ship *Ramdoolal Day* [sic] (47), but the selection of a copy of the Lansdowne portrait as a gift was especially significant. A full-length portrait of George Washington, the father of a new nation who was known for his virtuous character, was an acknowledgement of Dey's honesty and integrity, as well as a symbol of strengthening US-Indo relations.

Duncan Emrich believed that the painting should be repatriated to the United States. He attempted to interest the State Department in purchasing the portrait, but was unsuccessful because of lack of funds (48). In late 1962, Erick Kauders of Marblehead, Massachusetts, known in the fields of electronics and armaments and as the Czech-born co-inventor of the WWII bazooka, purchased the portrait from the Mallik family after Emrich brought it to his attention. After the painting arrived in the United States in 1963, Francis Sullivan, chief restorer of paintings for the National Gallery of Art, treated the painting, which was covered with "more than

a century and a half of Calcutta dust” (48). Based on his examination, Sullivan attributed the entire painting to Gilbert Stuart.

By 1966, the painting was on loan to the National Portrait Gallery (NPG), which was located temporarily in the Smithsonian’s Arts and Industries Building, while the “Old Patent Office” was undergoing renovation as its future home. During an interview by Russell Lynes for *Harper’s Magazine*, NPG director Charles Nagel showed Lynes the Ramdoolal Dey portrait and stated, “I think it is quite certain... that the head is by Stuart, though much of the rest of it was probably painted by someone else.” Nagel hoped to acquire the portrait and locate it in the entrance to the new galleries. Lynes went on to write, “It would be hard to think of anything more suitable except the original painting of which this is a replica... (49)” The National Portrait Gallery could not afford to purchase the painting, however, and Kauders could not afford to donate the portrait. Fortunately, the original Lansdowne was loaned to the NPG by the time of its opening in 1968 at its new location. The Ramdoolal Dey painting was returned to Erick Kauders.

Already by 1966, the attribution of the Ramdoolal Dey version of the Lansdowne portrait to Gilbert Stuart was being questioned. Experts at the National Portrait Gallery disagreed with the conservator at the National Gallery of Art. All agreed that it was artistically inferior to the original. That, of course, could be a function of the artist “having a bad day” or being in a hurry. By 1976, the portrait was also being attributed to William Winstanley. An Editor’s note “Whose Washington?” in the February, 1976 *Smithsonian* read,

“As with some other portraits of George Washington, there has long been speculation and controversy over the identity of the Ramdoolal Dey painting’s creator. When brought back to the United States a dozen years ago, the painting was authenticated as a Gilbert Stuart by an art restoration expert at the National Gallery of Art, who cleaned and restored it. Other authorities thought it more likely the work of William Winstanley, a contemporary and sometime copyist of Stuart. Still others believe Stuart may have done the head and other artists the rest of the painting. Today [1976] the National Portrait Gallery contends that whoever painted this picture, it was not Gilbert Stuart – and the same for the Washington portrait that has hung in the White House for 176 years. *Ed. (47)*”

By the late 1970s, the painting was offered for sale through the Hirschl-Adler Galleries of New York, which acted as an agent for Mr. Kauders. The portrait was purchased in 1980 by the David Warner Foundation, which presented the portrait as a gift to Washington and Lee University, which was the Alma Mater of Jonathan W. (Jack) Warner, Chairman of the Board of the Foundation. The painting was hung high in a specially designed niche on a prominent wall in the James G. Leyburn Library. In the mid 1980s, however, the painting returned to India for three years, where it was on display in the consulate in New Delhi as a loan through the State Department’s ART in Embassies Program. In the 1990s, the portrait was again on loan, exhibited in Richmond at both the Virginia Museum of Fine Arts and

Virginia Historical Society. After another eight-year loan to the Westervelt-Warner Museum in Tuscaloosa, Alabama (2003-2011), the painting finally came home.

Attribution of the portrait is still in question. Most recent theories center not only on William Winstanley, but possibly Edward Savage (50). And there are those who still believe the painting may be by Stuart himself. As Sylvia Hochfield stated in her 1982 article for *ARTnews* on the White House portrait, “It is sometimes difficult to tell if a particular example is a very bad Stuart or a very good copy” (46).

Analysis

The painting was analyzed entirely non-destructively by an undergraduate researcher under close curatorial supervision. Because the painting had spent so much time in Calcutta, India (whose hot and humid climate is not conducive to painting preservation) and was over two centuries old, we suspected we would find some significant areas of damage, in spite of the good condition of the painting that had been reported in 1976 (47). Thus, the painting was examined carefully under UV illumination, and visible fluorescence revealed many areas of retouching or inpainting. Additionally, the IR camera (*vide supra*) was particularly useful in revealing areas of damage. A photo of the sword tassel under UV illumination (Figure 20) revealed a difference in fluorescence to the right of the tassel, and an IR photograph of the same area (Figure 21) revealed the damage that had been repaired or overpainted. Similarly, a photograph of the UV fluorescence in the area of the pewter dog near the inkwell on the table (Figure 22) revealed likely damage underneath the dog’s feet, and the IR photograph (Figure 23) confirmed that damage. Several such areas were documented both under UV illumination and by IR photography. In some areas, it appeared that a few restoration efforts at some point in time may have overpainted larger portions of the canvas than were damaged.

Much more interesting was the detail the IR photography revealed in the black velvet clothing worn by Washington, and the detail in other black areas of the painting. Black passages can lose their tonal contrast with time and become visually muddy. There is agreement that the quality of this painting is not up to Stuart’s standard, but it was exciting to see that the quality was greater than is now evident to the naked eye. Many IR photographs were taken, and two show the detail visible in the IR that has been lost in the visible. For instance, an IR photograph of the vest area (Figure 24) revealed buttons, and an IR photograph of Washington’s proper left knee (Figure 25) revealed lost detail and brushwork.



Figure 20. Photograph of visible fluorescence under UV illumination of Washington's sword tassel.

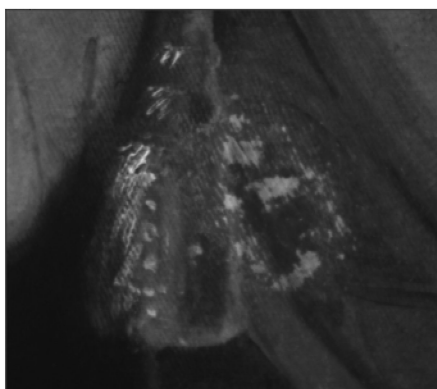


Figure 21. IR photograph (900-1700 nm) of the tassel area confirming overpaint in the damaged area revealed by the fluorescence difference under UV.



Figure 22. Photograph of visible fluorescence under UV illumination of the pewter dog near the inkwell on the table.

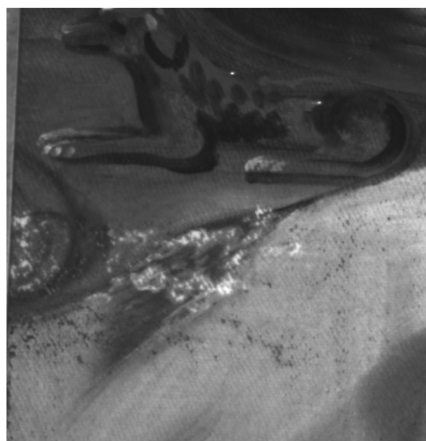


Figure 23. IR photograph (900-1700 nm) of the pewter dog near the inkwell on the table confirming overpaint in the damaged area revealed by the fluorescence difference under UV.

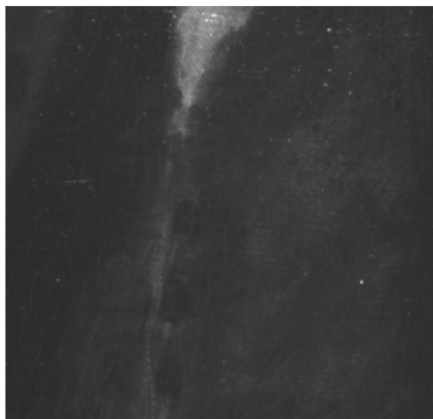


Figure 24. IR photograph (900-1700 nm) of the vest area of Washington's black velvet suit showing the presence of buttons that are not distinguishable to the unaided eye under visible light.



Figure 25. IR photograph (900-1700 nm) of the area around Washington's proper left knee showing detail in the brushwork and delineation of form that has been lost to the unaided eye under visible light.

IR photography of the hands (Figures 26 and 27), the feet (e.g., Figure 28), and the face (Figure 29) revealed artistic technique in the sweeping brush strokes that outline the fingers of the hands or the shoes., while an IR photograph of Washington's lower face revealed some slight modifications to the chin and neck area. It should be noted that no underdrawing was definitively detected in any of the images obtained (although see Figure 26).

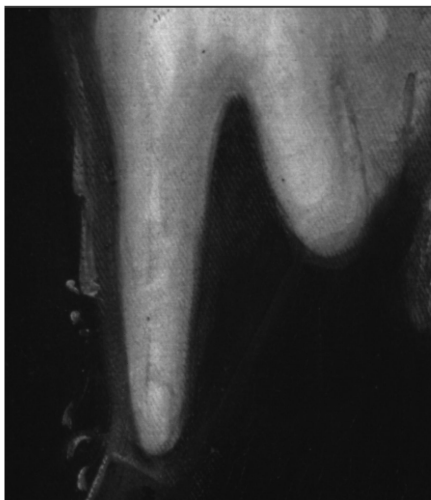


Figure 26. IR photograph (900-1700 nm) of Washington's proper left hand showing the sweeping brush strokes following the contours of the outline of the hand. Underdrawing lines may be visible between the fingers.



Figure 27. IR photograph (900-1700 nm) of Washington's proper right hand showing the sweeping brush strokes following the contours of the outline of the hand.

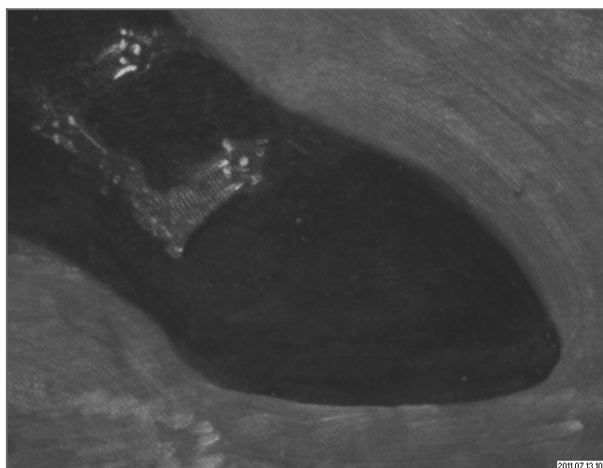


Figure 28. IR photograph (900-1700 nm) of Washington's proper left foot showing the sweeping brush strokes following the contours of the shoe.

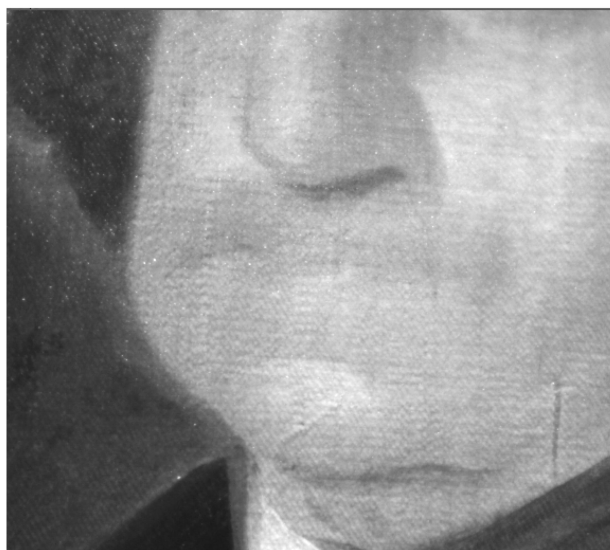


Figure 29. IR photograph (900-1700 nm) of the lower portion of Washington's face, showing the sweeping brush strokes following adjustment of the form of the proper right cheek and neck area.

pXRF analysis was very straightforward and revealed elements consistent with pigments in use at the turn of the 19th century (34); the spectra were similar to the Peale spectra obtained (*vide supra*). Differences were noted, however. A few of the spectra revealed zinc, which, although observed in zinc white since the turn of the nineteenth century, did not achieve much popularity with artists until roughly 1850 (51). These spectra may involve areas of retouching or inpainting that we did not detect under UV fluorescence or IR photography. No antimony (indicative of Naples Yellow) was observed. Lots of iron-based pigments were revealed, and, of course, mercury in the form of vermilion was detected in many red areas. The green areas did not show significant copper peaks. The blue areas did not show copper peaks either, and indigo (an organic dye) would be undetectable by pXRF, and Prussian blue, because of its high tinting strength (and therefore typical low abundance in use) and background iron peaks, also could not be confirmed or refuted. The black areas showed no clear presence of phosphorous, probably indicating one of the carbon blacks other than bone black or ivory black (40).

Conclusion

We have analyzed several objects either owned by George Washington or associated closely with him. Analysis of the Society of the Cincinnati porcelain provided a clear, unambiguous benchmark for detecting pieces employing chromium for the green coloration. Analysis of Charles Willson Peale's Lafayette painting confirmed areas of loss previously reported and showed his use of typical pigments for his era. IR photography of the Lansdowne copy, generally agreed on as not by Gilbert Stuart, shows that it is the work of a skilled, careful artist yet to be identified. We hope that the collection of IR photographs and pXRF spectra might be of future use in helping to determine the authorship of the Lansdowne copy.

Acknowledgments

The NSF is gratefully acknowledged for recently funding non-destructive analytical instrumentation (NSF 0959625) at W&L that was used in the examinations reported here; the NSF is also thanked for funding Chemistry in Art Workshops for many years. A 2009 State Council of Higher Education for Virginia Outstanding Faculty Award assisted ESU in various aspects of these projects. ESU thanks W&L for a Lenfest Summer Research Grant that facilitated two of these three projects. LFS, DSB, and DAGB thank W&L for summer undergraduate research support. ESU, PAH, and DAGB would like to thank Katherine Ridgway, Conservator, and Elizabeth Chambers, Collections Manager, Mount Vernon Estate and Gardens, for assistance with the Peale investigation during the Peale's loan to Mount Vernon. ESU would like to thank the following individuals for helpful conversations: Dr. Ellen G. Miles, Curator Emeritus, Smithsonian National Portrait Gallery; CindyLou Molnar, Head of Conservation, The National Portrait Gallery; Sarah L. Fisher, Head of Painting Conservation, National Gallery of Art (Washington, DC); Tiarna Doherty, Chief of

Conservation, Lunder Conservation Center, Smithsonian American Art Museum; Amber Kerr-Allison, Paintings Conservator, Smithsonian American Art Museum, Lunder Conservation Center; Jennifer Giaccai, Conservation Scientist, Museum Conservation Institute, Smithsonian Institution; Claire Walker, Smithsonian Postgraduate Conservation Fellow, Lunder Conservation Center, Smithsonian American Art Museum; and Dr. Bruce J. Kaiser. ESU, RWF, and LFS would like to thank Dr. Jennifer L. Mass, Senior Scientist, Scientific Research and Analysis Laboratory, Conservation Department, Winterthur Museum, for hosting discussions at Winterthur concerning George Washington's Society of the Cincinnati porcelain.

References

1. The reader should note that, because this is not a review paper, the references are not intended to be comprehensive, but should enable the reader new to porcelain and paintings investigations to get into relevant literature.
2. Myers, M., Jr. *Liberty without Anarch: A History of the Society of the Cincinnati*; University Press of Virginia: Charlottesville, VA, 1983.
3. *Yam Shiqua trade label, 58 x 33, Downs Collection*. In Winterthur Museum, Winterthur, DE, 1790–1810.
4. In *The Journals of Major Samuel Shaw*; Quincy, J., Ed.; W. Crosby and H. P. Nichols: Boston, 1847; pp 198–199.
5. Detwiler, S. In *George Washington's China Ware*; Harry N. Abrams, Inc.: New York, 1982; p 86.
6. Detwiler, S. In *George Washington's China Ware*; Harry N. Abrams, Inc.: New York, 1982; p 96.
7. de Butts, R., Jr. *The Virginia Magazine of History and Biography* **2001**, 109 #3 (3), 302–325.
8. Detwiler, S. In *George Washington's China Ware*; Harry N. Abrams, Inc.: New York, 1982; p 182.
9. *Fine Chinese Export Ceramics and Works of Art; lot 197, June 23, 1975*; In Christie's, Manson and Woods; London: 1975.
10. Bradley, L. P.; Meloni, S.; Uffelman, E. S.; Mass, J. L. Scientific Examination and Treatment of a Painting by Gijsbert Gillisz d'Hondecoeter in the Mauritshuis. In *Collaborative Endeavors in the Chemical Analysis of Art and Cultural Heritage Materials*; Lang, P. L., Armitage, R. A., Eds.; ACS Symposium Series 1103; American Chemical Society: Washington, DC, 2012; Chapter 2.
11. Uffelman, E. S.; Court, E.; Marciari, J.; Miller, A.; Cox, L. Handheld XRF Analyses of Two Veronese Paintings. In *Collaborative Endeavors in the Chemical Analysis of Art and Cultural Heritage Materials*; Lang, P. L., Armitage, R. A., Eds.; ACS Symposium Series 1103; American Chemical Society: Washington, DC, 2012; Chapter 3.
12. Bearden, J. A. In *CRC Handbook of Chemistry and Physics: A Ready-Reference Book of Chemical and Physical Data*, 60th ed.; CRC Press, Inc.: Boca Raton, Florida, 1979; pp E152–E190.

13. Mueller, S.; Mass, J. *The Magazine Antiques* **2011**, 82–84.
14. Kaiser, B. J.; Wright, A. *Draft Bruker XRF Spectroscopy User Guide: Spectral Interpretation and Sources of Interference*. Bruker: Billerica, MA, 2008.
15. Trentelman, K.; Bouchard, M.; Ganio, M.; Namowicz, C.; Patterson, C. S.; Walton, M. *X-Ray Spectrom.* **2010**, 39, 159–166.
16. Namowicz, C.; Trentelman, K.; McGlinchey, C. *Powder Diffraction* **2009**, 24, 124–129.
17. Shugar, A. N.; Mass, J. L. *Handheld XRF for Art and Archaeology*; Lueven: Belgium, 2012.
18. Greenwood, N. N.; Earnshaw, A. In *Chemistry of the Elements*; Butterworth Heinemann: Oxford, 1997; p 1002.
19. Preaud, T.; Ostergard, D. E. *The Sevres Porcelain Manufactory: Alexandre Brongniart and the Triumph of the Art and Industry, 1800-1847*; Yale University Press: New Haven, 1997.
20. Ward, D. C. *Charles Willson Peale: Art and Selfhood in the Early Republic*; University of California Press: Berkeley, 2004.
21. Miller, L. B.; Ward, D. C. *New Perspectives on Charles Willson Peale*; University of Pittsburgh Press: Pittsburgh, 1991.
22. Idzerda, S. J.; Loveland, A. C.; Miller, M. H. In *Lafayette, hero of two worlds: the art and pageantry of his farewell tour of America, 1824-1825: essays*; Idzerda, S. J., Loveland, A. C., Miller, M. H., Eds.; Queens Museum, Distributed by University Press of New England: Lebanon, NH, 1989; p 96.
23. Messing, C. H.; Rudder, J. B.; Shaw, D. W. In *A Son and his Adoptive Father: The Marquis de Lafayette and George Washington*; The Mount Vernon Ladies' Association: 2006; p 122.
24. Sellers, C. C. *Portraits and Miniatures by Charles Willson Peale*; Transactions of the American Philosophical Society: Philadelphia, PA, 1952; Vol. 42, Part 1.
25. Miller, L. B.; Hart, S.; Appel, T. A. In *The Selected Papers of Charles Willson Peale and His Family*; Yale University Press: New Haven, 1983; Vol. 1, pp 350–352.
26. In *The Writings of George Washington from the Original Manuscript Sources, 1745-1799*; Fitzpatrick, J. C., Ed.; United States Government Printing Office: Washington, DC, 1936; Vol. 20, p 463.
27. Miller, L. B.; Hart, S.; Appel, T. A. In *The Selected Papers of Charles Willson Peale and His Family*; Yale University Press: New Haven, 1983; Vol. 1, pp 356–357.
28. *Freeman's Journal and Philadelphia Daily Advertiser*; October 13, 1784.
29. *Marie Joseph Paul Yves Roch Gilbert Motier, Marquis De Lafayette*. http://www.nps.gov/museum/exhibits/revwar/image_gal/indeimg/lafayette.html (March 25, 2012).
30. Miller, L. B.; Hart, S.; Appel, T. A. In *The Selected Papers of Charles Willson Peale and His Family*; Yale University Press: New Haven, 1983; Vol. 1, pp 359–360.
31. Lee, R. E., Jr. In *Recollections and Letters of General Robert E. Lee*; Konecky and Konecky: New York, 1998; p 354.

32. Bomford, D. *Art in the Making: Underdrawings in Renaissance Paintings*; National Gallery (London) Company: London, 2002.
33. Delaney, J. K.; Zeibel, J. G.; Thoury, M.; Litteton, R.; Morales, K. M.; Palmer, M.; de la Rie, R. *Proc. SPIE* **2009**, 7391, 739103-1–739103-8.
34. Mayer, L.; Myers, G. *American Painters on Technique: The Colonial Period to 1860*; J. Paul Getty Trust: Los Angeles, CA, 2011.
35. Helwig, K. In *Artists' Pigments: A Handbook of Their History and Characteristics*; Berrie, B. H., Ed.; Archetype Publications: London, 2007; Vol. 4, pp 39–109.
36. Eastaugh, N.; Walsh, V.; Chaplin, T.; Siddall, R. *Pigment Compendium: A Dictionary and Optical Microscopy of Historical Pigments*; Butterworth-Heinemann: Oxford, 2008.
37. Wainwright, I. N. M.; Taylor, J. M.; Harley, R. D. In *Artists' Pigments: A Handbook of Their History and Characteristics*; Feller, R. L., Ed. Oxford University Press: New York, 1986; Vol. 1, pp 219–254.
38. Laver, M. In *Artists' Pigments: A Handbook of Their History and Characteristics*; Fitzhugh, E., Ed.; Oxford University Press: New York, 1997; Vol. 3, pp 295–355.
39. Gettens, R. J.; Feller, R. L.; Chase, W. T. In *Artists' Pigments: A Handbook of Their History and Characteristics*, Roy, A., Ed.; Oxford University Press: New York, 1993; Vol. 2, pp 159–182.
40. Winter, J.; Fitzhugh, E. W. In *Artists' Pigments: A Handbook of Their History and Characteristics*; Berrie, B. H., Ed.; Archetype Publications: London, 2007; Vol. 4, pp 1–37.
41. Evans, D. *The Genius of Gilbert Stuart*; Princeton University Press: Princeton, NJ, 1999.
42. Christman, M. C. S. In *George Washington: A National Treasure*; Smithsonian Institution: Washington, DC, 2002; pp 42–76.
43. Miles, E. G. In *George Washington: A National Treasure*; Smithsonian Institution: Washington, DC, 2002; pp 77–101.
44. Barratt, C. R.; Miles, E. G. *Gilbert Stuart*; The Metropolitan Museum of Art: New York, NY, 2004.
45. Miles, E. G. *George and Martha Washington: Portraits from the Presidential Years*. National Portrait Gallery, in association with the University Press of Virginia: Washington, DC, 1999.
46. Hochfield, S. *ARTnews* **1982**, January, 62–63.
47. Emrich, D. *Smithsonian* **1976**, February, 114–119.
48. Emrich, D. Historical notes prepared by Duncan Emrich, four-page typescript, signed and dated December 1963, object file U1980.1.1, University Collections of Art and History, Washington and Lee University; 1963.
49. Lynes, R. *Harper's Magazine* **1966**, June, 28.
50. Miles, E. G.; Molnar, C. Gilbert Stuart Lansdowne Portrait Discussion, personal communication, December 12; Washington, DC, 2011.
51. Kuhn, H. In *Artists' Pigments: A Handbook of Their History and Characteristics*; Feller, R. L., Ed.; Oxford University Press: New York, 1986; Vol. 1, pp 169–186.

Chapter 17

The Spectroscopic Analysis of Paints Removed from a Polychrome Wood Sculpture of *Male Saint*

Patricia L. Lang,* Shawn P. Leary, Rebecca F. Carey, Melissa
N. Coffey, Rick E. Hamilton, Amber L. Klein, Randall T. Short,
and Philip A. Kovac

Department of Chemistry, Ball State University,
2000 West University Avenue, Muncie, IN 47306

*E-mail: plang@bsu.edu

The examination of paints removed from a late 15th century South German sculpture known as *Male Saint* from the circle of Hans Multscher was performed utilizing both infrared spectroscopic and energy dispersive x-ray analysis. Pigments and paint components identified that are consistent with the sculpture's date include red ochre, azurite, gold, calcium carbonate, gypsum, China clay, hide glue, protein/oil binder, and linen fibers. The presence of a copper acetoarsenite in the green paint on the base is indicative of an application of paint after 1800.

Introduction

Unfamiliar to many is the genre of limewood sculptures that were made in Germany starting in the 15th century. Amongst the most distinguished and prodigious of the early craftsmen was Hans Multscher (1400-1467) of the German region of Swabia (1). Multscher's work spanned a period that marked a transition in this region from Gothic to more realistic forms of art (2). By 1430, his sculptures and those from his large workshop were characterized by a sense of movement exhibited under the naturalistic drape of the figure's cloak. Such features were, in part, facilitated by the use of the wood, *Tilia platyphyllos*, a broad-leafed limewood species indigenous to southern Germany. The wood's

uniform cellular structure gives rise to its elasticity, lightness, and tractability, traits important for the carver (1).

Additionally, until the end of the 15th century, it was traditional for the limewood sculptures to be painted. Although the polychrome palette was typically a limited one of blue, green, red, black, gold, and white pigments, a range of textures and patterns could be created by modifying the contour of the gesso ground by the use of textiles, and/or patterning tools (1).

The current work under study is a polychrome wood sculpture from the circle of Hans Multscher housed in the David Owsley Museum of Art at Ball State University. *Male Saint*, 2007.004.002, stands over 5 feet tall and is sculpted from the thick “C” of a limewood trunk which remains after the heartwood core is removed. See Figure 1. The dark beige paint on his neck, face, hands, and hair shows little deterioration. Substantial paint remains on the saint’s gold cloak, the blue inner lining of the cloak, and the green octagonal base, although there are scattered areas of loss. The binding of the red book that hangs from his belt shows substantial paint loss. Least intact is the yellow ochre-colored paint on the gown where there is uniform paint and ground loss. *Male Saint* was acquired by the museum in 2007.



Figure 1. Male Saint, Circle of Hans Multscher, 1450/1499. Gift of David Owsley via the Alconda-Owsley Foundation, 2007.004.002. Photo courtesy of the David Owsley Museum of Art at Ball State University. (see color insert)

The paint analysis was performed as a diagnostic prerequisite to a future conservation process. Although there are many chemical instrumental techniques available for analysis of pigments and paint components, including non-destructive techniques such as Raman microscopy, X-radiography, and X-ray fluorescence (3), the complementary techniques of infrared spectroscopy and scanning electron microscopy with energy dispersive x-ray detection (SEM-EDS) are a powerful combination of methods that are easy-to-use provided that a small sample can be removed. Many organic and inorganic colorants, binders, additives, grounds, and sizing agents are easily identified (4, 5) using the selective, molecular information provided in their infrared spectra, while those inorganics that have absorptions below the detector cut-off range or which are infrared inactive can often be identified with the characteristic elemental information provided in the EDS spectrum (6). Further, attenuated total reflection infrared *micro*spectroscopy has been used to identify pigments (7); however, the universal ATR accessory available on most instruments is sensitive enough to provide high quality spectra on extremely small paint samples as small as 500 μm (8) with no sample preparation. While the resolution or detection limit may not be as good as the infrared microscope, the information gained can be quite valuable as the paper describes, and the fact that it is a surface technique is useful as different spectral information can be obtained on each side of a paint sample.

The ease of analysis was an important consideration, given that the work was done as part of an immersive learning experience for undergraduate students in the Chemistry of Artists' Pigments course. Consequently, the analysis described is not an exhaustive study of the sculpture, but an initial investigation that yielded interesting results.

Experimental Section

Using a scalpel, samples approximately 250-750 μm in diameter, were obtained from areas that were unobtrusive or already deteriorating. (See Figure 2.) Removal of samples this size did not result in visible damage to the art.

Multiple paint samples and one fiber bundle were obtained from the locations (L) shown in Figure 3. The samples included a blue paint (L1 and L3), green paint (L2 and L4), red paint (L6), gold/red paint (L5), and a fiber bundle (L7). After removal, the samples were examined under a stereomicroscope to note the color, homogeneity, and general appearance of the samples.

A Perkin-Elmer 1600 infrared spectrometer fitted with a universal attenuated total reflectance accessory with a diamond element was used to acquire spectra at 4 cm^{-1} spectral resolution with four signal-averaged scans per spectrum. The infrared spectra were compared with those in Artists and Artisans Materials Infrared Spectral Library (9) or to the principal author's reference library for identification purposes. Multiple spectra were obtained on each paint sample.

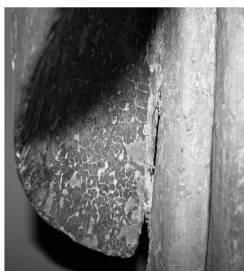


Figure 2. Close-up of bottom right of blue cloak on Male Saint showing localized areas of deterioration prior to sampling.

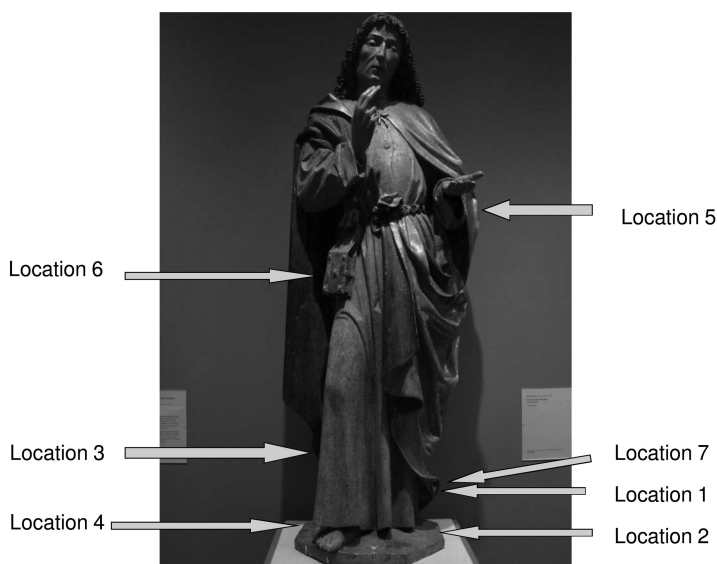


Figure 3. Sample locations.

SEM/EDS spectra were obtained using the electron beam source from a JEOL Scanning Electron Microscope as an excitation source and the emitted radiation was collected with a Noran 666B Energy Dispersive X-ray detector. The accelerating voltage was set to 15 keV, and the working distance was 30 mm. Paint samples were placed on carbon tab with no other preparation.

Microscopic analysis of the pigments was performed when additional information was needed for confirmation.

Results and Discussion

White on Back of Most All Samples

One of the pigments found on the back of the paints removed from all sampling locations was calcium carbonate, CaCO_3 , which was used in the ground. The infrared spectrum of a representative sample is shown in Figure 4. Characteristic CO_3^{2-} bands at 1420 cm^{-1} (asymmetric C-O stretching), 875 cm^{-1} (out-of-phase bending) and 728 cm^{-1} (OCO in-plane deformation) are marked in Figure 4 and assigned based on literature (10). Additionally, the spectrum matches reference spectra of its most common form, calcite (9).

Calcium carbonate has been an important artist's material since the classical times. CaCO_3 is found mainly in sedimentary rocks such as chalk and limestone but is also found in skeletal material of marine life. In German paintings on wood panels, the calcium carbonate used was typically from quarried chalk that had been ground and washed (11). The presence of the substance on the back of most of the paint samples, in a layer of about $500\text{ }\mu\text{m}$ thick, is consistent with the known preparation of the wood surface as discussed in the introduction (1).

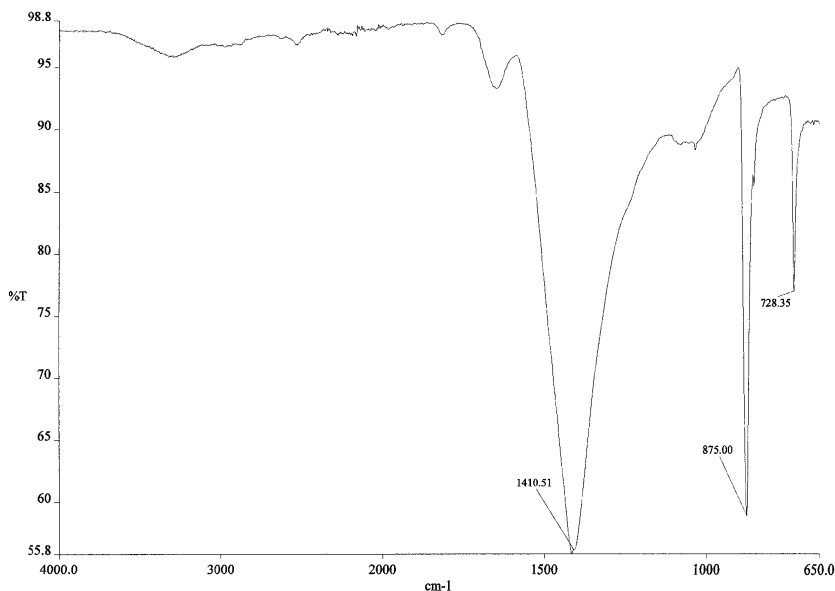


Figure 4. Infrared spectrum of white on back of all paints.

Blue Paint from Cloak Bottom

Samples were taken from the bottom left lining of the cloak (L1) outside of the fold (Figure 3) and the bottom right lining of the cloak (L3) as shown in Figures 2 and 3. When viewed under a polarizing microscope, a birefringent structure was clearly visible under cross-polars. A representative infrared

spectrum of the blue from that location is shown in Figure 5. The spectrum matches those of the blue basic form of copper, $2 \text{CuCO}_3 \cdot \text{Cu}(\text{OH})_2$, or azurite (11). Characteristic absorptions at 3426 cm^{-1} (O-H stretching), 1401 cm^{-1} (asymmetric CO_3^{2-} stretching), 949 cm^{-1} (C-O-H bending), and $834/814 \text{ cm}^{-1}$ (out-of-phase bending) are marked (12).

Azurite is one of the most important blue pigments in European painting during the middle ages and Renaissance, since its stable color is more economically convenient than the preferred ultramarine blue. It was prepared by grinding, washing, and levigating the natural mineral. Whilst the artificial basic copper carbonate, blue verditer, has an almost identical infrared spectrum (9), the blue particles in these samples from *Male Saint* have an irregular, broken fractured appearance characteristic of natural azurite (11).

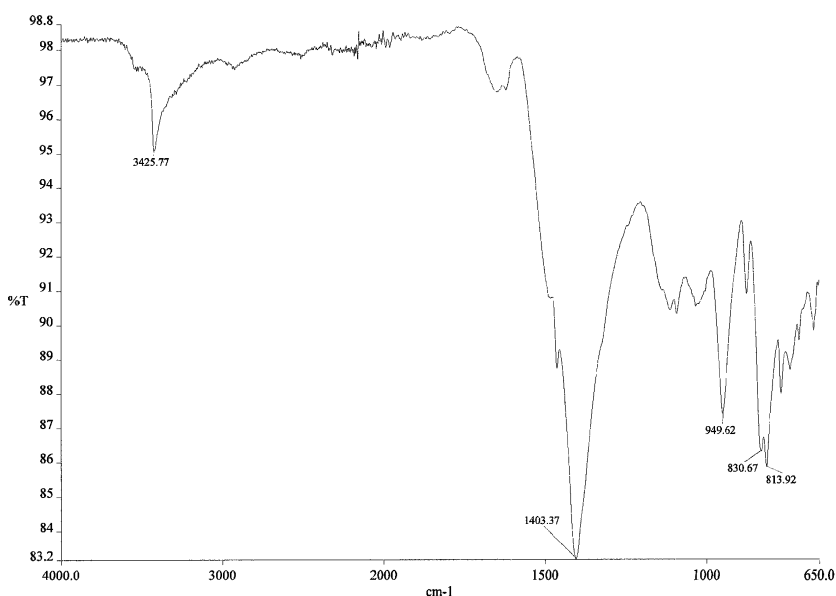


Figure 5. Infrared spectrum of blue paint from cloak identified as azurite. Blue side against the ATR element.

Green Paint from Base

A representative infrared spectrum of the green paint from both sides of the back of the base (L2 and L4) of the sculpture is shown in Figure 6. The presence of distinctive bands at 1555 cm^{-1} and 1451 cm^{-1} are indicative of the coupled carbonyl stretches of an acetate, the higher being the out-of-phase COO^- stretch and the lower, the COO^- in-phase stretch. This is strongly suggestive of verdigris, a hydrated basic copper acetate that can take on various forms, most of which are blue (11). However, the out-of-phase acetate stretching frequency does not match that found in verdigris which is at 1600 cm^{-1} (9, 13). There was no presence of

either blue or yellow pigments in our samples upon close examination under the microscope, which would indicate a mixture was used.

SEM/EDS data obtained on the green particles, indicated the presence of both copper and arsenic. This suggests Emerald Green, $\text{Cu}(\text{C}_2\text{H}_3\text{O}_2)_3 \cdot 3\text{Cu}(\text{AsO}_2)_2$, a copper acetoarsenite, and the acetate stretching frequencies match up with the reference spectrum (9) of Emerald Green. The identification of this pigment indicates that the green paint was applied later, since Emerald Green was not used until the early 19th century.

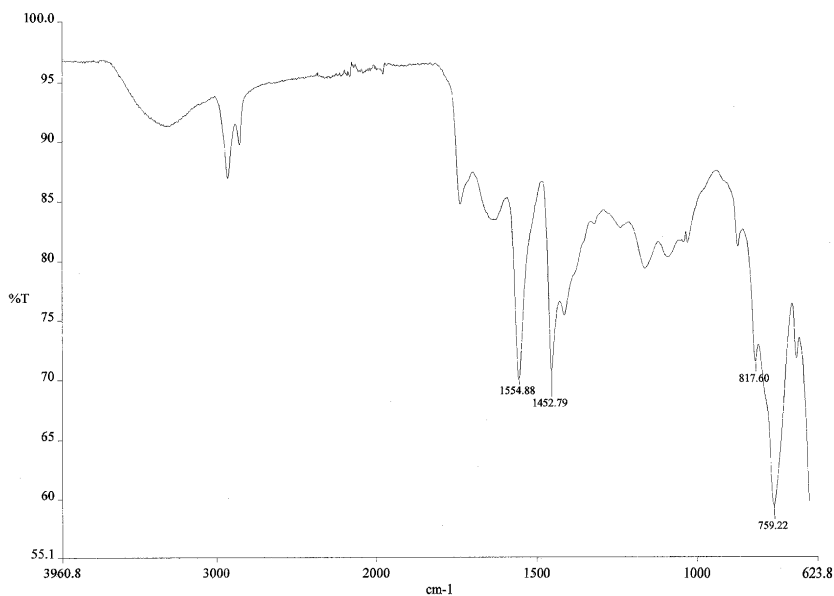


Figure 6. Infrared spectrum of green paint from base. Green side against ATR element.

The sample is much more complicated, however, as one observes additional bands in the spectrum shown in Figure 6. Under microscopic examination the green paint samples have a transparent “glaze” on top of the green paint, and a representative spectrum obtained from the glaze is shown in Figure 7.

The spectrum matches that of a natural protein, which could be a gelatin, egg white, or casein protein used as a binder or glaze (9). Characteristic broad bands due to natural polyamides are marked at 3290 cm^{-1} (N-H stretching), 3073 cm^{-1} (overtone of the amide II band), 1629 cm^{-1} (amide I, interaction of C=O stretch with NH_2 deformation), and 1540 cm^{-1} (amide II, involving the NH deformation and CN stretch) (14). An attempt to identify hydroxyproline present in the sample, which would indicate hide glue, using Erlich’s reagent was inconclusive due to the minimum sample size (15).

Although the identification of a protein in this sample allows the absorptions at 3300 and 1630 cm^{-1} to be assigned in the spectrum shown in Figure 6, still

unexplained are the absorptions at 2927, 2854, 1737, and 1160 cm^{-1} . These can be assigned to methylene asymmetric and symmetric stretching, respectively, and the C=O stretching and C-O stretching, respectively of an ester; all of which are consistent with the frequencies in linseed oil (9).

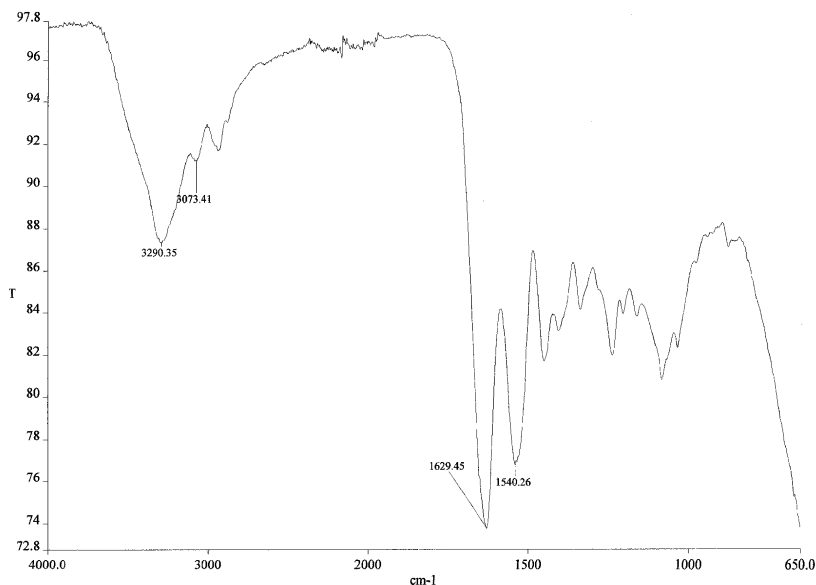


Figure 7. Infrared spectrum of the transparent glaze on green paint from base. Glaze side against ATR element.

Gold and Red Paint from Cloak

Samples taken from the *Saint's* cloak on his left (L5) were gold and red colored. Under microscopic examination of the samples' cross sections, a gold layer appeared to be the last applied, but in other samples, the gold looks intimately burnished into the red pigment. Under the gold/red layer was a white layer (500 μm thick), followed by an opaque, striated glaze layer (about 150 μm thick).

The pigment layers could not be physically separated as they were too thin and tightly bound. A representative spectrum of the paint, however, is shown in Figure 8. Absorptions at 3695, 3620, 1090, 1032, 998, and 907 cm^{-1} are most consistent with those of kaolin, in both frequency and relative intensity (9), although the frequencies are not an exact match. The sharp 3695 and 3620 cm^{-1} bands are non-hydrogen-bonded O-H stretching absorptions, while the lower frequency absorptions correspond to Si-O stretching modes. Kaolin, or China clay, is an aluminum silicate with the typical formula $\text{Al}_2\text{O}_3 \cdot 2\text{SiO}_2 \cdot 2\text{H}_2\text{O}$; it is a natural clay that is used to provide a paint with improved consistency. Additionally, the absorptions at 3532 and 3392 cm^{-1} are characteristic of the

asymmetric and symmetric O-H stretches found in gypsum, $\text{CaSO}_4 \cdot 2\text{H}_2\text{O}$ (9, 16) along with a 1619 cm^{-1} band and a shoulder at 1135 cm^{-1} that can be assigned to gypsum (9, 15). Additional spectra of these samples show more clearly the presence of the intense 1135 cm^{-1} absorption in gypsum, due to SO_4^{2-} asymmetric stretching (9, 16). Unassigned absorptions in the region between 1400 and 3000 cm^{-1} are indicative of an organic substance(s) presence, perhaps an oil and a protein.



Figure 8. Infrared spectrum of gold and red paint from cloak. Gold/red side was against the ATR element.

However, none of these findings indicate a pigment responsible for either the gold or red color present. The SEM/EDS data show the presence of gold, clearly indicating a gilding applied on top of the red. Elemental iron is also present, suggesting a red ochre, Fe_2O_3 , as a source of the red color in the second layer. Other elements identified (C, O, Al, Si, S, Ca) were consistent with the presence of China clay and gypsum, which are typically substances used with ochre pigments. Mg was also present, indicating the presence of another unidentified mineral, perhaps a silicate of calcium and magnesium. Overlapping bands in the Si-O stretching region would explain the apparent shifts in the kaolin absorptions in that region.

The findings suggest a water gilding technique was used where the thin gold leaf was applied to an adhesive layer of a colored clay mixed with hide glue. The red bole warms the color of the gilding and provides cushion against which to burnish (17).

Red Paint from Book Binding

A sample of red paint removed from the book binding (L6) consisted of a red colored layer on top, a white layer, followed by a striated glaze layer next to the wood. These appeared very similar under the microscope to those observed in the *three* layers found underneath the gold and red paint from the cloak (L5).

A representative infrared spectrum is shown in Figure 9. The spectrum shows previously discussed bands due to kaolin (stars), gypsum (circles), protein (triangles), and calcium carbonate (rectangles). The 2919 and 2850 cm^{-1} bands and the shoulder at about 1730 cm^{-1} (not marked), can be due to the presence of an esterified oil, such as linseed.

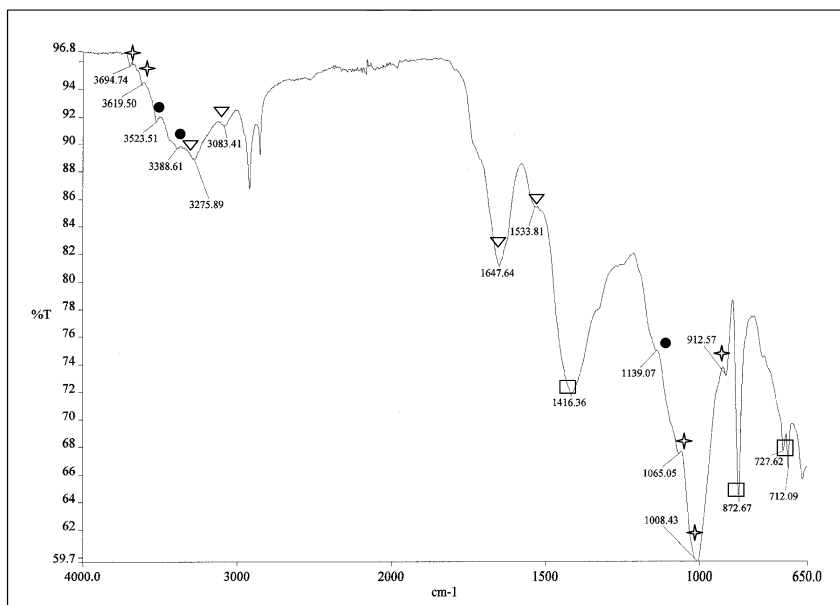


Figure 9. Infrared spectrum of red paint from book binding.

As in the case with gold and red paint removed from the cloak, there is no indication of a red pigment in the spectrum in Figure 9 or any taken from this sample. However, iron is present in the SEM/EDS spectrum, suggesting a red ochre as the compound responsible for the color as found in the outer cloak. Elements consistent with kaolin, gypsum, and calcium carbonate are also present (C, O, Al, Si, S, Ca). Mg was present, as in the paint of the outer cloak, suggesting that an additional silicate was also present. Although no gold was detected in

the elemental analysis, scattered metallic particles are apparent in some samples viewed under the microscope, and perhaps there was not enough gold present to be adequately detected. The book binding from which the red paint was removed was in an area with little paint remaining.

An infrared spectrum of the white layer confirmed the presence of calcium carbonate, and that of the striated, opaque glazed bottom layer confirmed the presence of protein. An Erlich's test on the latter was inconclusive.

Fiber Bundle Removed from Base of Cloak

A fiber bundle was removed from *Saint's* left side at the bottom of the cloak (L7). The sampling area is shown more clearly in Figure 10. The bundle was white and gradually turned very dark at the end that had been attached to the sculpture.

The spectrum at the white end of the bundle (Figure 11) showed bands consistent in frequency and intensity to the C-O stretching region of cellulose at 1107, 1152, 1027, 999, and 981 cm^{-1} . Under microscopic examination, the presence of fine lumen and cross-hatchings are visible in the fibers (18, 19), an indication that the cellulose fibers are from a linen textile.

The spectrum in Figure 11 also shows the presence of protein, as indicated by the amide I and II bands. As infrared spectra are taken of the fibers toward the darker end, the protein bands become more intense relative to the cellulose absorptions. Erlich's tests were positive for the fibers at the dark end indicating the presence of hydroxyproline, an amino acid present in hide glue. Thus, one can conclude that a linen was attached to the sculpture with a gelatin or an animal glue which has discolored over time. The linen was perhaps used for the purpose of joining two pieces of the sculpture together in this location. A publication on a similar sculpture of this genre reports that linen was applied to the entire wood surface before ground was applied (6).



Figure 10. Area on bottom left of cloak where textile fibers were sampled.

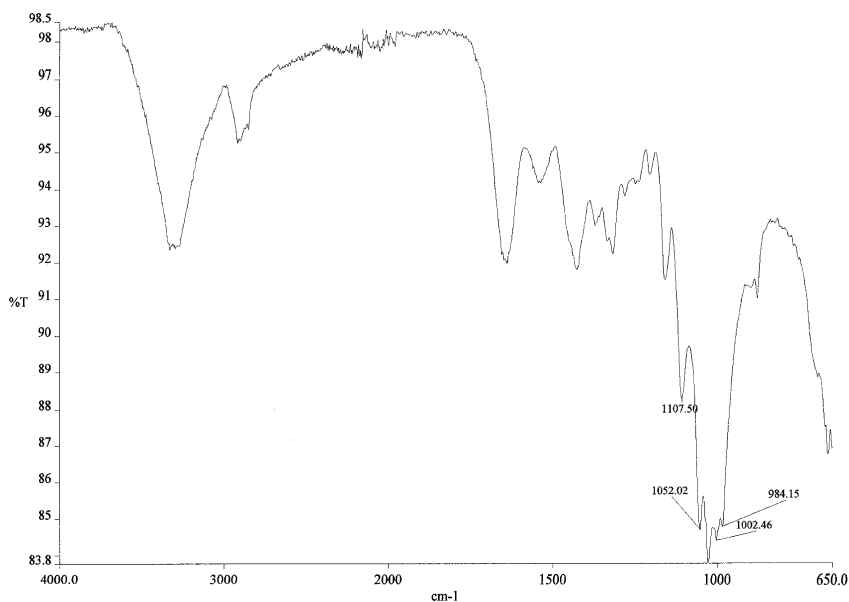


Figure 11. Infrared spectrum of white end of fibers.

Summary and Conclusions

Pigments and Components

With the exception of the Emerald Green identified on the base, all materials are consistent with the purported date of the sculpture. This finding, of course, does not verify that they are original paints, only that they *could* be. A summary is shown in Table I. with the layers listed from the last applied to those nearest to the wood.

The only evidence of possible unoriginal paint is that of the Emerald Green. Not only was that pigment not synthesized until well after the sculpture's date, the green base was the only area where there was a clear indication of a transparent protein glaze applied on top of the paint. On close examination of the sculpture's base, one can observe a very thin layer of a slightly different shade of green paint underneath the Emerald Green, which is most likely the original paint. Resampling of that area has not resulted in identification of this paint, as it adheres tightly to the sculpture and samples were not obtained.

The detection of protein and oil absorptions in all of the samples except for the blue azurite might be an indication that the artist used a combination of oil and protein as the binding medium. These bands might have been obscured in the spectra of the blue paint because the intense azurite absorption at 1400 cm^{-1} may

mask the amide II band, and the azurite particles were easily physically isolated from the rest of the paint. A band at 1650 cm⁻¹ in Figure 5 can be observed which could be the amide I band. There are also some indications of gypsum (1619 and 1130 cm⁻¹) and silicates (region around 1100 cm⁻¹) present, also common in the red paints.

Another conclusion is that the red on the outer cloak and the red on the book binding are the same paint formulations, consistent with the simple palette of the day.

Of particular interest is the striated, opaque, glazed *bottom* layer of the red paints. Identified as protein, most likely it is a hide-glue used as a sizing agent before the ground is applied, and the striations show the roughening of the wood's surface as preparation to accept the size.

“Macroscopic” ATR Analysis

The use of a universal ATR accessory for initial investigations of art and cultural objects has some obvious advantages, its ease of use being one. In this study, it allowed the analysts to quickly and easily gain surface information on samples as small as 500 x 500 μm. Infrared microspectroscopy has higher spatial resolution, but sample preparation and acquisition of spectra are more time-consuming. Thus, the use of a macroscopic universal ATR accessory served well as an efficient screening method for material identification, the results of which point to particular areas for future study.

Further Work

As discussed in the introduction and elaborated on in another publication in this monograph (20), the examination of *Male Saint* was undertaken as part of 15-week immersive learning course. To help increase the chance of finding an interesting result (for the students) using primarily infrared spectroscopy in the time period allowed, sampling was avoided in locations where there the paints *might* be composed of earth pigments, oxides, or non-infrared absorbing species. This was the reason the ochre-colored robe was not sampled in this study. The areas of the sculpture's hands, face, neck, and hair show paint that appears relatively undamaged and firmly attached and were not part of this study. However, before conservation proceeds, those areas will be sampled. The green paint on the sculpture's base will be re-sampled in the areas where one might find applications of the original paint. Infrared and EDS techniques will be used to identify the materials.

Additionally, the layering and chronology of paint and gilding application will be analyzed using microscopic examination of carefully prepared cross-sections. When a higher spatial resolution of samples is necessary, infrared *microspectroscopic* analysis will be used.

Table I. Summary of paint layering and pigments identified

<i>Area</i>	<i>Layering: appearance and color</i>	<i>Substances</i>
Cloak lining L1, L3	Top (1) Blue	Azurite
	(2) White	Calcite
	(3) striated, opaque, glaze	protein
Base L2, L4	Top (1) Transparent glaze	protein
	(2) green	Emerald green with protein, oil
	(3) White	Calcite
Outer Cloak L5	Top (1) Metallic gold, fluoresces with UV	Elemental gold, with protein, oil
	(2) Red-brown	Red ochre with protein, gypsum, clay, other silicates, calcite
	(3) White	Calcite
	(4) Striated, opaque glaze	Protein
Book binding L6	Top (1) Red	Red ochre with protein, gypsum, clay, other silicates
	(2) White	Calcite
	(3) Striated, opaque, glaze	Protein

Acknowledgments

The authors gratefully acknowledge Mr. Peter F. Blume, Director of the David Owsley Museum of Art at Ball State University for allowing us the privilege to sample *Male Saint*, Mr. Robert Galyen for the SEM/EDS analysis at TAWAS, Inc., and Michael Kutis, Department of Geology at Ball State, for assistance in microscopic examination.

References

- Baxandall, M. *The Limewood Sculptors of Renaissance Germany*; Yale University Press: New Haven, CT, 1980.
- Kahsnitz, R. *Carved Splendor, Late Gothic altarpieces in Southern Germany, Austria, and South Tirol*; Getty Publications: Los Angeles, CA, 2006.
- Burgio, L.; Clark, R. J. H.; Hark, R.; Rumsey, M. S.; Zannini, C. *Appl. Spectrosc.* **2009**, *63* (6), 611–620.
- Gomez, B. A.; Parera, S. D.; Siracusano, G., Maier, M. S. *e-preservation science* [online] **2010**, *7*, 1–7. <http://www.Morana-rtd.com/e-preservation-science/2010/Maier-30-06-2008.pdf> (accessed Jan. 2, 2012).

5. Lang, P. L.; Keefer, C. D.; Juenemann, J. C.; Tran, K. V.; Peters, S. M.; Huth, N. M.; Joyaux, A. G. *Microchem. J.* **2003**, *74*, 33–46.
6. Website of Art Conservator, Nina Owczarek http://ninasue.com/Research_files/Mourning%20St%20John%20Examination.pdf (accessed Jan. 2, 2012).
7. Rizzo, A. *Anal. Bioanal. Chem.* **2008**, *392*, 47–55.
8. Coombs, D. *Int. J. Vibr. Spec.* **2** [online] **1998**, *2*, 3–13. <http://www.ijvs.com/volume2/edition2/section1.html> (accessed Jan. 2, 2012).
9. *Infrared and Raman Users Group Spectral Database*; Price, B., Pretzel, B., Eds.; The Infrared and Raman Users Group: Philadelphia, PA, 2007; Volumes 1-2.
10. Andersen, F. A.; Brecevic, L. *Acta Chem. Scand.* **1991**, *45*, 1018–1024.
11. In *Artist Pigments, A Handbook of Their History and Characteristics*; Roy, A. Ed.; Oxford Press: New York, 1993; Vol. 2.
12. Frost, R. L.; Martens, W. N.; Mahmutagic, R. E.; Klopogge, J. T. *J. Raman Spectrosc.* **2002**, *33* (4), 252–259.
13. Kuhn, H. *Stud. Conserv.* **1970**, *15* (1), 12–36.
14. *The Coblenz Society Desk Book of Infrared Spectra*, 2nd ed.; Craver, C. D., Ed.; The Coblenz Society: Kirkwood, MO, 1982.
15. Neuman, R. E.; Logan, M. A. *J. Biol. Chem.* **1950**, *184*, 299–306.
16. Derrick, M. R.; Stulik, D. Landry, J. M. *Infrared Spectroscopy in Conservation Science*; Oxford University Press: New York, 1999.
17. Sandu, I. C. A.; Afonso, L. U.; Murta, E.; De Sa, M. H. *Int. J. Conserv. Sci.* **1** [online] **2010**, *1*, 47–62. http://www.ijcs.uaic.ro/pub/IJCS-10-06_Sandu.pdf (accessed Jan. 2, 2012).
18. Goodway, M. *JAIC* [online] **1987**, *26* (1), 27–44. <http://cool.conservation-us.org/jaic/articles/jaic26-01-003.html> (accessed Jan. 2, 2012).
19. McCrone, W. C.; Draftz, R. G.; Delly, J. G. *The Particle Atlas*; Ann Arbor Science Publishers: Ann Arbor, MI, 1967.
20. Lang, P. L. The Chemistry of Artists' Pigments: An Immersive Learning Course. In *Collaborative Endeavors in the Chemical Analysis of Art and Cultural Heritage Materials*; Lang P. L.; Armitage, R. A., Eds.; ACS Symposium Series 1103; American Chemical Society: Washington, DC, 2012; Chapter 14.

Subject Index

A

- AAA treatment. *See* Acid-alkali-acid (AAA) treatment
- Acacia catechu*, 124
- Accelerator mass spectrometry (AMS), 76
- Acid-alkali-acid (AAA) treatment, 147
- ACS. *See* American Chemical Society (ACS)
- American Chemical Society (ACS), 225
- American Institute for Conservation of Historic and Artistic Works (AIC), 220
- AMS. *See* Accelerator mass spectrometry (AMS)
- Archaic Mark codex, analysis, 197, 198
- blue paint, 201
- codicological analysis, 213
- conservator Marigene Butler's handwritten notes, 200*f*
- examination and photography, 203
- forgers' textual source, 215
- gold leaf coating, 210
- ink and brown-black paint analysis, 207
- paint analysis, 204
- paint and ink binding media, 207
- parchment, carbon dating, 211
- parchment coatings, 210
- photograph, 199*f*
- previous examinations, 200
- provenance and early history, 199
- Prussian blue in Orna et al. study, 201*f*
- ultraviolet fluorescence photograph, 202*f*
- white light photograph, 202*f*
- zinc-containing pigments, 202*f*
- Art and chemistry, bridging the gap, 241
- acids and bases chemistry, 243
- Bohr's atomic model, 242
- cochineal red dye, dilution
- UV-vis spectra, 246*f*
- elements, 242
- flame test, 243*f*
- organic chemistry, 244
- organic dyes, molecular structure, 244*f*
- properties, 242
- spectroscopy, 245
- stained glass, Sainte Chapelle, Paris, France, 243*f*
- Art conservators, macroscopic imaging techniques, 3
- Art/antiques market, 2
- Artists' pigments chemistry, 231
- 2009 chemistry class, 238*f*

- chemistry topics, progression, 232
- course structure and delivery details, 233
- curriculum, immersive learning course, 236
- Male Saint*, 232, 234*f*
- scanning electron microscope with energy dispersive X-ray (SEM/EDS), 233
- student learning outcomes, 236
- students experience, 231
- syllabus outline, 235*t*
- Azurite, 290*f*

B

- Baht Thailand bullet coin, 186
- Barium sulfate (BaSO₄)
- filler, 13
- FTIR residual spectrum, 15*f*
- BaSO₄. *See* Barium sulfate (BaSO₄)
- BCCE. *See* Biennial Conference on Chemical Education (BCCE)
- Beehive formation (BH), 103
- Beeswax, IR spectra, 247*f*
- BH. *See* Beehive formation (BH)
- Biennial Conference on Chemical Education (BCCE), 225
- Blue paint, FTIR spectrum, 204*f*
- Brown-black ink analysis, 207
- Byzantine manuscripts, 213

C

- Capsaicin, 136
- Carbon dating
- parchment, 211
- University of Arizona AMS facility, 213*t*
- Cardon, 124
- cCWCS. *See* Chemistry Coalitions, Workshops, and Communities of Scholars (cCWCS)
- Cellulose nitrate, FTIR spectrum, 204*f*
- Ceramics containing cocoa residues
- caffeine in mass spectra, 136*f*
- theobromine in mass spectra, 136*f*
- Charcoal, electron micrograph, 82*f*
- Chemistry and art efforts, 220
- Chemistry Coalitions, Workshops, and Communities of Scholars (cCWCS), 224

- scholars model, community evolution, 224*f*
 web banner and logo, 226*f*
 CHS. *See* Cultural Heritage Science (CHS)
 Cincinnati porcelain society
 blue border, 258*f*
 brown wing, 259*f*
 green dress, 260*f*
 pink sash, 259*f*
 white background, 258*f*
 Cochineal red dye
 dilution, UV-vis spectra, 246*f*
 molecular structure, 244*f*
Codex Vaticanus, 199
 Codicological analysis, 198, 213
 Codicological/text-critical analyses, 216
 Copper-containing blue pigment, 60
 Crucible damascus steel blades, 155, 156
 case study, 161
 ethics, 157
 ferrous technology, type, 156
 Koftgari inscription and pattern, 162*f*
 legacy and contributions, 160
 origins, 158
 Persian knife, 162
 18th century Persian Kard, 161*f*
 United Kingdom Institute for
 Conservation (UKIC's) Guidance, 158
 Crucible damascus steel kard, case study, 161
 Cueva la Conga rock art, 75, 76
 AMS radiocarbon dating, 80, 86
 benzoic acid, 86
 charcoal, electron micrograph, 82*f*
 fatty acid composition, graphs, 84*f*
 fatty acids ratios for distinguishing food
 residues, 85*t*
 microscopy methods, 77, 81
 paint samples, 83*t*
 plasma-chemical oxidation, 80, 86
 pretreatment and plasma conditions, 80*t*
 radiocarbon dating results, 87*t*
 rock painting
 photographs, 79*f*
 samples, 76
 samples description, 78*t*
 thermally assisted hydrolysis/
 methylation-gas chromatography-
 mass spectrometry, 77, 83
 X-ray fluorescence spectroscopy, 77, 82
 Cultural heritage objects, technical
 examination, 251
 George Washington's Society of
 Cincinnati porcelain, 252
 Authentic Society of Cincinnati plate,
 254*f*
 design, green dress, 260*f*
 plate with authentic decoration, 256*f*
 plate with later decoration, 255*f*, 256*f*
 portable X-ray fluorescence
 spectroscopy (pXRF) analysis,
 256
 Society of Cincinnati porcelain, 258*f*,
 259*f*, 260*f*
 Gilbert Stuart's Lansdowne Portrait,
 copy, 268
 analysis, 274
 background, 270
 face, IR photograph, 279*f*
 foot, IR photograph, 279*f*
 George Washington (Lansdowne
 Portrait), 269*f*
 hand, IR photograph, 278*f*
 sword tassel, UV illumination, 275*f*
 tassel area, IR photograph, 275*f*
 Washington's black velvet suit, IR
 photograph, 277*f*
 Washington's proper left knee, IR
 photograph, 277*f*
 pXRF uses, 58
 Washington's Charles Willson Peale
 Portrait
 analysis, 264
 Charles Willson Peale, 261
 Lafayette black collar, 268*f*
 Lafayette red curtain, 267*f*
 Lafayette red lips, 267*f*
 Lafayette retouched area, 266*f*
 Lafayette's gold sword hilt, 265*f*
 Lafayette's yellow pants, 266*f*
 The Marquis de Lafayette, 261, 263*f*
 portrait, 262
 Cultural Heritage Science (CHS), 227
 Curcuminoids, 125*t*

D

- DART ionization. *See* Direct analysis in
 real time (DART) ionization
 DART-TOF-MS. *See* Direct analysis in real
 time-time of flight mass spectrometry
 (DART-TOF-MS)
 Dealer cleaning, 41
 Direct analysis in real time (DART)
 ionization
 ceramic fragment, 133
 indigoid, flavonoid, and anthraquinone
 dye materials, 124
 JEOL AccuTOF mass spectrometer, 125,
 134

- Direct analysis in real time-time of flight mass spectrometry (DART-TOF-MS)
- ceramics, characterizing organic residues, 131
 - biomarker compounds, 134*t*
 - biomarkers in archaeology, 132
 - cacao, 134
 - chili peppers, 136
 - exact masses, 135*t*
 - garum (fish sauce), 137
 - materials and methods, 133
 - olive oil, 138
 - samples investigated, description, 134*t*
 - theobromine and caffeine, 136*f*
 - wine, 141
- organic dyes, identification
- colorant compound(s) and exact mass, 126*t*
 - curcuminoids present in French textile, 127*f*
 - dye material, 125*t*
 - materials and methods, 125
 - quercetin in cotton-dyed with quercitron bark, 128*f*
 - sandalwood-dyed French cotton samples, 128*f*
- E**
- EDS spectrum
- black paint on desk, 210*f*
 - flesh color, 206*f*
 - ink from text, 210*f*
 - zinc white pigment, 205
- EDXRF. *See* Energy dispersive X-ray fluorescence (EDXRF)
- Energy dispersive X-ray fluorescence (EDXRF)
- medieval Korean coinage, 167
 - spectrometry, 167
 - uses, 168
- Erlich's tests, 295
- EXAFS. *See* Extended X-ray absorption fine structure (EXAFS)
- Extended X-ray absorption fine structure (EXAFS), 57
- F**
- Face, IR photograph, 279*f*
- FAIC. *See* Foundation of the AIC (FAIC)
- Fish sauce (garum), DART mass spectra, 138*f*
- Flame test experiment, 243*f*
- Flesh color, EDS spectrum, 206*f*
- Foot, IR photograph, 279*f*
- Forensic investigators, macroscopic imaging techniques, 3
- Forger's palette, analysis, 11
- Forger's textual source, 198, 215
- Forgery, technical analysis, 1
- Fourier transform infrared (FTIR) microspectroscopy, 4
 - imaging techniques, 3, 6
 - invasive scientific analysis, 13
 - microfocus X-ray fluorescence, 3
 - noninvasive scientific analysis, 11
 - pyrolysis-gas chromatography-mass spectrometry (Py-GC-MS), 5
 - Raman microspectroscopy, 4
 - sampling and cross section preparation, 4
 - visual examination, 5
- Foundation of AIC (FAIC), 220
- Fourier transform infrared spectroscopy (FTIR), 4, 24, 92
- green paint and gum Arabic reference, 211*f*
 - hide glue, 14*f*
 - polymerized linseed oil, 14*f*
 - residual spectrum
 - barium sulfate, 15*f*
 - green paint, 15*f*
 - yellow stain, 212*f*
- FTIR. *See* Fourier transform infrared spectroscopy (FTIR)
- G**
- Gas chromatography-mass spectrometry (GC-MS), 77
- GC-MS. *See* Gas chromatography-mass spectrometry (GC-MS)
- George Washington (Lansdowne Portrait), 269*f*
- George Washington's Society of Cincinnati porcelain, 252
- Authentic Society of Cincinnati plate, 254*f*
 - design, green dress, 260*f*
 - plate with authentic decoration, 256*f*
 - plate with later decoration, 255*f*, 256*f*
 - portable X-ray fluorescence spectroscopy (pXRF) analysis, 256

Society of Cincinnati porcelain, 258*f*,
259*f*, 260*f*
Gijssbert Gillisz d'Hondecoeter, 23
cock and hens, 29*f*
condition and previous treatment history,
34
construction, 31
family, 26
methodology, 24
painting, 28
treatment, 40
Gilbert Stuart's Lansdowne Portrait, copy,
268
analysis, 274
background, 270
face, IR photograph, 279*f*
foot, IR photograph, 279*f*
George Washington (Lansdowne
Portrait), 269*f*
hand, IR photograph, 278*f*
pewter dog
IR photograph, 276*f*
UV illumination, 276*f*
sword tassel, UV illumination, 275*f*
tassel area, IR photograph, 275*f*
Washington's black velvet suit, IR
photograph, 277*f*
Washington's proper left knee, IR
photograph, 277*f*
Glazing, 34
Glue-bound CaCO₃, 31
Gold leaf coating, 210
Gray imprimatura, 33
Green paint sample
FTIR residual spectrum, 15*f*
reference spectra, FTIR spectrum, 14*f*
TMAH-derivatized sample, pyrogram,
16*f*
Green pigment particles, Raman spectra,
13*f*

H

Hand, IR photograph, 278*f*
Hansa Yellow (PY3) pigment, FTIR
residual spectrum, 15*f*
Helium purging, 3
Hide glue, FTIR spectrum, 14*f*
High performance liquid chromatography
(HPLC), 124
Hondecoeter's *Cock and Hens in a
Landscape*, 28, 29*f*
Hondecoeter's *oeuvre*, black and white
rabbit, 30*f*

Hondecoeter's original sky, 37
Horse's hindquarters, photomicrographs,
17*f*
HPLC. *See* High performance liquid
chromatography (HPLC)
Hydroxypropylcellulose, 42

I

Imaging techniques, 3, 6
INAA. *See* Instrumental Neutron
Activation Analysis (INAA)
Infrared photography (IR), 24
face, 279*f*
foot, 279*f*
hand, 278*f*
Pewter dog, 276*f*
Tassel area, 275*f*
Washington's black velvet suit, 277*f*
Washington's proper left knee, 277*f*
Infra-red spectroscopy, 246
Infrared spectrum
beeswax and paraffin wax, 247*f*
blue paint, 290*f*
gold/red paint from cloak, 293*f*
green paint from base, 291*f*
red paint, 294*f*
transparent glaze on green paint, 292*f*
white end of fibers, 296*f*
white on back, 289*f*
Ink and brown-black paint analysis, 207
Ink binding media, 207
Instrumental Neutron Activation Analysis
(INAA), 97
International Institute for Conservation of
Historic and Artistic Works (IIC), 220
Invasive scientific analysis, 13
IR. *See* Infrared photography (IR)
Iron-rich quartzite, 98
Iron-rich (limonite) sandstones, 98

J

*Joining Forces: Spreading Successful
Strategies*, 221

K

Kevex Spectrace Quanx spectrometer, 187
Klucel-G, 42

L

- LA-ICP-MS. *See* Laser ablation-inductively coupled plasma - mass spectrometry (LA-ICP-MS)
- Laser ablation-inductively coupled plasma - mass spectrometry (LA-ICP-MS), 93
- bivariate plots, 105
- coating and ancient paints chemistry, 101
- coating/paint samples, concentration, 102*t*
- dendrogram, Wards method, 103*f*
- elemental concentrations
- pelletized ochre and limonite samples, using XRF, 118
 - rock coatings, ochre, prehistoric paints, limonite, and an iron-rich quartzite (nodule), 108
- hierarchical cluster analysis, 103
- instrument settings, 99*t*
- instrumentation, data acquisition, and data reduction, 98
- laser depth profiling, intensity variation, 100*f*
- Log10(As/Fe) versus Log10(V/Fe), 106*f*
- Log10(Sb/Fe) versus Log10(V/Fe), 105*f*
- Lower Pecos rock paints
- physicochemistry, 94
 - pigment sources, 91
- pigments, sources, 96
- principle component analysis (PCA), 104
- rock paints, 93
- samples, types, 97
- iron-rich quartzite, 98
 - iron-rich (limonite) sandstones, 98
 - ochre, 97
 - oxalate coating, 98
 - prehistoric paints, 97
- X-ray fluorescence (XRF), 92, 101
- Lead soaps, 39
- imprimatura layer, 40
 - sky, disturbing dark lines visible, 40*f*
 - white pigment particles, 39
- Light shellac, TMAH-derivatized sample, pyrogram, 16*f*
- Linseed oil, FTIR spectrum, 14*f*
- Linseed oil, TMAH-derivatized sample, pyrogram, 16*f*
- Lithopone, 205
- Lithopone, zinc sulfide, 205
- Little Lost River Cave, Idaho
- perishable artifacts, nondestructive dating, 144
 - reed artifact, radiocarbon dates, 153*f*
- Lower Pecos archaeological region, 93*f*

- Lower Pecos paint pigments, 107
- Lower Pecos rock paints, SEM analysis, 96

M

- Macroscopic ATR analysis, 297
- Macroscopic imaging techniques
- art conservators, 3
 - forensic investigators, 3
- Madonna and Child with St. Elizabeth, the Infant St. John, and St. Catherine*, 59, 60, 61
- Male Saint* polychrome wood sculpture
- blue cloak, close-up, 288*f*
 - blue paint from cloak bottom, 289
 - bottom of cloak, 295*f*
 - Circle of Hans Multscher, 286*f*
 - fiber bundle removal from base of cloak, 295
 - gold/red paint from cloak, 292
 - green paint from base, 290
 - infrared spectrum
 - blue paint, 290*f*
 - gold/red paint from cloak, 293*f*
 - green paint from base, 291*f*
 - red paint, 294*f*
 - transparent glaze on green paint, 292*f*
 - white end of fibers, 296*f*
 - white on back, 289*f*
- macroscopic ATR analysis, 297
- paint layering, pigments identified, 298*t*
- paints removal, spectroscopic analysis, 285
- pigments, components, 296
- red paint from book binding, 294
- sample locations, 288*f*
- textile fibers, 295*f*
- white on back, 289
- Mauveine, Perkins' synthesis, 244*f*
- Medieval Korean coinage, energy dispersive X-ray fluorescence spectrometry, 167
- chemical compositions, 169
- Cu and Fe, 181*f*
- Cu and Pb, 182*f*
- Cu and Sn, 181*f*
- Cu and Zn, 180*f*
- KA, Cu and Pb, 173*f*
- KA, KB, KC, KD, KE, KF and Kmisc, 168
- KA, Zn, Fe and Sn, 173*f*
- KA composition, 170*f*
- KB, Cu and Pb, 174*f*
- KB, Zn, Fe and Sn, 174*f*

KB composition, 170*f*
KC, Cu and Pb, 175*f*
KC, Zn, Fe and Sn, 175*f*
KC composition, 171*f*
KD, Cu and Pb, 176*f*
KD, Zn, Fe and Sn, 176*f*
KD composition, 171*f*
KE, Cu and Pb, 177*f*
KE, Zn, Fe and Sn, 177*f*
KE composition, 172*f*
KF, Cu and Pb, 178*f*
KF, Zn, Fe and Sn, 178*f*
KF composition, 172*f*
Kmisc subsets, 179
Methyl linoleate, mass spectrum, 247*f*
Microfocus X-ray fluorescence, 3
Micro-X-ray absorption spectroscopy
(μ -XAS), 57
MSTFA. *See* N-Methyl-N-trimethylsilyl-
trifluoroacetamide (MSTFA)
 μ -XAS. *See* Micro-X-ray absorption
spectroscopy (m-XAS)

N

National Science Foundation (NSF), 219
Natural Yellow 3, 124
Near infrared (NIR) image, 3, 9*f*
NIR image. *See* Near infrared (NIR) image
N-Methyl-N-trimethylsilyl-
trifluoroacetamide (MSTFA), 127
Noninvasive scientific analysis, 11
NSF. *See* National Science Foundation
(NSF)

O

Ochre, 97
Olive oil, 138
 ceramics, characterizing organic
 residues, 138
 DART studies, 138
Omnicon software, 4
Overpaint removal, 42*f*, 44*f*
Oxalate coating, 98
Oxalate-rich coating
 pictograph paints, 95
 stratigraphy, 96*f*

P

Paint analysis, 204
Paint binding media, 207
Painting
 bottom tacking margin, 8*f*
 infrared spectrum of white on back, 289*f*
 near infrared (NIR) image, 3, 9*f*
 oak wood panel, glue-joined horizontal
 planks, 31*f*
 scientific examination and treatment, 23
 UV-induced visible fluorescence images,
 8*f*
Paint layering, pigments identified, 298*t*
Paints removal, spectroscopic analysis,
 Male Saint polychrome wood sculpture,
 285
Paraffin wax, IR spectra, 247*f*
Parchment, carbon dating, 211
Parchment coatings, 210
Parchment cross section
 ink, scanning electron micrograph, 208*f*
 photomicrograph of text area, 208*f*
 photomicrograph of ink, 208*f*
 proteinaceous coating, 208*f*
Particle induced X-ray emission (PIXE), 92
PCO. *See* Plasma-chemical oxidation
(PCO)
Pecos Style pictograph, photograph, 95*f*
Pewter dog
 IR photograph, 276*f*
 UV illumination, 276*f*
Photography, 199*f*, 203
Phthalocyanine green, PG7, Raman
 spectra, 13*f*
Pigments, components, 296
PittCon. *See* Pittsburgh Conference
(PittCon)
Pittsburgh Conference (PittCon), 225
PIXE. *See* Particle induced X-ray emission
(PIXE)
Plasma oxidation. *See* Plasma-chemical
oxidation (PCO)
Plasma-chemical oxidation (PCO), 76, 80,
86, 143
 dating of cleaned fragments, 150
 direct plasma oxidation, 145, 147*t*, 149
 juniper ring, 149*f*
 Little Lost River Cave, Idaho, 144, 146*f*,
 152*f*
 perishable artifacts, nondestructive
 dating, 143
 plasma-chemical oxidation procedure,
 148
 pretreatment and plasma oxidation
 conditions, 147*t*, 148*t*

- pretreatment protocol, for artifact fragments, 147
- radiocarbon, 150*t*
- reed artifact, 151*f*
- vacuum integrity checks (VIC), 145
- PLM. *See* Polarized light microscopy (PLM)
- Polarized light microscopy (PLM), 24, 58, 204
- azurite, 63*f*
- paint and ink samples, 204
- paint samples/cross sections, 58
- Polymerized linseed oil, FTIR spectrum, 14*f*
- Portable X-ray fluorescence spectroscopy (pXRF) analysis, 24, 51
- Apollo and Daphne, 66*f*
- George Washington's Society of Cincinnati porcelain, 256
- overpainted sky, 38*f*
- Veronese, Madonna and Child with St. Elizabeth, the Infant St. John, and St. Catherine, 62*f*
- cobalt, iron, and arsenic, 67*f*
- copper peaks, 63*f*
- copper resins, 68*f*
- lead tin yellow, 63*f*
- mercury and arsenic, 64*f*
- titanium white, 68*f*
- Port-hole cleaning, 41
- Potassium, SEM-EDS X-ray map, 39*f*
- Prehistoric paints, 97
- Proteinaceous coating, 208*f*
- Prussian blue, FTIR spectrum, 204*f*
- Prussian blue in Orna et al. study, 201*f*
- pXRF analysis. *See* Portable X-ray fluorescence spectroscopy (pXRF) analysis
- Py-GC-MS. *See* Pyrolysis-gas chromatography-mass spectrometry (Py-GC-MS)
- Pyrolysis-gas chromatography-mass spectrometry (Py-GC-MS), 5
- Q**
- Quercitron, 124
- Quercus velutina*, 124
- R**
- Radiocarbon dates
- direct plasma oxidation, 150*t*
- juniper ring, 152*f*
- reed artifact from Little Lost River Cave, Idaho, 153*f*
- Radiocarbon, PCO-AMS, 86
- Radiograph
- surface image, 13*f*
- Village Scene*, 10*f*
- Ragged Top (RT), 103
- Raman microspectroscopy, 4
- Raman spectroscopy
- green pigment particles, 13*f*
- phthalocyanine green, PG7, 13*f*, 205
- RATS. *See* Research and Technical Studies Group (RATS)
- Research and Technical Studies Group (RATS), 225
- Rock art, ¹⁴C analysis, 94
- Rock painting
- photographs, 79*f*
- samples, 76
- Rock paintings, 75
- Royal picture gallery Mauritshuis, cock/hens, 30*f*
- RT. *See* Ragged Top (RT)
- S**
- Scanning electron microscopy energy dispersive spectroscopy (SEM-EDS) analysis, 26, 33, 37, 57, 287
- cross-sectional microscopy, 37
- lead soaps, 39
- potassium and silicon, 39*f*
- X-ray maps, 37
- Scholars model, community evolution, 224*f*
- Science and art scholars
- Center for Workshops in the Chemical Sciences (CWCS), 222
- community development, 219
- community of scholars, 223
- early chemistry and art efforts, 220
- joining forces to ignite movement, 221
- NSF Research in Cultural Heritage Science (CHS), 227
- professional development workshops, 222
- undergraduate teaching and personal career, 226
- virtual chemistry and art community, 225
- Science, Technology, Engineering, and Mathematics (STEM) education, 224
- Secondary ion mass spectrometry (SIMS), 57

- Secondary support's vertical members, missing symmetry, 35*f*, 36
- SEM-BSE. *See* SEM in the backscattered electron mode (SEM-BSE)
- SEM-EDS. *See* Scanning electron microscopy energy dispersive spectroscopy (SEM-EDS)
- SEM in the backscattered electron mode (SEM-BSE), 24
- lead soap aggregate in imprimatura layer, 41*f*
- 1150× magnification, 41*f*
- SERS. *See* Surface enhanced Raman spectroscopy (SERS)
- Shallow grooves, 32*f*
- Siamese bullet coin, chemical composition, 185
- antimony, in Sib1-Sib15, 192*f*
- Baht Thailand bullet coin, elemental composition, 195*t*
- bullet coins, 186
- chemical compositions, 187
- contemporary counterfeits, examples, 186*f*
- copper, in Sib1-Sib15, 189*f*
- iron, in Sib1-Sib15, 190*f*
- silver, in Sib1-Sib15, 191*f*
- silver and gold lumps, 185
- tin, in Sib1-Sib15, 193*f*
- zinc, in Sib1-Sib15, 194*f*
- Silicon, SEM-EDS X-ray map, 39*f*
- SIMS. *See* Secondary ion mass spectrometry (SIMS)
- STEM education. *See* Science, Technology, Engineering, and Mathematics (STEM) education
- Surface enhanced Raman spectroscopy (SERS), 124
- Surface image, radiograph, 12*f*
- Sword tassel, UV illumination, 275*f*
- T**
- Tassel area, IR photograph, 275*f*
- Terpentina D, 34
- Tetramethylammonium hydroxide (TMAH), 5
- derivatized compound, peak identity, 18*t*
- derivatized sample, pyrogram, 16*f*
- The Journal of Chemical Education (JCE)*, 220
- Theobromine, 132
- Thermally assisted hydrolysis methylation (THM), 77
- Thermally assisted hydrolysis/methylation-gas chromatography-mass spectrometry (THM-GC-MS), 75
- Thin-sectioned paint sample, oxalate-rich coating, 96*f*
- THM. *See* Thermally assisted hydrolysis methylation (THM)
- THM-GC-MS. *See* Thermally assisted hydrolysis/methylation-gas chromatography-mass spectrometry (THM-GC-MS)
- TMAH. *See* Tetramethylammonium hydroxide (TMAH)
- U**
- Ultraviolet fluorescence photograph, 202*f*
- imitation fungal stains, 212*f*
- portrait of the evangelist Mark on folio 1 verso, 202*f*
- UVA lamps, wavelength, 6
- UV illumination
- Pewter dog, 276*f*
- Sword tassel, 275*f*
- UV-induced visible fluorescence images, painting, 6, 8*f*
- UV irradiation
- cross-section sample, 32*f*
- photomicrographs, 17*f*
- UV-vis spectra, dilution on cochineal red dye, 246*f*
- V**
- Varnish oxidation, 41
- Varnish/overpaint removal, 42*f*
- Veronese, Apollo and Daphne, 67*f*, 68*f*
- Veronese paintings, XRF analyses, 51
- cultural heritage objects, pXRF uses, 58
- Madonna and Child with St. Elizabeth, 54*f*, 55
- Paolo Veronese, 52
- small colorants, degradation/detection, 56
- technical examination
- Apollo and Daphne, 52, 53*f*, 61
- Condition Assessment, 61
- Madonna and Child with St. Elizabeth, 59
- pXRF Analysis, 65
- Village Scene*, radiograph, 10*f*
- Village Scene with Horse and Honn & Company Factory*, 2, 7*f*

Visual examination, 5

W

Ward's method, 103, 107

Washington's black velvet suit, IR
photograph, 277*f*

Washington's Charles Willson Peale
Portrait
analysis, 264

Charles Willson Peale, 261

Lafayette black collar, 268*f*

Lafayette red curtain, 267*f*

Lafayette red lips, 267*f*

Lafayette retouched area, 266*f*

Lafayette's gold sword hilt, 265*f*

Lafayette's yellow pants, 266*f*

The Marquis de Lafayette, 261, 263*f*

Portrait, 262

Washington's proper left knee, IR
photograph, 277*f*

White light photograph, 202*f*

White paint, XRF analysis, 12*f*

Winterthur/University of Delaware
Program in Art Conservation
(WUDPAC), 51

WUDPAC. *See* Winterthur/University of
Delaware Program in Art Conservation
(WUDPAC)

X

XANES. *See* X-ray absorption near-edge
spectroscopy (XANES)

1150x magnification, 41*f*

X-ray absorption near-edge spectroscopy
(XANES), 57

X-ray fluorescence (XRF) analysis
spectroscopy, 4, 11, 92

Veronese paintings, 51

white paint, 12*f*

X-ray radiation, 25

XRF. *See* X-ray fluorescence (XRF)

Z

Zinc white pigment, EDS spectrum, 205

Zinc-containing pigments, 202*f*